



# **The BCL6-IRF4-BLIMP1 Transcription Factor Axis as a Therapeutic Target in T- cell Lymphoma**

**PAUL DAVID GIBSON**

Thesis submitted for the degree of Doctor of Philosophy  
Northern Institute for Cancer Research, Newcastle University

September 2015



## **Abstract**

Peripheral T-cell lymphomas (PTCL) are a heterogeneous group of clinically aggressive malignancies derived from mature (post-thymic) T-cells or Natural Killer cells, which comprise approximately 10-15% of all non-Hodgkin lymphomas. In contrast to aggressive B-cell malignancies, which are often curable and for which advances in understanding disease biology have resulted in new targeted treatment approaches, the treatment of PTCL remains inadequate. Apart from those with ALK-positive anaplastic large cell lymphoma (ALCL), patients presenting with PTCL have a poor outcome with only approximately 25% cured of their disease. The pathogenesis of T-cell lymphoma is poorly understood and few new targeted therapies are emerging.

The transcription factors BCL6, IRF4 and BLIMP1 function in a regulatory network to direct mature B-cell differentiation. They are genetically altered and dysregulated in B-cell malignancy, and BCL6 and IRF4 represent potential therapeutic targets. These transcription factors also interact to regulate T-cell differentiation and emerging data indicated genetic alteration in some PTCL. This project investigated the importance of BCL6, IRF4, and BLIMP1 in the regulation of PTCL cell line proliferation and survival using ALCL cell lines *in vitro* as a model.

Lentiviral-mediated knockdown of BCL6 and IRF4, and overexpression of BLIMP1, each resulted in reduced proliferation / survival of some, but not all, ALCL cell lines tested, and no clear pattern of response emerged. These effects were associated with small changes in cell cycle progression and induction of apoptosis. Modulation of each of the transcription factors had small effects on the expression of the others, again with variable patterns between cell lines. IRF4 knockdown revealed a positive interaction with c-MYC and BLIMP1 $\alpha$  in 2/3 ALK+ ALCL cell lines. Intriguingly, ALK inhibition with crizotinib revealed different patterns of NPM-ALK mediated dysregulation of the transcription factors across the cell lines. These data support a positive role for BCL6 and IRF4 in the maintenance of ALCL, and an inhibitory / tumour suppressor role for BLIMP1, but show variability in dependencies between cell lines which could reflect clinically important disease heterogeneity which must be considered when targeting this transcription factor axis therapeutically.

“The mark of a person is defined by how they cope in the face of adversity”

## **Acknowledgements**

I must thank my supervisory team for giving me the opportunity to undertake my PhD, Dr. Chris Bacon, Dr. Vikki Rand, Dr. James Allan, and Dr. Luke Gaughan. I cannot express the gratitude for the teaching I have received, helping me to not only produce this thesis, but to further myself in ways I did not think possible. Special thanks go to Chris, who throughout the last three years has taught me not only to be independent but provided invaluable advice in every aspect of my life and has always encouraged me to push myself further. I am also thankful to Bright Red who provided me with the opportunity to complete my PhD by funding my studentship.

I am also thankful to Dr. Paul Sinclair who provided the BLIMP1-SIEW, and SIN-SIEW overexpression vectors for my BLIMP1 investigations.

I am grateful to all the members of the lymphoma research group who have given me technical help and advice throughout my project and offered a fresh perspective on many things I thought hopeless. Not least is the support I've received from Sarah and Holly who have always helped to brighten my day even after a string of failed experiments. I am also thankful to all members of the NICR who have been enormously friendly and always willing to help.

Finally, I am thankful to my loving wife Loren. She has heard it all, through good and bad results, angry rants about why things don't work, to just listening to me ramble on about my project. She has been my inspiration and encouragement to complete the PhD from the start.



## Contents

Abstract.....	ii
Acknowledgements.....	iv
List of figures.....	xi
List of tables.....	xiv
Abbreviations.....	xv
1. Introduction.....	22
1.1 The immune system.....	22
1.1.1 B-cell development.....	22
1.1.2 T-cell development.....	26
1.2 Lymphoma.....	31
1.3 B-cell Non-Hodgkin lymphoma.....	31
1.4 Peripheral T-cell lymphoma.....	34
1.4.1 Peripheral T-cell Lymphoma – Not otherwise Specified.....	36
1.4.2 Angioimmunoblastic T-cell lymphoma.....	38
1.4.3 Anaplastic Large Cell Lymphoma.....	39
1.4.3.1 Genetics of ALK+ ALCL.....	41
1.4.3.2 Genetics of ALK- ALCL.....	45
1.5 B-cell Lymphoma 6 (BCL6).....	47
1.5.1 BCL6 Structure.....	47
1.5.2 BCL6 in B-cells.....	49
1.5.3 BCL6 in B-cell lymphoma.....	51
1.5.4 BCL6 in T-cells.....	54
1.5.5 BCL6 in T-cell lymphoma.....	57
1.6 Interferon Regulatory Factor 4 (IRF4).....	58
1.6.1 IRF4 structure.....	58
1.6.2 IRF4 in B-cells.....	59
1.6.3 IRF4 in B-cell lymphoma.....	62
1.6.4 IRF4 in T-cells.....	63
1.6.5 IRF4 in T-cell lymphoma.....	69
1.7 B-lymphocyte Induced Maturation Protein 1 (BLIMP1).....	71
1.7.1 BLIMP1 structure.....	71
1.7.2 BLIMP1 in B-cells.....	72

1.7.3 BLIMP1 in B-cell lymphoma .....	73
1.7.4 BLIMP1 in T-cells .....	74
1.7.5 BLIMP1 in T-cell lymphoma .....	76
1.8 Aims .....	78
2. Materials and Methods .....	82
2.1 Mammalian cell culture .....	82
2.1.1 Cell culture conditions .....	82
2.1.2 Thawing of cryopreserved cells .....	83
2.1.3 Counting cells using a Haemocytometer and Trypan Blue exclusion.....	83
2.1.4 Freezing cells.....	83
2.1.5 Mycoplasma testing.....	85
2.2 Drugs/Inhibitors .....	85
2.2.1 BCL6 inhibitor, 79-6 .....	85
2.2.2 ALK inhibitor, Crizotinib .....	85
2.2.3 Lenalidomide .....	86
2.3 Resazurin viable cell assay.....	86
2.3.1 Principle .....	86
2.3.2 Method .....	86
2.4 siRNA knockdown.....	87
2.4.1 Principle .....	87
2.4.2 Method .....	88
2.5 Lentiviral-mediated transduction.....	89
2.5.1 Principle of shRNA .....	89
2.5.2 Principle of overexpression .....	91
2.5.3 Principle of lentivirus generation .....	91
2.5.4 Method .....	93
2.5.4.1 Culturing of lentiviral vector bacteria .....	93
2.5.4.2 Bacterial culturing of lentiviral vectors.....	93
2.5.4.3 Transfection of HEK 293T cells.....	94
2.5.4.4 Transduction of suspension cell lines .....	95
2.5.4.5 Induction and selection of transduced suspension cell lines .....	95
2.6 Protein analysis .....	96
2.6.1 Protein extraction .....	96

2.6.2 Protein quantification .....	96
2.6.3 SDS-PAGE .....	96
2.6.3.1 Principle.....	96
2.6.3.2 Method.....	97
2.7 Gene expression analysis by Quantitative-PCR (qPCR) .....	100
2.7.1 Principle .....	100
2.7.2 RNA extraction and cDNA synthesis .....	100
2.7.3 SYBR® Green qPCR .....	101
2.8 Flow cytometry.....	102
2.8.1 Principles of flow cytometry.....	102
2.8.2 Method .....	104
2.8.2.1 Propidium Iodide staining for cell cycle analysis .....	104
2.8.2.2 Detection of GFP and RFP transduced cells .....	105
2.8.2.3 BrdU/7-AAD staining for cell cycle analysis .....	106
2.8.2.4 Active caspase-3 staining for apoptosis analysis .....	106
3. The role of BCL6 in the maintenance of T-cell lymphoma.....	110
3.1 Introduction.....	110
3.2 Results .....	112
3.2.1 Characterisation of lymphoma cell lines .....	112
3.2.2 Knockdown of BCL6 using siRNA .....	114
3.2.3 BCL6 knockdown results in a modest reduction of proliferation/survival of lymphoma cell lines .....	116
3.2.4 BCL6 siRNA knockdown has cell line-specific effects on IRF4 and BLIMP1 expression .....	116
3.2.5 Doxycycline treatment of SUDHL1 cells results in reduced IRF4 expression.....	118
3.2.6 BCL6 shRNA knockdown results in reduced proliferation/survival of ALK+ ALCL cell lines.....	119
3.2.7 BCL6 shRNA knockdown results in small increases in G2/M populations ...	122
3.2.8 BCL6 shRNA knockdown affects transcription of IRF4 and c-MYC transcripts .....	124
3.2.10 ALCL cell lines are sensitive to 79-6 inhibitor .....	130
3.2.11 79-6 induces apoptosis in all lymphoma cell lines .....	130
3.2.12 79-6 fails to induce changes in B-cell targets in T-cell lymphoma cell lines .....	133

3.3 Discussion .....	135
4. IRF4 in the maintenance of T-cell lymphoma .....	144
4.1 Introduction.....	144
4.2 Results .....	146
4.2.1 IRF4 siRNA knockdown results in a slight reduction in proliferation/survival of SUDHL1 .....	146
4.2.2 IRF4 siRNA knockdown has minimal, cell line-specific effects on BCL6 and BLIMP1 expression.....	146
4.2.3 IRF4 shRNA knockdown results in reduced proliferation/survival of ALK+ ALCL cell lines.....	148
4.2.4 IRF4 shRNA knockdown results in a minor increase in G2/M populations..	150
4.2.5 IRF4 promotes the expression of c-MYC with variable effects on BLIMP1 expression in Karpas-299.....	153
4.2.6 PTCL cell lines are insensitive to Lenalidomide treatment.....	159
4.2.7 ALK+ ALCL cell lines demonstrate increased sensitivity to JQ-1 with Lenalidomide treatment .....	160
4.3 Discussion .....	162
5. The transcriptional repressor, BLIMP1, as a tumour suppressor in ALCL.....	170
5.1 Introduction.....	170
5.2 Results .....	171
5.2.1 BLIMP1 overexpression is achievable in ALK+ ALCL cell lines .....	171
5.2.2 BLIMP1 overexpression represses IRF4 and endogenous BLIMP1 in ALK+ ALCL .....	171
5.2.3 BLIMP1 overexpression reduces the proliferation/survival of ALK+ ALCL cell lines.....	173
5.2.4 BLIMP1 overexpression induces cell death in ALK+ ALCL cell lines.....	173
5.3 Discussion .....	178
6. NPM-ALK in the regulation of the BCL6-IRF4-BLIMP1 Transcription Factor Axis .....	186
6.1 Introduction.....	186
6.2 Results .....	187
6.2.1 ALK+ ALCL cell lines are selectively sensitive to Crizotinib.....	187
6.2.2 Inhibition of ALK reveals two distinct effects on RNA levels of BCL6, IRF4, BLIMP1, and c-MYC.....	187
6.3 Discussion .....	191
7. Conclusion and Discussion .....	196

8. References.....	208
--------------------	-----

## List of figures

- Figure 1.1** Differentiation of B and T-cells upon stimulus by Antigen Presenting Cell
- Figure 1.2** Germinal Center B-cell Maturation
- Figure 1.3** The BCL6-IRF4-BLIMP1 Transcription Factor Axis in the Germinal Center
- Figure 1.4** T-cell maturation
- Figure 1.5** Effect of cytokines upon the differentiation of CD4+ T-cells
- Figure 1.6** Differentiation of CD8+ T-cells
- Figure 1.7** Incidence of Lymphoma
- Figure 1.8** Peripheral T-cell Lymphoma
- Figure 1.9** Structure of BCL6 and the effect of inhibitors on the protein function
- Figure 1.10** Interaction of the BCL6-IRF4-BLIMP1 axis in CD4+ cells
- Figure 1.11** Structure and function of IRF4 with binding partners
- Figure 1.12** Interaction of IRF4 with binding partners in T-helper subsets
- Figure 1.13** Structure of BLIMP1 protein
- Figure 2.1** Structure of 79-6 inhibitor
- Figure 2.2** Structure of Crizotinib
- Figure 2.3** Structure of Lenalidomide
- Figure 2.4** Vector map of pTRIPZ taken from Thermo Scientific Manual
- Figure 2.5** Vector maps of packaging plasmids pMD2.G and pCMV  $\Delta$ R8.91 and expression vector pSIEW
- Figure 2.6** Formation of a lentivirus particle
- Figure 2.7** Principles of a flow cytometer
- Figure 2.8** RFP-gating strategy
- Figure 2.9** Compensation of fluorescent channels
- Figure 3.1** Interaction of BCL6 with IRF4 and BLIMP1 in B-cells vs. T-cells
- Figure 3.2** Expression of BCL6, IRF4, BLIMP1, and c-MYC in lymphoma cell lines
- Figure 3.3** Optimisation of siRNA voltages in SUDHL4
- Figure 3.4** Individual siRNAs vs. siRNA pool
- Figure 3.5** Counts of BCL6 knockdown lymphoma cells
- Figure 3.6** Effect of BCL6 knockdown on the BCL6-IRF4-BLIMP1 transcription factor axis

- Figure 3.7** Knockdown of BCL6 using shRNA and effect of doxycycline on IRF4 protein levels
- Figure 3.8** BCL6 knockdown results in reduced growth rates of ALK+ ALCL cell lines
- Figure 3.9** BCL6 knockdown results in accumulation of G2/M populations in ALK+ ALCL cell lines
- Figure 3.10** BCL6 knockdown results in no induction of apoptosis
- Figure 3.11** The effect of BCL6 shRNA knockdown on the expression of BCL6, IRF4, and BLIMP1 in SUDHL1
- Figure 3.12** The effect of BCL6 shRNA knockdown on the expression of BCL6, IRF4, and BLIMP1 in Karpas-299 and DEL
- Figure 3.13** Growth curve of lymphoma cell lines with Resazurin
- Figure 3.14** Resazurin profiles of 79-6 and DMSO treated cell lines
- Figure 3.15** Levels of apoptosis in lymphoma cell lines with 79-6 treatment
- Figure 3.16** Expression of BCL6 target genes after 8 hours with 79-6 treatment
- Figure 4.1** Interaction of IRF4 with BCL6 and BLIMP1 in B-cells vs. T-cells
- Figure 4.2** Counts of IRF4 knockdown lymphoma cells
- Figure 4.3** Effect of IRF4 knockdown on the BCL6-IRF4-BLIMP1 transcription factor axis
- Figure 4.4** IRF4 knockdown results in reduced growth rates of ALK+ ALCL cell lines
- Figure 4.5** IRF4 knockdown results in accumulation of G2/M populations in ALK+ ALCL cell lines
- Figure 4.6** IRF4 knockdown results in no induction of apoptosis
- Figure 4.7** The effect of IRF4 shRNA knockdown on the expression of BCL6, IRF4, and BLIMP1 in SUDHL1
- Figure 4.8** The effect of IRF4 shRNA knockdown on the expression of BCL6, IRF4, and BLIMP1 in Karpas-299
- Figure 4.9** The effect of IRF4 shRNA knockdown on the expression of BCL6, IRF4, and BLIMP1 in DEL
- Figure 4.10** Resazurin profiles of Lenalidomide treated cells
- Figure 4.11** Resazurin profiles of Lenalidomide and JQ-1 in combination
- Figure 5.1** Interaction of BLIMP1 with IRF4 and BCL6 in B-cells vs. T-cells

- Figure 5.2** Optimisation of pSIEW vector transduction in SUDHL1, SUPM2, and Karpas-299
- Figure 5.3** Overexpression of BLIMP1 $\alpha$  and BLIMP1 $\beta$  in ALK+ ALCL cell lines
- Figure 5.4** Overexpression of BLIMP1 affects cellular proliferation
- Figure 5.5** Overexpression of BLIMP1 induces cellular death
- Figure 6.1** Survival curve of ALCL cell lines treated with Crizotinib
- Figure 6.2** The effect of Crizotinib treatment on the expression of BCL6, IRF4, and BLIMP1 in ALK+ ALCL
- Figure 6.3** Summary of the interactions of ALK across ALK+ cell lines
- Figure 7.1** Summary of the interactions between the BCL6-IRF4-BLIMP1 transcription factor axis in ALK+ ALCL

## List of tables

- Table 1.1** Documented cases of translocations involving ALK in ALCL
- Table 1.2** CD4 T-helper cell subsets and roles of each
- Table 1.3** The Histological subgroups of ALCL as defined by the WHO Classification of Haematological Malignancies
- Table 2.1** List of cell lines used in this project
- Table 2.2** siRNA sequences and voltages for electroporation
- Table 2.3** shRNA sequences for TRIPZ vectors
- Table 2.4** Recipes for commonly used western blot reagents
- Table 2.4** List of antibodies used for western blot analysis
- Table 2.5** Primers used for quantitative PCR analysis

## Abbreviations

<b>7-AAD</b>	7-Aminoactinomycin D
<b>AICE</b>	AP1-IRF composite element
<b>AID</b>	Activation Induced Deaminase
<b>AITL</b>	Angioimmunoblastic T Cell Lymphoma
<b>AKT</b>	v-akt murine thymoma viral oncogene homolog
<b>ALCL</b>	Anaplastic Large Cell Lymphoma
<b>ALK</b>	Anaplastic Lymphoma Kinase
<b>ALL</b>	Acute Lymphoblastic Leukaemia
<b>AP1</b>	Activator Protein 1
<b>APC</b>	Antigen Presenting Cells
<b>APS</b>	Ammonium Persulphate
<b>ATL</b>	Adult T-cell Leukaemia
<b>ATM</b>	Ataxia Telangiectasia Mutated
<b>ATP</b>	Adenosine Triphosphate
<b>ATR</b>	Ataxia Telangiectasia and Rad3-related protein
<b>BACH2</b>	Basic Region-Leucine Zipper factor BTB and CNC homology 2
<b>BAT-3</b>	HLA-B-associated transcript 3
<b>BATF</b>	Basic Leucine Zipper Transcription Factor, ATF-like
<b>BBD</b>	BCL6 binding domain
<b>BCA</b>	Bicinchoninic acid
<b>BCL6</b>	B-cell Lymphoma 6
<b>BCOR</b>	BCL6 co-repressor
<b>BCR</b>	B-cell receptor
<b>BLIMP1</b>	B Lymphocyte-Induced Maturation Protein 1
<b>B-NHL</b>	B-cell Non-Hodgkin Lymphoma
<b>BSAC</b>	B-cell lineage-specific activator protein
<b>BTB</b>	BR-C, ttk and bab
<b>BRD4</b>	Bromodomain containing protein 4
<b>BrdU</b>	Bromodeoxyuridine
<b>C-ALCL</b>	Cutaneous Anaplastic Large Cell Lymphoma
<b>CCL3</b>	Chemokine (C-C motif) Ligand 3

<b>CTCF</b>	CCCTC-binding factor
<b>CDC</b>	Cell division cycle
<b>CDK</b>	Cyclin Dependent Kinase
<b>cDNA</b>	Complementary DNA
<b>CHOP</b>	Cyclophosphamide, Hydroxydaunorubicin (Doxorubicin), Oncovin (Vincristine), Prensione
<b>CtBP</b>	C-terminal Binding Protein
<b>CTCL</b>	Cutaneous T-cell Lymphoma
<b>gDNA</b>	Genomic DNA
<b>CHEK1</b>	Checkpoint Kinase 1
<b>ChIP</b>	Chromatin Immunoprecipitation
<b>cPPT</b>	Central Polypurine Tract
<b>CREBBP</b>	CREB binding protein
<b>CSR</b>	Class-Switch Recombination
<b>CXCR4</b>	C-X-C Chemokine Receptor Type 4
<b>DLBCL</b>	Diffuse Large B-cell Lymphoma
<b>DMEM</b>	Dulbecco's Modified Eagles Medium
<b>DMSO</b>	Dimethyl Sulfoxide
<b>DNA-PK<sub>cs</sub></b>	DNA-dependent protein kinase, catalytic subunit
<b>DNMT3A</b>	DNA (cytosine-5)-methyltransferase 3A
<b>EBV</b>	Epstein-Barr Virus
<b>ECL</b>	Electrochemiluminescence
<b>EICE</b>	ETS-IRF composite element
<b>EP300</b>	p300 lysine acetyltransferase
<b>ERK</b>	Extracellular Regulated Signal-Kinases
<b>FBX011</b>	F-box protein 1
<b>FCS</b>	Foetal Calf Serum
<b>FOXO1</b>	Forkhead Box Protein O1
<b>GADD45A</b>	Growth Arrest and DNA-damage-inducible, alpha
<b>GC</b>	Germinal Centre
<b>GFP</b>	Green Fluorescent Protein
<b>GSEA</b>	Gene Set Enrichment Analysis

<b>HAT</b>	Histone Acetyltransferase
<b>HDAC</b>	Histone Deacetylase
<b>HeBS</b>	HEPES-Buffered Saline
<b>HIF1a</b>	Hypoxia Inducible Factor 1a
<b>HMT</b>	Histone Methyltransferase
<b>HRP</b>	Horseradish Peroxidase
<b>HTLV-1</b>	Human T-cell Leukaemia Virus Type 1
<b>IBP</b>	IRF4-binding protein
<b>IFN<math>\gamma</math></b>	Interferon- $\gamma$
<b>Ig</b>	Immunoglobulin
<b>IL</b>	Interleukin
<b>IRF</b>	Interferon Regulatory Factor
<b>ISRE</b>	Inteferon-Stimulated Response Element
<b>JAK</b>	Janus Kinase
<b>JUN</b>	Jun Proto-Oncogene
<b>KLRG1</b>	Killer Cell Lectin-like Receptor Subfamily G Member 1
<b>LB</b>	Lysogeny Broth
<b>LTR</b>	Long Terminal Repeat
<b>MAPK</b>	Mitogen-Activated Protein Kinase
<b>MARE</b>	Maf Recognition Elements
<b>MCL</b>	Mantle Cell Lymphoma
<b>MCP</b>	Monocyte Chemoattractant Protein
<b>MDS1-EVI1</b>	Myelodysplasia syndrome 1 protein-ecotropic virus integration site 1 protein homolog
<b>MHC</b>	Major Histocompatibility Complex
<b>MITF</b>	Microphthalmia-associated Transcription Factor
<b>MIZ1</b>	Myc-Interacting Zinc Finger Protein 1
<b>MK</b>	Midkine
<b>MM</b>	Multiple Myeloma
<b>MRP</b>	Multidrug Resistance Protein
<b>MYC</b>	Myelocytomatosis Viral oncogene
<b>NCoR</b>	Nuclear Receptor Corepressor

<b>NFAT</b>	Nuclear Factor of Activated T-cells
<b>NF-κB</b>	Nuclear Factor kappa-light-chain-enhancer of Activated B-cells
<b>NHL</b>	Non-Hodgkin Lymphoma
<b>NK</b>	Natural Killer
<b>NPM</b>	Nucleophosmin
<b>NSCLC</b>	Non-small-cell lung carcinoma
<b>PBS</b>	Phosphate-Buffered Saline
<b>PC4</b>	Positive Cofactor 4
<b>PI</b>	Propidium Iodide
<b>PIN1</b>	Peptidylprolyl cis/trans Isomerase NIMA-interacting 1
<b>PI3K</b>	Phosphoinositide 3-kinase
<b>PLZF</b>	Promyelocytic Leukaemia Zinc Finger
<b>PMBL</b>	Primary Mediastinal B-cell Lymphoma
<b>PRDM1</b>	PR Domain Containing 1
<b>PTCL</b>	Peripheral T-cell Lymphoma
<b>PTCL-NOS</b>	Peripheral T-cell Lymphoma not otherwise specified
<b>PTN</b>	Pleiotropin
<b>RAS</b>	Rat Sarcoma
<b>RRE</b>	Rev Response Element
<b>RFP</b>	Red Fluorescent Protein
<b>RHOA</b>	Rho GTPase A
<b>RI-BPI</b>	Retro-Inverted BCL6 Peptide Inhibitor
<b>RIPA</b>	Radioimmunoprecipitation Assay
<b>RIZ</b>	Retinoblastoma protein-interacting zinc finger gene
<b>RPMI</b>	Roswell Park Memorial Institute medium
<b>rtTA</b>	Reverse Tetracycline Transactivator
<b>RT-PCR</b>	Real Time Polymerase Chain Reaction
<b>RISC</b>	RNA-Induced Silencing Complex
<b>SDF-1</b>	Stromal Cell-derived Factor-1
<b>SDS-PAGE</b>	Sodium Dodecyl Sulphate Polyacrylamide Gel Electrophoresis
<b>SHM</b>	Somatic Hypermutation
<b>shRNA</b>	Short-Hairpin RNA

<b>sinLTR</b>	Self-inactivating Long Terminal Repeat
<b>siRNA</b>	Short Interfering RNA
<b>SUMO-1</b>	Small Ubiquitin-like Molecule 1
<b>SMRT</b>	Silencing Mediator of Retinoid and Thyroid Receptor
<b>SPI</b>	Spleen Focus Forming Virus (SFFV) Proviral Integration Oncogene
<b>SRBCs</b>	Sheep Red Blood Cells
<b>STAT</b>	Signal Transducer and Activator of Transcription
<b>TBS</b>	Tris-Buffered Saline
<b>TCM</b>	Central memory T-cells
<b>TCR</b>	T-cell receptor
<b>TEM</b>	Effector memory T-cells
<b>TEMED</b>	Tetramethylethylenediamine
<b>TET</b>	Tet methylcytosine dioxygenase
<b>TF</b>	Transcription Factor
<b>T<sub>FH</sub></b>	Follicular B Helper T-cell
<b>T<sub>H</sub></b>	T-helper
<b>TP53</b>	Tumour Protein 53
<b>T<sub>reg</sub></b>	Regulatory T-cell
<b>WPRE</b>	Woodchuck Posttranscriptional Regulatory Element
<b>WHO</b>	World Health Organisation
<b>ZEB1</b>	Zinc finger E-box binding homeobox 1



## **Chapter 1: Introduction**



# 1. Introduction

## 1.1 The immune system

The key to the immune response in humans is the diverse nature of the lymphocytes present (figure 1.1). Lymphocytes are broadly divided into B-cells and T-cells; each cell type plays a specific role required for successful, adaptive immune response.

### 1.1.1 B-cell development

B and T-cells are produced in the bone marrow from progenitor haematopoietic stem cells. B-cells progress through a number of stages to reach a functional effector cell: pro-B-cell, large pre-B-cell, mature naïve B-cell, activated B-cell, Germinal Center (GC) B-cell, plasma cell/memory B-cell.

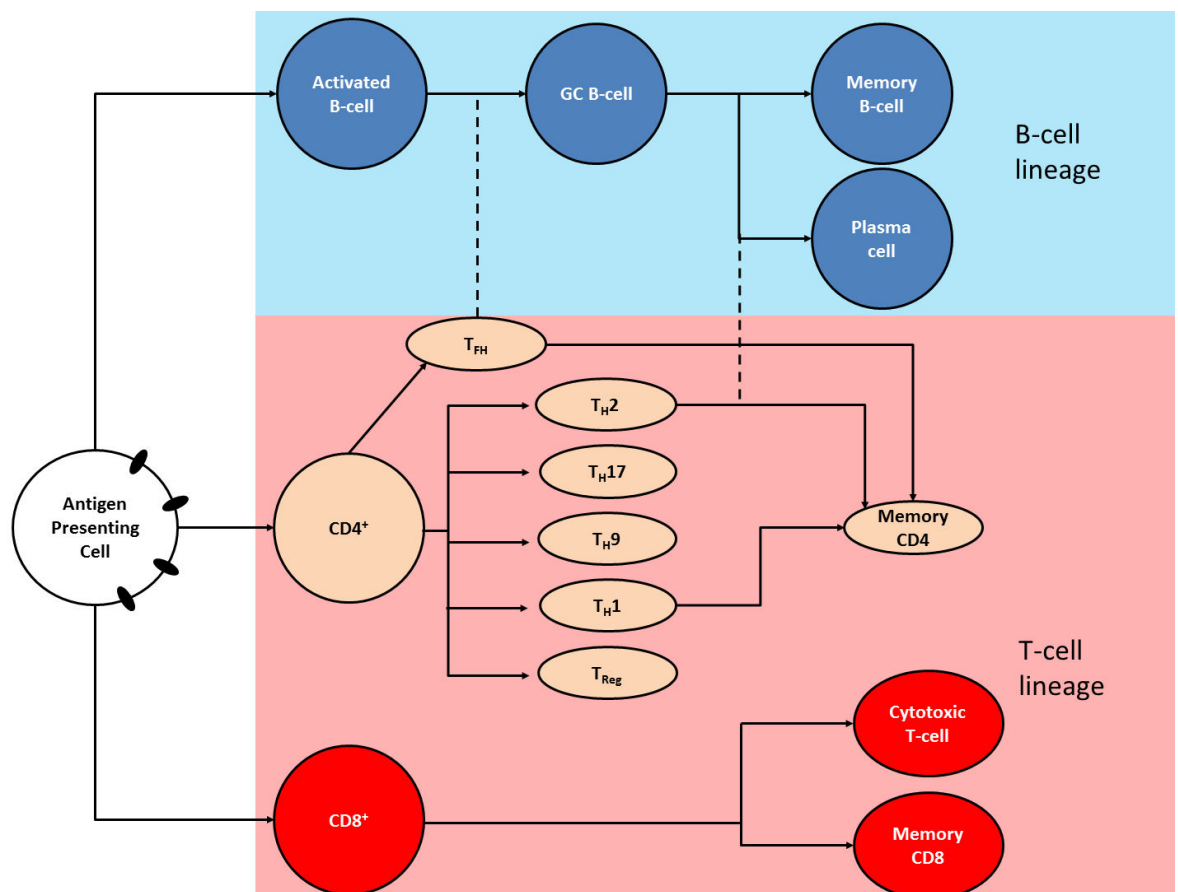


**Figure 1.1: Differentiation of B and T-cells upon stimulus by Antigen Presenting Cell**

The presence of a foreign antigen on the cell surface of antigen presenting cells (APCs) stimulates activation and differentiation of B-cells circulating the blood and T-cell precursors. GC = Germinal Centre,  $T_H$  = T helper cell,  $T_{Reg}$  = Regulatory T helper cell,  $T_{FH}$  = Follicular T helper cell. Dashed lines indicate where the T-helper cells presence is required for the formation of other cells of B-cell lineage.

To produce functional immunoglobulin (Ig) proteins on B-cell membranes, B-cell precursors interact with stromal cells and cytokine signals to stimulate Ig heavy and light chain locus rearrangements. The combination of rearranged light and heavy chain genes produce an antibody which is unique to the cell. Now a mature naïve B-cell, it is released into the blood.

Upon encountering a pathogen, antigen presenting cells (APCs), such as macrophages and dendritic cells, engulf and digest the pathogen to present foreign antigens on their cell surface via Major Histocompatibility Complexes (MHC). The antigens stimulate activation of B-cells and T-cells (figure 1.1) (Tangye and Tarlinton, 2009, Dudley et al., 2005). With help from antigen-activated T-cells naïve B-cells become activated and form or traffic to germinal centers where they differentiate into GC B-cells. Here, the GC B-cells undergo affinity maturation for their cognate antigen. There are two main processes undertaken by a GC B-cell to generate a mature antibody, Somatic Hypermutation (SHM) and Class-switch recombination (CSR). SHM is a process by which mutations are introduced into the coding sequence of immunoglobulin heavy and light chain genes. Mutations enhancing the affinity of immunoglobulin for antigen are positively selected within the germinal center microenvironment resulting in outgrowth of B-cells with high affinity antibody production. CSR is a process whereby deletional recombination changes the constant region segment used by a rearranged immunoglobulin gene to produce an immunoglobulin of a different isotype (figure 1.2).

Upon achieving affinity maturation, the GC B-cell will then differentiate into either a long-lived memory B-cell or an effector antibody-secreting Plasma cell. Central to this pathway is the regulation of the BCL6-IRF4-BLIMP1 transcription factor axis which governs progression through the GC maturation phases (figure 1.3) (De Silva and Klein, 2015).

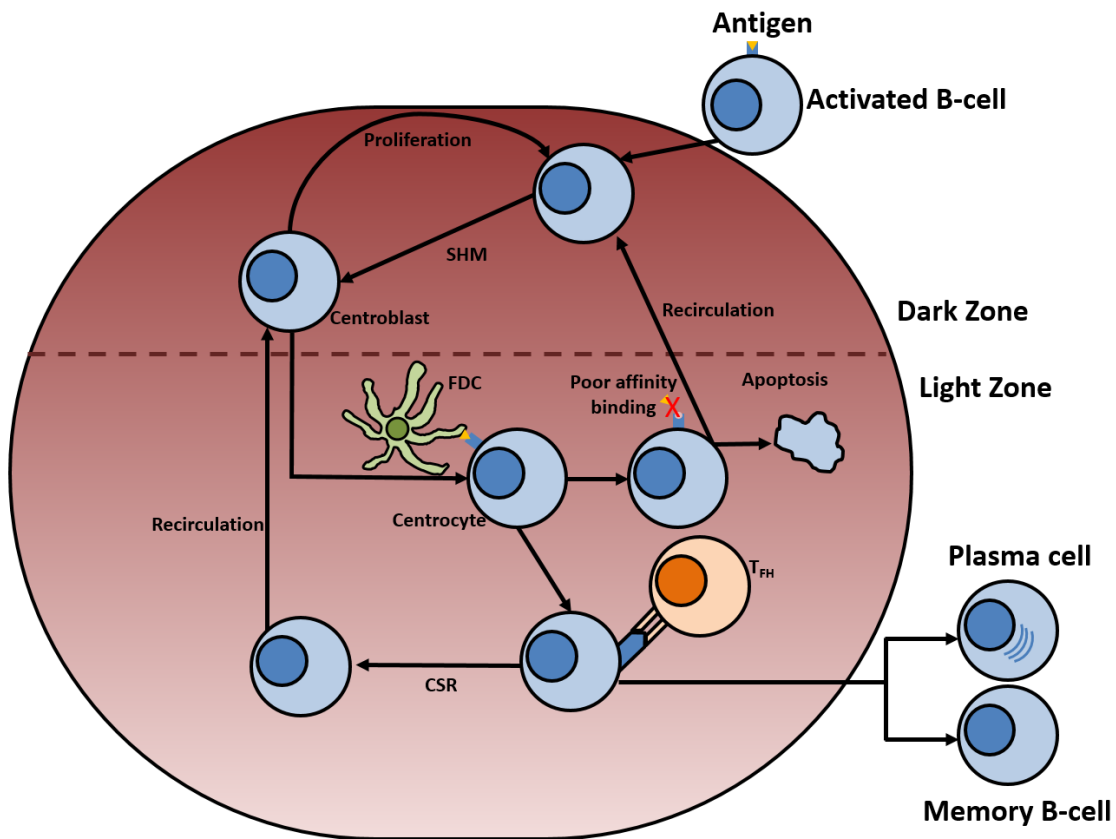


**Figure 1.2: Germinal Center B-cell maturation**

Prior to entry to the lymph node, naïve B-cells detect antigen and receive co-stimulatory signals from T-helper cells and enter the dark zone of the Germinal Center (GC). The B-cell, now termed a centroblast, undergoes one or more rounds of proliferation and somatic hypermutation (SHM) through upregulation of Activation Induced Deaminase (AID). After this, the centroblast migrates to the light zone of the GC and are subjected to Follicular Dendritic Cells (FDCs) with target antigen present on their cell surface. At this point the mutated B-cell Receptor (BCR), a product of SHM, will bind the antigen. If binding affinity is too low the centrocyte undergoes apoptosis due to lack of survival signals from the FDCs. At this point, B-cells are defined as centrocytes. Centrocytes then undergo another round of selection by interaction of CD40 with CD40L found on follicular B-helper T-cells (T<sub>FH</sub>). A small subset of centrocytes which do not achieve the required affinity can recirculate into the dark zone to undergo further SHM. In addition, light zone centrocytes may undergo immunoglobulin class-switch recombination (CSR) before recirculating into the dark zone before undergoing further proliferation and SHM. Finally, the centrocytes can either leave the germinal center as a mature plasma cells or memory B-cells.

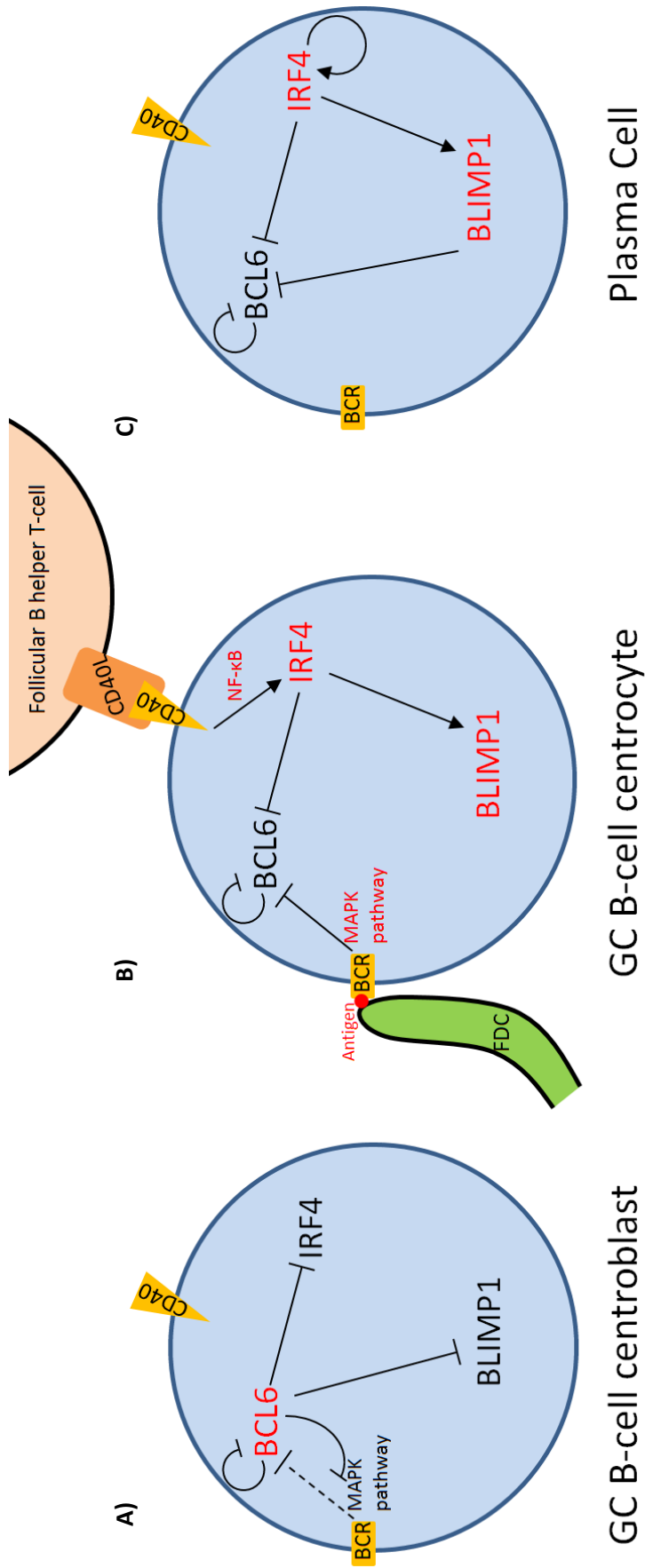


**Figure 1.3: The BCL6-IRF4-BLIMP1 Transcription Factor Axis in the Germinal Center**

A) Transcription Factor axis at the centroblast stage of B-cell development. Germinal Centre signals promote the expression of BCL6, in turn BCL6 directly represses BLIMP1, a key component in plasma cell determination. BCL6 represses key DNA damage response genes to facilitate somatic hypermutation. B) Upon stimulation of B-cell receptor (BCR), through antigen binding from follicular dendritic cells (FDC), a MAP-kinase (MAPK) pathway is induced leading to the phosphorylation and degradation of BCL6 whilst simultaneous IRF4 upregulation is stimulated by NF- $\kappa$ B via activation of the CD40 receptor present on the centrocyte. CD40 receptor is stimulated through interaction with a follicular B helper T-cell, IRF4 expression leads to the promotion of BLIMP1 expression. C) Differentiation to the plasma cell is completed. BLIMP1 and IRF4 are expressed and BCL6 is repressed. Differentiated morphology is maintained by the self-promoting loop IRF4 exhibits upon itself. GC = Germinal Centre. Red text indicates actively transcribed genes, black text indicates repressed genes.

### 1.1.2 T-cell development

Like B-cells, T-cells pass through a number of intermediate cell stages to produce a mature T-cell: Pre-thymic precursor, early thymic precursor, double negative thymocyte (CD4-CD8-), double positive thymocyte (CD4+CD8+), single positive thymocyte (CD4+CD8- or CD4-CD8+), and finally a single positive CD4<sup>+</sup> or CD8<sup>+</sup> T-cell (Godfrey and Zlotnik, 1993) (figure 1.4).

CD4<sup>+</sup> T-cells regulate the mammalian immune response, facilitating adaptive immunity of the host. CD4<sup>+</sup> T-cells can differentiate into one of many T helper cell types, which function to aid other lymphocytes in their specialisation through the production of cytokines (table 1.1). Helper T-cells are not necessarily terminally differentiated; further differentiation to other subsets can be achieved. T-helper cell plasticity is controlled by the presence of certain cytokines and expression of specific genes (figure 1.5) (Luckheeram, 2012). CD4<sup>+</sup> T-cells also have the ability to differentiate into memory CD4 T-cells characterised by expression of BCL6 (Choi et al., 2013). Memory CD4<sup>+</sup> T-cells remain a controversial topic with regards to which T-helper cells can contribute (Hale and Ahmed, 2015). Multiple studies have demonstrated long-term retention of both T<sub>H1</sub> and T<sub>FH</sub> cells for up to 150 days post-infection clearance which, upon reinfection, rapidly proliferated and recall the T<sub>FH</sub>

T-helper subset	Interleukins required	Master regulator	Role
Follicular B Helper T-cell (T <sub>FH</sub> )	IL6, IL21	BCL6	Involved in the development of antigen-specific B-cell immunity through germinal center production and antibody maturation induction (Bollig et al., 2012, Breitfeld et al., 2000, Vinuesa et al., 2005).
T-helper 2 (T <sub>H2</sub> )	IL2, IL4	GATA3	Maintain the persistence of allergies through B-cell interaction (Del Prete, 1992, Sokol et al., 2009).
T-helper 9 (T <sub>H9</sub> )	TGF-β, IL4	RBPJ	Maintain the persistence of allergies through B-cell interaction (Staudt et al., 2010).
T-helper 1 (T <sub>H1</sub> )	IL12, IFNγ	T-bet	Enhance macrophage activity and produce opsonising antibodies (Murray et al., 1985, Afkarian et al., 2002, Lugo-Villarino et al., 2003).
T-helper 17 (T <sub>H17</sub> )	IL6, TGF-β	RORγT	Mount immune responses against extracellular pathogens (Annunziato et al., 2007, Ivanov et al., 2006, Weaver et al., 2006).
Regulatory T-cell (T <sub>reg</sub> )	TGF-β, IL12	FOXP3	Suppression of the immune system (Jutel and Akdis, 2008).

**Table 1.1: CD4 T-helper cell subsets and roles of each**

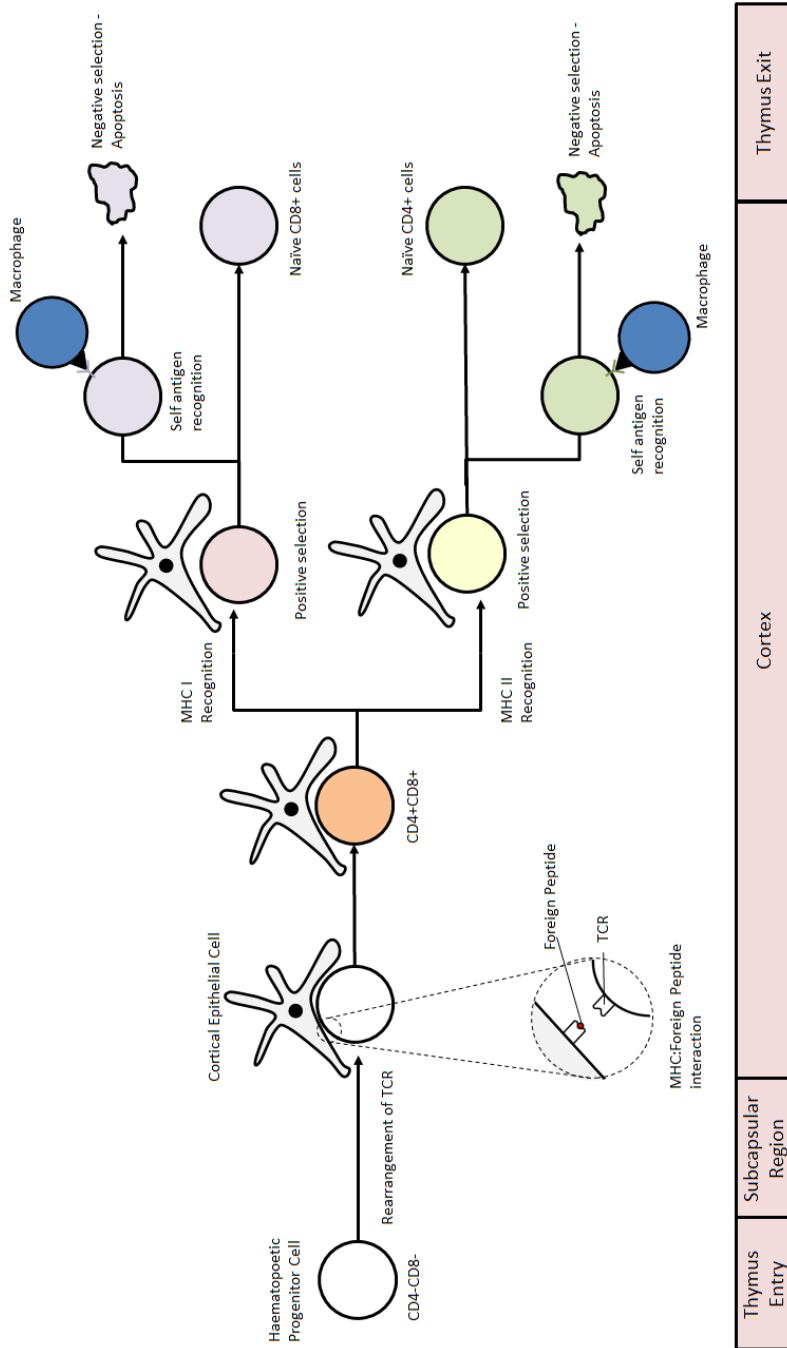


**Figure 1.4: T-cell maturation**

Haematopoietic Progenitor Cells enter the thymus and move to the subcapsular region where T-cell receptor (TCR) genes begin to rearrange (Mombaerts et al., 1992, Petrie et al., 1995, Philpott et al., 1992, Shinkai et al., 1993). As maturation proceeds, the T-cells begin to express specific cell surface receptors leading them into the cortex of the thymus. As the T-cells move they interact with thymic cortical epithelial cells (Zerrahn et al., 1997) which contain MHC:foreign peptide complexes upon their cell surface. MHC (Major Histocompatibility Complex) comes in two classes, MHC class I and MHC class II, these are vital for T-cell maturation. Upon interaction with MHC, thymocytes express CD4 and CD8 upon their cell surface (at this stage the cells are defined as CD4<sup>+</sup>CD8<sup>+</sup> T-cells). A cell recognising MHC class I undergoes positive selection and receives maturation signals from thymic cortical epithelial cells preventing the expression of CD4 on the T-cell surface and develops characteristics of cytotoxic CD8 T-cells (Petrie et al., 1995, Zerrahn et al., 1997). Conversely, T-cells recognising MHC Class II molecules receive maturation signals from thymic cortical epithelial cells preventing expression of CD8 on the T-cell surface and develop CD4 T-cell characteristics (Shaffer et al., 2004, McCarthy et al., 2012). In addition to positive selection, TCRs which bind antigen with excessive or poor avidity will undergo negative selection. A TCR with high avidity has potential to recognise self-antigen and cause an autoimmune response, whereas a low avidity TCR will not initiate immune responses to foreign pathogens. The surviving T-cells migrate to the medulla to undergo another round of negative selection with dendritic cells and macrophages expressing self-antigen. The remaining selected T-cells, now naïve CD4 and CD8 T-cells leave the thymus.

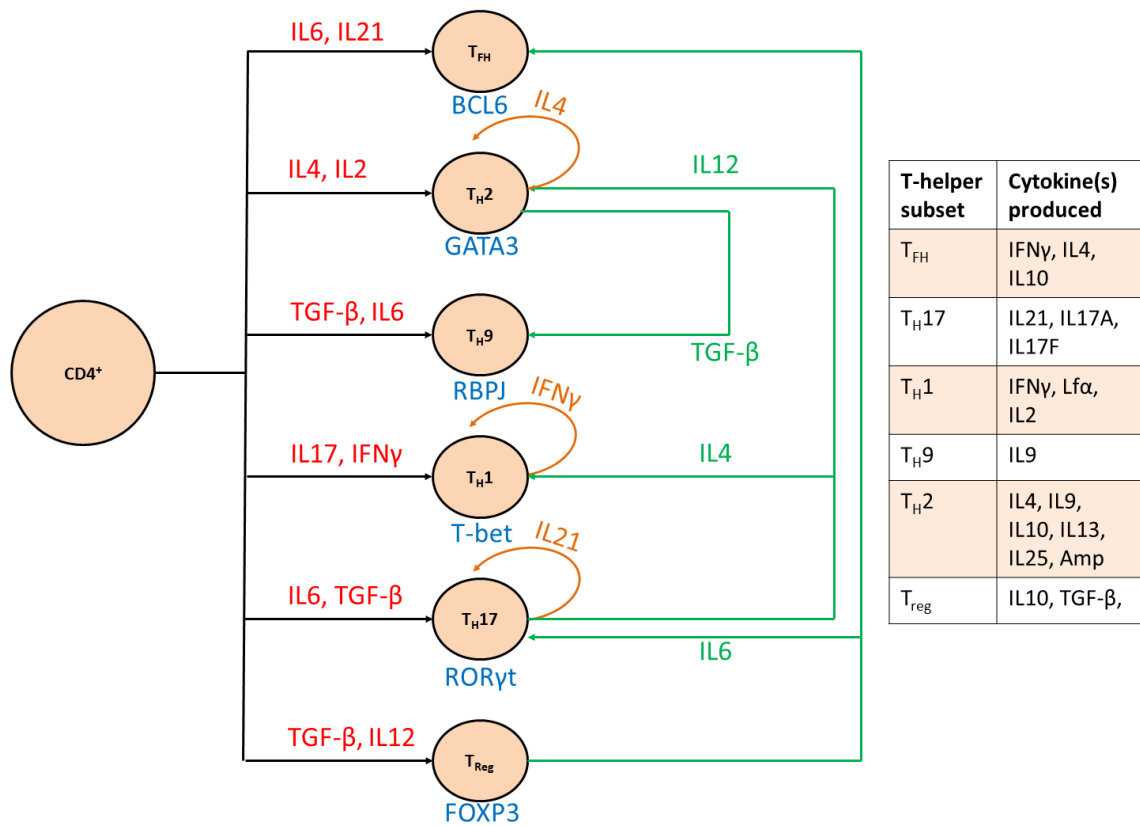


**Figure 1.5: Effect of cytokines upon the differentiation of CD4+ T-cells.**

Black arrows indicate the differentiation of the naïve CD4+ T-cell to the helper T-cell subsets in the presence of particular cytokines (red text). Orange arrows and text indicates the cytokine produced by the specific T-helper subset which promotes self-amplification. Blue text indicates the “master regulator” of each T-helper subset. Green arrows indicate the further differentiation T-helper cells can undergo when stimulated by specific cytokines (green text). Although the transcription factor, RBPJ, has been found to be upregulated in Th9 cells (van den Ham et al., 2010) it has not yet been verified as the regulator of Th9 cells.

phenotype (Luthje et al., 2012, Pepper et al., 2011, Hale et al., 2013). In another study, T<sub>H</sub>2 cells derived from mice infected with *N.brasiliensis*, transferred into an immunocompromised mouse recipient and rested for 30 days before reinfection with the parasite, were sufficient to clear infection (Zaph et al., 2006). Therefore, currently it is believed that T<sub>H</sub>1, T<sub>H</sub>2, and T<sub>FH</sub> cells are able to form long lived memory CD4<sup>+</sup> T-cells.

Naïve CD8<sup>+</sup> T-cells undergo a large proliferative stage upon detection of foreign antigen; this clonal expansion gives rise to differentiated CD8<sup>+</sup> T-cells which can either develop into cytotoxic T-cells with a short lifespan or longer-living memory T-cells. If another encounter with the corresponding antigen occurs, then memory cells can rapidly proliferate and differentiate into cytotoxic T-cells (Harty and Badovinac, 2008, Williams and Bevan, 2007) (figure 1.6).

Cytotoxic CD8<sup>+</sup> T cell populations are defined by the ability to secrete interferon- $\gamma$  (IFN $\gamma$ ) and to produce characteristic effector molecules used in cell lysis such as Granzyme B and Perforin (Belz and Kallies, 2010). Memory CD8<sup>+</sup> T cell populations, conversely, are divided into two subgroups, categorised by the expression of specific markers. The two groups are defined as Central memory T-cells (TCM) and Effector memory T-cells (TEM). TCM express high levels of the chemokine receptor, CCR7 as well as CD62L whereas TEM express these proteins at a lower level whilst producing cytokines and cytolytic molecules (Sallusto et al., 1999). Interestingly, TEM are very similar to cytotoxic CD8<sup>+</sup> T-cells in their features but differ in the ability to exist once foreign antigen has been removed (Gebhardt et al., 2009, Hikono et al., 2007). Therefore, it is generally accepted that TEM are the long-lived effector T-cells whilst TCM require further differentiation to achieve their cytotoxic potential, suggesting a longer-lived memory T-cell subset. The co-ordination of these cell types allows for an efficient defensive system against invading pathogens and facilitates a more effective clearance of the disease should it arise again.

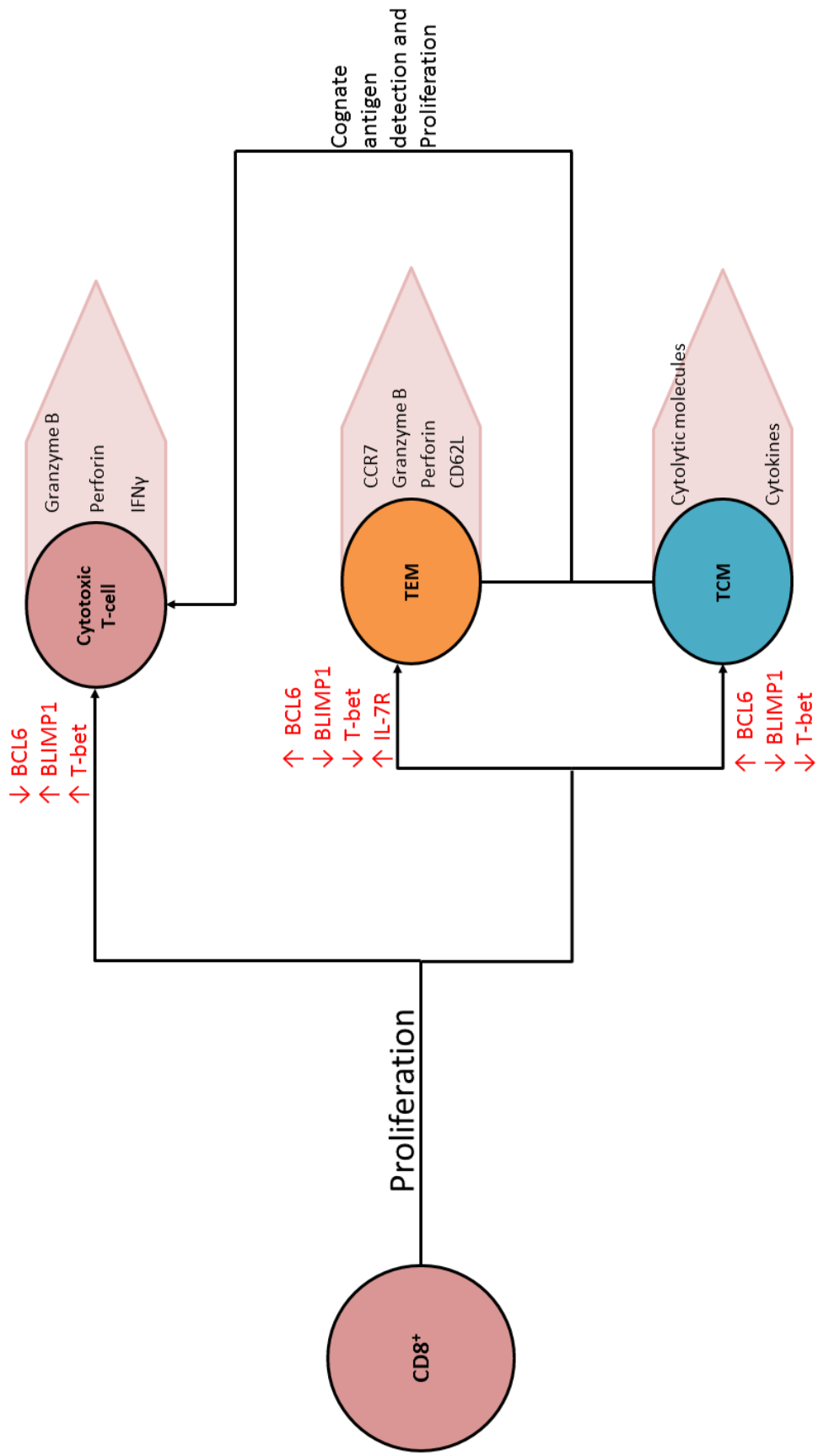


**Figure 1.6: Differentiation of CD8<sup>+</sup> T-cells**

TEM = Effector memory CD8<sup>+</sup> T-cell, TCM = Central memory CD8<sup>+</sup> T-cell. Black arrows indicate differentiation of naive CD8<sup>+</sup> T-cells in the presence of particular transcription factors (red text). Green arrow indicates the further differentiation of TEM and TCM in the presence of cognate antigen. Expressed molecules for each subtype are indicated in pink arrows. BCL6 and BLIMP1 transcription factors act antagonistically to one another to allow cellular differentiation.

## **1.2 Lymphoma**

Most cancers are believed to adhere to specific hallmarks outlined by Hanahan and Weinberg, namely: the ability to evade growth suppressors, ability to activate invasion and metastasise to other tissue types, to reproduce indefinitely, to induce angiogenesis, to escape cell death, and to sustain proliferation (Hanahan and Weinberg, 2000). Lymphomas are neoplasms of lymphoid cells which form solid tumours in lymph nodes or extranodal tissues and may be present as indolent or aggressive disease (Swerdlow et al., 2008). As lymphocytes circulate around the body, lymphomas do not necessarily need to acquire new invasive qualities. Like all cancers, lymphomas are genetic diseases, typically being caused by multiple genetic lesions such as translocations, point mutations, and deletions which target similar pathways. Generally, genetic lesions associated with lymphoma dysregulate genes involved in cancer hallmark pathways critical for lymphocyte development, proliferation, differentiation and survival.

According to the World Health Organisation (WHO) Classification of lymphomas, these neoplasms can be sub-divided into categories. Firstly, lymphomas are defined as Hodgkin or Non-Hodgkin Lymphoma (NHL), somewhat arbitrarily and based on the early historical characterisation of Hodgkin lymphoma defined by the presence of Reed-Sternberg cells, a multinucleated CD30+CD15+ B-cell (Kuppers et al., 2012). Non-Hodgkin lymphomas are then subdivided according to origin from B-cells or T/Natural-Killer (NK)-cells and subsequently sub-classified based upon clinical, pathologic and genetic features (Swerdlow et al., 2008). The incidence of each subclass can be found in figure 1.7.

### **1.3 B-cell Non-Hodgkin lymphoma**

The most common B-cell Non-Hodgkin Lymphomas (B-NHL) subtypes are Diffuse Large B-cell Lymphoma (DLBCL) and Follicular Lymphoma (FL). DLBCL accounts for approximately 30% of all NHL whilst FL also accounts for 30% of all NHL in the Western World (Ott and Rosenwald, 2008, Hartmann et al., 2008). Investigation into DLBCL through gene expression profiling has allowed further subdivision of the group. DLBCLs with strong expression of GC gene signatures are categorised into Germinal Center B-cell Diffuse Large B-cell Lymphoma (GCB-DLBCL), whilst those with gene signatures relating to activated B-cells give rise to lymphomas which resemble post-

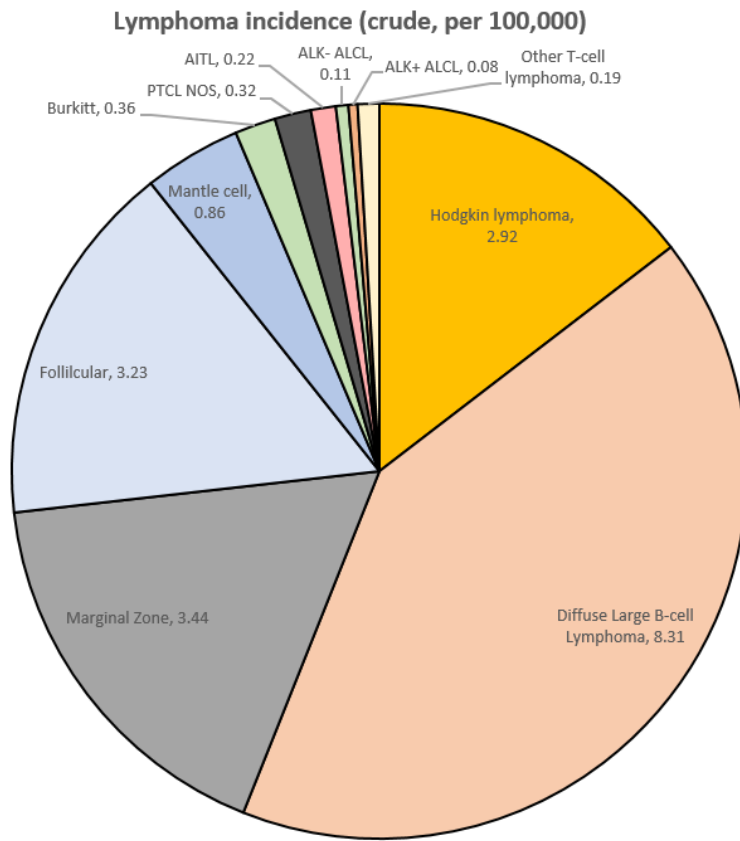


**Figure 1.7: Incidence of lymphomas (adapted from (Smith et al., 2015))**  
 Crude incidence of lymphoma subtypes per 100,000 people in the UK from data collected from the UK's Haematological Malignancy Research Network. PTCL NOS = Peripheral T-cell lymphoma, Not otherwise specified, AITL = Angioimmunoblastic T-cell lymphoma, ALK = Anaplastic Lymphoma Kinase, ALCL = Anaplastic Large Cell Lymphoma

germinal center B-cells, regarded as Activated B-cell Diffuse Large B-cell Lymphoma (ABC-DLBCL). Finally, a third group of DLBCL is defined as neoplasms arising from thymic B-cells and are termed Primary Mediastinal B-cell lymphoma (PMBL).

GCB-DLBCL typically exhibit amplifications of the *MIHG1* gene on chromosome 13, which harbours the *miR-17-92* microRNA, gains of a 7.6Mb region of 12q, and amplification of *REL* on chromosome 2, together with losses of *PTEN* on chromosome 10 by array CGH (Lenz et al., 2008b). ABC-DLBCLs are typically characterised by trisomy 3, gains of 18q and a 9Mb gain of 19q, as well as 6q losses and deletion of the *INK4 $\alpha$ /ARF* locus of 9p (Lenz et al., 2008b). PMBLs exhibit gains of 9p24 (encompassing the *JAK2* gene) and 20p as well as monosomy 10 (Lenz et al., 2008b). In addition, DLBCLs often carry translocations of *BCL2*, *c-MYC*, and/or *BCL6* singly, or in combination as aggressive “double-hit” or “triple-hit” (Snuderl et al., 2010). These translocations give rise to aberrant gene expression through promoter/enhancer substitution, often with immunoglobulin genes. *BCL6* (3q27) translocations have been reported to be present in 19.5% of DLBCL cases giving rise to constitutive expression of B-cell Lymphoma (BCL6) protein (Shustik et al., 2010). The t(14;18)(q32;q21) translocation involving *IGH* and *BCL2* is present in 10-40% of DLBCL cases (Tsujiimoto et al., 1985) whilst translocations involving *c-MYC* (8q24) are rarer, present in up to 14% of DLBCL cases (Barrans et al., 2010). *BCL6* is highly expressed in GCB-DLBCL, as the cell of origin naturally expresses high levels of *BCL6*, however translocations of *BCL6* occur in both GCB- and ABC-DLBCL (Thieblemont and Briere, 2013). *BCL6* may also be dysregulated in DLBCL by other means. Loss of 6q across DLBCL is of particular interest in this regard as this region contains *PRDM1*, the gene encoding B Lymphocyte-Induced Maturation Protein 1 (BLIMP1), a transcriptional repressor of *BCL6* (Bea et al., 2005). ABC-DLBCLs typically demonstrate high Nuclear Factor kappa-light-chain-enhancer of Activated B-cells (NF- $\kappa$ B) activation, in many cases brought about by constitutively active B-cell Receptor (BCR) signalling (Lenz et al., 2008a). In one study, approximately 10% of ABC-DLBCL and 4% of GCB-DLBCL harboured mutations in *CARD11*, a gene required for NF- $\kappa$ B transcription via BCR stimulation (Lenz et al., 2008a). In addition to *CARD11*, activating mutations in *MYD88*, *CD79A/B*, and inactivating mutations in *TNFAIP3* give rise to constitutive NF- $\kappa$ B activity in ABC-DLBCL (Pasqualucci and Dalla-Favera, 2014).

Generally, FL is a less-aggressive lymphoma than DLBCL but does have the ability to transform into a more aggressive lymphoma (Ott and Rosenwald, 2008). Approximately 80-90% of FL cases contain the t(14;18)(q32;q21) translocation juxtaposing *BCL2* with the *IGH* promoter region (Ott and Rosenwald, 2008). Despite this, published data suggests that the translocation alone is not sufficient to produce FL (Liu et al., 1994, McDonnell et al., 1989). Therefore, other genetic aberrations are believed to contribute to the transformation of these cells. The genetics of the disease are quite variable. A recent publication demonstrated, through use of whole-exome sequencing, that FL harbour genetic lesions such as copy number variations and single nucleotide mutations in genes required for apoptosis, chromatin remodelling, cell cycle and immune evasion such as *FAS*, *CREBBP*, *c-MYC*, *TP53*, and *B2M* (Pasqualucci et al., 2014).

#### **1.4 Peripheral T-cell lymphoma**

Peripheral T-cell lymphomas (PTCL) are neoplasms of NK cells or mature T-cells (either  $\alpha\beta$  or  $\gamma\delta$  T-cells) which account for approximately 12% of all non-Hodgkin Lymphoma (Piccaluga et al., 2011).

The World Health Organisation (WHO) classification of PTCL recognises a number of PTCL subtypes (figure 1.8A and 1.8B, (Swerdlow et al., 2008)), the most common of which are:

- PTCL not otherwise specified (PTCL-NOS)
- Angioimmunoblastic T cell Lymphoma (AITL)
- ALK+ (Anaplastic Lymphoma Kinase) Anaplastic Large Cell Lymphoma (ALCL)
- ALK- ALCL

These lymphomas are clinically, genetically and pathologically heterogeneous and, from a pathological perspective, are often difficult to classify. Clinical behaviour and prognosis of PTCL is highly variable but systemic (as opposed to cutaneous) PTCL are generally aggressive in nature as shown in figures 1.8C and 1.8D (Pileri and Piccaluga, 2012, Vose et al., 2008). Most systemic PTCL are initially treated with the same CHOP chemotherapy regimen (cyclophosphamide, doxorubicin, vincristine, prednisolone) but relapse is common and despite aggressive second-line chemotherapy treatment, long-

**A) Mature T-cell and NK-cell neoplasms**

- T-cell prolymphocytic leukemia
- T-cell large granular lymphocytic leukemia
- Chronic lymphoproliferative disorder of NK cells\*
- Aggressive NK cell leukemia
- Systemic EBV+ T-cell lymphoproliferative disease of childhood
- Hydroa vacciniforme-like lymphoma
- Adult T-cell leukemia/lymphoma
- Extranodal NK/T-cell lymphoma, nasal type
- Enteropathy-associated T-cell lymphoma
- Hepatosplenic T-cell lymphoma
- Subcutaneous panniculitis-like T-cell lymphoma
- Mycosis fungoides
- Sézary syndrome
- Primary cutaneous CD30+ T-cell lymphoproliferative disorders
  - Lymphomatoid papulosis
  - Primary cutaneous anaplastic large cell lymphoma
  - Primary cutaneous gamma-delta T-cell lymphoma
  - Primary cutaneous CD8+ aggressive epidermotropic cytotoxic T-cell lymphoma\*
  - Peripheral T-cell lymphoma, NOS
  - Angioimmunoblastic T-cell lymphoma
  - Anaplastic large cell lymphoma, ALK+
  - Anaplastic large cell lymphoma, ALK-\*

35

**B)**

**Prevalence of common PTCL types**

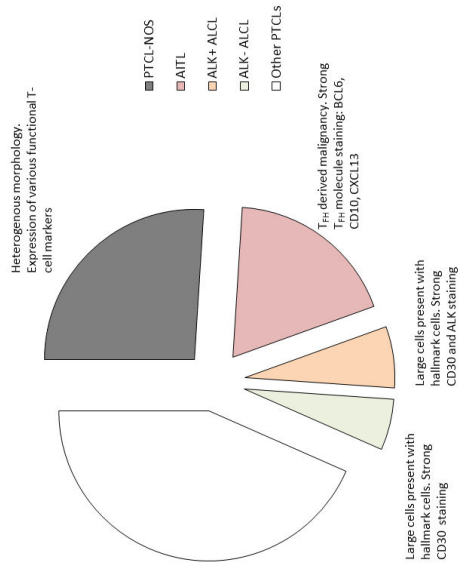


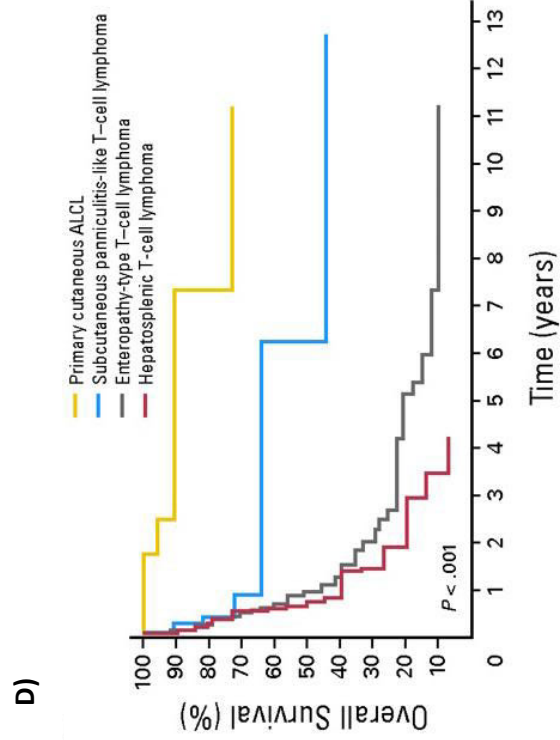
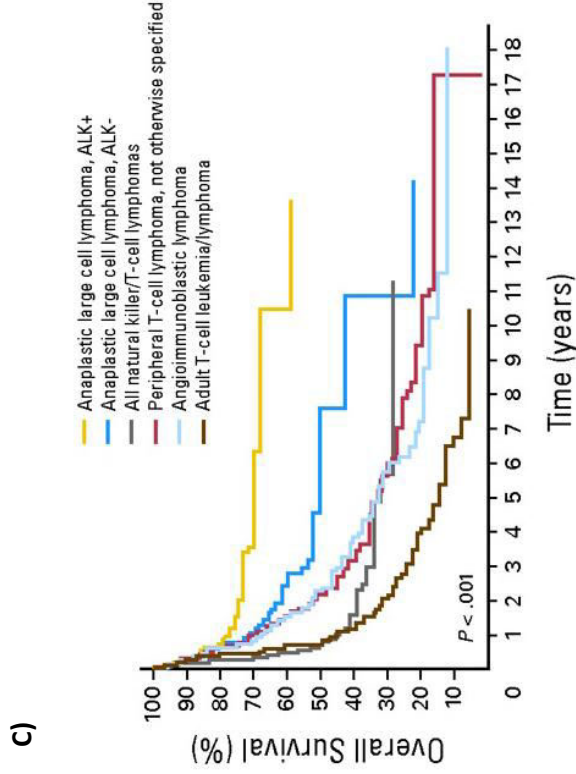
**Figure 1.8 Peripheral T-cell Lymphoma (adapted Swerdlow et al, 2008)**

A) WHO Classification of Peripheral T-cell Lymphoma. 2008 PTCL classification according to the WHO.

Entries marked with \* indicate provisional entries requiring additional evidence to be recognised as distinct diseases. B)

Prevalence of the four most common PTCL subtypes with histological markers identified. Histological features of each lymphoma subtype described next to each section. T<sub>FH</sub> = Follicular T-helper cell. C) and D) PTCL patient survival organised by subtype.

Overall survival of patients presenting with PTCL, most common C) and less common D). Patients presenting with ALK+ ALCL and Primary Cutaneous ALCL show good 5 year overall survival rates whilst ALK- ALCL and Subcutaneous panniculitis-like T-cell lymphoma present intermediate survival rates. Angioimmunoblastic T-cell lymphoma, Peripheral T-cell lymphoma, not otherwise specified, Natural killer/T-cell lymphoma, Enteropathy-type T-cell lymphoma, and Hepatosplenic T-cell lymphoma have a poor 5 year overall survival.



term disease-free survival is not achievable for most patients. Novel therapeutic approaches to the treatment of PTCL are desperately needed. Recently, the Histone Deacetylase (HDAC) inhibitors Belinostat and Romidepsin, and the antifolate agent Prelatraxate, have been approved for use for relapsed or refractory PTCLs due to the reasonable sensitivity to these drugs demonstrated in clinical trials (Bates et al., 2015, McDermott and Jimeno, 2014). It is unknown why PTCLs exhibit high sensitivity to HDAC inhibition as gene expression changes of PTCLs treated with these drugs vary widely between samples. However, down-regulation of the NF- $\kappa$ B pathway is present in many samples which could be indicative of potential mechanism of action (Bates et al., 2015).

#### **1.4.1 Peripheral T-cell Lymphoma – Not otherwise Specified**

PTCL-NOS are a group of mature T-cell lymphomas which do not show features of any other PTCL subgroup as defined by the WHO and are primarily nodal neoplasms (Vose et al., 2008). Typically, PTCL-NOS presents at a median age of 50-60 years with 50-70% of patients being male (Weisenburger et al., 2011, Schatz et al., 2015). The 5-year overall survival rate of PTCL-NOS is currently 30% (figure 1.8C) (Weisenburger et al., 2011). Of all PTCL-NOS patients, most receive combination chemotherapy with anthracycline treatment (80%) or combination chemotherapy without anthracycline (7%) (Weisenburger et al., 2011). However, studies have revealed no overall benefit to 5-year overall survival with the addition of anthracycline (Vose et al., 2008).

Until recently, the genetic changes underlying PTCL-NOS genetics have remained largely unknown but, in the last few years, studies have begun to identify recurrent alterations in the tumours. Studies have reported recurrent gains across 7q22-ter harbouring the *CDK6* gene and losses of 6q21, 9p21, and 17p13 regions encompassing *PRDM1*, *CDKN2A* and *CDKN2B*, and *TP53* tumour suppressor genes respectively (Fujiwara et al., 2008, Zettl et al., 2004).

Despite the low incidence of the t(5;9)(q33;q22) *SYK-ITK* translocation in PTCL-NOS (Streubel et al., 2006), it has been reported that expression of the proliferative gene, *SYK*, is high across PTCL-NOS presenting a potential therapeutic avenue for this group of lymphoma (Fujiwara et al., 2008). More recently, recurrent translocations involving *TP63* in PTCL-NOS have been identified (Vasmatzis et al., 2012). The clinical

relevance of this translocation is unknown to date, but it is currently believed to cause dysregulation of the P53 pathway in order to promote lymphomagenesis (Vasmatazis et al., 2012).

Mutations are common in PTCL-NOS and multiple studies have confirmed a number of mutated targets. In one study of 28 diagnostic PTCL-NOS, a novel set of recurrently mutated genes were found across multiple pathways (Schatz et al., 2015), most harboured mutations in one or more genes involved in epigenetic modification such as *TET1*, *TET2*, *MLL2*, *KDM6A*, *MLL*, and *CREBBP* (Schatz et al., 2015). Another study confirmed the presence of *TET2* mutations in 38% of PTCL-NOS cases (Palomero et al., 2014). In addition, recurrent frameshift/missense mutations in *DNMT3A* have been identified in 48.5% of PTCL-NOS (Sakata-Yanagimoto et al., 2014) and, in some rare cases, present simultaneously in *TET2*-mutated PTCL-NOS (Couronne et al., 2012). These mutations are believed to give rise to inactivation of both Tet methylcytosine dioxygenase (TET)2 and DNA (cytosine-5)-methyltransferase 3A (DNMT3A) as knock-out mouse studies have demonstrated that deficiency of both genes results in increased self-renewal capabilities of haematopoietic stem cells (Challen et al., 2012, Quivoron et al., 2011).

Recently the presence of a recurrent *RHOA* c.G50T gene mutation, giving rise to a Rho GTPase A (RHOA) G17V protein mutation, was identified in both AITL and PTCL-NOS. This mutation leads to inhibition of the  $\rho$ -signalling pathway as well as upregulation of the NF- $\kappa$ B, p38 mitogen-activated protein kinase, and mitogen-activated protein kinase kinase/extracellular signal-regulated kinase pathways (Palomero et al., 2014, Manso et al., 2014). The authors surmise that PTCL-NOS patients presenting with this mutation could benefit from NF- $\kappa$ B inhibitors. Another study demonstrated the presence of a recurrent *PLCG1* mutation, giving rise to a *PLCG1* S345F protein mutation, in PTCL-NOS (Manso et al., 2015). *PLCG*-mutated PTCL-NOS neoplasms exhibited lower overall survival rates compared to non-mutated counterparts. In addition, this mutation was associated with increased CD30-staining by immunohistochemistry (Manso et al., 2015). Therefore, it is believed that these tumours may benefit from CD30-targeted treatments.

### **1.4.2 Angioimmunoblastic T-cell lymphoma**

AITL is a lymphoma believed to be derived from follicular helper T-cells ( $T_{FH}$ ) based upon the expression of PD1, CXCL13, ICOS, CD57, CD10, BCL6 and other antigens similar to that of  $T_{FH}$  present in the germinal center (Piccaluga et al., 2007, de Leval et al., 2007, Grogg et al., 2007).

Patients presenting with AITL typically appear at a median age of 69 years with a 5-year overall survival rate of 33% (Xu and Liu, 2014). The treatment regimens for AITL are not standardised, as a result patients are treated with combination chemotherapy, steroids, or immunomodulators (Mosalpuria et al., 2014). However, AITL patient survival has not improved in the last 20 years (Xu and Liu, 2014).

Cytogenetic and SNP array analysis of AITL has demonstrated recurrent trisomies of chromosome 21 and 19, as well as gains of 5q, 11q13, 20q13, 22q, and 3q. In addition, recurrent losses of 6q, 13q22-q23, 8p22, and 9p21 were reported (Fujiwara et al., 2008, Lepretre et al., 2000, Nelson et al., 2008). Of particular interest is the loss of 9q21, harbouring the tumour suppressor gene *CDKN2A*, highlighting a potential mechanism of transformation of AITL (Fujiwara et al., 2008). AITL has been linked with viral associations which contribute to homeostasis of the AITL microenvironment. Epstein-Barr Viruses (EBV) are found in the B-cells of almost half of all AITL cases and, whilst the mechanism has not been defined, the viruses are believed to control cytokine/chemokine production (Foss et al., 2011).

Three independent gene expression studies of AITL have highlighted a set of genes involved in vascular biology as upregulated in AITL, most notably Vascular Endothelial Growth Factor (VEGF), which has been suggested to be a potential therapeutic avenue for AITL treatment (Piccaluga et al., 2007, Zhao et al., 2004, Iqbal et al., 2014).

Many mutations have been identified in AITL recently. One study demonstrated, through targeted sequencing of 219 candidate genes, that 76% of AITLs harboured mutations in *TET2*, 33% exhibited mutations in *DNMT3A*, and 20% exhibited mutations in *IDH2* (Odejide et al., 2014). Further, albeit less frequent, mutations were found in *TP53*, *CCND3*, *EP300*, *JAK2*, and *STAT3* (Odejide et al., 2014). As previously

Variant	Specific Histological Features
Common	Cohesive neoplastic cells found predominantly in lymph node sinuses
Giant-cell rich	Presence of large multi-nucleated cells with Reed-Sternberg characteristics
Hodgkin-like	CD30+ anaplastic cells surrounded by sclerotic bands, typically with ALK protein expression
Small-cell type	Variable neoplastic cell sizes with irregular nuclei, can contain sheets of CD30+ blasts
Lympho-histiocytic	Variable neoplastic cell sizes with irregular nuclei with abundance of reactive histiocytosis containing irregular nuclei

**Table 1.2: The Histological subgroups of ALCL as defined by the WHO Classification of Haematological Malignancies**

mentioned in PTCL-NOS, AITL also harbour mutations in *RHOA* although at a higher frequency. The most common mutation identified in *RHOA* is the RHO G17V mutation. Multiple studies have confirmed the presence of this mutation in AITL (Palomero et al., 2014, Sakata-Yanagimoto et al., 2014, Yoo et al., 2014). In normal T-cells, *RHOA* is required for T-cell migration and motility, as well as adhesion and cell-cell interactions (Heasman et al., 2010). Investigation into this mutation in AITL has revealed it exhibits a dominant-negative phenotype resulting in loss of *RHOA* function (Sakata-Yanagimoto et al., 2014, Yoo et al., 2014). This effect is believed to improve motility of the T<sub>FH</sub> cell to the follicular environment whereby it can drive proliferation (Ahearne et al., 2014).

### **1.4.3 Anaplastic Large Cell Lymphoma**

ALCL are tumours of large pleomorphic cells which express CD30 (previously termed Ki-1). Histologically, most ALCLs are defined by the presence of “hallmark” cells which have enlarged nuclei with a characteristic horseshoe shape (Swerdlow et al., 2008). However, the ALCL histotype encompasses multiple morphological variants: common, giant cell-rich, Hodgkin-like, small-cell type, and lympho-histiocytic defined in table 1.2 (Piccaluga et al., 2010).

Cumulatively, ALCL encompass 3 separate subgroups as defined by the WHO (Swerdlow et al., 2008):

- Systemic ALCL, divided into:
  - o ALK+ ALCL
  - o ALK- ALCL
- Primary Cutaneous Anaplastic Large Cell Lymphoma (C-ALCL)

Accounting for 10-15% of all paediatric NHL, systemic ALK+ ALCLs typically present at a median age of 10-11 years with a predominance towards males (Kinney et al., 2011). ALK- ALCLs are more common in adults, typically presenting at a median age of 40-65. Multiple studies have detailed the observation that the 5 year overall survival of ALCL varies between ALK+ (80%) and ALK- (48%) subgroups (Falini et al., 1999, Gascoyne et al., 1999, Lechner et al., 2012). The reason for the favourable prognosis of ALK+ ALCL is unclear, however it may be attributed to the younger age and relatively lower genetic complexity of ALK+ ALCL compared to ALK- ALCLs. Typically ALK+ ALCLs demonstrate few genetic lesions aside from the characteristic ALK translocation whilst ALK- ALCLs harbour lesions across multiple regions (Boi et al., 2013).

C-ALCL, conversely, present as nodular, often ulcerated, tumours of the skin which are typically CD30+ and granzyme B-positive but lack ALK expression, with a median age of 60 years (Stein et al., 2000, Su et al., 1997, Wood et al., 1996). C-ALCL accounts for approximately 9% of all cutaneous T-cell lymphoma (CTCL) and has a much better prognosis than systemic ALCL counterparts with a 5 year overall survival of 90-95% (Querfeld et al., 2010).

Patients presenting with systemic ALCL are typically given the standard combination chemotherapy, CHOP. Intensive chemotherapy in combination with stem-cell transplant may be prescribed for patients with a poorer prognosis (Armitage, 2012).

Despite being well studied, the cell-of-origin for ALCLs has not been elucidated. Independent of histological subtype, most ALCLs demonstrate strong expression of membranous CD30 (Falini et al., 1995, Gascoyne et al., 1999). CD30 is a 120kDa protein which is required for regulation of apoptosis and induction of NF- $\kappa$ B expression in activated B and T-cells (Wright et al., 2007). Expression of CD30 is not exclusive to ALCL however, with reported cases of DLBCL also expressing the glycoprotein (Piccaluga et al., 2010). Therefore, other common markers are used to distinguish ALCL such as granzyme B, perforin, and TIA-1 (Piccaluga et al., 2010).

Recent work has focused on profiling the molecular signature for ALCLs. Recently, two independent groups have attempted to define ALCL at the molecular level (Agnelli et al., 2012, Iqbal et al., 2014). Through gene expression profiling, ALCLs

demonstrate high expression of *CD30*, *BATF3* and *TMOD1* with low expression of T-cell receptor genes: *LCK*, *FYB*, and *CSK1* (Iqbal et al., 2014).

#### **1.4.3.1 Genetics of ALK+ ALCL**

Genetically, ALK+ ALCL typically exhibit gains of 12p and 17q24-qter, and losses of 4q13-q21 and 11q14 (Salaverria et al., 2008). However, the most common aberration is the *ALK* translocation. *ALK* is a gene, located at chromosome 2p23, that encodes a receptor tyrosine kinase of 177kDa which, after post-translational modifications, can increase to 220kDa in size (Stoica et al., 2001). *ALK* contains several domains: an extracellular ligand-binding domain, a transmembrane domain, and a cytoplasmic kinase catalytic domain (Stoica et al., 2001, Stoica et al., 2002). Part of the insulin-receptor superfamily, *ALK* shares homology with Leukocyte Tyrosine Kinase (LTK) (Stoica et al., 2001). The exact role of *ALK* in normal tissues has yet to be definitively identified but restricted expression of *ALK* in the nervous system during foetal development suggests a physiological role in this context. The putative *ALK* ligands Pleiotropin (PTN) and Midkine (MK) are similarly expressed in the foetal nervous system but specific interactions between *ALK* and these ligands in human cells has yet to be demonstrated (Moog-Lutz et al., 2005, Motegi et al., 2004, Mourali et al., 2006, Mathivet et al., 2007).

Recurrent translocations involving *ALK* were originally observed in the 1980s (Benz-Lemoine et al., 1988, Fischer et al., 1988) however the translocation partners were not identified until 1994 by two separate groups (Morris et al., 1994, Shiota et al., 1994). *ALK* translocations, producing *ALK* fusion genes have been observed across many types of cancer such as: Inflammatory Myofibroblastic Tumours, DLBCLs, Renal Medulla Carcinoma, Serous Ovarian Carcinoma, and non-small-cell lung cancer (NSCLC) (Hallberg and Palmer, 2013). The most common chromosomal translocation of *ALK* in ALCL, is the t(2;5)(p23;q35) accounting for up to 80% of all ALK+ ALCL cases (Amin and Lai, 2007, Stein et al., 2000). However, other translocation partners fusing to the 5' end of *ALK* have been identified including: *RNF213* (Cools et al., 2002), *ATIC* (Colleoni et al., 2000, Cools et al., 2002, Ma et al., 2000), *TFG* (Hernandez et al., 1999), *MSN* (Tort et al., 2001), *TPM3* (Lamant et al., 1999, Siebert et al., 1999), *TPM4* (Meech et al., 2001), *MYH9* (Lamant et al., 2003), and *CLTCL* (Touriol et al., 2000) (summarised in table 1.3). All *ALK* fusion genes share common features; each partner is highly expressed in

Gene name	Gene symbol	Translocation
Nucleophosmin	NPM	t(2;5)(p23;q35)
Ring finger protein 213	RNF213 (ALO17)	t(2;17)(p23;q25)
5-aminoimidazole-4-carboxamide ribonucleotide formyltransferase/IMP cyclohydrolase	ATIC	inv(2)(p23;q35)
TRK-fused gene	TFG	t(2;3)(p23;q21)
Moesin	MSN	t(2;X)(p23-q11-12)
Tropomyosin 3	TPM3	t(1;2)(p23;q35)
Tropomyosin 4	TPM4	t(2;19)(p23;p13.1)
Myosin Heavy Chain 9	MYH9	t(2;22)(p23;q11.2)
Clathrin Heavy Chain	CLTCL	t(2;17)(p23;q23)

**Table 1.3: Documented cases of translocations involving ALK in ALCL**

normal cells and is the cause of constitutive fusion gene expression. In addition partners contain, either complete or in part, an oligomerisation domain which is believed to mediate auto-associative interactions of ALK by mimicking ligand-mediated activation of the tyrosine kinase (Hernandez et al., 1999, Lamant et al., 1999, Lamant et al., 2003). Critically, each translocation also retains the complete tyrosine kinase domain of ALK.

Constitutively active, ligand-independent ALK, derived from fusion genes mediates its activity through a number of important signalling pathways. ALK interacts with the RAS-ERK, PI3K-AKT, and the Janus Kinase (JAK)-Signal Transducer and Activator of Transcription (STAT)3 pathways to promote expression of transcription factors involved in cellular growth, differentiation, and anti-apoptotic pathways such as Jun Proto-Oncogene (JUN)B, C/EBP $\beta$ , BCL2A1, MMP9, INK4A, and Hypoxia Inducible Factor 1a (HIF1A) (Hallberg and Palmer, 2013). Of particular interest is the JAK-STAT3 pathway, as this is believed to play a key role in survival of ALCL. STAT3 is activated through phosphorylation either by ALK directly, or via JAK3 signalling (Chiarle et al., 2008). Activated STAT3 induces the expression of many targets, most importantly *BCL6*, *IRF4*, *PRDM1 $\alpha$* , *BCL2*, *BCL-XL*, *C/EBP $\beta$* , *Survivin*, and *MCL1* (Chiarle et al., 2008, Kwon et al., 2009, Walker et al., 2013). In agreement with this, ChIP-Seq analysis of phosphorylated STAT3 (p-STAT3) demonstrates binding to *BCL6* in the breast cancer cell line, SK-BR-3, resulting in increased expression of *BCL6* mRNA (Walker et al., 2013). Furthermore, knockout of *Irf4* in normal murine T-cells abolishes a STAT3-dependent *PRDM1* luciferase reporter construct signal compared to wild-type controls suggesting Interferon Regulatory Factor (IRF)4 is also a direct p-STAT3 target (Zamo et al., 2002).

Taken together these data, with the observation that p-STAT3 is highly expressed in ALK+ ALCLs (Khoury et al., 2003, Zamo et al., 2002), suggests that STAT3 is vital for cellular survival and presents an attractive therapeutic target for ALK+ ALCLs.

Inhibition of ALK as a therapeutic avenue has gained popularity in recent years due to the large spectra of cancers which harbour an ALK translocation. The only Food and Drug Administration approved drugs currently available for ALK are Crizotinib and Ceritinib. Crizotinib is a dual ALK and c-Met inhibitor which is approved for use in NSCLC patients harbouring an ALK translocation (Sahu et al., 2013). Crizotinib and Ceritinib can bind ALK and inhibit the phosphorylation of the tyrosine kinase (Cui et al., 2011, Sahu et al., 2013, Friboulet et al., 2014). Recently, Crizotinib has entered clinical trials for treatment of patients with relapsed or refractory ALCL (Mosse et al., 2013). Despite initial good response for patients, there is worry that resistant-forms of the cancer will arise with prolonged treatment. One study demonstrated the generation of resistance to Crizotinib *in vitro* by subjecting Karpas-299 cells to low levels of drug (Zdzalik et al., 2014). Interestingly, sequencing of the resistant Karpas-299 cells revealed an activating ALK mutation, specifically I1171T, which was believed to confer resistance (Zdzalik et al., 2014). Another study performed sequencing of *NPM-ALK* gene mutations in ALK+ ALCL tumours which received standard chemotherapy regimens and detected two missense mutations in the gene across the ALCL tumour panel (Lovisa et al., 2015). The mutations detected in this study however, did not result in activation of ALK. The c.872G>A (corresponding to a R291Q protein mutation) resulted in autophosphorylation of NPM-ALK, comparable to wild-type NPM-ALK, when introduced into HEK-293T cells (Lovisa et al., 2015). However the second mutation detected, c.1004G>A (corresponding to a R335Q protein mutation), markedly reduced NPM-ALK autophosphorylation as well as STAT3 phosphorylation and resulted in increased sensitivity to Crizotinib (Lovisa et al., 2015). However, in other ALK-driven malignancies such as Neuroblastoma as well as accelerated mutagenesis screens, activating ALK mutations have been detected which confer resistance to Crizotinib (Bresler et al., 2011, Zhang et al., 2011). Therefore taken together, these studies demonstrate that, although rare, mutations in *NPM-ALK* are a possibility in ALK+ ALCLs and therefore novel therapeutic alternatives are required. Currently, novel inhibitors

of ALK, HSP90, or mTOR are under investigation to attempt to overcome resistance (Zdzalik et al., 2014).

Specific gene signatures have been defined for ALK+ and ALK- ALCLs from gene expression profiling. According to one study, ALK+ ALCLs are enriched for gene signatures involved in cellular proliferation and survival, such as HIF1A, Interleukin (IL)-10, and K-RAS target genes compared to ALK- ALCLs (Iqbal et al., 2014). Previously published data from this group also revealed that ALK+ ALCLs are enriched for cytokine signalling regulators of *STAT3*, *IL-26* and *IL-31R* (Iqbal et al., 2010). Other gene expression profiling studies have found that *BCL6*, *PTPN12*, *CEBPB*, *SERPINA1* and *GAS* are overexpressed in ALK+ ALCL. In addition, ALK+ ALCLs demonstrated high levels of BCL6, C/EBPbeta, and SERPINA1 protein by tissue microarray staining (Lamant et al., 2007). Another independent study has demonstrated that ALK+ ALCLs also over-express signal transduction molecules such as SYK, LYN, and CDC37 (Thompson et al., 2005).

In addition to changes in protein-coding genes, microRNAs have now been implicated in the pathogenesis of many malignancies. MicroRNAs are important for normal T-cell development as well as regulation of cancer biology. These RNAs bind to processed mRNA and lead to the degradation or inhibition of translation (Lawrie, 2013). Recently, through use of a transgenic-ALK mouse models in combination with primary ALCL tumours, microRNA profiles for ALCL have been established (Merkel et al., 2010). Specifically, ALK+ ALCLs express high levels of different *miR-17-92* cluster members: *miR-20b*, *miR106a*, *miR-20a*, *miR-886-3p*, and *miR-17* (Merkel et al., 2010). Common to both ALCL subgroups, *miR-101* is downregulated and, interestingly over-expression of the microRNA in ALK+ ALCL cells reduced proliferation of these cells (Merkel et al., 2010). In addition, a separate independent study also revealed that ALK+ ALCLs down-regulate *miR15A/16-1*, which is known to regulate HIF1A and VEGF expression in ALCL (Dejean et al., 2011).

As a whole, these data highlight the common gene expression and microRNA alterations that occur across ALCL suggesting that ALCLs may share a common precursor. Important variances between gene expression profiles of the subsets would

not only allow tailored treatment but highlight the differences in transforming mechanism.

#### **1.4.3.2 Genetics of ALK- ALCL**

ALK- ALCLs are genetically less well characterised than ALK+ ALCLs, but by definition they lack the ALK translocation (Swerdlow et al., 2008). ALK- ALCLs typically exhibit gains of 1q and 6p21 as well as losses of 17p13 and 6q21 (encompassing *TP53* and *PRDM1* respectively) (Boi et al., 2013, Zettl et al., 2004).

Translocations have been observed in a small number of ALK- and c-ALCL cases, specifically the t(6;7)(p25.3;q32.3) translocation involving *DUSP22* and *IRF4* leading to downregulation of *DUSP22* mRNA expression (Feldman et al., 2011). The clinical relevance of this lesion has yet to be determined, but those harbouring the translocation exhibit an overall survival rate of 90%, higher than the average for ALK- ALCLs (Parrilla Castellar et al., 2014). Another exclusive ALK- ALCL rearrangement involving the *TP63* gene has also been identified. In this study, it was revealed that *TP63* rearrangements give rise to fusion proteins homologous to a dominant-negative form of P63 ( $\Delta$ NP63) which is believed to be oncogenic (Vasmatazis et al., 2012). The most common translocation partner was *TBL1XR1*. The study also revealed that *TP63* rearranged neoplasms resulted in significantly lower overall survival rates than non-rearranged counterparts (Vasmatazis et al., 2012).

A transcriptional profiling meta-analysis of 309 PTCLs has identified a number of genes which allow specific identification of ALK- ALCL from other PTCL. In this study, ALK- ALCL is defined by expression of *TNFRSF8*, *BATF3*, *TMOD1*, *TMEM158*, *MSC* and *POPDC3* (Agnelli et al., 2012). Further gene signature studies have allowed the reclassification of some PTCL-NOS as ALK- ALCL. In one study, ALK- ALCLs exhibit enriched expression of c-Myelocytomatosis Viral oncogene (c-MYC) and *IRF4* gene signatures compared to PTCL-NOS (Iqbal et al., 2014). Other studies have demonstrated that ALK- ALCLs overexpress *CCR7*, *CNTFR*, *IL-22*, and *IL-10* (Lamant et al., 2007, Piva et al., 2010), as well as the anti-apoptotic proteins *BCL2*, *BIC*, and *BIRC6* (Thompson et al., 2005).

Whole exome sequencing of ALK- ALCL has revealed the sub-group exhibits recurrent activating mutations of *JAK1* and *STAT3* genes and inactivating mutations of

*PRDM1*, *TP53*, and *CSMD2* (Crescenzo et al., 2015). In this study, mutations in *STAT3* clustered in the SH2 domain whilst *JAK1* mutations clustered primarily in the kinase domain. Recurrent missense mutations of *STAT3* included Y640F, N647I, D661Y, and A662V. The result of these mutations is constitutive activation of the *JAK/STAT3* pathway with p-*STAT3* levels comparable to ALK+ ALCL (Crescenzo et al., 2015). This mechanism is believed to be oncogenic for ALK- ALCL. Furthermore, cell lines harbouring these mutations exhibited reduced cellular growth upon *JAK/STAT3* pathway inhibition (Crescenzo et al., 2015).

MicroRNAs are also believed to play a key role in ALK- ALCLs as overexpression of *miR155* is present in these lymphomas (Merkel et al., 2010). Further investigation into *miR155* demonstrated that the microRNA is specifically oncogenic in ALK- ALCL (Merkel et al., 2015). In this study, high levels of promoter methylation were detected in ALK+ ALCL cell lines compared to ALK- ALCL and resulted in low expression of *miR155*. Furthermore, subcutaneous injection of Mac1 and Mac2a ALK- ALCL cell lines, transfected with *pre-miR155* RNA, into mice resulted in increased tumour growth compared to controls (Merkel et al., 2015). Thus, *miR155* is deemed important for ALK- ALCL proliferation. In addition, a specific microRNA signature consisting of 4 upregulated microRNAs: *miR-210*, *miR-197*, *miR-191*, and *miR-512-3p* and 7 downregulated microRNAs: *miR-451*, *miR-22*, *miR-146a*, *miR455-3p*, *miR455-5p*, *miR-494*, and *miR-143* has been identified to allow delineation of ALK- ALCL from other PTCLs (Liu et al., 2013).

## 1.5 B-cell Lymphoma 6 (BCL6)

### 1.5.1 BCL6 Structure

*BCL6* is a gene, located at chromosome 3q27, which encodes a zinc finger transcriptional repressor (figure 1.9A). *BCL6* encodes three transcripts, two of which produce the full-length BCL6 protein whilst the third encodes a truncated form of the protein (BCL6S) lacking exon 7, encoding the RD2 domain (Shen et al., 2008). The BCL6 protein comprises three main domains: the C-terminal zinc finger domain, the RD2 domain, and the N-terminal POZ/BTB domain. The zinc finger domain comprises six zinc fingers which facilitate precise binding to BCL6 binding motifs (core sequence TTCCTA/CCGGA) within the regulatory regions of BCL6 target genes. The role of the RD2 domain has only recently been discovered and is currently believed to involve repressive activity of specific target genes, which allows progression through GC B-cell development. The RD2 domain interacts with HDAC2, MTA3/NuRD complex, as well as CtBP (Bereshchenko et al., 2002, Fujita et al., 2004, Huang et al., 2014, Mendez et al., 2008). By recruiting HDAC2, gene transcription of targets such as: *EBI2*, *S1PR1*, and *S1PR2* are silenced (Huang et al., 2014). The POZ/BTB domain is vital to allow BCL6 to form homodimers and heterodimers with other POZ/BTB domain-containing transcription factors such as Myc-Interacting Zinc Finger Protein-1 (MIZ-1) and

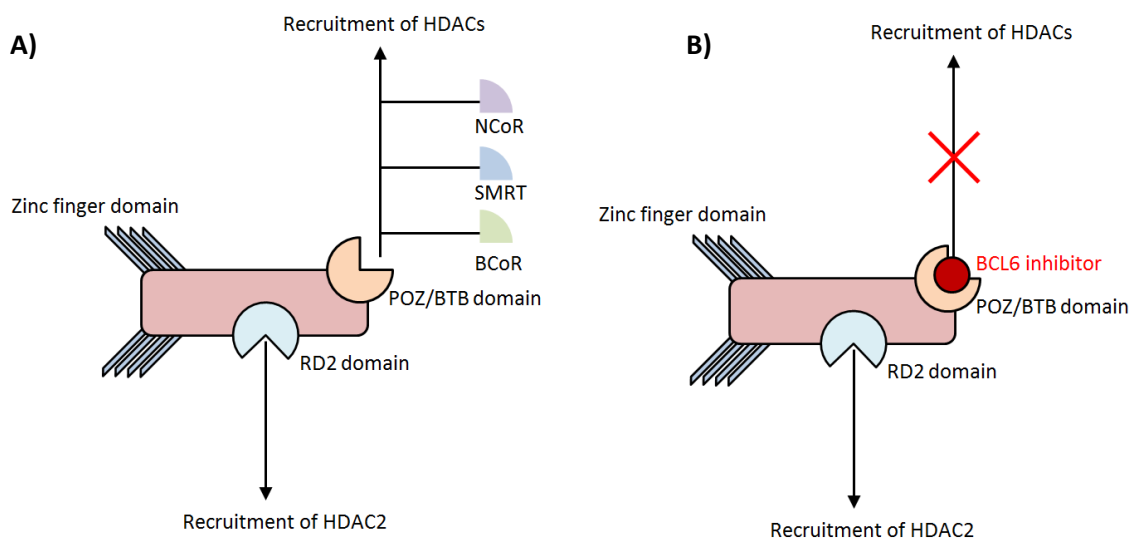


**Figure 1.9: Structure of BCL6 and the effect of inhibitors on the protein function**

A) Structure of BCL6 protein with binding partners. B) Mechanism of BCL6 inhibition. All available BCL6 inhibitors, 79-6, RI-BPI, Rifamycin SV, and Apt48 bind and prevent interactions of the POZ/BTB domain with co-repressor molecules rendering the repressive activity of domain non-functional.

Promyelocytic Leukaemia Zinc Finger (PLZF) (Dhordain et al., 2000, Phan et al., 2005). The formation of these complexes creates 2 lateral grooves through which, the domain recruits co-repressor molecules such as BCL6 Corepressor (BCoR), Nuclear receptor corepressor (NCoR), and Silencing mediator for retinoid and thyroid hormone receptors (SMRT), amongst others, to facilitate the recruitment of HDACs to target genes and thereby effect transcriptional repression (Ahmad et al., 2003, Dhordain et al., 1997, Dhordain et al., 1998, Huynh et al., 2000). For example, when BCoR interacts with the BCL6 BTB domain, it can create characteristic repression complexes with both class I and class II HDACs that allow histone deacetylation and ultimately silencing of genes (Huynh et al., 2000, Polo et al., 2004). All three co-repressor proteins bind the lateral groove via a BCL6 binding domain (BBD). The BBD domain of SMRT and BCoR share high homology with only 3/17 residues differing between the molecules whereas BCoR possess low homology, harbouring a completely different sequence (Ahmad et al., 2003, Ghetu et al., 2008).

Genetically, *BCL6* contains an autoregulatory binding site within the first exon of the gene which allows suppression of its own transcription (Kikuchi et al., 2000, Pasqualucci et al., 2003). This occurs via recruitment of CtBP and, subsequently, the corepressor Zinc finger E-box binding homeobox 1 (ZEB1) to this site (Mendez et al., 2008, Papadopoulou et al., 2010). Other *BCL6* regulatory elements have been detected upstream of the transcription start site (Tang et al., 2002) and, more recently, in intron 1 of the *BCL6* gene, which can be bound by CCCTC-binding factor (CTCF) (Kikuchi et al., 2000, Saito et al., 2007, Batlle-Lopez et al., 2015).

Post-translational modifications of BCL6 are also utilised to regulate BCL6 activity. Phosphorylation of BCL6 by Mitogen-Activated Protein Kinase (MAPK) pathways results in degradation of the transcription factor, whilst BCL6 can also be targeted for ubiquitination directly by F-box protein 11 (FBX011) (Niu et al., 1998, Saito et al., 2007, Duan et al., 2012). The PEST domain overlapping the RD2 domain of BCL6 can also undergo p300-mediated acetylation resulting in inactivation of transcriptional suppressive activity by blocking HDAC association (Bereshchenko et al., 2002).

### 1.5.2 BCL6 in B-cells

With the introduction of gene expression profiling it has been possible to investigate in detail the expression and activity of BCL6 in B-cells. This technology has led to the discovery that BCL6 suppresses genes involved in lymphocyte activation, differentiation, and apoptosis by recruiting HDACs to silence target genes (Shaffer et al., 2012).

Although not fully elucidated, expression of BCL6 is believed to be initiated by MEF2B, IRF8, and IRF4 within naïve B-cells interacting with T-cells and antigen (Basso and Dalla-Favera, 2015). At the centroblast stage of lymphocyte development, BCL6 fine-tunes its own expression via an autoregulatory mechanism (Pasqualucci et al., 2003, Mendez et al., 2008) and inhibits differentiation of the GC B-cells through interaction with other transcription factors (figure 1.4A) (Saito et al., 2007). In addition, BCL6 blocks the expression of inflammation genes such as *IL-10*, *CCL3* and *STAT1* (Barish et al., 2010, Toney et al., 2000); this may also explain why *BCL6* deficient mice in these studies developed fatal inflammatory diseases.

BCL6 is critical for GC-formation. BCL6 mutant mice, expressing a truncated form of BCL6 which lacks DNA-binding activity, displayed a failure to form germinal centres during a T-cell-dependent immune response and developed a fatal systemic inflammatory disease characterised by the presence of T<sub>H</sub>2 cells (Dent et al., 1997, Ye et al., 1997). Recently, the RD2 domain of BCL6 has shown to be important in early GC-cell development (Huang et al., 2014). The domain has been demonstrated to directly bind the co-repressor MTA3 via coimmunoprecipitation assays (Bereshchenko et al., 2002, Fujita et al., 2004, Huang et al., 2014) and exert repressive functions on target genes through recruitment of HDAC2 (Huang et al., 2014). Mutation of a critical lysine residue in the RD2 domain abolishes this repressive activity resulting in aberrant GC B-cell formation (Huang et al., 2014). In addition, RD2-mutant mice failed to produce detectable levels of GC B-cells after immunisation with Sheep Red Blood Cells (SRBCs) (Huang et al., 2014).

Genomic instability is believed to be maintained by BCL6 activation due to repression of specific B-cell targets in GC B-cells. It is believed that in order for GC B-cells to tolerate the high rates of DNA damage brought about by CSR and SHM, BCL6

represses genes encoding regulators of the DNA damage response (namely *TP53*, *ATR*, *CHEK1*, *GADD45A*, *PC4* as well as CDK inhibitors *P21* and *P27KIP1*) (Phan and Dalla-Favera, 2004, Ranuncolo et al., 2008a, Ranuncolo et al., 2008b). In particular, the interactions between Tumour Promoter 53 (TP53) and BCL6 are important. TP53 requires suppression by BCL6 in GC B-cells as the TP53 pathway would induce apoptosis due to the large-scale genomic aberrations occurring from SHM. Interestingly, the pathways involved in activation of TP53 as a transcription factor (ATM-mediated phosphorylation and PIN1 interactions) are important for the degradation of BCL6 (Phan et al., 2007, Zacchi et al., 2002, Zheng et al., 2002). The actions of these pathways may help to ensure that healthy B-cell proliferation and cell death is controlled and that constitutive BCL6 expression does not result in tumorigenesis.

BCL6 facilitates cell-cycle progression by repressing inhibitors of cyclin dependent kinases (CDKs) such as P21 and P27KIP1 (Phan et al., 2005, Shaffer et al., 2000). Cell cycle progression is key for GC B-cells to allow rapid proliferation and expansion of centroblasts before migration and selection.

A well-established target of BCL6 is BLIMP1 and interactions between the transcription factors have been studied extensively. BCL6 prevents plasma cell differentiation through inhibition of *PRDM1* (figure 1.4A). Initially, it was shown, using DNaseI footprinting that *PRDM1* contained two binding sites for BCL6 (Tunyaplin et al., 2004) and that there was a two-fold increase in the number of antibody secreting cells (a characteristic of BLIMP1 expression) in *Bcl6*<sup>-/-</sup> mice compared to *Bcl6*<sup>+/-</sup> controls, suggesting that expression of the *PRDM1* gene was repressed by BCL6. Further studies have confirmed the antagonistic interactions between BLIMP1 and BCL6 (Cimmino et al., 2008, Crotty et al., 2010, Shaffer et al., 2002, Shaffer et al., 2012, Shapiro-Shelef and Calame, 2005, Tunyaplin et al., 2004, Alinikula et al., 2011, Basso et al., 2010). Although it has been postulated that BCL6 may bind and repress *PRDM1* directly, other studies have suggested alternate mechanisms (Alinikula et al., 2011, Basso et al., 2010). One study found, through CHIP-on-CHIP screening, that *PRDM1* was not the sole BCL6 target gene (Basso et al., 2010). In agreement with this, another study (Alinikula et al., 2011) found that BCL6 exerts its effects indirectly on *PRDM1* through activation of BACH2 (basic region-leucine zipper (bZip) factor BTB and CNC homology 2) and MITF

(microphthalmia-associated transcription factor) in DT40 cells. BACH2 has been found to inactivate BLIMP1 expression via interaction with two Maf Recognition Elements (MARE-elements) present on the *PRDM1* gene (Ochiai et al., 2006). MITF has also been found to inactivate IRF4 (Lin et al., 2004). It is for these reasons that BCL6 is believed to repress BLIMP1 activity by a number of pathways: by directly repressing the transcription of *PRDM1*, by increasing inhibition of *PRDM1* via BACH2 expression, and by repressing activators of *PRDM1*, such as IRF4, through MITF expression. More recent studies into BCL6-BACH2 interactions have suggested the dependency of BACH2 on BCL6 for BLIMP1 $\alpha$  inhibition (Huang et al., 2013a). In this study, through ChIP-Seq *PRDM1 $\alpha$* , but not *PRDM1 $\beta$* , binding sites of BCL6 and BACH2 overlapped in the DLBCL cell line OCI-Ly7. Furthermore, knockdown of each protein individually caused increased levels of *BLIMP1* mRNA with further increase in a double knockdown (Huang et al., 2013a). The authors suggest BACH2 protein may recruit BCL6, or vice versa, allowing repressive activity on *PRDM1 $\alpha$* , whereas *PRDM1 $\beta$*  may be inhibited by BCL6 alone.

### **1.5.3 BCL6 in B-cell lymphoma**

BCL6 plays a central role in the pathogenesis of several types of B-cell lymphoma (Basso and Dalla-Favera, 2012, Shaffer et al., 2012, Shaffer et al., 2000). The proto-oncogene was first identified as the target of chromosome 3q27 translocation, which is found in approximately 40% of all Diffuse Large B-cell Lymphoma (DLBCL) (Ye et al., 1993, Butler et al., 2002). In addition, BCL6 was found to be highly expressed in germinal center B-cells (Cattoretti et al., 1995). This suggested that B-cell lymphomas derived from germinal centers may in fact be a result of aberrant BCL6 expression. BCL6 translocations are associated with the *Ig* loci in approximately 50% of all B-cell cases, with 75% of these locating to the *Ig* heavy chain locus (Akasaka et al., 2000), as well as non-*Ig* loci (such as the *IL-21* locus) in approximately 40% of B-cell cases (Ueda et al., 2002). *BCL6* translocations cluster in the 5'UTR of the gene resulting in the substitution of the *BCL6* promoter region, causing subsequent overexpression of the gene (Butler et al., 2002, Ye et al., 1997, Chen et al., 1998). In addition, studies into *BCL6* translocations revealed that the event leads to loss of autoregulation by BCL6, as well as regulation by other targets by disruption of the promoter binding site (Gearhart et al., 2006, Mendez et al., 2008).

In addition to translocations, the *BCL6* promoter region undergoes SHM to dysregulate *BCL6* regulation. The *BCL6* exon 1 region and the 696 base pair sequence downstream is subject to SHM in normal GC B-cells, however the majority of mutations do not cause alteration in transcriptional activity (Zan et al., 2000). One study demonstrated that introduction of GC B-cell-generated *BCL6* mutants, harbouring mutations in the *BCL6* regulatory region present within exon 1 of *BCL6*, into DLBCL cell lines gave rise to increased expression of *BCL6* mRNA which was not found in BL, FL, or B-cell chronic lymphocytic leukaemia (Pasqualucci et al., 2003). In agreement with this, a second independent study demonstrated that introduction of *BCL6* constructs, lacking the DNA-binding domain, into mice deficient in *BCL6* protein resulted in marked increase in *BCL6* mRNA levels compared to full-length counterparts (Wang et al., 2002). Furthermore, approximately 15% of DLBCL harbour mutations in *BCL6* in this autoregulatory sequence. Collectively, these data demonstrate that *BCL6* can escape autoregulation via SHM of its own regulatory elements during the GC B-cell reaction.

*BCL6* is also dysregulated in B-cell lymphoma through inactivation of histone acetyltransferases (HATs). One study demonstrated, by ChIP analysis, that the p300 lysine acetyltransferase gene (*EP300*) and its cofactors gene, HLA-B-associated transcript 3 (*BAT-3*), are physically bound by *BCL6* (Cerchietti et al., 2010b). Furthermore, inhibition of *BCL6* via a peptide inhibitor, resulted in increased lysine-acetyltransferase activity of P300 in DLBCL cell lines as well as increase *EP300* and *CREBBP* mRNA levels suggesting *BCL6* repressed *EP300* and CREB-binding protein (*CREBBP*) acetyltransferase activity (Cerchietti et al., 2010b). Importantly, P300-mediated acetylation of heat-shock protein 90 (HSP90) regulates its chaperone activity (McClellan et al., 2007). In normal GC B-cells, *CREBBP* acetylates and subsequently inactivates *BCL6* (Andersen et al., 2012). Thus, it is currently hypothesised that *BCL6* maintains HSP90 activity via inhibition of P300-mediated acetylation as well as downregulating *CREBBP* expression to promote survival (Cerchietti et al., 2010b, Andersen et al., 2012).

In B-cell biology orphan F-box protein (*FBXO11*) is required for *BCL6* ubiquitylation and degradation, however in DLBCL inactivating mutations or deletions of *FBXO11* are present (Duan et al., 2012). In one study, deletions/mutations of

*FBXO11* in DLBCL cell lines exhibited greater stability of BCL6 protein levels (Duan et al., 2012). Furthermore, introduction of *FBXO11* into *FBXO11*-null cells resulted in ubiquitylation and degradation of BCL6 (Duan et al., 2012). Therefore, BCL6 expression and stability is believed to be maintained in some DLBCL via *FBXO11* inactivation.

Normal BCL6 functions allow for cancer development. For example, aberrant constitutive activation of BCL6 facilitates survival and proliferation of cancerous cells, genomic instability, and the blocking of GC B-cell differentiation through repression of *PRDM1*, in DLBCL (Shaffer et al., 2000). Furthermore, transgenic mice mimicking a t(3;14)(q27;q32) translocation, common to human DLBCL, facilitates production of B-cell and T-cell lymphomas and upon administration of N-ethyl-N-nitrosourea caused a marked increase in the incidence of T-cell lymphomas (Baron et al., 2004).

In recent years several inhibitors of BCL6 have been created, a synthetic peptide inhibitor (Cerchietti et al., 2009), a peptide aptamer (Chattopadhyay et al., 2006), and a small molecular inhibitor (Cerchietti et al., 2010a). These inhibitors rely on specifically binding and blocking the BTB domain of the BCL6 protein (figure 1.8B), preventing the recruitment of co-repressors mandatory for biological activity (Ahmad et al., 2003, Cerchietti et al., 2010a, Cerchietti et al., 2010b, Cerchietti et al., 2009). Retro-inverted BCL6 peptide inhibitor (RI-BPI) is a 41 amino acid long peptide designed specifically to target the lateral groove of the BCL6 BTB/POZ domain (Cerchietti et al., 2009). The inhibitor was able to induce apoptosis in DLBCL cell lines and primary DLBCL patient samples *in vitro* (Cerchietti et al., 2009, Cerchietti et al., 2010b, Polo et al., 2004), and in addition could reduce the proliferation of xenografted DLBCL cell lines, SUDHL4 and SUDHL6, in SCID mice with no obvious side effects (Cerchietti et al., 2009, Cerchietti et al., 2010b). The small molecular inhibitor, 79-6, was also shown to selectively kill “BCL6-dependent” DLBCL cell lines and administration at low concentrations upregulated a number of known BCL6 target genes in “BCL6-dependent” DLBCL cell lines SUDHL4 and SUDHL6 but not in the “BCL6-independent” cell line Toledo (Cerchietti et al., 2010a). Another BCL6 inhibitor is a peptide aptamer (Apt48), produced from a library of randomly generated peptides and able to bind the BCL6 BTB/POZ domain in a manner distinct from the BCL6-SMRT interaction (Chattopadhyay et al., 2006). Specifically, this peptide could even bind a mutated BTB/POZ domain which could not be bound by SMRT. In addition, treatment of cell

lines *in vitro* with Apt48 lead to upregulation of a BCL6-repressed luciferase reporter as well as increasing mRNA levels of BCL6-repressed targets, *BLIMP1*, *CD69*, and *CyclinD2* (Chattopadhyay et al., 2006). Furthermore, this peptide aptamer facilitated IL-2 and IL-5-mediated suppression of growth of cells expressing BCL6 (Chattopadhyay et al., 2006). Recently, through use of X-ray crystallography, the antibiotic Rifamycin SV has also been shown to bind to the BCL6 lateral groove, by a similar mechanism to RI-BPI and 79-6 (Evans et al., 2014), suggesting a novel foundation for the development of new BCL6 inhibitors. Collectively these data demonstrate the potential to inhibit BCL6 through the BTB/POZ domain suggest a means to BCL6 therapeutically.

Other mechanisms for BCL6 inhibition can also be postulated. In addition to the BTB domain, the RD2 domain mediates transcriptional repression of some BCL6 target genes and has been implicated in DLBCL. Gene Set Enrichment Analysis (GSEA) of GCB-DLBCL cells harbouring a BCL6 knockdown and rescued with BCL6 containing a mutant RD2 domain revealed RD2 domain-dependent repression of a number of genes known to be BCL6 targets in B-cell lymphoma (Huang et al., 2014, Shaffer et al., 2000) suggesting that RD2 domain inhibition may also be useful in DLBCL.

BCL6 could also be inhibited indirectly. For example, one study (Ying et al., 2013) found that somatic mutations of *MEF2B* in DLBCL cell lines resulted in deregulated overexpression of BCL6. Introduction of mutated *MEF2B* or *BCL6* via viral-transduction into SUDHL4 cells caused marked reduction in the proliferative activity of these cells as well as reduced BCL6 expression. The study suggests that MEF2B, and perhaps other BCL6 regulators, may represent alternative targets for indirectly blocking BCL6 activity.

#### **1.5.4 BCL6 in T-cells**

BCL6 is vital for normal T-cell differentiation and maturation, with roles identified in T-helper cell specification, effector T-cell differentiation and T-cell memory. There are multiple hypotheses for the mechanism of BCL6 action in effector CD4<sup>+</sup> T cells. One well documented hypothesis is that each CD4<sup>+</sup> T-cell subset has a known master regulator transcription factor (figure 1.5), which, for T<sub>FH</sub> cells is believed to be BCL6 (Johnston et al., 2009). Expression of BCL6 is normally regulated by IL-6 and IL-21, however, constitutive overexpression of BCL6 has been shown to promote the

expression of T<sub>FH</sub>-related genes (Nurieva et al., 2009), whilst in contrast, CD4<sup>+</sup> cells lacking BCL6 fail to differentiate into T<sub>FH</sub> cells (Johnston et al., 2009, Nurieva et al., 2009, Yu et al., 2009). In addition, *BCL6* mRNA has been shown, by real-time reverse transcription polymerase chain reaction (RT-PCR), to be significantly upregulated in naïve CD4<sup>+</sup> cells upon administration of IL-6 and IL-21 (Nurieva et al., 2009). Another hypothesis for the involvement of BCL6 in T-cell differentiation is the “balanced model” whereby the fate of CD4<sup>+</sup> T-cells is determined by strict regulation of a gene expression profile (Inghirami et al., 2015). In this model, CD4<sup>+</sup> T-cells initially develop into T<sub>H1</sub> or T<sub>H2</sub> cell types as determined by their master regulators (T-bet and GATA3 respectively), however maintenance of this differentiation fate is mediated via expression of other master regulator genes (Inghirami et al., 2015). Therefore, a T<sub>H</sub> cell committed to T<sub>H1</sub> lineage may activate expression of a BCL6 gene expression profile, leading to terminal differentiation to a T<sub>FH</sub> cell subset.

Therefore, BCL6 has been implicated as the key regulator of T<sub>FH</sub> cell differentiation, a process which has been shown to be antagonised by BLIMP1 (Crotty et al., 2010, Johnston et al., 2009). Intriguingly, the only CD4<sup>+</sup> cell type which has high expression of BCL6 is the T<sub>FH</sub> cell, the remaining groups (T<sub>H1</sub>, T<sub>H2</sub>, T<sub>H17</sub>, and T<sub>Reg</sub>) show a high expression of BLIMP1 (Crotty et al., 2010, Fazilleau et al., 2009, Johnston et al., 2009, Cimmino et al., 2008). In Blimp1-deficient murine CD4<sup>+</sup> cells, *Bcl6* mRNA was shown to have a two-fold increase against wild-type controls (Cimmino et al., 2008). This evidence suggests that respective expression and inhibition of either BLIMP1 or BCL6 is the key to determining CD4<sup>+</sup> cell fate decision (figure 1.10).

A recent study into targets of BCL6 in T<sub>FH</sub> cells has also demonstrated that BCL6 represses a number of targets involved in T-cell differentiation, signalling, and migration. These targets include: *STAT4*, *IFNGR1*, *GIMAP1*, *RORA* and *GATA3* (Hatzi et al., 2015). In addition, this study demonstrated that BCL6 can bind to Activator Protein 1 (AP1) motifs in T<sub>FH</sub> cells, in conjunction with AP1, to repress AP1-mediated activity on these targets (Hatzi et al., 2015).

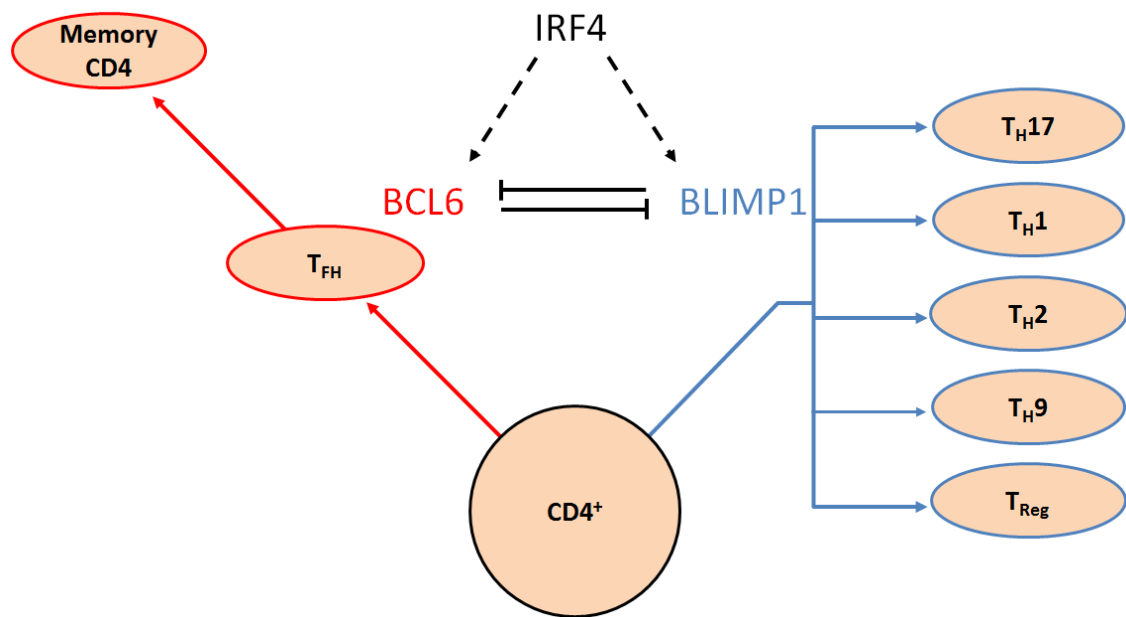


**Figure 1.10: Interaction of the BCL6-IRF4-BLIMP1 axis in CD4<sup>+</sup> cells**

BCL6 activity promotes differentiation to follicle helper T-cell [T<sub>FH</sub>] whilst BLIMP1 activity promotes differentiation to the remaining T-helper [T<sub>H</sub>] cells. Both BCL6 and BLIMP1 activity is facilitated by IRF4; however the interaction between IRF4 and either transcription factor is poorly understood. Cells overexpressing BCL6 will favour T<sub>FH</sub> specialisation but in BCL6 deficient cells, T<sub>FH</sub> differentiation is not possible. BCL6 has also been implicated as important for memory CD4 T-cell development. BLIMP1 expression is present in all remaining T<sub>H</sub> subsets. BCL6 and BLIMP1 can physically bind each other's promoter and actively prevent transcription (Cimmino et al., 2008, Johnston et al., 2009).

A certain threshold of BCL6 is believed to be required to achieve CD8<sup>+</sup> differentiation into memory T-cells (figure 1.8). BCL6-deficient mice exhibited lower detectable levels of CD44 and Ly6C (CD8<sup>+</sup> memory T –cell surface markers) than wild-type mice (Ichii et al., 2004). In agreement with these findings, overexpression of BCL6 in the transgenic *Ick-BCL6* mouse model resulted in elevated levels of memory T-cells compared to wild type mice (Ichii et al., 2002, Ichii et al., 2004). However, in the spleens of Bcl6-deficient mice phenotypic memory T-cells were still detectable (Ichii et al., 2004) suggesting that the formation of memory T-cells is not wholly reliant upon BCL6 expression.

Recently, BCL6 has been shown to repress the glycolytic pathway in primary CD4<sup>+</sup> and CD8<sup>+</sup> murine T-cells (Leavy, 2014, Man and Kallies, 2014, Oestreich et al., 2014). In this study, a BCL6 expression construct was shown to inhibit the expression of luciferase reporter constructs for a number of glycolytic molecules (Oestreich et al., 2014). Furthermore qPCR analysis of glycolytic pathway member mRNAs, in CD4<sup>+</sup> T-cells cultured in T<sub>H</sub>1 conditions with a BCL6 expression construct, revealed that BCL6 represses a number of targets, including *SLC2A1*, *SLC2A3*, *PKM*, and *HK2* (Oestreich et

al., 2014). In addition, CHIP-PCR also revealed that BCL6 specifically bound the promoter region of *SLC2A3* (Oestreich et al., 2014). The data as a whole suggests that BCL6 is responsible for the maintenance of glycolytic pathway repression exhibited in memory CD8<sup>+</sup> T-cells.

Interestingly, BCL6 may not utilise the BTB/POZ domain in T-cells as it does in B-cells. Recent evidence shows that a knock-in mouse model containing BCL6 with a non-functional BTB domain did not produce fatal inflammatory responses found within *Bcl6*<sup>-/-</sup> mice (Huang et al., 2013b). In addition, T<sub>FH</sub> cells containing this mutated BCL6 gave rise to normal GC responses whilst normal T-helper cell differentiation was achieved with the same construct (Huang et al., 2013b). Thus, BCL6 may exert its actions through a different domain, such as RD2. In agreement with this, mice harbouring BCL6 with an inactivated RD2 domain resulted in a 40% reduction of GC-T<sub>FH</sub> cell formation in comparison to wild type mice suggesting the domain is important for T<sub>FH</sub> cell formation (Huang et al., 2014).

### **1.5.5 BCL6 in T-cell lymphoma**

From our current understanding of BCL6 functions in B-cells, it is logical to assume it may act as a pro-tumour factor in some PTCL. In fact, BCL6 overexpression results in the overproduction of T<sub>FH</sub> cells and contributes to T<sub>FH</sub> cell-derived lymphomas as well as other T-cell lymphomas (de Leval et al., 2007, Duy et al., 2011, Kerl et al., 2001). Indeed, deficiency of BCL6 in CD8<sup>+</sup> T-cell reduces the proliferation of these cells (Ichii et al., 2002) and a further study found that cytotoxic T-cell proliferation correlates with Bcl6 expression in mice (Ichii et al., 2004).

BCL6 has been shown to be vital for pre-B-cell renewal in B-cell leukaemias due to its inhibitory effect on DNA damage response genes (Duy et al., 2011, Hurtz et al., 2011) and it is plausible that the same process may be occurring within T-cell lymphomas, although the BCL6 target genes of B-cells have not been confirmed in T-cells as of yet. Importantly, BCL6 promotes the formation of long-lived memory T-cells with self-renewal capabilities; equally it represses terminal effector T-cell differentiation associated with low proliferative potential providing evidence of potential oncogenic effect in PTCL.

In ALK+ ALCL, deregulation of BCL6 appears prominent. It has been suggested this deregulation is mediated through the constitutive activation of ALK driven by the t(2;5)(p23;q35) NPM-ALK translocation. In agreement with this, gene expression profiling and IHC staining of systemic ALCLs demonstrated that BCL6 expression is higher in ALK+ ALCL (Saglam and Uner, 2011, Lamant et al., 2007).

A study investigating overexpression of a construct containing full length NPM-ALK under the control of a CD4 promoter in transgenic mice, restricting NPM-ALK expression to the T-cell lineage only, revealed mice expressing the cassette developed spontaneous thymic lymphomas, strongly reinforcing the fusion genes role in lymphomagenesis (Chiarle et al., 2003). Another study investigating overexpression of full-length NPM-ALK in HEK-293T cells resulted in increased phosphorylation of STAT3 compared to inactive NPM-ALK (Chiarle et al., 2005, Zamo et al., 2002). Furthermore, ALK+ ALCL cell lines expressed considerably more phosphorylated STAT3 in contrast to ALK- cell lines (Zamo et al., 2002). Collectively, the data suggests that NPM-ALK drives ALK+ ALCL to phosphorylate, and thus activate, STAT3. Phosphorylated STAT3 has been shown to activate the expression of a number of targets, most importantly BCL6. Induction of phosphorylated STAT3 expression in the breast cancer cell line, SK-BR-3, resulted in increased expression of *BCL6* mRNA (Walker et al., 2013). In addition, ChIP-Seq analysis of human cells revealed STAT3 binding directly to the *BCL6* gene (Walker et al., 2013) suggesting STAT3 directly drives the expression of BCL6. Taken together, the data suggests that the initial transforming mechanism, NPM-ALK fusion could result in the constitutive expression of BCL6 and therefore may constitute potential therapeutic targets in these lymphomas.

## **1.6 Interferon Regulatory Factor 4 (IRF4)**

### **1.6.1 IRF4 structure**

Located at chromosome 6p25.3, *IRF4* was initially characterised by the generation of *Irf4*<sup>-/-</sup> mice (Mittrucker et al., 1997) which lacked GCs and plasma cells and could not generate cytotoxic T-cell responses. This finding was reinforced with immunohistochemistry analysis of human and mouse lymphoid tissue for IRF4 protein which showed high expression in plasma cells, but a lack of expression in most, but not all, GC B-cells (Falini et al., 2000).

IRF4 is a member of the IRF family of transcription factors. Most members of the IRF family consist of a tryptophan-rich DNA-binding domain coupled to a regulatory domain and an IRF-associated domain (IAD), the exception being IRF6 which lacks an IAD (Shaffer et al., 2009). IRF4 is unique in that it is one of two IRF family members expressed solely in lymphocytes, the other being IRF8 (Shaffer et al., 2009). IRF4 possesses poor DNA binding ability despite containing a DNA binding domain. This is currently believed to be the result of an autoinhibitory domain present at the C-terminal of the protein (Brass et al., 1996). However, through binding of a co-factor, such as SPI1/PU.1 (Spleen Focus Forming Virus (SFFV) Proviral Integration Oncogene), SPIB, STAT3, or Basic Leucine zipper transcription factor, ATF-like (BATF) the autoinhibitory effect can be alleviated allowing IRF4 to exert DNA-binding activity to ETS-IRF composite elements (EICEs) or AP1-IRF4 composite elements (AICEs) (Brass et al., 1996, Escalante et al., 2002, Li et al., 2012) (figure 1.11). IRF4 can exert inhibitory effects on target genes through binding of interferon-stimulated response elements (ISREs) present in the promoters of genes (Brass et al., 1996, Yamagata et al., 1996). IRF4 successfully bound ISREs coupled to a GAL4 reporter construct and repressed IRF1-mediated expression of the reporter (Brass et al., 1996). Therefore it is hypothesised that IRF4 prevents the binding of other IRF family members to target genes through interaction with ISREs, in the absence of PU.1, and acts to inhibit transcriptional activation.

### **1.6.2 IRF4 in B-cells**

Although it is required during early B-cell development, IRF4 also performs a vital part in late B-cell differentiation. During selection of GC B-cells, increased expression of IRF4, brought about by CD40 signalling and subsequent activation of NF- $\kappa$ B (Gupta et al., 1999), alters the balance of TFs (figure 1.4B) causing repression of *BCL6* transcription and activation of *BLIMP1* transcription (De Silva et al., 2012). Activation of the NF- $\kappa$ B pathway stimulates the formation of NF- $\kappa$ B heterodimers upon promoter regions of *IRF4*, activating *IRF4* transcription (Gupta et al., 1999, Saito et al., 2007, Shaffer et al., 2006, Sharma et al., 2000). In addition to CD40, IRF4 expression can also be induced by IL-4, mediated by STAT6 (Grumont and Gerondakis, 2000, Gupta et al., 1999). In agreement with previous findings, evidence shows low levels of NF- $\kappa$ B

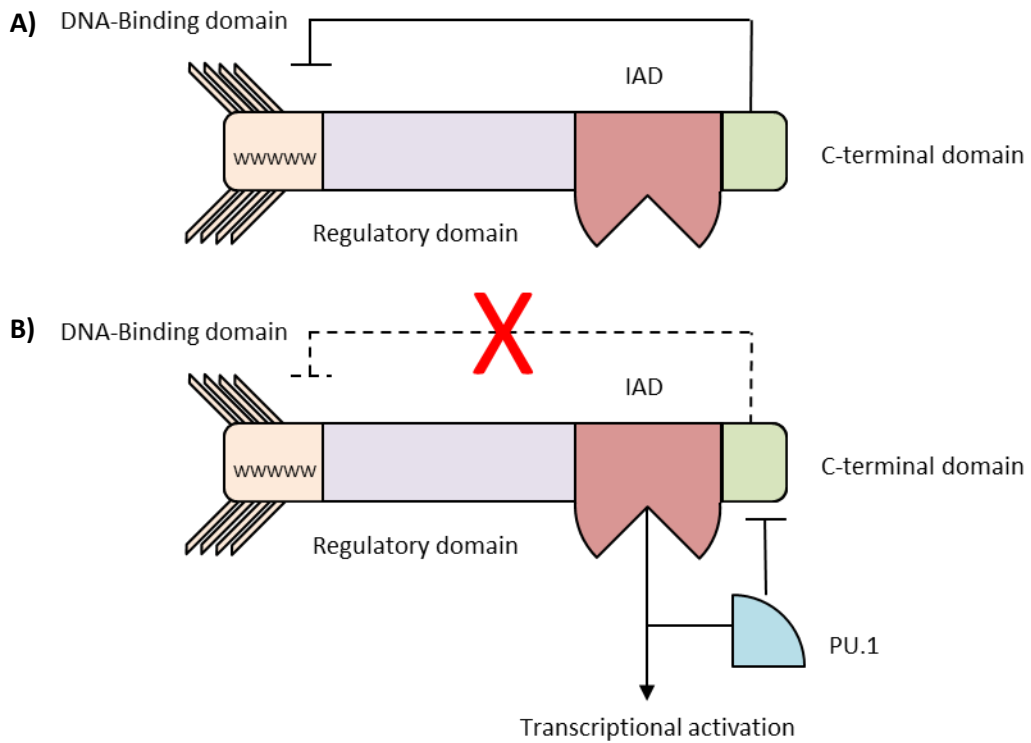


**Figure 1.11: Structure and function of IRF4 with binding partners**

A) Protein structure of IRF4 protein. IRF4 consists of four domains: a DNA-binding domain containing five tryptophan repeats, a regulatory domain, an IRF-associated domain (IAD), and a C-terminal inhibitory domain. Whilst IRF4 is not interacting with binding partners, the C-terminal domain exerts inhibitory activity on the DNA-binding domain preventing efficacious binding to IRF4 consensus sequences. B) Effect of binding of PU.1 by the IRF-associated domain. Interaction of PU.1 with the IAD allows the PEST domain of PU.1 to inhibit C-terminal domain inhibitory activity. IRF4 can now bind consensus sequences with 5-fold greater avidity and activate transcriptional activity (Escalante et al., 2002).

within GC B-cells (Shaffer et al., 2001) as well as IRF4, whilst expression of IRF4 is highest within plasma cells.

The positive feedback loop of IRF4, and the inhibition by IRF4 of BCL6, maintains the plasma cell in the differentiated form (Sciammas et al., 2006, Shaffer et al., 2008) (figure 1.4C). Studies investigating the distribution of B-cell populations in *Irf4*<sup>-/-</sup> mice show that, in comparison to wild type mice, there was a dramatic decrease in the number of plasma cells present (Klein et al., 2006, Mittrucker et al., 1997), suggesting a vital role of IRF4 in inducing terminal differentiation.

IRF4 has also been shown to be required for CSR (Klein et al., 2006, Sciammas et al., 2006). In these studies, loss of IRF4 in B-cells resulted in poor expression of AID. Upon restoration of IRF4, CSR was restored, indeed more so than restoring AID alone (Sciammas et al., 2006), thus suggesting that IRF4 is important for CSR, both independently and through AID expression.

The levels of IRF4 differ between B-cell development stages (figure 1.4). As well as being promoted by STAT6 and NF- $\kappa$ B, IRF4 is believed to be repressed by MITF (Lin et al., 2004). Loss of MITF resulted in high rates of B-cell activation and differentiation into plasma cells, which promoted an autoimmune response (Lin et al., 2004). Currently however, no further studies into MITF/IRF4 interactions have been published. Nonetheless the data as a whole suggests IRF4 regulation plays an important role in B-cell maturation.

As well as affecting plasma cell differentiation, IRF4 in conjunction with IRF8, promotes the rearrangement of Ig light-chain genes during early B-cell development (Johnson et al., 2008). In non-transformed pre-B-cells with *IRF4*<sup>-/-</sup> *IRF8*<sup>-/-</sup> genotype,  $\kappa$  light-chain recombination does not occur but can be induced by re-introducing IRF4 (Inlay et al., 2002, Johnson et al., 2008, Lu et al., 2003). IRF4 has also been shown to upregulate CXCR4, a receptor for the chemokine SDF-1 (Tokoyoda et al., 2004). It is proposed that this encourages pre-B-cells in the bone marrow to preferentially migrate towards stromal cells expressing SDF-1 rather than IL-7. As IL-7 represses light-chain gene rearrangement (Johnson et al., 2008), IRF4 expression tends to promote light chain gene rearrangements. Due to the observation that immature B-cells recognising self-antigen upregulate their IRF4 expression (Pathak et al., 2008), one study

concluded that IRF4 allow these B-cells further *Ig* gene alterations in order to escape apoptosis.

### **1.6.3 IRF4 in B-cell lymphoma**

IRF4 has been implicated in the development and maintenance of ABC-DLBCL, Multiple Myeloma, Hodgkin lymphoma, Primary effusion Lymphoma, and Chronic lymphocytic leukaemia. As a result, therapeutic intervention targeting IRF4 has become an attractive prospect in these malignancies.

Studies have found that, using RNA-interference-based genetic screens, loss of IRF4 was toxic to myeloma cell lines irrespective of the transforming mechanism of the myeloma (Shaffer et al., 2008). In addition, chromosomal translocations bringing *IRF4* under control of the Ig heavy-chain regulatory regions have been identified in MM cases (Iida et al., 1997, Tsuboi et al., 2000). A particularly important target gene of IRF4 in MM is *c-MYC*. Regulation of the *c-MYC* gene is commonly lost in MM (Dib et al., 2008) and IRF4 also binds to the *c-MYC* promoter, activating its expression. Expression of *c-MYC* also increases IRF4 expression by binding a conserved intronic region of *IRF4*, effectively creating a positive autoregulatory feedback loop (Shaffer et al., 2008). In agreement with this, levels of IRF4 and *c-MYC* expression correlate well in MM patients (Shaffer et al., 2008). *c-MYC* is an important target as the protein is known to regulate the expression of vital cell cycle regulators such as P27, as well as cyclins and CDKs (Eilers, 2008, Dang et al., 2006). In mouse T-cells, deficiency of *c-MYC* resulted in a reduced induction of cyclin A, CDKs 2 and 4, and CDC25A however P27 remained unaffected (Wang et al., 2011b). These data collectively highlights the importance of an IRF4/*c-MYC* interaction for tumour proliferation and survival.

Additionally, in approximately 2% of all MM cases, a common amino acid substitution is found amongst the DNA binding domain (specifically K123R) (Chapman et al., 2011). Although the implication of the mutation has not yet been discovered, the frequency of recurrence suggests it may provide a selective advantage.

In another study, a role for IRF4 in mantle cell lymphoma (MCL) has been discovered. MCL cell lines which had selected resistance to bortezomib (a proteasome inhibitor which induces remission in 30-50% of MCL patients) showed elevated

expression of both IRF4 and BLIMP1 (Perez-Galan et al., 2011). However, knockdowns of IRF4 in the bortezomib-resistance MCL cell lines sensitised them to the drug, implicating IRF4 as an important factor for cancer mortality. IRF4 has also been targeted for therapies for ABC-DLBCL, by using the drug Ibrutinib which targets the B-cell receptor/NF- $\kappa$ B signalling pathway in these cells and, in conjunction with another drug Lenalidomide, causes them to undergo apoptosis (Yang et al., 2012). These drugs have been used in other lymphomas, such as chronic lymphocytic leukaemia (Herman et al., 2011) with promising results as well as MM (Li et al., 2011, Lopez-Girona et al., 2011, Zhu et al., 2011, McCarthy et al., 2012). Thus reinforcing the importance IRF4 plays in the transformation of lymphocytic cells.

#### **1.6.4 IRF4 in T-cells**

IRF4 has also been implicated as a regulator of T-helper cell differentiation, playing roles in the development of several T<sub>H</sub> cell subsets (Bollig et al., 2012, Brustle et al., 2007, Honma et al., 2008, Lohoff et al., 2002). It appears to play an accommodating role to both BLIMP1 and BCL6, and other master regulators, in determining T-cell differentiation but the exact mechanism of this is not well defined (figure 1.10).

IRF4 is important in mature CD4<sup>+</sup> T-cell function. Initial studies demonstrated that whilst *Irf4*<sup>-/-</sup> mice did not have abrogated T-cell development, the proliferation of these CD4<sup>+</sup> T-cells was diminished when stimulated with CD3, concanavalin A, or staphylococcal enterotoxin A antibodies compared to *Irf4*<sup>+/+</sup> mice (Mittrucker et al., 1997). Furthermore, these cells lacked the ability to produce IL-2, IL-4, and IFN- $\gamma$  (Mittrucker et al., 1997). Further studies into IRF4s involvement in IL-2, IL-4, and IFN- $\gamma$  production demonstrated that IRF4 exerts T-helper cell-specific regulation of these interleukins (Honma et al., 2008).

Deficiency of IRF4 *in vitro* and *in vivo* demonstrated that IRF4 was required for T<sub>H</sub>2 differentiation (Honma et al., 2008, Lohoff et al., 2002, Rengarajan et al., 2002, Tominaga et al., 2003). Intriguingly, effector/memory CD4<sup>+</sup> T-cells obtained from *Irf4*<sup>-/-</sup> mice produced lower levels of IL-2, IL-4, and IL-5 compared to wild-type cells (Honma et al., 2008). In addition, *Irf4*-deficient mice failed to sustain T<sub>H</sub>2 immune responses to infections (Honma et al., 2008, Lohoff et al., 2002, Tominaga et al., 2003). Therefore, it

is believed that IRF4 is critical for the differentiation and function of CD4<sup>+</sup> T-cells to T<sub>H</sub>2 cells. In agreement with this, CD4<sup>+</sup> T-cells derived from *Irf4*-deficient mice fail to produce T<sub>H</sub>2 cytokines (IL-4, IL-5, IL-13, and IL-21) when stimulated with T<sub>H</sub>2-promoting factors (Lohoff et al., 2002, Rengarajan et al., 2002, Tominaga et al., 2003).

The role of IRF4 in the determination of T<sub>H</sub>1 cells remains difficult to ascertain. Studies of CD4<sup>+</sup> T-cells in *Irf4*-deficient mice demonstrated that these cells exhibited higher expression of IFN- $\gamma$ , a T<sub>H</sub>1 cytokine, compared to wild type controls (Rengarajan et al., 2002, Tominaga et al., 2003). However, a separate study into murine *Irf4*<sup>-/-</sup> CD4<sup>+</sup> T-cells stimulated with TCR antigen demonstrated that these cells exhibited lower expression of IFN- $\gamma$  than wild-type CD4<sup>+</sup> T-cells (Honma et al., 2008). Furthermore, in an infectious model utilising *Leishmania major*, *Irf4*<sup>-/-</sup> mice failed to produce both T<sub>H</sub>1 and T<sub>H</sub>2 responses (Sacks and Noben-Trauth, 2002).

In addition to promoting T<sub>H</sub>2, and potentially T<sub>H</sub>1 responses, IRF4 is important in T<sub>H</sub>17 differentiation. CD4<sup>+</sup> T-cells deficient in IRF4 lose the ability to differentiate into T<sub>H</sub>17 cells and produce IL-17 under stimulation (Brustle et al., 2007, Chen et al., 2008, Huber et al., 2008). IRF4 activity on IL-17 expression is strictly controlled by IRF4-binding protein (IBP). It has been demonstrated that deficiency of IBP resulted in enhanced IRF4 binding to IL-17 and IL-21 regulatory regions suggesting IBP typically inhibits IRF4 binding (Chen et al., 2008). Inhibition of IRF4 has been implicated as a potential therapy in T<sub>H</sub>17-mediated inflammatory diseases as loss of the gene confers resistance to mouse models of some T<sub>H</sub>17-associated diseases such as multiple sclerosis (Brustle et al., 2007). Furthermore, *IRF4*<sup>-/-</sup> T-helper cells fail to express the T<sub>H</sub>17 regulator, ROR $\gamma$ t, when primed with IL-6 and TGF- $\beta$  (T<sub>H</sub>17 conditions) (Brustle et al., 2007). Further investigation into IRF4 revealed the protein can bind to the T<sub>H</sub>17 cytokine promoter, *IL-21*, and activate its expression in conjunction with Nuclear Factor of Activated T-cells (NFAT)c2 (Chen et al., 2008). IRF4 has been revealed to play an important role in the differentiation of CD4<sup>+</sup> T-cells via interaction with a variety of binding partners (figure 1.11). Recently, through genome wide ChIP analysis, IRF4's role in T<sub>H</sub>17 differentiation has been explored further (Ciofani et al., 2012). Interactions between IRF4 and BATF facilitate chromatin remodelling and, along with STAT3, allow access to a transcriptional program resulting in the differentiation of T<sub>H</sub>17 cells.

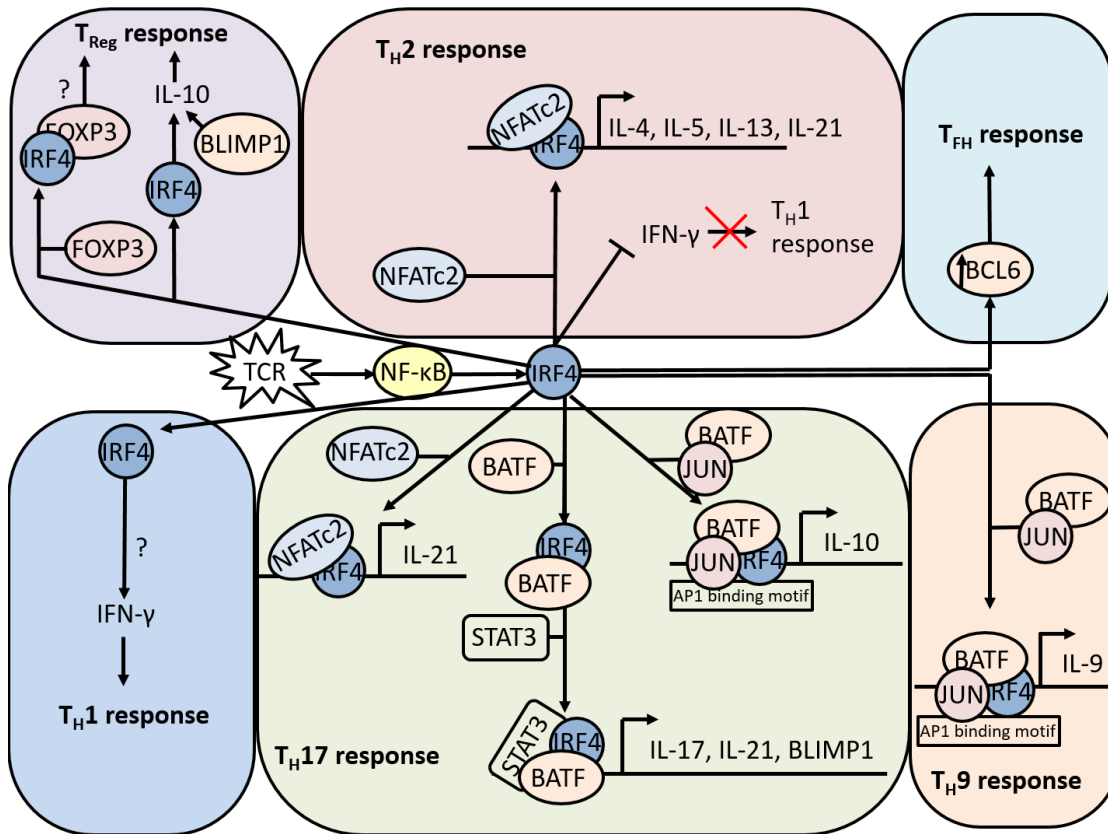


**Figure 1.12: Interaction of IRF4 with binding partners in T-helper cell subsets**

TCR stimulation upregulates NF- $\kappa$ B in  $T_H$  responses resulting in upregulation of IRF4 expression. Associations of IRF4 with different molecules results in localisation to different transcriptional target regulatory regions.  $T_{Reg}$  responses are believed to be mediated through IRF4s interaction with FOXP3, however little is known about the exact mechanisms of this action. IRF4 and BLIMP1 are required for IL-10 production in  $T_{Reg}$  cells and are believed to contribute to  $T_{Reg}$  response.  $T_H1$  responses remain undetermined, however data currently suggests IRF4 facilitates differentiation through IFN- $\gamma$ .

Moreover, through ChIP-Seq analysis, IRF4 binding sites overlapped with BATF binding sites in approximately 54% of all IRF4 targets, most notably *PRDM1* and interleukin genes: *IL21*, *IL17a*, and *IL10* in CD4<sup>+</sup> and T<sub>H</sub>17 cells (Li et al., 2012). IRF4 also interacts with AP1 binding sites in pre-activated T-cells as a method of overcoming the intrinsically low levels of PU.1 protein (Li et al., 2012, Kwon et al., 2009, Murphy et al., 2013), the partner required in B-cells for IRF4 activity (Brass et al., 1996, Escalante et al., 2002). Through Electrophoretic Mobility Shift Assays (EMSAs) the authors show that IRF4, via interaction with AP1 sites, required the BATF-JUN complex to bind target sites within the *IL10* gene within transfected 293T cells suggesting that BATF-JUN is required for IRF4 to exert transcriptional activity within the T-cell lineage (Li et al., 2012). It is therefore generally accepted that IRF4 mediates the differentiation of T<sub>H</sub>17 cells as well as T<sub>H</sub>2.

Another member of the BATF family is BATF3. Through deficiency studies, BATF3 has been demonstrated to be required for CD8<sup>+</sup> dendritic cell development (Hildner et al., 2008). Furthermore, BATF3 and IRF8 have overlapping targets in these cells suggesting a possible interaction (Bachem et al., 2010). Direct interaction of IRF8 and BATF3 has been suggested, but never proven (Murphy et al., 2013). Despite this, due to the similarities between IRF4 and IRF8 structures (Jo et al., 2010) and the potential for IRF8 to bind BATF (Murphy et al., 2013), it is plausible that IRF4 may interact with BATF3 for T-cell development as well. In addition to BATF, IRF4 has also been demonstrated to bind NFATc2 in transfected HEK 293T cells (Rengarajan et al., 2002). Introduction of NFATc2 to these cells in combination with immunoprecipitation for IRF4 demonstrated a strong interaction between the two transcription factors (Rengarajan et al., 2002). Furthermore, IRF4 knockout T<sub>FH</sub> cells failed to induce *IL-4* expression, an NFATc2 target (Rengarajan et al., 2002). Further studies have revealed that IRF4 interacts with NFATc2 to drive the expression of multiple interleukins such as IL-21, IL-5, and IL-13 in the CD4<sup>+</sup> T-cell compartment (Hermann-Kleiter and Baier, 2010, Rengarajan et al., 2002). IRF4 is also believed to be important for the development of T<sub>Reg</sub> cells. Whilst interaction of IRF4 and endogenous FOXP3 has not been demonstrated, the two transcription factors are believed to share common T<sub>Reg</sub>-related gene targets (Zheng et al., 2009). In addition, GFP-tagged FOXP3 gave rise to strong binding affinity between itself and IRF4 (Zheng et al., 2009); however, further

study is required to elucidate if this interaction occurs with endogenous FOXP3. In addition, reports have shown that T<sub>Reg</sub>-specific IRF4 deficiencies lead to an autoimmune syndrome in mice (Chen et al., 2008, Zheng et al., 2009), suggesting IRF4 is critical for T<sub>Reg</sub> cell functions.

However, due to the large repertoire of interactions IRF4 exhibits, it has also been found to affect the formation of other T-helper cells. Lohoff et. al show that *Irf4*<sup>-/-</sup> mice fail to generate T<sub>FH</sub> cells and, in addition, showed dramatic loss of BCL6 expression in *Irf4*<sup>-/-</sup> CD4<sup>+</sup> T-cells strongly implicating a positive interaction between IRF4 and BCL6 (Lohoff et al., 2002); a striking contrast to B-cells where IRF4 is responsible for suppression of *BCL6* transcription (figure 1.4) (Saito et al., 2007). Moreover, IRF4 has been shown to physically bind BCL6 (Gupta et al., 1999). Therefore, IRF4 may also direct differentiation of T<sub>FH</sub> cells as well as T<sub>Reg</sub>, T<sub>H2</sub> and T<sub>H17</sub> cells (figure 1.12).

IRF4 expression is also required for the differentiation of T<sub>H9</sub> cells. Murine *Irf4*<sup>-/-</sup> CD4<sup>+</sup> T-cells fail to induce IL-9 production under T<sub>H9</sub>-stimulating conditions (Staudt et al., 2010). Furthermore, in a mouse model for allergic asthma, *Irf4*<sup>-/-</sup> mice were resistant to induction of the disease strongly implicating T<sub>H9</sub> involvement. Further investigation, using microarray studies, demonstrated that BATF is specifically enriched in T<sub>H9</sub> cells (Jabeen et al., 2013). In addition, T-cells deficient in either BATF or IRF4 exhibited poor expression of IL-9. Re-introduction of either BATF or IRF4 separately to these cells promoted a 2-fold increase in IL-9 production, however re-introduction of both resulted in dramatically larger increases in IL-9 production (Jabeen et al., 2013). Thus, it is believed that both IRF4 and BATF are required for efficient T<sub>H9</sub> responses (figure 1.12).

Multiple studies have confirmed the importance of IRF4 in the expansion and function of cytotoxic CD8<sup>+</sup> T-cells (Man et al., 2013, Raczkowski et al., 2013, Yao et al., 2013). One study found that IRF4-deficient CD8<sup>+</sup> T-cells expanded poorly in comparison to wild-type controls *in vitro* when stimulated with dendritic cells and alpha-CD3 (Yao et al., 2013). IRF4-deficient CD8<sup>+</sup> T-cells in mice also incorporated less BrdU than wild-type mice when infected with influenza virus indicating the importance of IRF4 for proliferation *in vivo* (Yao et al., 2013). In agreement with this finding, another study

found *IRF4*<sup>-/-</sup> T-cells proliferated slower than wild-type counterparts and were outcompeted within a 5-day period in competitive transfer experiments against wild-type T-cells (Rackowski et al., 2013). In addition to slowing proliferation, IRF4 is important in preventing apoptosis. T-cell cultures of *IRF4*<sup>-/-</sup> CD8<sup>+</sup> T-cells induced apoptosis to a greater frequency than *IRF4*<sup>+/+</sup> CD8<sup>+</sup> T-cells (Man et al., 2013). Though it is not understood how IRF4 prevents apoptosis, the data reinforces the notion that IRF4 is critical for CD8<sup>+</sup> T-cell survival and proliferation.

IRF4 has also been implicated in the metabolic activity of CD8<sup>+</sup> T-cells. ChIP-Seq analysis of murine *Irf4*<sup>-/-</sup> T-cells stimulated with N4 antigen yielded two important targets in regulation of T-cell metabolism, Forkhead Box Protein O1 (*Foxo1*) and *Hif1a* (Man et al., 2013). In addition, loss of IRF4 in these cells reduced the rate of oxygen consumption, decreased ATP production, and exhibited lower glycolytic activity than *Irf4*<sup>+/+</sup> T-cells (Man et al., 2013), all hallmarks of mitochondrial respiration. Currently, it is believed that IRF4 interacts with a number of key targets to regulate CD8<sup>+</sup> T-cell differentiation. In addition to upregulation of BLIMP1 expression, another independent study confirmed that *IRF4*<sup>-/-</sup> CD8<sup>+</sup> T-cells exhibit lower expression of T-bet (*Tbx21*) and *Hif1a*, as well as disrupting the binding of T-bet protein to targets (Yao et al., 2013), genes which are known to be important in CD8<sup>+</sup> T-cell differentiation (Finlay et al., 2012). This suggests that IRF4 regulates the expression of these targets in order to sustain activated CD8<sup>+</sup> T-cell differentiation.

Recent work has identified IRF4 associations with BLIMP1. IRF4 is believed to directly bind to sites within and around the *PRDM1* locus and subsequently increase transcriptional activity of BLIMP1 in both CD4<sup>+</sup> and CD8<sup>+</sup> T-cells (Kwon et al., 2009, Man et al., 2013, Rackowski et al., 2013, Yao et al., 2013). It has been found that IRF4 indirectly affects the *PRDM1* gene through binding of a response element 3' to the gene, in conjunction with STAT3 (Kwon et al., 2009), which caused greatly increased levels of *BLIMP1* mRNA in CD4<sup>+</sup> cells. Whilst loss of IRF4 in these cells did not affect STAT3 phosphorylation, it did result in a striking reduction in STAT3 binding activity (Kwon et al., 2009), suggesting a requirement of IRF4 for STAT3 activity. In CD8<sup>+</sup> T-cells, IRF4 was able to bind multiple sites within the *PRDM1* gene, including the promoter region (Yao et al., 2013). In congruence with this data, a separate study found that *IRF4*<sup>-/-</sup> CD8<sup>+</sup> T-cells, when stimulated with T-cell activating cytokines, had lower BLIMP1

protein expression than *IRF4*<sup>+/+</sup> counterparts (Raczkowski et al., 2013). However, when IRF4 was reintroduced retrovirally, *BLIMP1* mRNA levels increased in these cells (Raczkowski et al., 2013).

Taken together the studies described indicate an important role for IRF4 in many aspects of T-cell function and differentiation. Our understanding of the interactions between IRF4 and its targets in T-cells however, and thus the mechanisms by which IRF4 acts in these cells, is still incomplete.

### **1.6.5 IRF4 in T-cell lymphoma**

IRF4 has an ambiguous part to play within PTCL currently. Although translocations involving the gene do exist in some PTCL (Feldman et al., 2011, Feldman et al., 2009, Karai et al., 2013); the oncogenic nature of the translocation has yet to be shown. Initial investigation into these translocations revealed that they are predominantly present in c-ALCL, but were also found in PTCL-NOS and ALK- ALCL cases. In this study, 2 PTCL-NOS cases exhibited a t(6;14)(p25;q11.2) *IRF4-TCRA* translocation whilst partners for the remaining cases were undetermined (Feldman et al., 2009). However, further investigation into 6p25.3 translocations in ALK- ALCL revealed a recurrent translocation, specifically t(6;7)(p25.3;q32.3) (Feldman et al., 2011). Interestingly, the majority of ALK- ALCL cases did not involve *IRF4* but *DUSP22*, the gene adjacent and telomeric to *IRF4*. However, all cases shared a common breakpoint adjoining to the *FRA7H* fragile site on 7q32.3. Specifically, 8/29 ALK- ALCL cases exhibited translocations involving *IRF4* whilst 15/29 cases involved *DUSP22*, with the remaining undetermined (Feldman et al., 2011). Despite the translocation, *IRF4* mRNA expression was found to be constant between 6p25.3 rearranged and non-rearranged samples (Feldman et al., 2011). Recently, a case of PTCL-NOS with marked splenomegaly has been reported to harbour a t(6;14)(p25;q11.2) *IRF4-TRCA* translocation suggesting the translocation may be a determinant of aggressive PTCL. In addition, this tumour exhibited high expression of IRF4 by immunohistochemistry staining suggesting IRF4 could be the driver of the aggressive lymphoma (Somja et al., 2014).

Translocations involving 6p25.3 have not been reported in ALK+ ALCL however IRF4 expression is still high (Feldman et al., 2009). It has been suggested that STAT3

may drive the expression of IRF4 in ALK+ ALCL. As previously mentioned, NPM-ALK drives the phosphorylation and activation of STAT3 (Chiarle et al., 2005, Zamo et al., 2002). STAT3 and IRF4 interactions are pivotal for normal T-cell function. *IRF4*<sup>-/-</sup> mice, stimulated with IL-21, failed to induce the expression of a STAT3-dependent *PRDM1* response element coupled to a luciferase reporter compared to *IRF4*<sup>+/+</sup> counterparts strongly implicating interactions between IRF4 and STAT3 (Kwon et al., 2009).

In human malignancies involving oncogenic viruses such as Human T-cell leukaemia virus type 1 (HTLV-I) and EBV, IRF4 may play a vital role in maintaining the adult T-cell leukaemia (ATL) malignancy (Wang et al., 2011a, Sharma et al., 2000). The HTLV-I virus transforms cells by activating the NF-κB pathway and subsequently causes overexpression of IRF4, in a manner similar to EBV-transformed lymphoblastoid cells (Xu et al., 2008). Furthermore, IRF4 can transactivate IL-15 receptor α-chain gene (Mariner et al., 2002) and in some ATL, IL-15 has been associated as a growth factor (Kukita et al., 2002). Further investigation into IRF4 in ATL demonstrated that constitutive expression of IRF4 in Jurkat cells results in downregulation of a number of targets involved in cell cycle regulation, DNA repair, apoptosis, immune recognition and metastasis including: Cyclin B1, EB1, RHOA, GRB2, PCNA, RP-A, NIP3, GRB2, and LFA-1 (Mamane et al., 2002). These targets are believed to contribute to HTLV-I-mediated transformation and promote cell survival (Mamane et al., 2005).

In recent studies, IRF4 has been demonstrated to promote its own expression via a novel positive-feedback loop (Boddicker et al., 2015). ChIP-analysis of ALCL cell lines revealed that IRF4 binds to *c-MYC*, *TNFRSF8* (CD30), *P52*, and *RELB* promoters (Boddicker et al., 2015). In addition, knockdown of NF-κB subunits, P52 and RELB, resulted in decreased IRF4 expression in ALCL cell lines suggesting NF-κB directly targets IRF4 in ALCL (Boddicker et al., 2015). Stimulation of CD30 with ligand also resulted in activation of NF-κB and subsequent increase in IRF4 expression (Boddicker et al., 2015). Taken together, the data suggests that in ALCL, IRF4 promotes its own expression via upregulation of CD30 and NF-κB subunits.

## 1.7 B-lymphocyte Induced Maturation Protein 1 (BLIMP1)

### 1.7.1 BLIMP1 structure

*PRDM1* is a gene located at chromosome 6q21 which encodes the BLIMP1 protein. The protein contains five zinc-finger motifs which allows sequence-specific DNA binding activity (Keller and Maniatis, 1992, Tunyaplin et al., 2000). There are two known protein isoforms of BLIMP1: BLIMP1 $\alpha$  and BLIMP1 $\beta$ . BLIMP1 $\alpha$  results from a full length transcript of the *PRDM1* gene whilst BLIMP1 $\beta$  lacks amino acids 1-101 at the N-terminus of the protein (Gyory et al., 2003) (figure 1.13). A third, naturally occurring variant of BLIMP1 has been described recently in NK-cells and lymphoblastoid cell lines which lacks exon 6 (termed BLIMP1 $\Delta$ 6) (Smith et al., 2010, Vrzalikova et al., 2012). This BLIMP1 isoform has been poorly characterised to date however.

BLIMP1 contains three domains which are required for the function of the protein: the PR-domain, the proline-rich region, and the zinc-finger domain. The PR-domain exhibits homology to SET domains within histone methyltransferases (HMTs) (Bellefroid et al., 1989, Huang et al., 1998). The proline-rich region has been demonstrated to recruit corepressor molecules, such as HDAC1, HDAC2, as well as GROUCHO proteins (Ren et al., 1999, Yu et al., 2000). The zinc-finger domain is

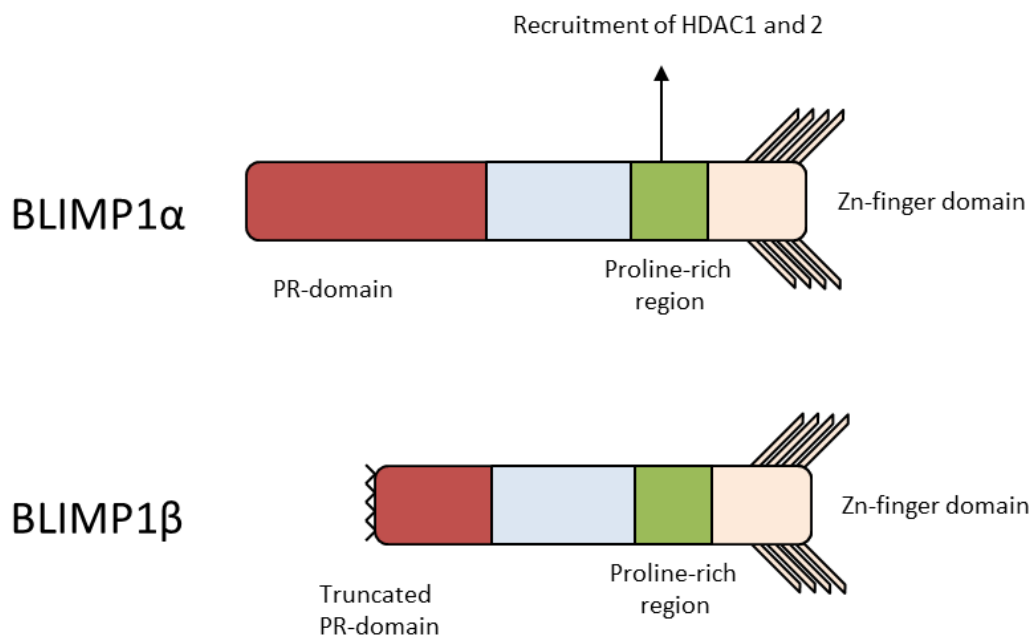


**Figure 1.13: Structure of BLIMP1 proteins**

BLIMP1 is comprised of two isoforms: BLIMP1 $\alpha$  and BLIMP1 $\beta$ . BLIMP1 contains three primary domains: the PR-domain, proline rich region, and the zinc finger domain. BLIMP1 $\alpha$  and BLIMP1 $\beta$  are transcribed from alternative promoters giving rise to a full length BLIMP1 $\alpha$  and a BLIMP1 $\beta$  with a truncated PR-domain. BLIMP1 exerts its repressive activity through recruitment of co-repressors.

required for the binding of BLIMP1 protein to DNA-binding sites. Through DNase fingerprinting it was revealed that only a portion of the zinc-finger domain is required for adequate binding to the BLIMP1 target sites, PRDI (Keller and Maniatis, 1992).

Through use of a luciferase reporter gene construct coupled to the DNA binding domains of BLIMP1 $\alpha$  and BLIMP1 $\beta$ , it has been demonstrated that BLIMP1 $\beta$  exhibited lower repressive activity when compared to BLIMP1 $\alpha$  (Gyory et al., 2003).

### **1.7.2 BLIMP1 in B-cells**

Differentiation of plasma cells critically relies upon the expression of BLIMP1 as well as the inhibition of BCL6 (Shapiro-Shelef and Calame, 2005). The role of BLIMP1 was first unearthed by demonstrating antibody secretion occurring in the immature B-cell line, BAL17, when transfected with a BLIMP1 construct (Turner et al., 1994). This role was reinforced with deletions of *Prdm1* in mice, which showed dramatic loss of Ig secretion in plasma cells in response to appropriate stimuli (Shapiro-Shelef et al., 2003) suggesting BLIMP1 is also vital for maturation of B-cells. In addition, studies confirmed that forced expression of BLIMP1 in the DLBCL cell line, SUDHL4, and in the Burkitt lymphoma cell line, Raji, is sufficient to drive differentiation of B-cells to Ig secreting cells (Shaffer et al., 2002).

The BLIMP1 protein exerts its effects by inhibiting transcription of multiple effector pathways (Cimmino et al., 2008, Shaffer et al., 2002). Of most interest, BLIMP1 represses genes involved in regulating B-cell receptor signalling such as *SPIB* and *ID3*, as well as inhibiting Ig class-switching by blocking the expression of AID, KU70, KU86, DNA-PK $\text{cs}$ , and STAT6 proteins (Shaffer et al., 2002).

Importantly, BLIMP1 also inhibits the expression of genes involved in proliferation, most notably *BCL6* (Cimmino et al., 2008) and *c-MYC* (Lin et al., 1997). Ectopic expression of BLIMP1 in B-cells, transformed with the Abelson murine leukaemia virus, repressed endogenous c-MYC expression and induced apoptosis (Lin et al., 1997). It is these inhibitory effects of BLIMP1 which, in conjunction with IRF4 self-promotion, contribute to maintaining the differentiated plasma cell (figure 1.4C). Taken together, these data coined the term “master regulator of plasma cell differentiation” for BLIMP1.

BLIMP1 has also been found to indirectly regulate expression of BACH2 in plasma cells via repression of PAX5 (Muto et al., 2010, Ochiai et al., 2008). Much like BCL6, BACH2 and BLIMP1 have antagonistic roles. BACH2 also inhibits expression of BLIMP1 in follicular B-cells (Ochiai et al., 2008). In BACH2 deficient cells, BLIMP1 is prematurely expressed and, subsequently, antibody secreting cell differentiation is enhanced. In addition, CSR and SHM rates are decreased in these cells (Muto et al., 2010).

### **1.7.3 BLIMP1 in B-cell lymphoma**

BLIMP1 is well established as a tumour suppressor gene in DLBCL. Initial studies into ABC-DLBCL revealed that *PRDM1* was inactivated in 24% of all cases, on both alleles, through gene truncations, nonsense mutations, or splice site mutations, giving rise to aberrant BLIMP1 $\alpha$  and BLIMP1 $\beta$  proteins (Pasqualucci et al., 2006, Tam et al., 2006). A more recent study demonstrated that *PRDM1* is inactivated by homozygous deletions, mutations, or constitutive BCL6 expression in 53% of ABC-DLBCL (Mandelbaum et al., 2010). In this study, it was shown that the *PRDM1* gene was genetically inactivated in 31% of ABC-DLBCL cases but a further 22% of cases, which did not harbour *PRDM1* inactivation, also contained a *BCL6* translocation (Mandelbaum et al., 2010). Furthermore, lentiviral-mediated knockdown of BCL6 in the RCK8 ABC-DLBCL cell line resulted in upregulation of *BLIMP1* mRNA and protein (Mandelbaum et al., 2010). The data suggests that *PRDM1* is either physically abrogated or mutated, or BLIMP1 expression is suppressed by constitutive BCL6 expression as a mechanism of transformation through suppression of GC B-cell differentiation.

As well as the repressive roles BLIMP1 has been shown to have, evidence has found that the protein may also be required for MM activity. An immunohistological study of B and T-cell lymphomas showed 100% of MM tumours were positive for BLIMP1 (Garcia et al., 2006), whereas other subsets of lymphomas showed lower or occasional positivity for BLIMP1. In agreement with this, a study into mice with a deficiency of BLIMP1 expression, brought about by the truncated *Blimp1<sup>gfp/gfp</sup>* gene (Kallies et al., 2004), revealed that lack of BLIMP1 expression prevented the formation of plasmacytomas (D'Costa et al., 2009). Specifically, this study demonstrated that

deficiency of BLIMP1 did not abrogate plasma cell formation but resulted in reduction in plasma cell transformation. Some mice reconstituted with *Blimp1<sup>gfp/gfp</sup>* however, developed tumours which were not plasma cell-based.

BLIMP1 depletion in chronic myeloid leukaemia is believed to be important to the transformation of these neoplasms due to interactions with BACH2. The inhibition of BLIMP1 alongside its interactions with CSR and SHM (Muto et al., 2004), makes BACH2 another potential tumour promoter. Indeed, in chronic myeloid leukaemia, the resulting BCR-ABL fusion gene targets and upregulates BACH2 expression (Vieira et al., 2001), thus loss of regulation by BLIMP1 may be sufficient to increase genomic instability.

#### **1.7.4 BLIMP1 in T-cells**

Originally, it was believed that the sole purpose of BLIMP1 in lymphocytes was to allow the terminal differentiation of antibody-producing plasma cells. However, more recently, BLIMP1 expression has been suggested to be crucial in T-cell homeostasis. Multiple studies have demonstrated that the overexpression of BLIMP1 resulted in the accumulation of T-cells, within the CD8 lineage, with an effector phenotype through suppression of memory cell differentiation potential (Kallies et al., 2006, Kallies et al., 2009, Martins et al., 2006, Rutishauser et al., 2009, Shin et al., 2009).

BLIMP1 is important for limiting T-cell responses. One well annotated mechanism of BLIMP1 function is through repression of IL-2 production during T-cell activation (Gong and Malek, 2007, Martins and Calame, 2008). Naïve T-cells, upon activation, express IL-2 which in turn causes potent transcription of *BLIMP1* mRNA (Gong and Malek, 2007). However, ectopic expression of BLIMP1 in activated T-cells *in vitro* resulted in marked reduction of IL-2 after 24 hours suggesting BLIMP1 inhibited IL-2 (Gong and Malek, 2007). Thus, IL-2 appears important for initial proliferation upon T-cell activation before suppression by BLIMP1 expression.

Studies into BLIMP1 expression revealed that the protein is expressed in only a subset of effector and memory CD8<sup>+</sup> T-cells. Loss of BLIMP1 expression in mice led to the accumulation of large numbers of CD4<sup>+</sup> and CD8<sup>+</sup> memory T-cells in comparison to

wild type counterparts (Kallies et al., 2006, Martins et al., 2006). This evidence suggested BLIMP1 regulated the numbers of CD8<sup>+</sup> T-cells as well as the number of CD4<sup>+</sup> T-cells. In agreement with these findings, it was also found that CD8<sup>+</sup> T-cells express high levels of *BLIMP1* mRNA (Intlekofer et al., 2007) suggesting a suppressive role for BLIMP1 in CD8<sup>+</sup> T-cell proliferation. Recent evidence has revealed that BLIMP1 deficient CD8<sup>+</sup> cells preferentially differentiate into a memory T-cell phenotype (Kallies et al., 2009, Rutishauser et al., 2009, Shin et al., 2009). Virus-mediated BLIMP1-deficient CD8<sup>+</sup> cells lose the ability to differentiate into KLRG1<sup>hi</sup>IL-7R<sup>lo</sup> cells (a phenotype associated with effector T-cell properties which have a characteristically limited ability to survive and undergo memory cell conversion (Kaech and Wherry, 2007)) and instead differentiate into KLRG1<sup>lo</sup>IL-7R<sup>hi</sup> cells (a memory CD8<sup>+</sup> precursor cell phenotype) (Kallies et al., 2009, Rutishauser et al., 2009). In agreement with these findings, these cells also exhibited a lower expression of granzyme B, an important effector molecule required for cytotoxic T-cells (Kallies et al., 2009, Rutishauser et al., 2009, Shin et al., 2009). However, the effect was not substantial enough to abolish effector functions of these T-cells as they could still clear acute infections with lymphocytic choriomeningitis or influenza viruses (Kallies et al., 2009, Rutishauser et al., 2009). The loss of granzyme B is thought to be caused by constitutive expression of BCL6 (Yoshida et al., 2006), arising from the lack of BLIMP1 expression. *BCL6*<sup>-/-</sup> CD8<sup>+</sup> cells overexpress large quantities of granzyme B (Yoshida et al., 2006) (figure 1.7), therefore, the data signifies the antagonistic interaction between BCL6 and BLIMP1 in the CD8<sup>+</sup> cell lineage too.

Recent studies have elucidated that BLIMP1 expression is promoted, at least in part, by IRF4 expression to determine cytotoxic T-cell fate (Man et al., 2013, Raczkowski et al., 2013, Yao et al., 2013). One study demonstrated that deficiency of *Irf4* in murine CD8<sup>+</sup> T-cells resulted in abrogation of cytotoxic T-cell formation upon infection with *L.monocytogenes* concurrent with loss of BLIMP1 protein expression (Raczkowski et al., 2013). This effect was been confirmed by another independent study demonstrating IRF4 directly promoted the expression and function of BLIMP1 and that ablation of *Irf4* in murine T-cells abrogated antiviral CD8<sup>+</sup> T-cell responses (Yao et al., 2013).

During CD4 determination, BLIMP1 is expressed in T<sub>Reg</sub> and T<sub>H2</sub> cells and is believed to commit CD4<sup>+</sup> T-cells to these lineages via repression of effector molecules (Cimmino et al., 2008, Fazilleau et al., 2009, Johnston et al., 2009, Martins et al., 2008). In T<sub>Reg</sub> cells, BLIMP1 expression is believed to contribute to the immune-suppressive function of these cells. Mice deficient in T-cell-specific BLIMP1 expression develop colitis which is believed to be attributed to excessive IL-2 production (Kallies et al., 2006, Martins et al., 2006). BLIMP1 expression is driven by IRF4 in T<sub>Reg</sub> cells to induce immune-suppression is via induction of *IL-10* resulting in suppression of T<sub>H1</sub> and T<sub>H2</sub> immunity (Cretney et al., 2011, Huber and Lohoff, 2014).

In agreement with BCL6 data, deficiency of BLIMP1 in the CD4<sup>+</sup> lineage caused these cells to preferentially differentiate into T<sub>FH</sub> cells (Johnston et al., 2009). Moreover, these cells also show an increase in proliferation in comparison to wild type CD4<sup>+</sup> cells (Martins et al., 2006), suggesting BCL6 promotes, and BLIMP1 inhibits, proliferation in this lineage.

Taken together studies have shown that BLIMP1 is critical for differentiation of both CD4<sup>+</sup> and CD8<sup>+</sup> T-cells and required to be under strict control by both IRF4 and BCL6.

### **1.7.5 BLIMP1 in T-cell lymphoma**

Multiple studies have highlighted the *PRDM1* gene as an important potential tumour-suppressor gene of T-cell lymphoma. Early investigations showed loss of *PRDM1* expression through gene deletions in NK-cell neoplasms in comparison to normal NK cells (Iqbal et al., 2009, Karube et al., 2011). In one particular study (Karube et al., 2011), regions of 6q21 were frequently lost in NK lymphomas. But upon re-expression of *PRDM1* in these neoplasms, suppression of cell proliferation was achieved. In addition, further studies have confirmed that 3% of primary ALK<sup>+</sup> ALCL and 39% of primary ALK<sup>-</sup> ALCL contain BLIMP1 inactivations/deletions (Boi et al., 2013). As a whole, these studies strongly implicate the role of *PRDM1* as a tumour suppressor gene.

BLIMP1 $\beta$  levels appear to correlate with poorer survival outcome in PTCL. One study (Zhao et al., 2008), showed that BLIMP1 $\beta$ -positive patients had a significantly

lower rate of survival than BLIMP1 $\beta$ -negative patients. In addition to this, inhibition of BLIMP1 $\beta$  via treatment with bortezomib, a proteasome inhibitor, reduced RNA and protein levels of IRF4 and c-MYC in the T-cell lymphoma cell line HUT78, suggesting BLIMP1 $\beta$  may interact with these target genes in PTCL (Zhao et al., 2008). The authors believe that NF- $\kappa$ B upregulation leads to subsequent BLIMP1 $\beta$  upregulation, which in turn, results in increased activity of c-MYC and IRF4 prompting lymphomagenesis. The authors do not prove whether the effect seen is caused by NF- $\kappa$ B upregulation alone or through the effect of BLIMP1 $\beta$  increase; however they argue that BLIMP1 $\beta$  may act like its analogs, *PRDM2* (Retinoblastoma protein-interacting zinc finger gene, RIZ) and *PRDM3* (Myelodysplasia syndrome 1 protein-ecotropic virus integration site 1 protein homolog, MDS1-EVI1), each of which contain truncated PR domains but are required for leukaemogenesis (Sasaki et al., 2002, Cuenco et al., 2000). The work demonstrates the contrasting contributions of the BLIMP1 isoforms to oncogenesis of lymphoma, however further work is required to fully understand the role of BLIMP1 $\beta$ .

Recently, BLIMP1 $\alpha$  was shown to inhibit the expression of *miR155* in ALK+ ALCL (Boi et al., 2013). The pro-tumour activity of *miR155* in ALK- ALCL has recently been elucidated by another publication (Merkel et al., 2015). In this study, deficiency of *miR155* in ALK- ALCL cell lines resulted in increased levels of cleaved caspase 3 as well as a reduction in proliferation (Merkel et al., 2015). Furthermore, the study demonstrated that, using ALK+ ALCL cell lines, *miR155* expression was unaffected by Crizotinib, suggesting that, if *miR155* is oncogenic in ALK+ ALCL, its expression is not mediated through ALK. Therefore, these data collectively suggest that BLIMP1 $\alpha$  may be lost in ALK+ ALCL as a mechanism of promoting *miR155* expression.

These data highlight the diversity of BLIMP1 between T-cell lymphomas, potentially highlighting it as both a tumour suppressor and an oncoprotein.

## 1.8 Aims

The interactions between BCL6, IRF4 and BLIMP1 are well characterised in B-cell non-Hodgkin lymphoma and this understanding has led to novel therapeutic targets for these neoplasms. However, their roles and interactions in T-cell non-Hodgkin lymphoma, or indeed in normal T-cells, are poorly understood. Evidence suggests analogous roles for BCL6, IRF4 and BLIMP1 between B-cells and T-cells (Crotty et al., 2010, De Silva et al., 2012, Johnston et al., 2009, Shapiro-Shelef et al., 2003), such as the mutual repression of BCL6 and BLIMP1 which may suggest potential common ground for treatment options. Conversely, subtle differences, such as the conflicting interactions of BCL6 and IRF4 between B and T-cells (Bollig et al., 2012, De Silva et al., 2012), may provide insight into the important variances that contribute to each disease.

Collectively, the data described above highlights the BCL6-IRF4-BLIMP1 axis as an important aspect of PTCL which, as for B-cell lymphoma, could potentially be dysregulated. Indeed, the incorrect expression of any of these genes could be considered tumorigenic. Thus the central hypothesis to be tested is: “BCL6 and IRF4 may promote, while BLIMP1 may repress, T-cell lymphoma development and/or maintenance and hence constitute a putative therapeutic target”. This will be explored in four parts:

- Aim 1: To analyse the role of BCL6 in the survival and proliferation of PTCL
- Aim 2: To analyse the role of IRF4 in the survival and proliferation of PTCL
- Aim 3: To analyse the role of BLIMP1 as a tumour suppressor in PTCL
- Aim 4: To evaluate the role of ALK in ALK+ ALCL in the regulation of BCL6, IRF4, and BLIMP1





## **Chapter 2: General Materials and Methods**



## 2. Materials and Methods

### 2.1 Mammalian cell culture

#### 2.1.1 Cell culture conditions

Lymphoma cell lines were cultured in plastic 75cm<sup>2</sup> flasks with a vent cap (Corning) at 37°C in Roswell Park Memorial Institute (RPMI) 1640 medium (Gibco) supplemented with L-glutamine and foetal calf serum (FCS) (Gibco) in a humidified atmosphere containing 5% CO<sub>2</sub>. HEK 293T cells were cultured in Dulbecco's Modified Eagles Medium (DMEM) 6171 (Sigma) supplemented with 10% (v/v) foetal calf serum (Gibco), 4mM L-glutamine (Sigma), and 10mM Sodium Pyruvate (Sigma). The cell lines used are listed in table 2.1. Table 2.1: List of cell lines used in this project. Suspension lymphoma cells were routinely sub-cultured every 2-3 days by transferring a fraction of culture to a new 75cm<sup>2</sup> flask with fresh 37°C medium. Adherent HEK 293T cells were sub-cultured every 2-3 days by initially separating the cells from DMEM medium and

Cell line	Lymphoma type	Media
SUDHL1	ALK+ Anaplastic Large Cell Lymphoma	RPMI-1640 + 10% FCS
Karpas-299	ALK+ Anaplastic Large Cell Lymphoma	RPMI-1640 + 10% FCS
DEL	ALK+ Anaplastic Large Cell Lymphoma	RPMI-1640 + 10% FCS
SUPM2	ALK+ Anaplastic Large Cell Lymphoma	RPMI-1640 + 10% FCS
SR786	ALK+ Anaplastic Large Cell Lymphoma	RPMI-1640 + 10% FCS
Mac1	ALK- Cutaneous Anaplastic Large Cell Lymphoma	RPMI-1640 + 10% FCS
Mac2a	ALK- Cutaneous Anaplastic Large Cell Lymphoma	RPMI-1640 + 10% FCS
FEPD	ALK- Anaplastic Large Cell Lymphoma	RPMI-1640 + 10% FCS
DL40	ALK- CD30+ Large T-cell Lymphoma	RPMI-1640 + 10% FCS
Karpas-384	γδ T-cell Non-Hodgkin Lymphoma	RPMI-1640 + 10% FCS
HDLM2	T-cell Hodgkin Lymphoma	RPMI-1640 + 20% FCS
SUDHL4	GCB Diffuse Large B-cell Lymphoma	RPMI-1640 + 20% FCS
Karpas-422	GCB Diffuse Large B-cell Lymphoma	RPMI-1640 + 20% FCS
Toledo	GCB Diffuse Large B-cell Lymphoma	RPMI-1640 + 10% FCS
Pfeiffer	GCB Diffuse Large B-cell Lymphoma	RPMI-1640 + 10% FCS
HLY-1	ABC Diffuse Large B-cell Lymphoma	RPMI-1640 + 10% FCS
H929	Multiple Myeloma	RPMI-1640 + 10% FCS
LP1	Multiple Myeloma	RPMI-1640 + 10% FCS
HEK 293T	-	DMEM + 10% FCS

**Table 2.1: List of cell lines used in this project**

Mac1 and Mac2a cell lines derived from the same patient. ALK = Anaplastic lymphoma kinase, GCB = Germinal Centre B, ABC = Activated B-cell, DLBCL = Diffuse Large B-cell lymphoma, RPMI = Roswell Park Memorial Institute, DMEM = Dulbecco's Modified Eagles Medium, FCS = Foetal Calf Serum.

washing briefly with 37°C phosphate buffer saline (PBS) (137mM Sodium Chloride, 2.7mM Potassium Chloride, 10mM Disodium Phosphate, 1.8mM Monopotassium Phosphate). Cells were then treated with 1ml of 1X Trypsin-EDTA solution (Sigma) and incubated at 37°C for 1 minute to allow detachment of cells from the flask. Next, trypsin-EDTA solution was neutralised using 9ml 37°C DMEM medium; cells were then transferred into a new 75cm<sup>2</sup> flask with fresh DMEM medium. All cell lines used were validated through LGC Standards prior to use.

### **2.1.2 Thawing of cryopreserved cells**

Cells, stored in freezing medium (section 2.1.4) in cryovials, were recovered from liquid nitrogen storage, thawed at 37°C and combined with 5ml of appropriate culture medium pre-warmed to 37°C. After brief centrifugation at 300g for 5 minutes to remove Dimethyl Sulfoxide (DMSO)-containing freezing medium, cells were resuspended in the appropriate medium and incubated at 37°C.

### **2.1.3 Counting cells using a Haemocytometer and Trypan Blue exclusion**

A haemocytometer contains two chambers of four gridded areas of 1mm<sup>2</sup> each of which containing sixteen individual 0.25cm<sup>2</sup> squares. A coverslip is applied to the grid which is held 0.1mm above the grid allowing accurate determination of the total volume in each grid square. To determine total number of cells, a sample is first combined in a 1:1 ratio with 0.4% Trypan Blue (Sigma) before being loaded into a single chamber and all non-blue cells which are encompassed inside the four 1mm<sup>2</sup> chambers are counted. The impermeable dye, Trypan Blue, cannot be taken up by living cells with intact membranes however dead cells will be stained blue by invasion of the dye and hence constitute a simple method of determining cell viability. Total viable cell number is calculated using the following formula:

$$\frac{\text{Total cell count}}{\text{Number of } 1\text{mm}^2 \text{ grids counted}} \times \text{Dilution factor} = \text{cells/ml} \times 10^4$$

### **2.1.4 Freezing cells**

For cryopreservation, exponentially growing cells were counted using Trypan Blue exclusion (section 2.1.3) and 5x10<sup>6</sup> cells were collected and centrifuged at 300g for 5 minutes. Supernatant was removed and cells were resuspended in 1ml standard



culture medium + 10% DMSO. DMSO is used as a cryopreservation agent. Cells were then transferred to cryovials (1ml/cryovial) and stored at -80°C, in a freezing container, for 24 hours before transferring to liquid nitrogen maintained at -196°C.

### **2.1.5 Mycoplasma testing**

All cell lines were routinely screened for mycoplasma infections by combining aspirates of cell culture medium with a mycoplasma detection reagent using the MycoAlert Mycoplasma Detection Kit (Lonza) according to the manufacturer's protocol. The kit measures the activity of mycoplasma enzymes which can be detected colourmetrically using a FLUOStar Omega Plate Reader (BMG Labtech). Cells were routinely screened for mycoplasma on a 6-week basis.

## **2.2 Drugs/Inhibitors**

### **2.2.1 BCL6 inhibitor, 79-6**

The BCL6 inhibitor, 79-6, was designed to target the BTB/POZ domain of BCL6 and prevent the interaction of BCL6 with co-repressors such as NCoR, BCoR, and HDACs (Cerchietti et al., 2010a). 79-6 was ordered from Merck Millipore, 50mg, product code: 197345. The drug was initially reconstituted in DMSO to a concentration of 100mM. Further dilutions were performed in DMSO and stored at -20°C. The chemical structure of 79-6 is shown in figure 2.1.

### **2.2.2 ALK inhibitor, Crizotinib**

Crizotinib is a dual c-MET and ALK inhibitor originally designed as a c-MET inhibitor. The drug was designed to target the ATP-binding site of c-MET thereby preventing the phosphorylating activity of the kinase (Cui et al., 2011). Crizotinib was ordered from SelleckChem, 5mg, product code: S1068. The drug was reconstituted in DMSO to a concentration of 40mM and subsequently diluted to working stocks in the µM range using sterile water and stored at -20°C. The chemical structure of Crizotinib is shown in figure 2.2. Recently the drug has been approved for use for use in ALK+ non-small cell lung carcinoma (NSCLC) due to its ability to also bind ALK with high avidity and prevent the phosphorylating activity of ALK (Gerber and Minna, 2010).

### **2.2.3 Lenalidomide**

Lenalidomide is a thalidomide analogue which has been utilised across multiple cancers. The drug works by targeting and inhibiting Cereblon, an E3 ubiquitin ligase, resulting in both direct anti-tumour and immunomodulatory effects (Breitkreutz et al., 2008, Gandhi et al., 2014). Lenalidomide was ordered from SelleckChem, 50mg, product code: S1029. The drug was reconstituted to a concentration of 200mM in DMSO. Chemical structure can be found in figure 2.3.

## **2.3 Resazurin viable cell assay**

### **2.3.1 Principle**

Resazurin is a blue dye which can be metabolised by mitochondrial enzymes to the pink fluorescent dye, Resorufin and hence used as a measure of metabolically active cells. Resorufin can be detected by absorbance at 570nm or by fluorescence at 585nm when excited at 570nm. The fluorescence produced is proportional to the metabolic activity of the population and therefore to the number of metabolically active cells in a given population but the assay cannot readily distinguish cytostatic or cytotoxic effects of a treatment.

### **2.3.2 Method**

Resazurin sodium salt was ordered from Sigma, 5g, product code: R7017. Upon arrival, Resazurin was reconstituted in sterile water (Gibco) to a final concentration of 100µg/ml and stored in 1ml aliquots at -20°C in the dark. In order to perform the assay, cells were first subjected to growth curve analysis to ascertain the correct seeding density required for up to 4 days growth at 37°C, 5% CO<sub>2</sub> (see chapter 3, section 3.2.9). Briefly, cells were counted by Trypan Blue exclusion (see section 2.1.3) before centrifuging at 300g for 5 minutes. Supernatant medium was then aspirated off and cells were then reconstituted in fresh medium to 1x10<sup>6</sup> cells/ml. This culture was then serially diluted to achieve a range of concentrations for analysis (see chapter 3, section 3.2.9). 100µl of each concentration of cells was then plated out, in triplicate, in a 96-well plate (COSTAR). Wells were surrounded with 100µl PBS to avoid evaporation. A control well containing medium-only was added to all plates to serve as a blank, the plate was then incubated at 37°C, 5% CO<sub>2</sub>, for 96 hours. After incubation, 11µl of

100µg/ml Resazurin reagent was added to each well, in the dark, and incubated at 37°C, 5% CO<sub>2</sub>, for a further 2 hours. After, fluorescence was detected using a FLUOStar Omega Plate Reader (BMG Labtech). Fluorescence was recorded at 590nm, data was normalised with respect to medium-only control well. For drug experiments, cells were counted by Trypan Blue exclusion (see section 2.1.3) before centrifuging at 300g for 5 minutes, supernatant was aspirated off and cells were reconstituted in fresh medium to double the final concentration required as determined by growth curve analysis (see chapter 3, section 3.2.9). 50µl of cell culture was then plated out, in triplicate, in a 96-well plate. To this 50µl of appropriate drug, at double the final concentration required, was added accordingly to the wells. Control wells containing either medium-only (blank) or cells and medium only (zero) were added and all wells were surrounded with 100µl PBS. Cells were then incubated at 37°C, 5% CO<sub>2</sub> for 72-120 hours according to experimental parameters. Resazurin reagent was added and measured as previously described. To analyse data, raw fluorescent values were calculated as a proportion of the zero control well. Values were plotted and respective IC<sub>50</sub> values determined using cell viability curves on GraphPad Prism 6.0 software.

## **2.4 siRNA knockdown**

### **2.4.1 Principle**

Naturally occurring short-interfering RNA (siRNA) is a double-stranded length of RNA, typically between 21 and 25 nucleotides, derived from double-stranded RNA (dsRNA), that utilises the RNA interference (RNAi) pathway to prevent translation of specific RNA sequences (Agrawal et al., 2003). Double-stranded RNA is cleaved by an RNase III nuclease, Dicer, creating an siRNA duplex with a two 3' nucleotide overhang on each strand. This duplex is then processed through the cellular RNAi machinery into single-stranded RNA (ssRNA) complementary to the target mRNA. The ssRNA combines with RNA-induced silencing complex (RISC) proteins, directing these to complementary mRNA sequences and where they effect post-transcriptional silencing either by mRNA degradation or by translational inhibition. Translational inhibition is favoured if sequence similarity is not perfect (Pratt and MacRae, 2009). Experimentally, synthetic siRNAs (usually 19-25 nucleotides in length) mimicking Dicer products are delivered to cells to artificially silence target transcripts. Typically, multiple siRNAs to the same target are used in combination to reduce the non-specific effects that a single siRNA

may exhibit, a single siRNA may knockdown other vital targets within a cell if too abundant.

### 2.4.2 Method

Sequences of siRNAs can be found in table 2.2. Lyophilised siRNA oligonucleotides (GE Dharmacon) were reconstituted using 1X siRNA Buffer (GE Dharmacon) to a final concentration of 20 $\mu$ M, divided into 5 $\mu$ l aliquots, and stored at -20 $^{\circ}$ C. To transfect suspension lines with siRNA, cells were first counted using Trypan Blue exclusion (section 2.1.3), 2x10<sup>6</sup> cells were then centrifuged at 300g for 5 minutes and medium was removed. Cell pellet was then resuspended in 200 $\mu$ l fresh 37 $^{\circ}$ C medium (final concentration 5x10<sup>6</sup> cells/ml) and loaded into a 4mm Electroporation Cuvette (Peqlab) before the adding 5 $\mu$ l of 20 $\mu$ M appropriate siRNA to achieve a final concentration of 500nM. Cells were then electroporated using the EPI2500 Pulse Generator (Fischer Scientific) according to voltages found in table 2.2. Optimal voltages were determined for each individual siRNA to achieve a voltage which resulting in sufficient knockdown with the least toxic effects (see chapter 3, section 3.2.2). Cells were electroporated for 10ms at appropriate voltages before standing at room

	Construct	Target Sequence (5'-3')	Voltage		
			SUDHL1	Karpas-299	SUDHL4
BCL6 SMARTPool siRNA	BCL6-001	CCUUAUUCGUCUCCGGAGU	260V	280V	340V
	BCL6-002	GUAUAUACCCGUACAACGU	260V	280V	340V
	BCL6-003	GUUAUAACUACUCCGGAGA	260V	280V	340V
	BCL6-004	CAUCAAGCCUCCUGUGAA	260V	280V	340V
IRF4 siRNA pool	IRF4-001	CCCACGGGCTCTATGCGAAA	260V	280V	340V
	IRF4-002	CAGGCCGTTTCTCATACTACA	260V	280V	340V
	Dharmacon Non-silencing siRNA #2	Sequence not provided	260V	280V	340V

Table 2.2: siRNA sequences and voltages for electroporation

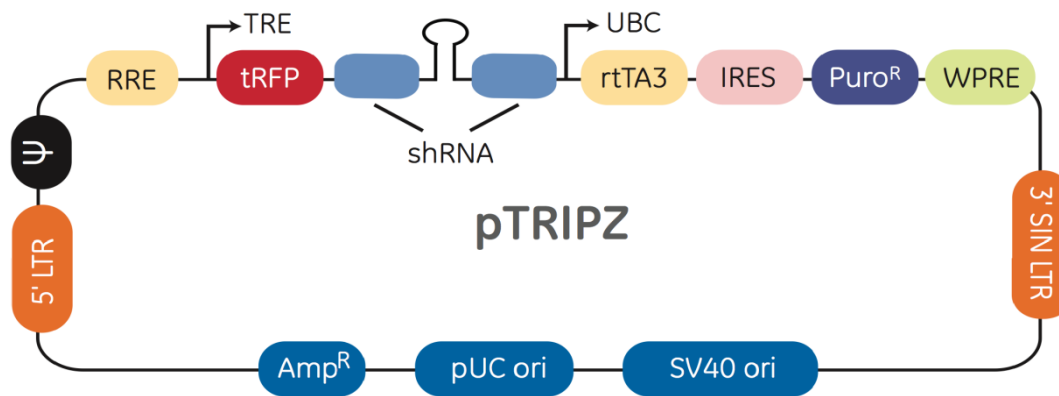


**Figure 2.4: Vector map of pTRIPZ taken from Thermo Scientific Technical Manual**

TRIPZ is a doxycycline-inducible vector driving the shRNA of choice and red fluorescent protein (RFP) from a doxycycline responsive cytomegalovirus promoter (TRE). The vector also contains an Internal Ribosome Entry Site (IRES) sequence which facilitates translation initiation from the within mRNA sequences. In addition, the vector contains bacterial antibiotic resistance genes for ampicillin (Amp<sup>R</sup>) and Zeomycin (Zeo) as well as the mammalian antibiotic resistance gene for puromycin (Puro<sup>R</sup>). Expression of puromycin resistance gene is constitutive and independent of doxycycline induction, driven by a Ubiquitin C (UBC) promoter, whilst expression of Amp<sup>R</sup> and Zeo is driven by the University of California (pUC) promoter. To allow integration into the host genome, 5' Long Terminal Repeat (LTR) and Self-inactivating LTR (sinLTR) regions are present. Additional plasmid components include: Central Polypurine Tract (cPPT) required for translocation of vector to the nucleus of non-dividing cells, Woodchuck Posttranscriptional Regulatory Element (WPRE) element which facilitates translational stability of transcripts, Reverse tetracycline transactivator (rtTA3) required for efficient induction via doxycycline, and Psi packaging sequence ( $\Psi$ ) which facilitates packaging of the vector. To induce the plasmid, doxycycline binds the rtTA3 element resulting in activation of the element. This then allows rtTA3 to bind the TRE promoter resulting in activation of transcription.

temperature for 15 minutes. Cells were then diluted to an appropriate concentration using fresh 37°C medium and transferred to a 6-well plate (CORNING) for culture at 37°C, 5% CO<sub>2</sub>.

## 2.5 Lentiviral-mediated transduction

### 2.5.1 Principle of shRNA

Lentiviral short-hairpin RNA (shRNA) knockdown is a mechanism of RNAi that can be used to inducibly or stably knockdown targets. Unlike siRNA, shRNA is introduced into a cell via a vector which can integrate into the genome. The inducible shRNA vector used in this project, pTRIPZ (figure 2.4), is designed to utilise the endogenous micro-RNA 30 (*miR-30*) pathway by incorporating a 22 nucleotide dsRNA and a 19 nucleotide loop from *miR-30* to the shRNA. This addition allows the shRNA to be recognised as a primary *miR-30* transcript and allows processing by Drosha in the nucleus to a pre-shRNA. After processing, pre-shRNA is exported out of the nucleus by

Exportin 5 before associating with Dicer resulting in the removal of the stem loop. At this point, the shRNA sequence is processing in the same manner as siRNA (see section 2.4.1) (Boden et al., 2004).

The shRNA system is more desirable over siRNA knockdown as the system utilises the endogenous micro RNA processing machinery that is used by the cell to produce functional micro-RNAs (Rao et al., 2009). However, high levels of shRNA may elicit an anti-viral response causing the activation of the innate immune system resulting in degradation of cellular mRNAs (Bumcrot et al., 2006).

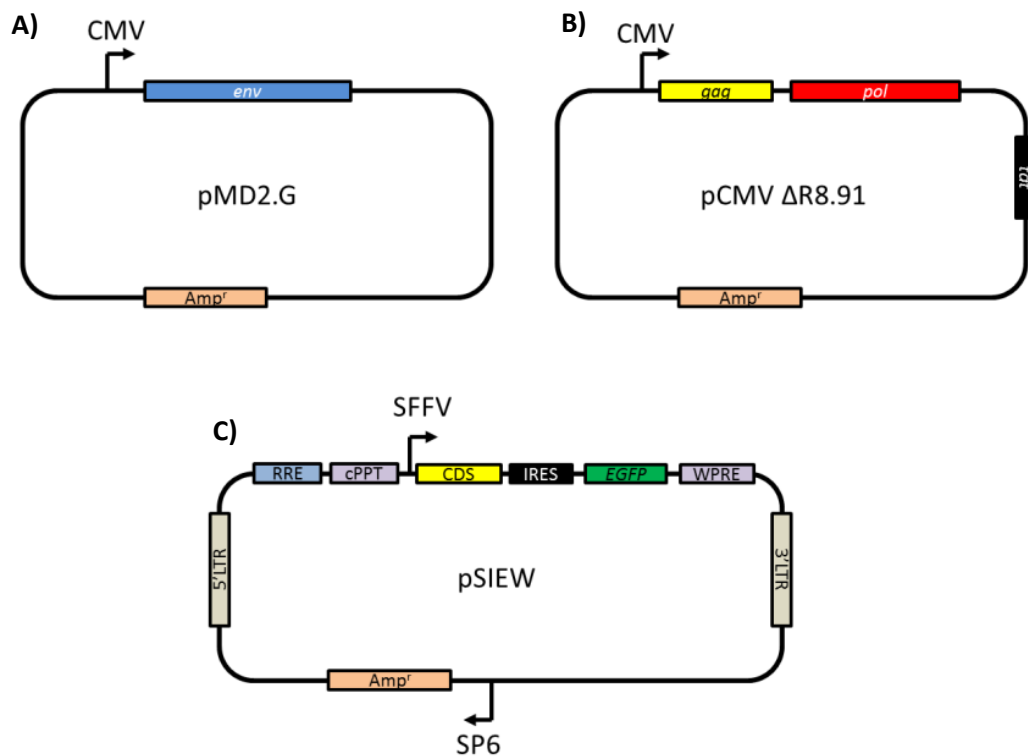


**Figure 2.5: Vector maps of packaging plasmids pMD2.G and pCMV ΔR8.91, and expression vector pSIEW**  
 Packaging vectors are used during transfection of cells: A) pMD2.G and B) pCMV ΔR8.91. The vectors contain the viral genes *pol*, *env*, and *gag* that together create a lentivirus as well as the *tat* gene to enhance transcription driven from a Cytomegalovirus (CMV) promoter. Viral genes are distributed between two vectors to prevent the formation of self-replicating lentivirus. C) Vector map for pSIEW. SIEW vector constitutively expresses a coding sequence of interest (CDS) and Green Fluorescent Protein (EGFP) from the Spleen Focus Forming Virus (SFFV) promoter. The vector also contains an Internal Ribosome Entry Site (IRES) sequence which facilitates translation initiation from within mRNA sequences. All vectors contain an ampicillin resistance gene (*Amp<sup>r</sup>*). SIEW resistance gene is driven by a SP6 promoter. To allow integration into the host genome, 5' and 3' Long Terminal Repeat (LTR) regions are present in the SIEW vector. Other elements in the SIEW vector include: Rev Response Element (RRE) and cPPT element both of which facilitate RNA translation, and the Woodchuck Posttranscriptional Regulatory Element (WPRE) required for enhancing expression from the vector.

### **2.5.2 Principle of overexpression**

In addition to TRIPZ, the pSIEW expression vector was utilised in this project (figure 2.5C). The expression vector allows constitutive transcription of a coding sequence resulting in significant production of target mRNA sequences. Expression constructs are used for multiple purposes such as: assessing the effect of ectopic expression of potential tumour suppressor genes on the survival of cells, or to produce peptides and antibodies.

For functional studies, reintroduced mRNA sequences typically lack 5' Untranslated Region (UTR) and 3'UTR elements; this can allow simultaneous knockdown of endogenous target (by targeting shRNA to UTR sequences) whilst expressing sequence of choice. This method is particularly useful for assessing the effect of mutated gene sequences on cellular function.

### **2.5.3 Principle of lentivirus generation**

One method of introducing viral vectors is lentiviral transduction whereby a lentivirus is engineered to deliver shRNA directly into the host genome. To produce functional lentivirus for transduction, transfer vectors must be packaged. Our packaging protocol involves transfecting HEK 293T cells with the transfer vector and two packaging vectors, using the calcium phosphate method (Kwon and Firestein, 2013). Simultaneous expression of the viral *pol*, *env*, and *gag* genes, together with the transfer vector, allows intracellular formation of intact viral particle, which is released into the culture medium (figure 2.6).

Cells of interest can be transduced with lentivirus to stably introduce a construct into the genome. It is important to achieve a balance between the level of expression of construct and the number of integrations, as the greater the number of integrations, the greater the chance of non-specific disruption of gene functions via integration of vector into the gene.

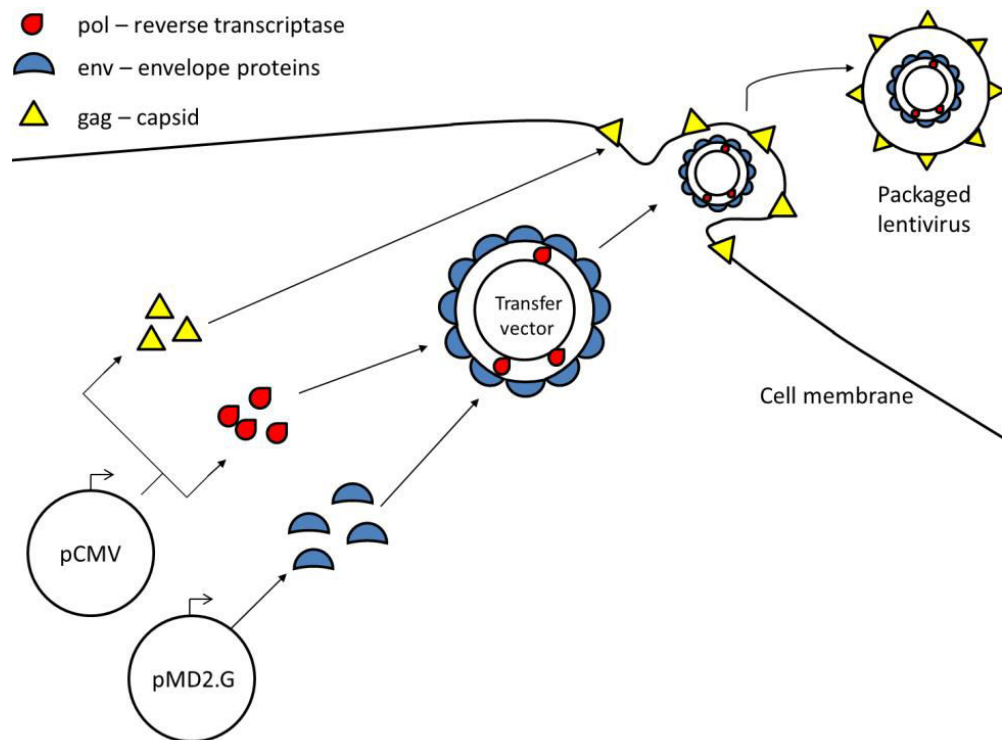


**Figure 2.6 Formation of a lentivirus particle**

Lentiviruses require three core components to create a functional infectious particle: a reverse transcriptase/integrase (encoded by the *pol* gene), envelope proteins (encoded by the *env* gene), and capsid proteins (encoded by the *gag* gene). After appropriate vectors, pCMV and pMD2.G, are transfected into HEK 293T cells transcription of the *pol*, *env*, and *gag* genes occurs from the vectors. The Pol integrase and transfer vector (pTRIPZ or pSIEW) are encapsulated by envelope proteins. Meanwhile, gag capsid protein coats the cell membrane. Finally, encapsulated transfer vector combines with gag-bound cellular membrane and is exocytosed producing a functional packaged lentivirus.

Target	Reference	Target Sequence (5'-3')
BCL6	V3THS_333939	TGACTGATGTTGTCATTGT
	V3THS_404721	AGGTGAACCATGTCAGCAA
	V2THS_132926	CAAAGGATACTGTAACACT
IRF4	V3THS_377531	CCAGCAGGTTCACTACTAC
	V3THS_377532	GGGGCTACGATTACCAGA
Non-silencing control	RHS4743	Not supplied

Table 2.3: shRNA sequences for TRIPZ vectors

## 2.5.4 Method

### 2.5.4.1 Culturing of lentiviral vector bacteria

All bacterial cultures were grown in Lysogeny Broth (LB) (10g Bacterial Tryptone, 10g Sodium Chloride, 5g Yeast Extract, 1L sterile water) containing 1µg/ml ampicillin at 37°C, with shaking, in autoclaved, foil-covered conical flasks unless stated otherwise. Cultures were split 1:500 with fresh LB for 16 hour incubations for general culturing. All bacteria work was conducted around a blue Bunsen burner flame.

### 2.5.4.2 Bacterial culturing of lentiviral vectors

Glycerol stocks of TRIPZ vector-containing bacteria were acquired from GE Thermo Scientific, sequences and references are found in table 2.3. pSIEW glycerol stocks were kindly donated by Dr. Paul Sinclair. Upon arrival, all glycerol stocks were stored at -80°C. To produce further stocks, a scraping of the current glycerol stock was taken using a sterile needle and mixed in 3ml of 1µg/ml ampicillin LB and incubated at 37°C for 8 hours with shaking in a sterile 20ml universal tube (Thermo Scientific) to produce a pre-culture. After 8 hours, up to 100µl of culture was pipetted onto an LB-1.5% agar plate (4g Bacto Agar (BD Biosciences, product code: 214010), 250ml LB) and spread evenly using a sterile spreader. LB-agar plates were then incubated at 37°C overnight. After incubation, individual colonies were selected for pre-culture. Briefly, using a p200 tip, individual colonies were lifted from agar plate and mixed with 3ml fresh 1µg/ml ampicillin LB in separate 20ml universal tubes. Cultures were then incubated at 37°C for 8 hours with shaking. After incubation, 1ml of each culture was centrifuged at 7,000g for 3 minutes whilst the remaining culture was stored at 4°C. Bacterial DNA was then isolated from centrifuged bacteria using a QIAprep Spin Miniprep kit (product code: 27106) according to the manufacturer's protocol. Presence

of plasmid was confirmed through use of restriction endonuclease digests and agarose gel electrophoresis. After confirmation, 200µl of plasmid-containing cultures were recovered from 4°C storage and mixed with 3ml fresh 1µg/ml ampicillin LB, in a universal tube, before incubating at 37°C with shaking for 8 hours. Cultures were then transferred to conical flasks and mixed with 150ml of fresh 1µg/ml ampicillin LB before incubating at 37°C for with shaking for 16 hours. To produce glycerol stocks, 500µl of bacterial culture was then combined with 500µl of 80% autoclaved glycerol (diluted with sterile water) and transferred to a cryovial. Samples were then stored at -80°C. The remaining culture was utilised for large-scale isolation of bacterial vector. Cultures were divided evenly into 50ml falcon tubes (CORNING) and centrifuged at 3,000g for 15 minutes. LB supernatant was then removed and plasmid DNA isolated from bacterial pellet using the Endofree Plasmid Maxi Kit (Qiagen) according to the manufacturer's protocol. All plasmids were reconstituted in 100µl TE Buffer (10mM Tris.Cl, pH 8.0, 1mM EDTA) and stored at -20°C. PlasmidDNA was quantified using a NanoDrop ND-1000UV spectrophotometer 128 (NanoDrop Technologies). Vector maps can be found in figures 2.4 and 2.5.

#### ***2.5.4.3 Transfection of HEK 293T cells***

2x10<sup>5</sup> HEK 293T cells were suspended in 10ml DMEM medium in 100mm culture dishes (COSTAR) prior to transfection and incubated at 37°C, 5% CO<sub>2</sub> for 24 hours. Next, for each individual transfection plate; 5µg of pMD2.G vector, 15µg pCMV ΔR8.91 vector, and 20µg transfer vector (TRIPZ or SIEW) were combined with 2.5µM HEPES in sterile water, pH 7.3 (Sigma, product code: H3375) at room temperature to a final volume of 250µl in a 1.5ml tube. To this, 250µl 0.5M Calcium Chloride solution to a final concentration of 0.25M and 500µl 2XHeBS solution (560mM NaCl, 100mM HEPES, 3mM Na<sub>2</sub>HPO<sub>4</sub>, pH 7.0) was added to the vector mixture and incubated at room temperature for 30 minutes to form calcium phosphate precipitates. After incubation, the transfection solution was added directly to HEK 293T plates and incubated at 37°C, 5% CO<sub>2</sub> for 24 hours. Next, medium was aspirated off the plates and cells were washed in PBS before applying fresh medium. Cells were incubated at 37°C, 5% CO<sub>2</sub> for 72 hours to allow formation of lentiviral particles. Finally, supernatant was harvested and centrifuged at 86,000g for 120 minutes at 4°C to concentrate virus.

Concentrated virus was resuspended in RPMI+10% FCS media and stored at -80°C in 50µl aliquots. All vectors were packaged using this technique.

#### **2.5.4.4 Transduction of suspension cell lines**

Prior to transduction, cells were counted using Trypan Blue Exclusion (section 2.1.3).  $5 \times 10^5$  cells were then centrifuged at 300g for 5 minutes, and resuspended in 5ml of fresh medium in a universal tube. To this, 5µl of 8mg/ml polybrene (Merck Millipore, product code: TR-1003-G, stored at -20°C) was added to achieve a final concentration of 8µg/ml. 500µl of culture was then immediately plated in a 48-well plate (COSTAR) and surrounding wells filled with 500µl PBS to avoid evaporation. Cells were then treated with appropriate concentrations of viral particles, sealed using Parafilm, and transduced by centrifuging at 900g for 50 minutes at 34°C. After spinfection, Parafilm was removed, and cells were cultured as normal at 37°C, 5% CO<sub>2</sub>.

#### **2.5.4.5 Induction and selection of transduced suspension cell lines**

To induce TRIPZ-transduced cells, doxycycline was required. Doxycycline was acquired from Sigma, product code: D9891-1G, resuspended in sterile water and stored at -20°C in 1ml aliquots. Transduced cells were treated with doxycycline to a final concentration of 2µg/ml and incubated at 37°C for 72 hours. Red Fluorescent Protein (RFP) levels for TRIPZ vectors, and Green Fluorescent Protein (GFP) levels for SIEW vectors, were detected using a FACSCalibur (BD Biosciences) (see section 2.8.2.2). For each cell line, optimal puromycin (Santa Cruz Biotechnology, product code: CAS 58-58-2, stored at -20°C) concentration for selection was determined by incubation of cells for 72 hours with a range of puromycin concentrations followed by assessment by Resazurin. Briefly, 100µl of non-transduced cells were seeded in a 96-well plate at  $1 \times 10^5$  cells/ml and treated with 1µl puromycin to a final concentration of either 0µg/ml, 0.5µg/ml, 1µg/ml, 2µg/ml, or 4µg/ml. Wells were then surrounded with 100µl PBS and cells were incubated at 37°C. After 72 hours, cells survival was assessed by Resazurin (section 2.3). The concentration of puromycin which killed all cells after 72 hours was selected for each cell line. Concentrations of puromycin used were: 4µg/ml for SUDHL1, 2µg/ml for Karpas-299 and DEL, and 1µg/ml for SUDHL4. Puromycin was acquired from Santa Cruz Biotechnology, product code: sc-108071A, resuspended in sterile water and stored in 100µl aliquots at -20°C. Volumes of virus that produced

approximately 30% RFP/GFP-positivity as determined by flow-cytometry (the Poisson distribution dictates that a 30% transduction efficiency denotes a high probability of a single integration per cell across the culture) were selected using puromycin.

## **2.6 Protein analysis**

### **2.6.1 Protein extraction**

5x10<sup>6</sup> cells were centrifuged at 300g for 5 minutes at 4°C and washed twice in cold PBS. Cell pellets were then lysed in Radioimmunoprecipitation buffer (RIPA) lysis buffer (50mM Tris, 150mM NaCl, 1% Sodium Deoxycholate, 1% Triton X-100, 0.1% SDS) (Harlow and Lane, 2006) supplemented with protease and phosphatase inhibitors (1mM Aminoethyl benzenesulfonyl hydrochloride, 800nM Aprotinin, 50µM Bestatin, 15µM E-64, 5µM EDTA, 20µM Leupeptin, 10µM Pepstatin A) and incubated on ice for 30 minutes. Following incubation, samples were subjected to sonication using a Soniprep 150 Plus Sonicator (Measuring and Scientific Equipment) for 10 seconds at an amplitude of 5.0. Finally, lysate was centrifuged at 16,000g for 15 minutes at 4°C and supernatant collected. Lysate was stored in RIPA buffer at -20°C.

### **2.6.2 Protein quantification**

Protein was quantified using the Pierce Bicinchoninic Acid (BCA) Assay and FLUOStar Omega microplate reader (BMG-Labtech) according to the manufacturer's protocol. The BCA assay measures the reduction of Cu<sup>2+</sup> ions to Cu<sup>+</sup> ions by proteins which then reacts with BCA to produce a purple colouring which can be detected at an absorbance of 562nm (Tuszynski and Murphy, 1990). By plotting a standard curve of known protein concentration, unknown protein concentrations can be determined by their absorbance.

### **2.6.3 SDS-PAGE**

#### **2.6.3.1 Principle**

Sodium Dodecyl Sulphate Polyacrylamide Gel Electrophoresis (SDS-PAGE) is a process by which proteins can be separated on a gel according to their molecular weight. Protein separation is achieved by conferring a negative charge to proteins by combining protein sample with a loading buffer, typically containing SDS and β-mercaptoethanol, and boiling the protein sample. When loaded into a gel and a

current applied, charged protein will be repelled from the anode and migrate through the gel. Once separated, proteins are transferred to membrane by the same electrical stimulus. Proteins of interest are visualised by using primary antibodies against the denatured form of that protein. Once bound, a secondary antibody is applied with a conjugated horseradish peroxidase (HRP)-tagged epitope attached. The addition of Electrochemiluminescence (ECL) results in the metabolism of HRP resulting in the emission of light, therefore allowing antibody-bound proteins to be detected using an X-Ray film.

### **2.6.3.2 Method**

Reagents used for SDS-PAGE are found in table 2.4. SDS-PAGE was performed using a 1.5mm 8% acrylamide gel due to the range of protein sizes detected (~140-50kDa in size) (table 2.4). 20µg of total protein lysate was combined with 5µl of 4X sample loading buffer (1ml 4X SDS sample buffer table 2.4, 5% β-mercaptoethanol, 0.04% Bromophenol Blue) and combined with RIPA buffer to a final volume of 20µl in a clean 1.5ml tube. Sample was then denatured by heating to 100°C for 5 minutes before centrifuging at full speed for 10 seconds. Gels were then assembled into a Mini-PROTEAN® 3 system tank (Bio-Rad) and filled with 500ml 1X Running Buffer (100ml 10X Running Buffer (table 2.4), 900ml deionised water). Protein samples were then pipetted into wells of gel; 15µl of Spectra™ Multicolour Broad Range Protein Ladder Standards (Thermo Scientific) was also loaded adjacent to protein samples. After, gel tank was filled with remaining 500ml 1X Running Buffer. Electrophoresis was then performed at a constant 120V for 90 minutes.

Western blot analysis was performed by transferring proteins from SDS-PAGE gel to an Immobilon-P PVDF membrane (Millipore) at 100V for 1 hour using the Mini Trans-Blot System (Bio-Rad). Briefly, PVDF membrane was activated by incubating in methanol for 5 minutes at room temperature, before equilibrating in 1X Transfer buffer (200ml 5X Transfer Buffer (table 2.4), 200ml Methanol, 600ml deionised water) for 5 minutes at room temperature. After, gel and PVDF membrane were placed together and flanked by two sponges and two transfer buffer-soaked filter papers.

Product	Reagent	Ingredients	Storage	Volume required
Acrylamide Gel	8% Resolving Gel	Protogel: 30% acrylamide, 0.8% bisacrylamide (Gene Flow, product code: A2-0072)	Room temperature	2.7ml
		4X Resolving Gel Buffer: 1.5M Tris-HCl, 0.4% SDS, pH 8.8 (Gene Flow, product code: B9-0012)	Room temperature	2.6ml
		N, N, N', N'- Tetramethylethylenediamine (TEMED) (Sigma, product code:T9281-25ml)	Room temperature	10µl
		Ammonium Persulphate (APS) (Sigma, product code: A3678-25g)	Powder: Room temperature Liquid: combine 500mg with 5ml of sterile water, aliquot into 100µl and store at -20C	30µl
		Sterile Water (Gibco, product code:10977-049)	Room temperature	4.7ml
	6% Stacking Gel	Protogel	Room temperature	1ml
		Protogel Stacking Buffer: 0.5M Tris-HCl, 0.4% SDS, pH 6.8 (Gene flow, product code: B9-0014)	Room temperature	1.25ml
		TEMED	Room temperature	10µl
		APS	Powder: Room temperature Liquid: combine 500mg with 5ml of sterile water, aliquot into 100µl and store at -20C	50µl
		Sterile Water	Room temperature	2.75ml
		4X SDS Sample buffer (50ml)	250mM Tris pH 6.8	Room temperature
	40% Glycerol		Room temperature	20ml
	8% SDS		Room temperature	4g
	Sterile Water		Room temperature	Add until 40ml total volume, pH to 6.8, then top up to 50ml with sterile water
10X Running Buffer	25mM Tris	Room temperature	60g	
	192mM Glycine	Room temperature	288g	
	0.1% SDS	Room temperature	20g	
	Sterile Water	Room temperature	Add until total volume 2L	
5X Transfer Buffer	25mM Tris	Room temperature	4g	
	192mM Glycine	Room temperature	14.4g	
	0.0075% SDS	Room temperature	750mg	
	Sterile Water	Room temperature	Add until total volume 2L	
10X TBS pH 7.6	20mM Tris	Room temperature	48.4g	
	150mM Sodium Chloride	Room temperature	175.32g	
	Sterile Water	Room temperature	Add until total volume 1.6L, pH to 7.6 with HCl, then add until total volume is 2L	

Table 2.4: Recipes for commonly used western blot reagents

Antibody	Clone ID	Company	Dilution
BCL6	SP155	Spring Biosciences	1/1,000
IRF4	EP5699	Epitomics	1/10,000
BLIMP1	C14A4	Cell Signalling	1/1,000
c-MYC	Y69	Abcam	1/1,000
$\alpha$ -tubulin	DM1A	Sigma	1/10,000
Polyclonal Goat Anti-Rabbit, HRP tagged	P0448	Dako	1/10,000
Polyclonal Goat Anti-Mouse, HRP tagged	P044701	Dako	1/10,000

**Table 2.5: List of antibodies used for western blot analysis**

All membranes were incubated with primary antibodies overnight at 4°C and secondary antibodies were incubated for 1 hour at room temperature.

Transfer membranes were blocked in 1XTBS (100ml 10X TBS (table 2.4), 900ml deionised water)-0.1% Tween+5% milk for 1 hour at room temperature. Membranes were then incubated with primary antibody, diluted in 1XTBS-0.1% Tween-5% milk overnight. After incubation, membranes were subjected to 2x10 minute washes in 1XTBS-0.1% Tween before incubating with the appropriate secondary antibody, diluted in 1XTBS-0.1% Tween-5% milk for 1 hour at room temperature. All antibodies used are found in table 2.5.

To detect protein, membranes were subjected to 4x10 minute washes in 1XTBS-0.1% Tween before addition of 1ml ECL detection reagent (GE Healthcare, product code: RPN2209) per membrane and incubation at room temperature for 1 minute. Membranes were then wrapped in Saran Wrap and affixed to an X-Ray film cassette. Amersham Hyperfilm (GE Healthcare, product code: 28-9068-37) was then exposed to the membrane, in a dark room, and developed using an automated developer.

To strip membranes for future antibody probing, membranes were incubated in a glass container with 20ml stripping buffer (2.5ml 0.5M Tris pH 6.8, 2ml 20% SDS, 140 $\mu$ l 2- $\beta$ -mercaptoethanol, 15.4ml sterile H<sub>2</sub>O) in a 60°C shaking water bath for 30 minutes. Membranes were then subjected to 4x10 minute 1XTBS-0.1% Tween washes, at room temperature, before blocking in 1XTBS-0.1% Tween-5% milk for 1 hour at room temperature. After which, membranes were ready for fresh primary antibody.

## 2.7 Gene expression analysis by Quantitative-PCR (qPCR)

### 2.7.1 Principle

Quantitative Reverse Transcription PCR (qRT-PCR) is a method used to quantify relative RNA levels between samples through use of a DNA-binding fluorescent dye. For qRT-PCR to assess mRNA transcript level, RNA is first extracted from cells and reverse transcribed to produce cDNA. The cDNA is combined with the fluorescent SYBR® Green compound which, when bound to nucleic acids, emits a green fluorescent light which can be detected 520nm. Therefore, absolute and relative cDNA levels between samples can be calculated by measurement of fluorescence intensity at 520nm. To produce fluorescent signal strong enough to detect, forty rounds of PCR are undertaken with target-specific primers. Each successive PCR product is bound by SYBR® Green and hence doubles the original level of fluorescing compounds, qPCR machines can detect the intensity of fluorescence after each cycle of PCR and can quantify DNA levels by measuring the number of cycles required to achieve a certain threshold (Cycle Threshold – Ct) of fluorescence intensity. Relative expression of one product compared to another can then be calculated using the  $2^{\Delta\Delta Ct}$  method (Livak and Schmittgen, 2001):

$$\Delta Ct = Ct_{target} - Ct_{reference}$$

$$Relative\ Expression = 2^{(\Delta Ct_{target} - \Delta Ct_{control})}$$

### 2.7.2 RNA extraction and cDNA synthesis

$2 \times 10^6$  cells were harvested for RNA extraction by centrifuging cell cultures at 300g for 5 minutes in a 20ml universal tube. RNA was extracted from cell lines using the EZ-RNA (Biological Industries, product code: K1-0120) extraction kit, following the manufacturer's protocol, and eluted in RNase-free water (Gibco). RNA was stored at -80°C. The concentration of each sample was determined using a NanoDrop ND-1000 UV spectrophotometer 128 (NanoDrop Technologies). Reverse transcription was performed with 500ng of RNA using the RevertAid™ H Minus First Strand cDNA Synthesis kit (Fermentas International Inc., product code: K1632), using a random hexamer primer and reverse transcriptase provided in the kit, according to the

manufacturer's instructions. Briefly, the reverse transcription was performed with the following parameters: 25°C for 10 minutes, 42°C for 60 minutes, 70°C for 5 minutes. Samples were then stored at -20°C until required.

### 2.7.3 SYBR® Green qPCR

Relative gene expression assays were performed on a 384-well plate using the 7900HT Sequence Detection System (Applied Biosystems) with the SYBR® Green Assay kit (Invitrogen). Expression of target genes was analysed using primers in Table 2.5.

Primers were designed using PrimerQuest software (Integrated DNA Technologies) to the following criteria: a GC content of 50%, a melting temperature of 60-65°C, and an amplified sequence that spans an intron-exon boundary of approximately 200 bases. The specificity of each primer was determined using a melting curve analysis to ensure no primer dimers were formed. Lyophilised primer oligonucleotides were synthesised by Sigma and reconstituted in sterile water (Gibco) to a final concentration of 100µM. Primers were then stored at -20°C. Each qPCR well contained: 5µl Platinum SYBR® Green (Invitrogen), 0.4µl of 2.5µM forward primer (final concentration 100nM), 0.4µl of 2.5µM reverse primer (final concentration 100nM), 3.2µl nuclease-free H<sub>2</sub>O, 1µl cDNA. Each sample was plated in triplicate for each primer set and every primer set contained a null-template control well to confirm absence of contamination. Plate was then sealed with a MicroAmp film lid (Life technologies, product code: 4309849). The plate was then centrifuged at 1,000g for 1 minute prior to PCR cycling.

Target	Forward (5'-3')	Reverse (5'-3')
BCL6	CAAGACCGTCCATACCGGTG	GCCCCACAGATGTTGCAAC
IRF4	AGGATTGTTCTGAGGGAGCCAAA	ACCAATGTCCCATGACGTTTGGAC
BLIMP1α	TCCAGCACTGTGAGGTTTCA	TCAAACCTCAGCCTCTGTCCA
BLIMP1β	GTA CTCTGTGGTGGGTTAATCG	ACACAAATGTTCA TTTAAGGAGCTG
c-MYC	GTCTCCACACATCAGCACAAC	GTTTCGCCTCTTGACATTCTCCT
GAPDH	GAAGGTGAAGGTCGGAGTC	GAAGATGGTGATGGGATTTTC
RPL13A	TGAGTGAAAGGGAGCCAGAAG	CAGACCTGGCATT CATGTGGCTTT
p21	CCTCATCCCGTGTTCCTTT	GTACCACCCAGCGGACAAGT
TP53	CCCTTCCAGAAAACCTACC	AATCAACCCACAGCTGCAC
ATR	TCTCTGCAGGGTTTGTGGCTGTTT	AAGTGCTTCACCCATGCTCCCTAT
B2M	GCCGTGTGAACCATGTGACT	GCTTACATGTCTCGATCC
HPRT	CGTCTTGCTCGAGATGTGAT	GCACACAGAGGGCTACAATGTG

Table 2.5: Primers used for quantitative PCR analysis

The following cycling parameters were used: 95°C for 2 minutes followed by 40 cycles of 95°C for 15 seconds (melting) and 60°C for 1 minute (annealing/extension). Data was analysed using Applied Biosystems Sequence Detection System v2.3. Relative gene expression was calculated for each sample using the  $2^{-\Delta\Delta C_t}$  method (Livak and Schmittgen, 2001). The results were normalised to either RPL13A or GAPDH expression. RPL13A was chosen for 79-6 experiments (see chapter 3, section 3.2.10) for consistency with previously published literature. However, both RPL13A and GAPDH expression did not vary with 79-6 inhibitor treatments in this study.

## **2.8 Flow cytometry**

### ***2.8.1 Principles of flow cytometry***

Flow cytometry is a laser-based technique used to detect fluorescent particles on or within individual cells in a stream passing through a detection apparatus. Cells can be fixed to prevent the degradation and lysis of cells during preparation. Cells can be chemically fixed by two means: with a cross-linking reagent such as formaldehyde or with a denaturing solution such as ethanol (Warnes, 2014). Cross-linking reagents bind to intracellular components and cause intramolecular and intermolecular bonds to form resulting in a “stasis” of cellular components. Denaturing solutions replace the intracellular fluids and cause denaturation of protein tertiary structures (Warnes, 2014). Fixed cells are then treated with either fluorescent antibodies to specific cell surface or intracellular proteins or a fluorescent dye for analysis. Cells are passed through a flow cytometer and fluorescence data is collected as illustrated in figure 2.7.

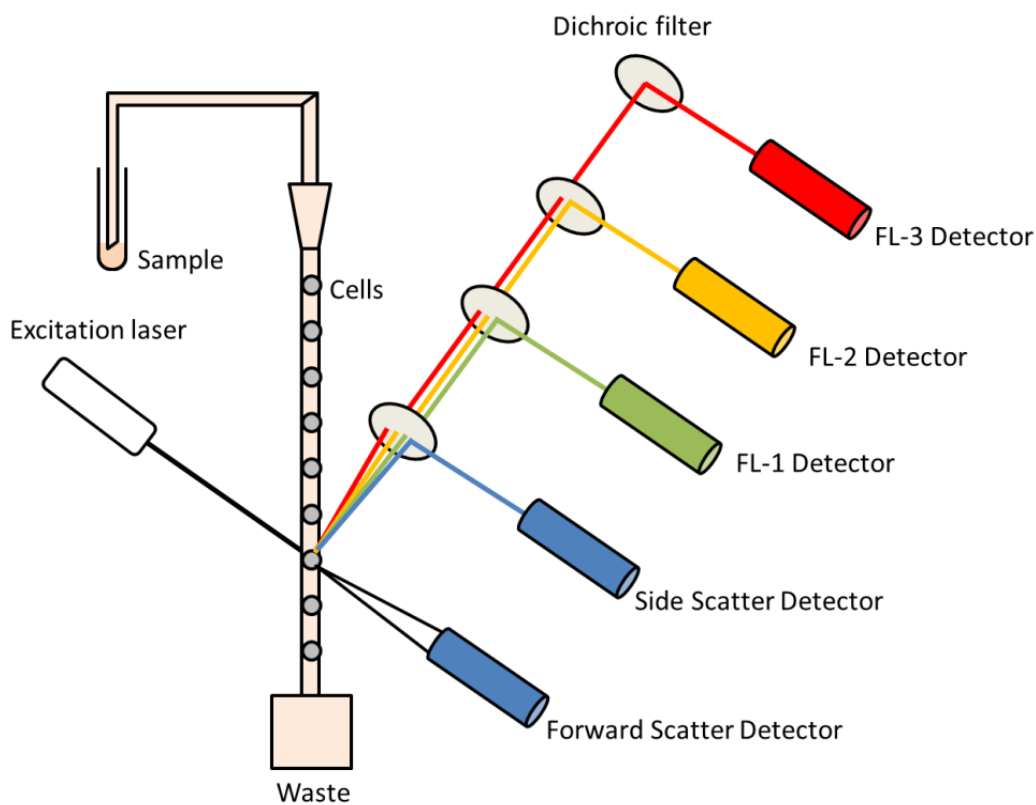


**Figure 2.7: Principles of a flow cytometer**

Cells are aspirated into the flow cytometer and combined with an isotonic fluid which helps align and force the cells into a single stream. The cells then pass through an excitation laser of known wavelength (typically 488nm) which, upon contact with the cell, is split into two directions. Light scattered by cells at an angle  $<10^\circ$  are detected by a forward scatter detector; this is generally regarded as a measure of the size of a cell. The remaining light is scattered  $90^\circ$  in relation to the original source and passes through a number of dichroic filters to separate out the various wavelengths. The first wavelength filtered is 488nm which is detected by a side scatter detector; this is generally regarded as a measure of cellular granularity. Further filters are applied separating wavelengths of 515-545nm (FL-1), 564-606nm (FL-2),  $>650$ nm (FL-3) which are detected by various fluorescent detectors. Other fluorescent detectors are available for specialist flow cytometers.

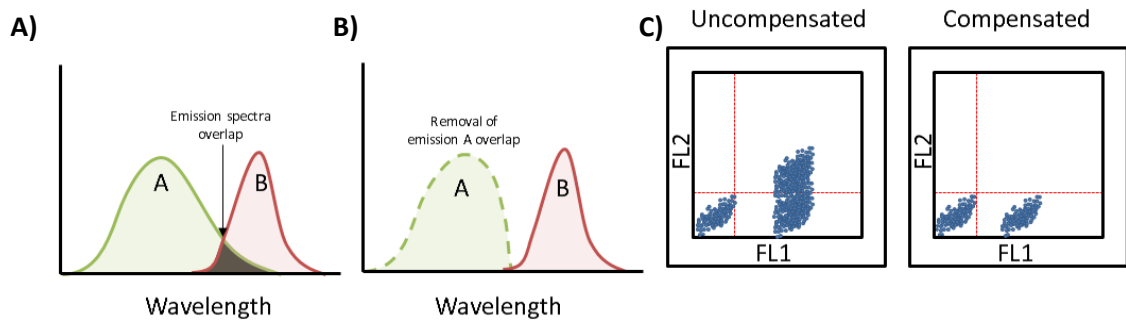


**Figure 2.8: Compensation of fluorescent channels**

A) Emission spectra for two fluorochromes. The emission spectrum of fluorochrome A overlaps the emission spectrum of fluorochrome B. B) Compensation subtracts the fluorescence observed from fluorochrome A to accurately measure fluorochrome B. C) Example of uncompensated and compensated plots for an FL1 fluorochrome observed during the compensation process. Each quadrant defines a population. The bottom-left quadrant is defined by non-stained cells, the top-left quadrant is an FL2-positive population, bottom-right quadrant is an FL1-positive population, and top-right is an FL1 and FL2-positive population. Uncompensated FL1 fluorescence is detected by the FL2 detector, compensation removes aberrant FL2 readings.

To analyse multiple fluorescent channels at once, a process known as compensation must be undertaken. This process involves the removal of emission spectrum from one fluorochrome from a detector designed to measure emission from a different fluorochrome to accurately conduct multicolour analysis. Compensation is necessary when the physical emission spectra of two fluorochromes overlap (figure 2.8).

Lymphoma cell lines: SUDHL1, DEL, Karpas-299, and SUDHL4 underwent compensation before any experiments were conducted. The FL1 fluorescent channel was compensated using GFP-expressing cells, the FL2 channel was compensated using RFP-expressing cells, and the FL3 channel was compensated using 7-aminoactinomycin D staining (7-AAD).

## **2.8.2 Method**

### **2.8.2.1 Propidium Iodide staining for cell cycle analysis**

Propidium Iodide (PI) is a dye which binds cellular DNA and RNA which can be used to visualise cell cycle profiles. To stain,  $1 \times 10^6$  cells were harvested by centrifuging at 300g for 5 minutes, supernatant removed and resuspended in 1ml PBS before centrifuging at 300g for 5 minutes. After, PBS supernatant was removed and cells were immediately fixed with 500 $\mu$ l 4 $^{\circ}$ C 70% ethanol in a 1.5ml tube for 30 minutes on ice. At this stage, fixed cells could be stored at 4 $^{\circ}$ C until required. Next, cells were washed

twice in PBS (400g for 5 minutes), supernatant removed, and resuspended in 50µl of 100µg/ml RNase (Sigma, product code: R6513-10MG) and transferred to a Polystyrene Falcon Round Bottom Tube (CORNING, product code: 352054). The addition of RNase causes the degradation of RNA within a sample so that only DNA is stained. Next, 200µl of 50µg/ml PI (Sigma, product code: 81845-25mg) was added to each sample and incubated at room temperature, in the dark, for 30 minutes. PI-stained cellular DNA content was analysed using the FACSCalibur flow cytometer (BD Biosciences). A total of 10,000 events were analysed. Cell cycle data was collected using CellQuest software (BD Biosciences, England) and analysed using Cyflogic software (CyFlo, Finland). RNase was resuspended in sterile water (Gibco) and stored at 4°C.

### 2.8.2.2 Detection of GFP and RFP transduced cells

5x10<sup>5</sup> cells containing pSIEW or induced pTRIPZ vectors were harvested by centrifuging at 300g for 5 minutes, washed once in PBS (300g for 5 minutes), PBS was then removed and cells were fixed for 30 minutes on ice with 500µl Cytofix/Cytoperm solution (BD Biosciences, product code: 554722). Cells were then centrifuged at 300g for 5 minutes, supernatant removed, then washed once with 500µl Perm/Wash Buffer (BD Biosciences, product code: 554723) (300g for 5 minutes) and resuspended in 500µl

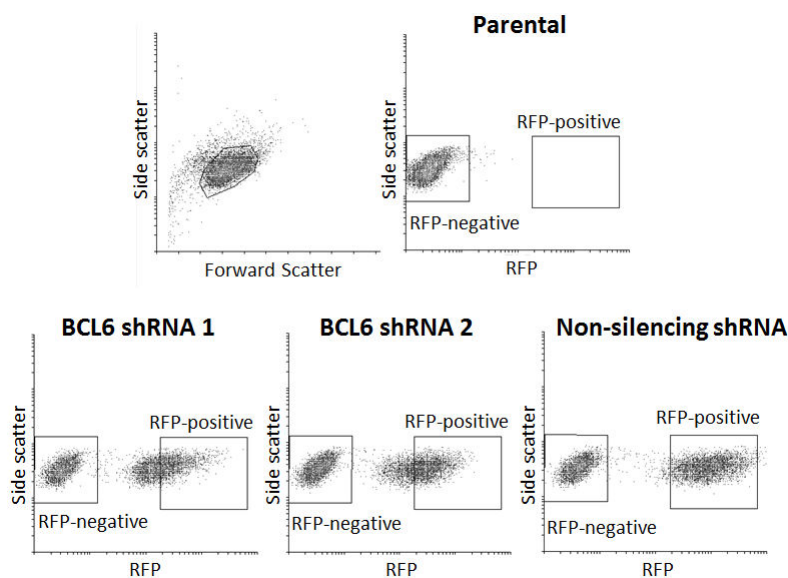


**Figure 2.9: RFP-gating strategy**

A) Gating strategy for all RFP-tracking experiments. Live cell population defined by left panel, RFP trace for non-transduced cells defined in the right panel. Subsequent RFP expression is assessed from live cell population only. B) Example traces of RFP expression in a mixture of Parental cells and Non-silencing shRNA TRIPZ-transduced cells induced with 0.5µg/ml doxycycline for 72 hours. RFP-positive cells are defined as expressing RFP at greater-than-or-equal-to 1 log greater than the highest expressing RFP-negative population to prevent any overlap of the two populations.

Perm/Wash Buffer before transferring to a Polystyrene Round Bottom Tube (CORNING). Data was collected using the FACSCalibur flow cytometer (BD Biosciences) with CellQuest software (BD Biosciences, England). A total of 10,000 events were collected. RFP-positive cell populations are defined as in figure 2.9. GFP-positive populations are defined separately for each experiment. Data was analysed using Cyflogic software (Cyflo, Finland).

### **2.8.2.3 BrdU/7-AAD staining for cell cycle analysis**

Bromodeoxyuridine (BrdU) is a thymidine analogue which can be incorporated into newly synthesised DNA (Lehner et al., 2011). 7-AAD is a DNA-stain. Together, the two molecules allow accurate identification of the cell cycle phase of cells within a sample. BrdU-positive cells represent those undergoing replication (S-phase) whilst 7-AAD staining produces two populations, based on fluorescent intensity, of G1/G0 and G2/M stage cells. By allowing the incorporation of BrdU into cellular DNA and treating with a fluorescent antibody against BrdU before staining with 7-AAD these populations can be measured.

Cells to be analysed were treated with 10µl of 1mM BrdU per 1ml of culture and incubated for 30 minutes at 37°C, 5% CO<sub>2</sub> before being harvested by centrifuging at 300g for 5 minutes, at least 5x10<sup>5</sup> cells were harvested. The supernatant was then removed, and the cell pellet was fixed with 500µl Cytofix/Cytoperm solution (BD Biosciences) for 30 minutes on ice. Cells were then treated using the FITC BrdU/7-AAD assay kit (BD Biosciences, product code: 559619) according to the manufacturer's protocol. Data was collected using the FACSCalibur flow cytometer (BD Biosciences) using CellQuest software (BD Biosciences, England). A total of 10,000 events, determined to be RFP-positive and high expressors by FL-2 gating, were analysed. High expressing RFP-positive cells were defined as shown in figure 2.9. Data was analysed using Cyflogic software (CyFlo, Finland).

### **2.8.2.4 Active caspase-3 staining for apoptosis analysis**

Caspase-3 is a procaspase protein which is cleaved to an active caspase-3 protein to initiate apoptosis (McIlwain et al., 2013). FITC-labelled anti active caspase-3 fluorescent antibodies can be used as an indicator of apoptosis in cells. The level of

FITC fluorescence is directly proportional to the levels of active caspase-3 present in cells and is hence an indicator of apoptosis.

Cells to be analysed were first harvested by centrifuging at 300g for 5 minutes ( $5 \times 10^5$  cells). Supernatant was then removed and cells were washed once in PBS (300g for 5 minutes). PBS was then removed and the cell pellet was then fixed in Cytotfix/Cytoperm solution (BD Biosciences) for 30 minutes on ice. The cells were then centrifuged at 300g for 5 minutes and washed twice in Perm/Wash Buffer (BD Biosciences) (300g for 5 minutes) before resuspending cell pellet in in 25 $\mu$ l FITC active caspase-3 antibody (BD Biosciences – product code: 550480, diluted 1:5 in Perm/Wash Buffer) for 30 minutes at room temperature. 500 $\mu$ l of Perm/Wash Buffer was then added to the cells and transferred to Polystyrene Round Bottom Tubes (CORNING). Data was collected using the FACSCalibur flow cytometer (BD Biosciences) and CellQuest software (BD Biosciences, England). A total of 10,000 events were collected. Data was analysed using Cyflogic software (CyFlo, Finland).

## **Chapter 3: The role of BCL6 in the maintenance of PTCL**



### 3. The role of BCL6 in the maintenance of T-cell lymphoma

#### 3.1 Introduction

BCL6 is a transcriptional repressor which plays vital roles in both B- and T-cell development through regulation of lymphocyte proliferation and differentiation (Mendez et al., 2008, Pasqualucci et al., 2003, Saito et al., 2007). Importantly, BCL6 demonstrates B-cell specific mutual inhibition of IRF4 and BLIMP1 and T-cell-specific mutual inhibition of BLIMP1 but is activated by IRF4 in T-cells (figure 3.1). BCL6 has been implicated as a driver of many B-cell lymphomas, however its role in T-cells is not well established. Overexpression of the protein has been detected in many T-cell malignancies suggesting a potential role in lymphomagenesis (de Leval et al., 2007, Duy et al., 2011, Kerl et al., 2001). Furthermore, in ALK+ ALCL, evidence suggests that BCL6 expression is driven by the NPM-ALK translocation (Chiarle et al., 2005, Zamo et al., 2002).

Research into BCL6 inhibition has yielded several peptides and drug compounds, all of which exploit BCL6's unique BTB/POZ domain. Indeed, treatment of BCL6-dependent cell lines with the peptides RI-BPI or Apt48, or the molecular inhibitor, 79-6, result in anti-tumour effects (Cerchiatti et al., 2010a, Cerchiatti et al., 2009, Chattopadhyay et al., 2006).

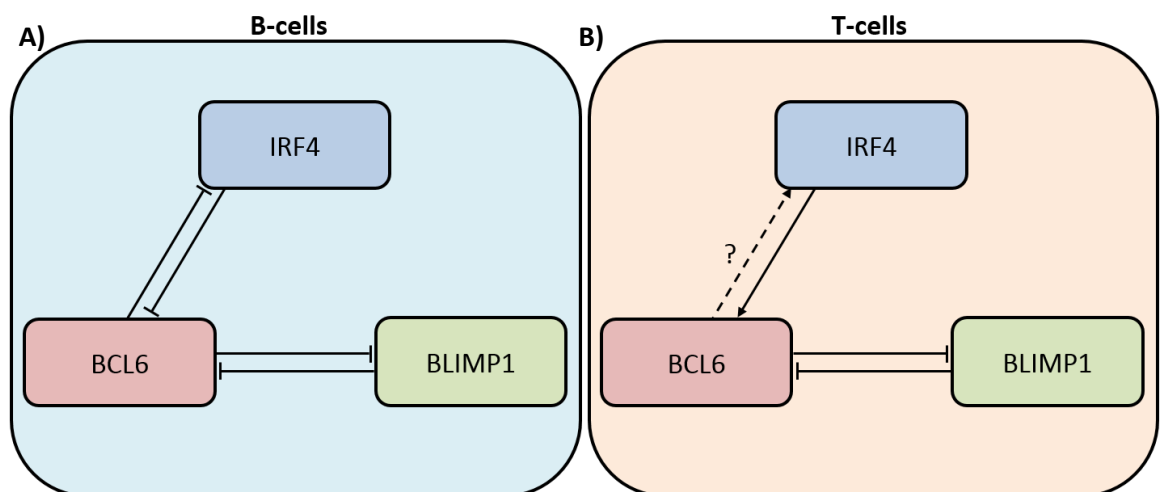


**Figure 3.1: Interaction of BCL6 with IRF4 and BLIMP1 in B-cells vs. T-cells**

A) In B-cells, BCL6 exhibits mutual inhibition with BLIMP1 and IRF4 B) In T-cell differentiation, BCL6 retains this mutual inhibition activity with BLIMP1, however interactions with IRF4 differ. BCL6 expression, and subsequent  $T_{FH}$  cell differentiation is abrogated in  $Irf4^{-/-}$  mice demonstrating a positive interaction of IRF4 on BCL6 (Lohoff et al., 2002). However, the effect of BCL6 upon IRF4 expression is not known to date.

The aim of this chapter is to investigate BCL6 as a potential oncoprotein in T-cell lymphoma by exploring the effect of BCL6 deficiency on proliferation, cell cycle, and induction of apoptosis of T-cell lymphoma cell lines. The chapter then investigates the effect of targeting BCL6 therapeutically using 79-6, as well as the determining the effect of BCL6 deficiency on expression of downstream targets IRF4 and BLIMP1.

## 3.2 Results

### 3.2.1 Characterisation of lymphoma cell lines

To understand the heterogeneous nature of peripheral T-cell lymphoma in the context of the BCL6-IRF4-BLIMP1 transcription factor axis, western blotting for BCL6, IRF4, BLIMP1, and c-MYC protein levels were evaluated using whole-cell extracts from exponentially growing lymphoma cell lines. Expression of c-MYC was assessed to investigate if c-MYC protein levels correlated with IRF4 protein levels. Cells were cultured as normal at 37°C for 24 hours before lysing with RIPA buffer.

The majority of cell lines included in this PTCL panel are ALCL due to availability. HDLM2 was also included due to the similar histological features the cell line exhibits to an ALK- ALCL. H929 and LP1 were included as positive controls for expressed IRF4, BLIMP1, and c-MYC whilst SUDHL4, HLY-1, and Karpas-422 were included as positive controls for expressed BCL6.

As shown in figure 3.2, ALCL cell lines exhibited heterogeneous expression of BCL6 and BLIMP1 whilst IRF4 levels were expression at similar levels to MM cell lines in all PTCL cell lines apart from SUDHL1.

BCL6 protein was expressed to similar levels to those found in the ABC-DLBCL cell line, HLY-1, but less than GCB-DLBCL cell lines SUDHL4 and Karpas-422 (figure 3.2B), and is present in all ALK+ ALCL cell lines but variable across the remaining cell lines. This result is consistent with published gene expression profiling data demonstrating high expression of BCL6 in ALK+ ALCL compared to ALK- ALCLs (Lamant et al., 2007).

IRF4 protein expression was generally consistent across all T-cell lines with levels reaching those found in MM cell lines (figure 3.2A). The low IRF4 protein detected in SUDHL1 (figure 3.2A) was deemed anomalous as protein expression levels were higher in all subsequent western blots for this cell line (figure 3.2B).

Levels of c-MYC protein also appeared consistent with MM cell lines in all PTCL cell lines apart from Karpas-384. BLIMP1 protein expression was variable across T-cell lines with only SR786 and DL40 reaching levels similar to MM cell lines (figure 3.2A).

In addition, expression of BCL6 and BLIMP1 appear reciprocal in SUDHL1, Karpas-299, DEL, SUPM2, Mac1, Mac2a, and DL40 whereby BCL6 is high and BLIMP1 is low or vice versa. ALK- ALCL cell lines Mac1 and Mac2a are derived from the same patient, Mac1 is a presentation cell line whilst Mac2a is a relapse cell line. Interestingly, Mac2a gains expression of BCL6 and subsequently loses expression of BLIMP1 $\alpha$  upon relapse. BCL6 protein levels in SUDHL1, Karpas-299, SUPM2, and Mac2a are comparable to that of the ABC-DLBCL cell line HLY-1 (figure 3.2B).

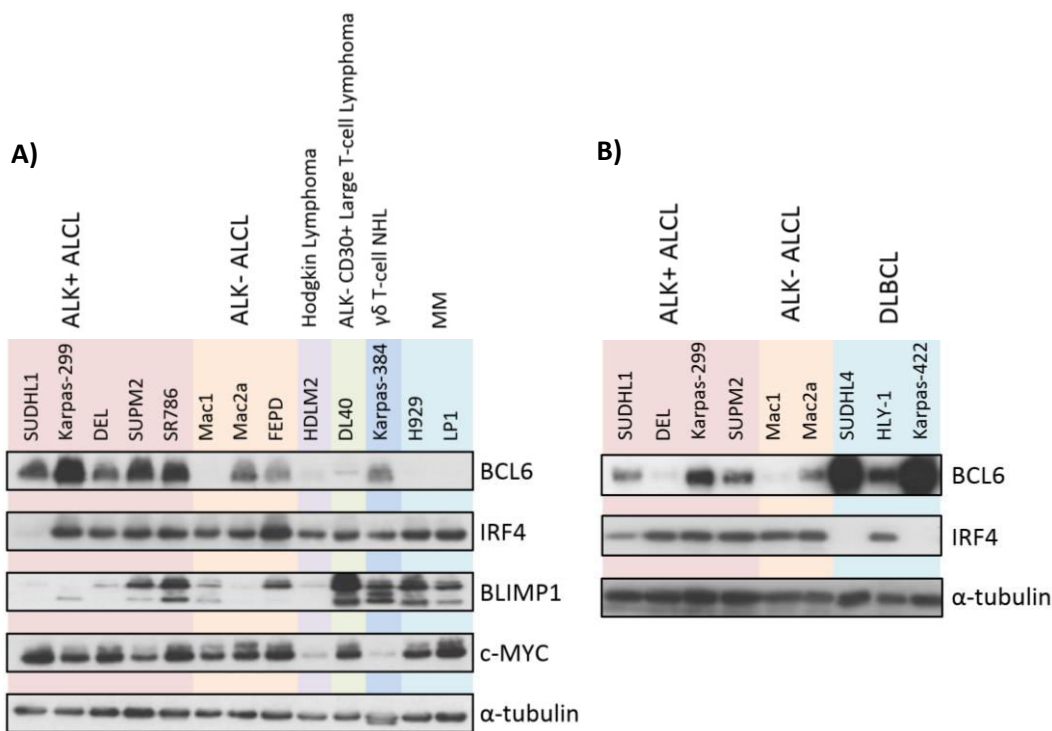


**Figure 3.2: Expression of BCL6, IRF4, BLIMP1, and c-MYC in lymphoma cell lines**

A) Expression of transcription factors in peripheral T-cell lymphoma, Hodgkin lymphoma, and multiple myeloma cell lines. The BLIMP1 antibody detects both isoforms of BLIMP1: BLIMP1 $\alpha$  and BLIMP1 $\beta$  (upper and lower molecular weight bands respectively). The identity of the third intermediate, band is unknown, possibly a truncated form of BLIMP1 $\alpha$ . B) Expression of BCL6 and IRF4 by western blot of ALCL cell lines compared to DLBCL cell lines. Equal loading assessed by blotting for  $\alpha$ -tubulin. ALK = Anaplastic Lymphoma Kinase, ALCL = Anaplastic large cell lymphoma, NHL = Non-Hodgkin lymphoma, MM = Multiple Myeloma, DLBCL = Diffuse large B-cell Lymphoma

### 3.2.2 Knockdown of BCL6 using siRNA

To investigate if BCL6 might regulate proliferation and/or survival of ALCL cell lines, siRNA-mediated knockdown was undertaken in the ALCL cell line, SUDHL1, and a control GCB-DLBCL cell line, SUDHL4. Optimal siRNA voltage was previously determined by members of the lymphoma group for SUDHL1, but this was not available for SUDHL4. To evaluate optimal voltage,  $2 \times 10^6$  SUDHL4 cells were electroporated at either 280V, 300V, 320V, or 340V for 10ms with either a pool of 4 BCL6 siRNAs or a non-silencing siRNA, incubated at room temperature for 15 minutes before seeding out at  $5 \times 10^5$  cells/ml in 6-well plates and incubating at 37°C. After 24 hours, cells were counted by Trypan Blue exclusion and protein extracts were collected and assessed by western blotting. Figure 3.3A shows the greatest level of BCL6 knockdown occurs with 320V and 340V electroporation. However, treatment of cells at voltages above 300 volts was toxic (figure 3.3B). Therefore, to compensate for toxicity, all subsequent BCL6 siRNA knockdown experiments were performed with  $4 \times 10^6$  cells and electroporated at 320V for SUDHL4.

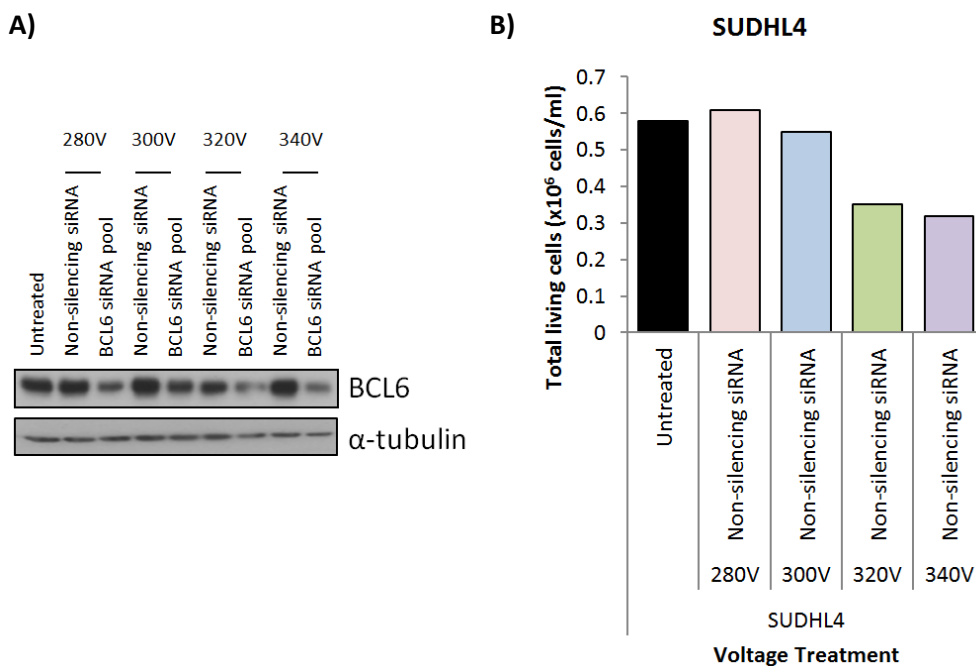


**Figure 3.3: Optimisation of siRNA voltage in SUDHL4**

Cells were electroporated and seeded at  $5 \times 10^5$  cells/ml. After 24 hours, protein lysates were collected. A) Level of BCL6 knockdown at electroporation voltages for 10ms. B) Total number of live cells as determined by Trypan blue exclusion. Results are representative of 2 independent experiments.

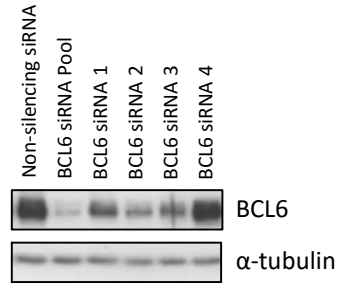


**Figure 3.4: Individual siRNAs vs. BCL6 siRNA pool**

Knockdown of BCL6 in SUDHL1 cells electroporated at 260V for 10ms with 500nM of each siRNA. Protein collected 24 hours post-transfection.

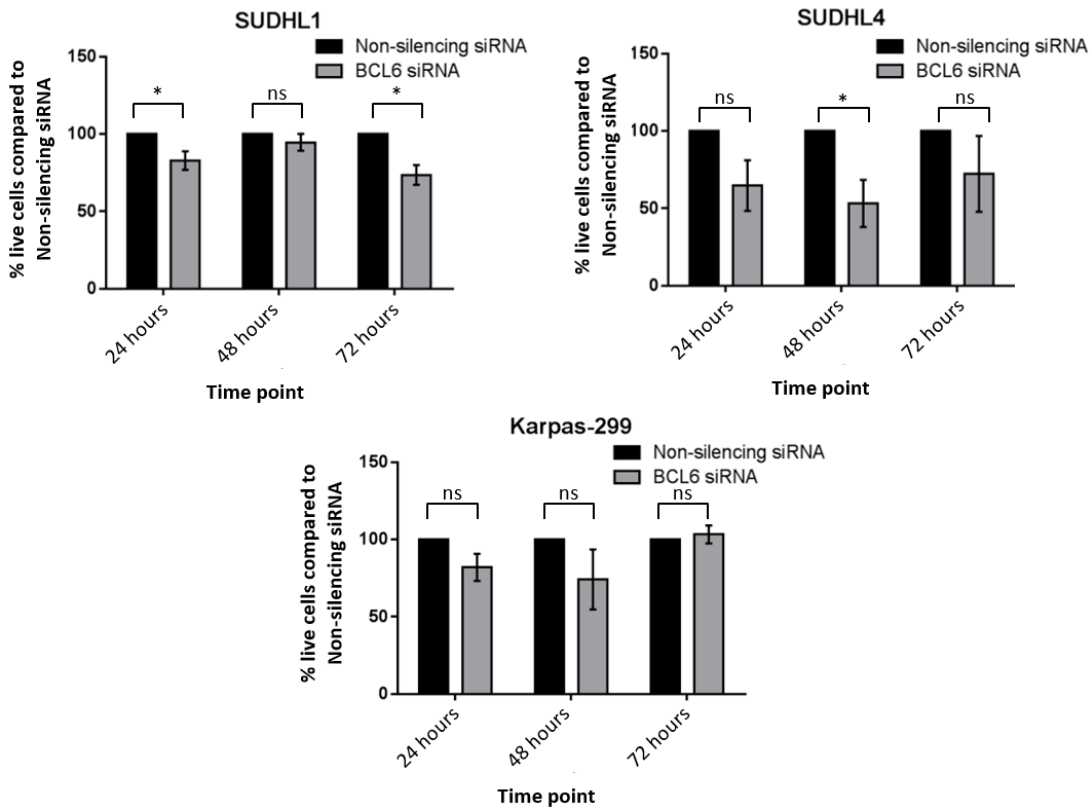


**Figure 3.5: Counts of BCL6 knockdown lymphoma cells**

Data expressed as live cells remaining after BCL6 siRNA knockdown normalised to those treated with non-silencing siRNA. Data represents the mean +/- standard error of the mean, of 3 independent experiments. Significance calculated using a paired students t-test, \* p<0.05, ns = not significant.

In addition to determining the optimum voltages for electroporation, the knockdown efficiency of 500nM of each of the individual siRNAs that constitute the siRNA pool was compared to 500nM of the siRNA pool in SUDHL1 cells (figure 3.4). No individual siRNA produced a greater knockdown than the siRNA pool so the siRNA pool was used in all BCL6 siRNA knockdown experiments.

### ***3.2.3 BCL6 knockdown results in a modest reduction of proliferation/survival of lymphoma cell lines***

In order to investigate if BCL6 knockdown affected the proliferation/survival of lymphoma cell lines, SUDHL1, Karpas-299, and SUDHL4 cells were electroporated with 500nM of BCL6 siRNA or non-silencing siRNA and viable cells were counted every 24 hours for 3 days. All cell lines showed some degree of decrease in their proliferation/survival after BCL6 knockdown (figure 3.5). SUDHL4, a GCB-DLBCL dependent upon BCL6 expression, showed the greatest decrease in cell number with knockdown (24 hours  $p=0.9297$ , 48 hours  $p=0.047$ , 72 hours  $p=0.7212$ ) (figure 3.5) whilst SUDHL1 showed a limited effect (24 hours  $p=0.0451$ , 48 hours  $p=0.136$ , 72 hours  $p=0.0144$ ) and Karpas-299 exhibited a trend but was not found to be significant (24 hours  $p=0.1083$ , 48 hours  $p=0.2535$ , 72 hours  $p=0.6065$ ) (figure 3.5).

### ***3.2.4 BCL6 siRNA knockdown has cell line-specific effects on IRF4 and BLIMP1 expression***

In order to investigate if BCL6 knockdown affected IRF4 and BLIMP1 expression in lymphoma cell lines, protein and RNA were collected every 24 hours for 3 days post-electroporation and assessed by qRT-PCR and western blot. Successful knockdown was achieved in all cell lines tested (figure 3.6A); the greatest knockdown being recorded at 24 hours across all cell lines. RNA levels of *BCL6* were significantly reduced in SUDHL1 at all timepoints (24 hours  $p=0.0155$ , 48 hours  $p=0.0095$ , 72 hours  $p=0.0201$ ) and at 24 hours in Karpas-299 but returned to basal levels after 48 hours (24 hours  $p=0.0002$ , 48 hours  $p=0.9142$ , 72 hours  $p=0.3802$ ) (figure 3.6B). In addition, BCL6 protein levels were decreased in these cell lines after 24 hours but increased slowly over the course of 72 hours (figure 3.6A). Knockdown of BCL6 had no effect on IRF4 or BLIMP1 protein levels in either SUDHL1 or Karpas-299 (figure 3.6A). However, BCL6 knockdown resulted in an initial increase in *IRF4* and *BLIMP1* mRNA in SUDHL1 cells at 24 hours (*IRF4*  $p=0.0365$ ,

BLIMP1  $p=0.0174$ ) which gradually recovered to basal levels with increased BCL6 protein levels over time (IRF4: 48 hours  $p=0.1265$ , 72 hours  $p=0.2496$ , BLIMP1: 48 hours  $p=0.0833$ , 72 hours  $p=0.7529$ ) (figure 3.6B). This effect was not seen in Karpas-299 in either IRF4 (24 hours  $p=0.5334$ , 48 hours  $p=0.4399$ , 72 hours  $p=0.3263$ ) or BLIMP1 (24 hours  $p=0.7556$ , 48 hours  $p=0.4694$ , 72 hours  $p=0.3397$ ) (figure 3.6B).

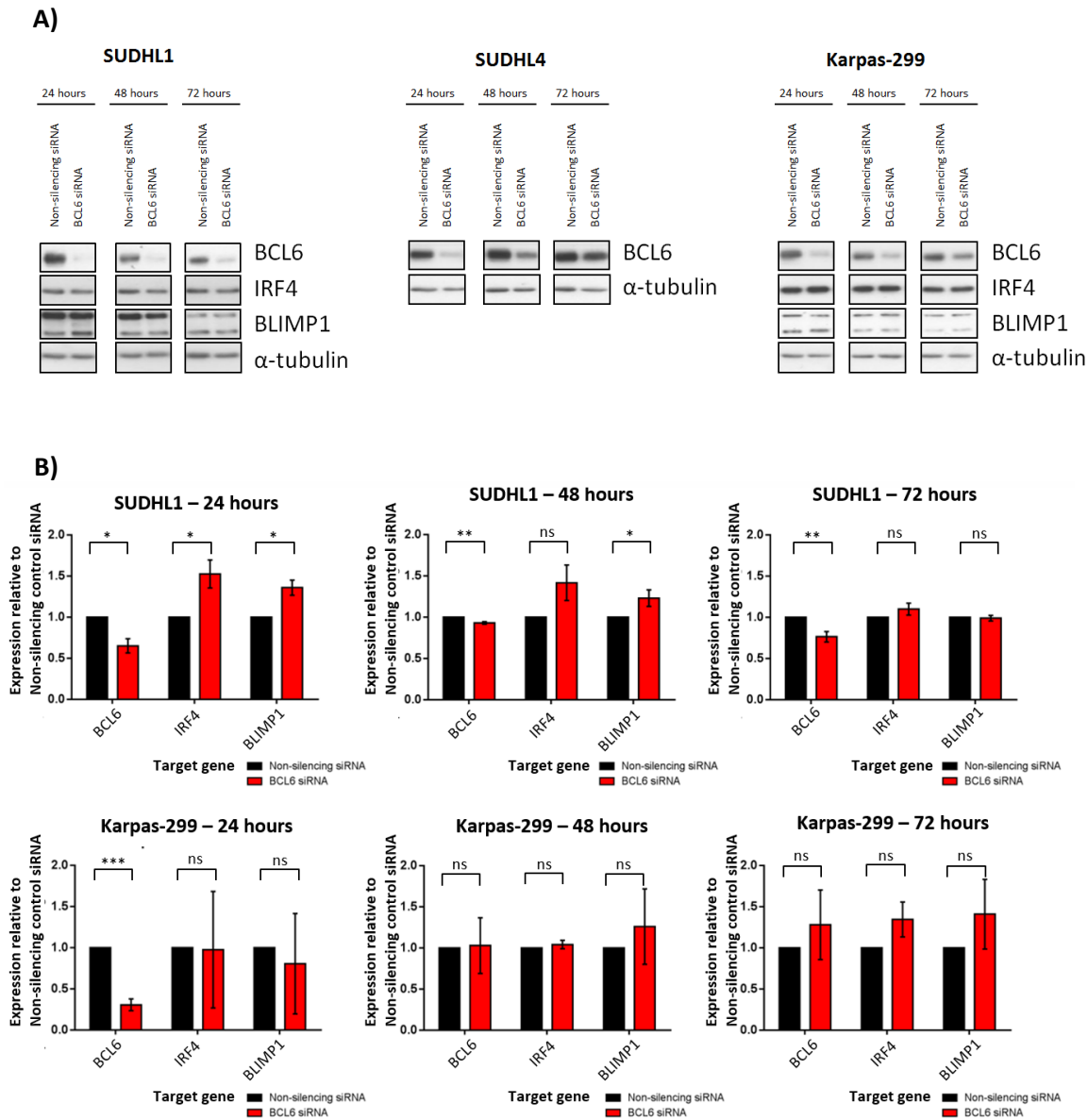


**Figure 3.6: Effect of BCL6 knockdown on the BCL6-IRF4-BLIMP1 transcription factor axis**

A) Timecourse western blot of lymphoma cell lines treated with non-silencing or BCL6 siRNA and assessed after the indicated time points. Data representative of 3 independent experiments. B) Relative mRNA levels in ALCL cell lines SUDHL1 and Karpas-299, Data represents the mean  $\pm$  standard error of the mean, of 3 independent experiments.

### 3.2.5 Doxycycline treatment of SUDHL1 cells results in reduced IRF4 expression

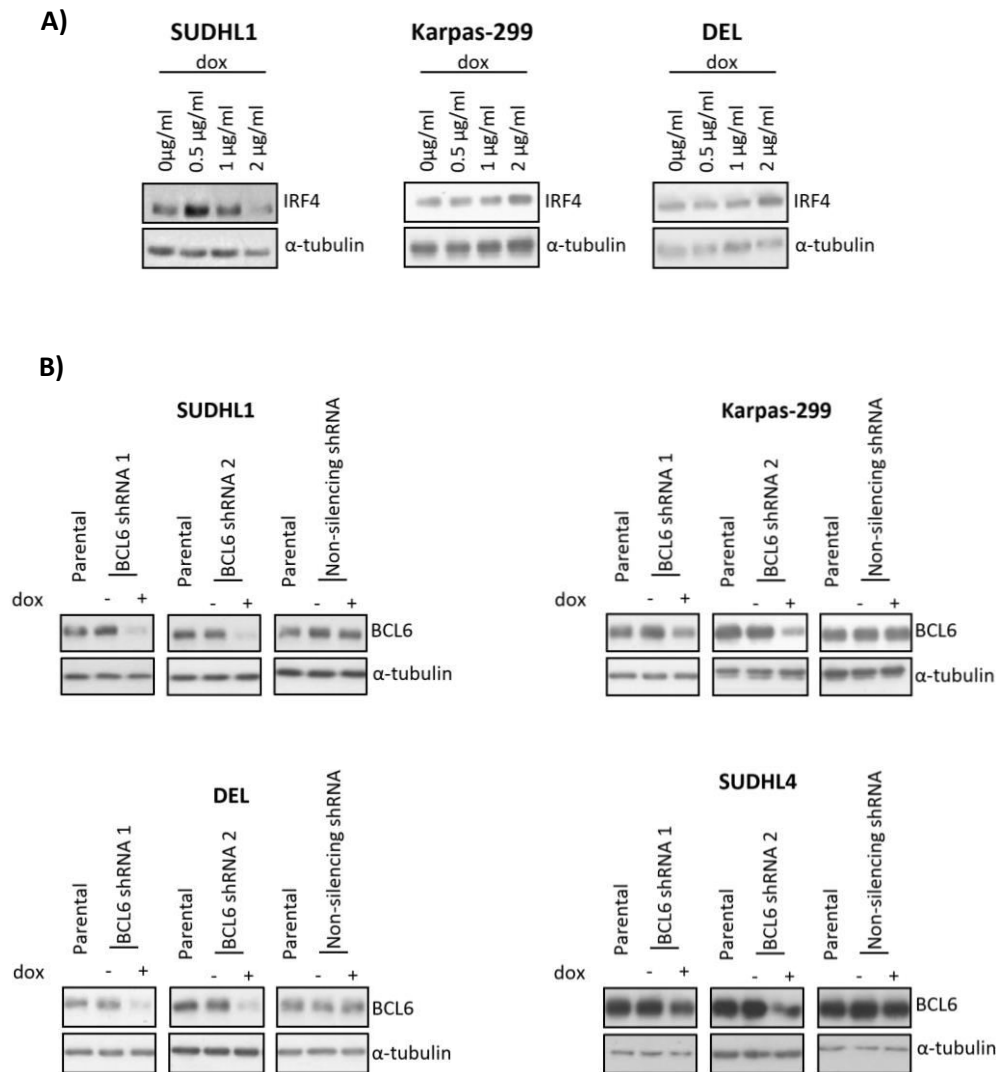


**Figure 3.7: Knockdown of BCL6 using shRNA and effect of doxycycline on IRF4 protein levels**  
 A) Effect of culturing cells in increasing concentrations of doxycycline for 7 days on IRF4 protein levels in lymphoma cell lines. Dox=doxycycline. B) Representative western blots of shRNA-transduced cells treated with 0.5  $\mu$ g/ml doxycycline (SUDHL1) or 2  $\mu$ g/ml doxycycline (Karpas-299, DEL, SUDHL4) for 72 hours in SUDHL1, Karpas-299, DEL, and SUDHL4. Data representative of 3 independent experiments.

Considering the subtle proliferation/survival phenotype caused by the siRNA knockdown of BCL6, shRNA knockdown was pursued to investigate if stable, prolonged, knockdown of BCL6 would produce a more marked effect. Initially, non-transduced cells were treated with increasing concentrations of doxycycline to ascertain the highest concentration of doxycycline that could be used to induce lentiviral constructs with the least adverse effects on the transcription factors. Previously published data has demonstrated that high levels of doxycycline (5  $\mu$ g/ml) can induce changes in key signalling pathways and result in reduced proliferation of cell lines (Ahler et al., 2013, Pulvino et al., 2015). Therefore, cells were maintained in various concentrations of doxycycline for 1 week before protein levels of BCL6, IRF4,

and BLIMP1 were assessed. BCL6 and BLIMP1 was unaffected by doxycycline however, IRF4 exhibited a dose-dependent suppression in SUDHL1 cells (figure 3.7A). The remaining cell lines, Karpas-299 and DEL, were unaffected by doxycycline (figure 3.7A). As a result, Karpas-299 and DEL were treated with 2µg/ml doxycycline to ensure maximum induction of vector, as defined in the TRIPZ manual, whilst SUDHL1 was treated with 0.5µg/ml doxycycline to minimise non-specific effects for all experiments.

### **3.2.6 BCL6 shRNA knockdown results in reduced proliferation/survival of ALK+ ALCL cell lines**

To ensure that both BCL6 shRNAs achieved BCL6 knockdown, cells were transduced with BCL6 shRNA or non-silencing shRNA constructs, selected in puromycin for 1 week (4µg/ml puromycin – SUDHL1, 2µg/ml puromycin – DEL and Karpas-299, 1µg/ml puromycin – SUDHL4), and induced with doxycycline. After 72 hours, western blotting showed marked decrease in BCL6 levels upon induction of BCL6 shRNA in all cell lines with both constructs (figure 3.7B). Knockdown was more prominent in SUDHL1 and DEL and less in Karpas-299 and SUDHL4 (figure 3.7B). Consistent with this, knockdown of *BCL6* mRNA was greater in SUDHL1 and DEL than Karpas-299 (figures 3.11 and 3.12).

To evaluate the role of BCL6 on the proliferation of cell lines, transduced cell lines were induced for 72 hours with doxycycline to induce shRNA knockdown and RFP expression, before combining in a 50:50 ratio with non-transduced cells and cultured in doxycycline-containing medium; the time of mixing is indicated as day 0 in all experiments. RFP levels were then tracked by flow cytometry for 2 weeks post-mixing. 2 of 3 cell lines containing BCL6 shRNA exhibited a reduction in RFP levels after 14 days (figure 3.8A). SUDHL4 DLBCL cells were also used as a positive control for BCL6 sensitivity. BCL6 shRNA RFP-positive cells, which are indicative of BCL6 knockdown cells, were significantly reduced at day 14, in proportion with non-silencing shRNA cells, 2 days post-mixing (shRNA 1 p=0.00001, shRNA 2 p = 0.001) (figure 3.8A). Karpas-299 showed the greatest effect on RFP-positivity with both BCL6 shRNAs, reducing RFP-positive populations 2 days after mixing (figure 3.8A). Both BCL6 shRNAs populations resulted in significantly reduced RFP populations in relation to non-silencing shRNA populations by day 14 (shRNA 1 p=0.004, shRNA 2 p=0.001). BCL6 shRNA populations in SUDHL1 were significantly reduced at day 14 with both shRNAs

compared to non-silencing shRNA populations (shRNA 1  $p=0.043$ , shRNA 2  $p=0.0001$ ) but only showed a reduction from day 11 (figure 3.8A). DEL exhibited the lowest effect on growth, day 14 was the only time point to have both BCL6 shRNAs significantly reduce RFP levels compared to control shRNA (shRNA 1  $p=0.044$ , shRNA 2  $p=0.003$ ) (figure 3.8A). Despite the significant effect, DEL was deemed insensitive as only shRNA 2 caused RFP populations to drop below 100% (figure 3.8A). In a parallel experiment, SUDHL1-transduced cells were also induced with 0.5 $\mu$ g/ml doxycycline and counted every 2-3 days, by Trypan Blue exclusion, for 14 days. In this experiment, BCL6 knockdown with shRNA 1 cells also caused a significant reduction in the number of living cells in the SUDHL1 cell line compared to non-silencing shRNA cells, after 14 days, by counting ( $p=0.011$ ) (figure 3.8B). However, SUDHL1 BCL6 shRNA 2 cells failed to achieve a significant difference in cell number ( $p=0.165$ ) (figure 3.8B).

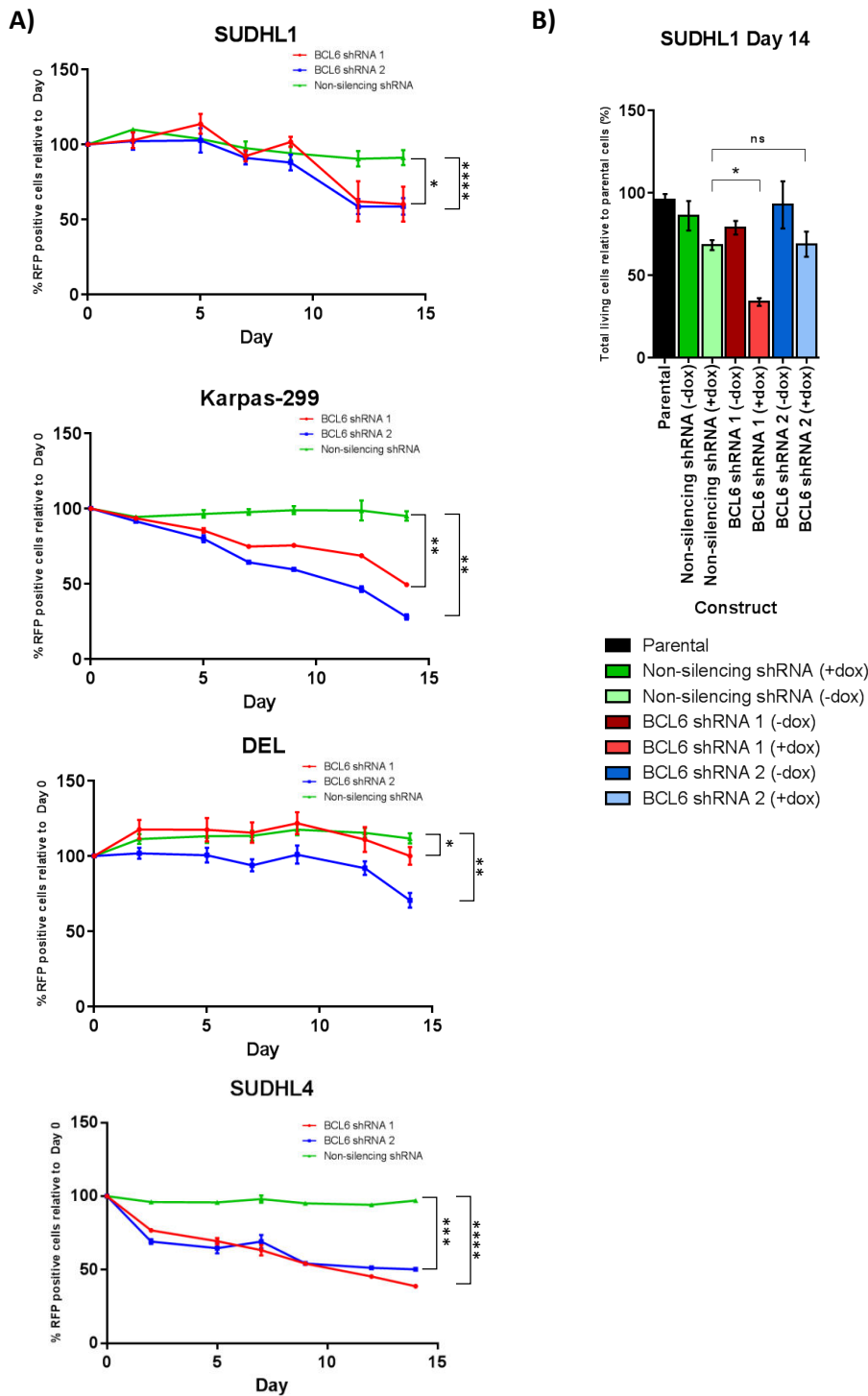


**Figure 3.8: BCL6 knockdown results in reduced growth rates of ALK+ ALCL cell lines**

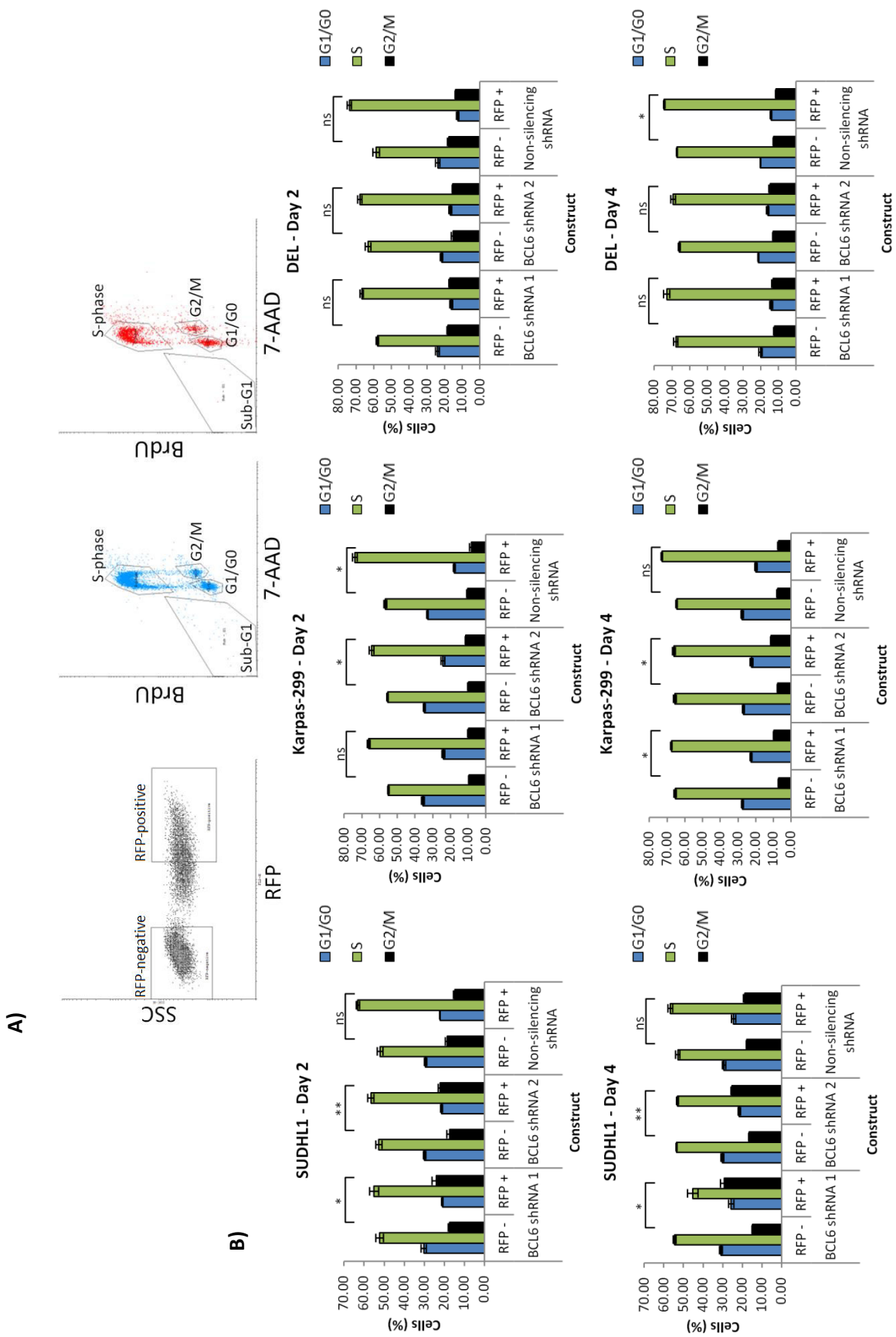
A) RFP-tracking experiments in lymphoma cell lines, cells were mixed in a 50:50 ratio transduced to non-transduced cells at day 0 and treated with doxycycline. Cells were maintained in doxycycline for the duration of the experiment. Data is equal to 3 independent replicates; error bars indicate standard error of the mean. B) Total cell numbers in SUDHL1 relative to parental cells after 14 days in culture, data is equal to 4 independent replicates; error bars indicate standard error of the mean. Significance calculated using a paired students t-test, \*  $p < 0.05$ , \*\*  $p < 0.01$ , \*\*\*  $p < 0.001$ , \*\*\*\*  $p < 0.0001$ .

### **3.2.7 BCL6 shRNA knockdown results in small increases in G2/M populations**

To investigate whether BCL6 knockdown affected the cell cycle of ALCL cell lines, samples were taken for BrdU/7-AAD staining at days 2 and 4 of the RFP-tracking experiments shown in figure 3.8A. RFP-positive populations of SUDHL1, Karpas-299, and DEL harbouring BCL6 shRNA showed varying effects (figure 3.9). All shRNA constructs across all cell lines increased S-phase and decreased G1/G0 between RFP-negative and RFP-positive populations (figure 3.9B). Despite this effect, there was a variable effect on the G2/M populations across the cell lines. SUDHL1 showed a small but significant increase in the proportion of G2/M populations with BCL6 knockdown after 2 days in culture (shRNA 1  $p=0.049$ , shRNA 2  $p=0.005$ ) whilst non-silencing shRNA decreased G2/M populations ( $p=0.06$ ) (figure 3.9B). This effect is more pronounced after 4 days in culture (shRNA 1  $p=0.021$ , shRNA 2  $p=0.005$ , non-silencing shRNA  $p=0.134$ ) (figure 3.9B). BCL6 knockdown also increased the G2/M population in Karpas-299 to a lower degree than SUDHL1. Whilst both shRNAs significantly increase G2/M populations at day 4 (shRNA 1  $p=0.033$ , shRNA 2  $p=0.01$ , non-silencing shRNA  $p=0.118$ ) the effect is minimal (figure 3.9B). At day 2, shRNA 1 fails to significantly increase G2/M populations ( $p=0.367$ ) whilst shRNA 2 increases slightly ( $p=0.039$ ) and control shRNA decreases ( $p=0.036$ ) (figure 3.9A). DEL failed to significantly alter G2/M populations at day 2 with BCL6 knockdown (shRNA 1  $p=0.258$ , shRNA 2  $p=0.904$ , non-silencing shRNA  $p=0.118$ ). In addition, after 4 days in culture, G2/M populations across all shRNA-positive cells are statistically not significant to shRNA-negative counterparts in DEL, however non-silencing shRNA significantly decreased G2/M populations (shRNA 1  $p=0.228$ , shRNA 2  $p=0.07$ , non-silencing shRNA  $p=0.012$ ) (figure 3.9B). Generally, SUDHL1 and Karpas-299 ALCL cell lines demonstrate an increase in G2/M populations following BCL6 shRNA induction by day 4.

**Figure 3.9: BCL6 knockdown results in accumulation of G2/M populations in ALK+ ALCL cell lines**

A) Representative cytograms for BrdU/7-AAD staining and gating strategy employed for SUDHL1, RFP-negative cell cycle trace is depicted in blue (middle pane) whilst RFP-positive cell cycle trace is depicted in red (right pane). B) Respective cell cycle profiles of RFP-negative and RFP-positive cells within a culture as assessed by BrdU/7-AAD staining at 2 and 4 days post mixing. Data is derived from 3 independent experiments; error bars indicate standard error of the mean. \*  $p < 0.05$ , \*\*  $p < 0.01$ , ns = not significant.



To assess apoptosis, samples were also taken at days 2 and 4 in culture, stained with active caspase-3 antibody, and assessed by flow cytometry (figure 3.10A). Most cell lines failed to significantly induce apoptosis with either BCL6 shRNA compared to non-silencing shRNA, apart from shRNA 1 in SUDHL1 and DEL at day (SUDHL1: shRNA 1 day 2  $p=0.0162$ , day 4  $p=0.0071$ , shRNA 2 day 2  $p=0.359$ , day 4  $p=0.2179$ , Karpas-299: shRNA 1 day 2  $p=0.3107$ , day 4  $p=0.1394$ , shRNA 2 day 2  $p=0.3409$ , day 4  $p=0.2903$ , DEL: shRNA 1 day 2  $p=0.0385$ , day 4  $p=0.4975$ , shRNA 2 day 2  $p=0.0699$ , day 4  $p=0.7019$ ) (figure 3.10B).

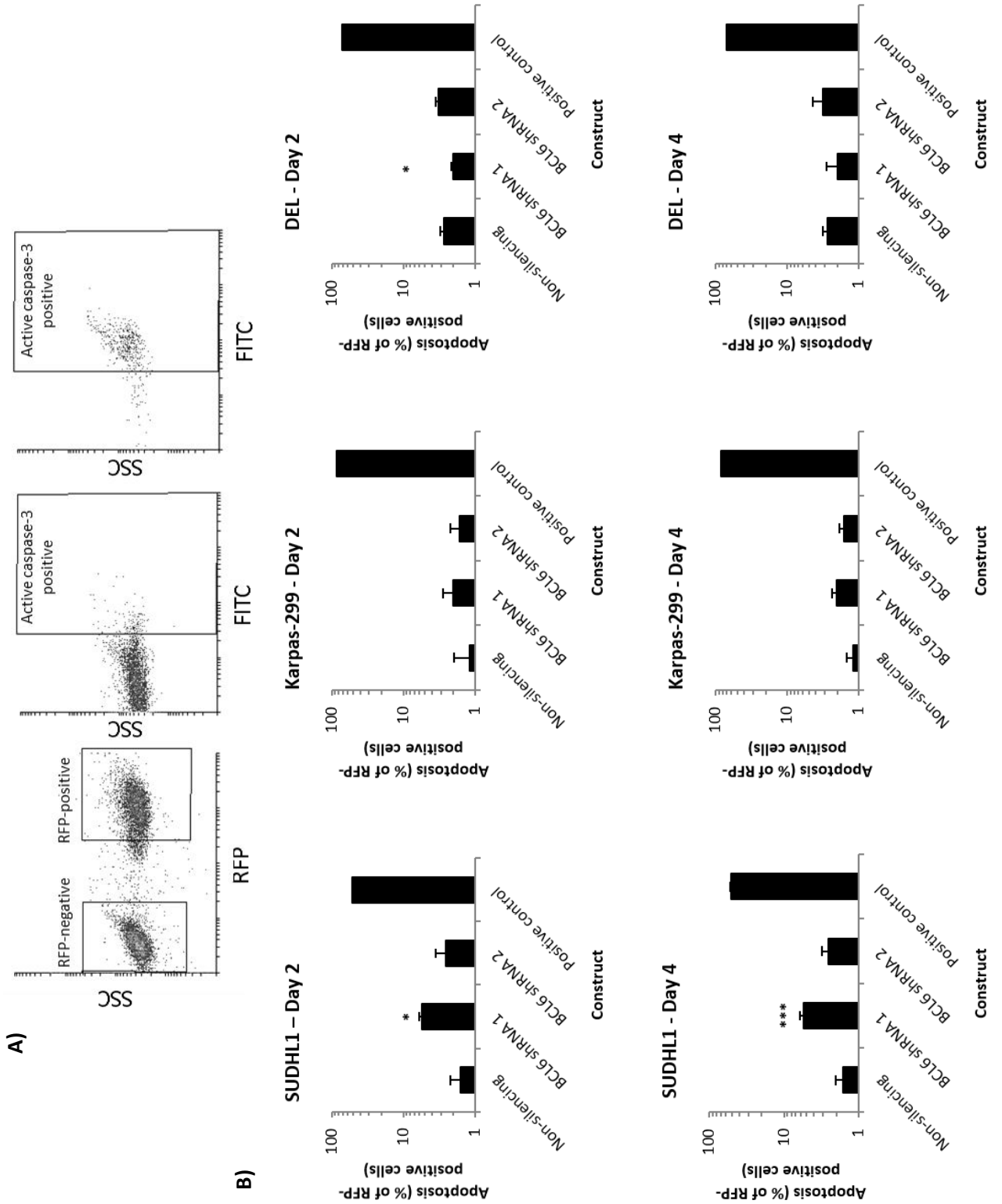
### **3.2.8 BCL6 shRNA knockdown affects transcription of IRF4 and c-MYC transcripts**

To assess the effect of BCL6 knockdown upon expression of *BCL6*, *IRF4*, *BLIMP1*, and *c-MYC*, shRNA-transduced cells were treated with doxycycline for two weeks and lysed for RNA and protein analysis after 3, 10, and 17 days treatment. SUDHL1 cells achieved significant BCL6 knockdown at both the RNA and protein level across a two-week period (shRNA 1: day 3  $p<0.0001$ , day 10  $p=0.2576$ , day 17  $p=0.01559$ , shRNA 2: day 3  $p<0.0001$ , day 10  $p<0.0001$ , day 17  $p=0.0156$ ) (figure 3.11). IRF4 transcripts in SUDHL1 showed a subtle, but not significant, increase upon BCL6 knockdown at day 3 (shRNA 1:  $p=0.0161$ , shRNA 2:  $p=0.1536$ ) (figure 3.11A), however this effect was lost by day 10 (shRNA 1: day 10  $p=0.0959$ , day 17  $p=0.7647$ , shRNA 2: day 10  $p=0.2669$ , day 17  $p=0.4742$ ) (figure 3.11B-C). No other significant changes to either the RNA or protein levels of the transcription factors were observed in SUDHL1 cells (figure 3.11). A similar trend was observed in Karpas-299 as in SUDHL1; *BCL6* mRNA was significantly reduced (shRNA 1  $p<0.0001$ , shRNA 2  $p<0.0001$ ) which resulted in marginal increases in IRF4 transcript levels (shRNA 1  $p=0.0453$ , shRNA 2  $p=0.1939$ ) but not protein levels after 72 hours induction (figure 3.12A). No other significant changes in transcription factor RNA or protein were observed in Karpas-299 (figure 3.12A). In DEL, BCL6 knockdown caused a significant reduction in *BCL6* mRNA levels (shRNA 1  $p<0.0001$ , shRNA 2  $p<0.0001$ ) resulting in a marginal, but not significant, increase in *c-MYC* transcript levels only (shRNA 1  $p=0.0644$ , shRNA 2  $p=0.1848$ ), this was not observed at the protein level (figure 3.12B) and had no effect on the remaining transcription factors (figure 3.12B).

### 3.2.9 Growth curves of cell lines for drug treatments

To evaluate the seeding density required for effective assessment of drug potency for cell survival assays, cells were seeded in 96-well plates at varying concentrations and allowed to grow for 72 hours before assessing with Resazurin. After 4 days of growth, it was decided that the seeding concentration of  $1 \times 10^5$  cells/ml was sufficient for all cell lines as the fluorescent signal had not plateaued across all cell lines at this concentration (figure 3.13).

**Figure 3.10: BCL6 knockdown results in no induction of apoptosis**



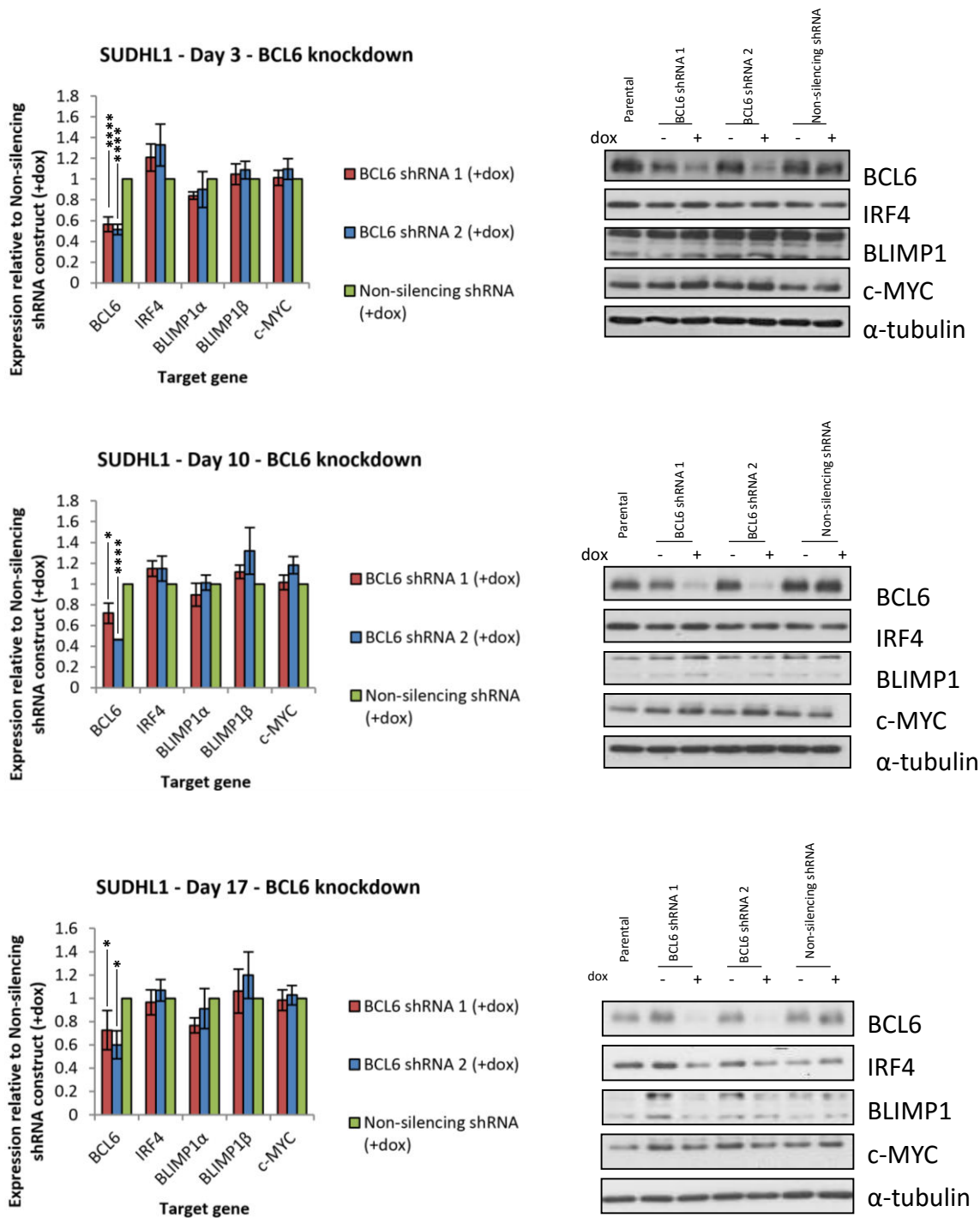


**Figure 3.12: The effect of BCL6 shRNA knockdown on the expression of BCL6, IRF4, and BLIMP1 in SUDHL1**  
 Transcript and protein levels of transcription factors after induction of shRNA and maintenance of culture with 0.5 $\mu$ g/ml doxycycline-containing medium at A) Day 3, B) Day 10, C) Day 17. Data is derived from 4 independent replicates; error bars indicate standard error of the mean. Significance calculated using a paired students t-test, \*  $p < 0.05$ , \*\*  $p < 0.01$ , \*\*\*  $p < 0.001$ , \*\*\*\*  $p < 0.0001$ .

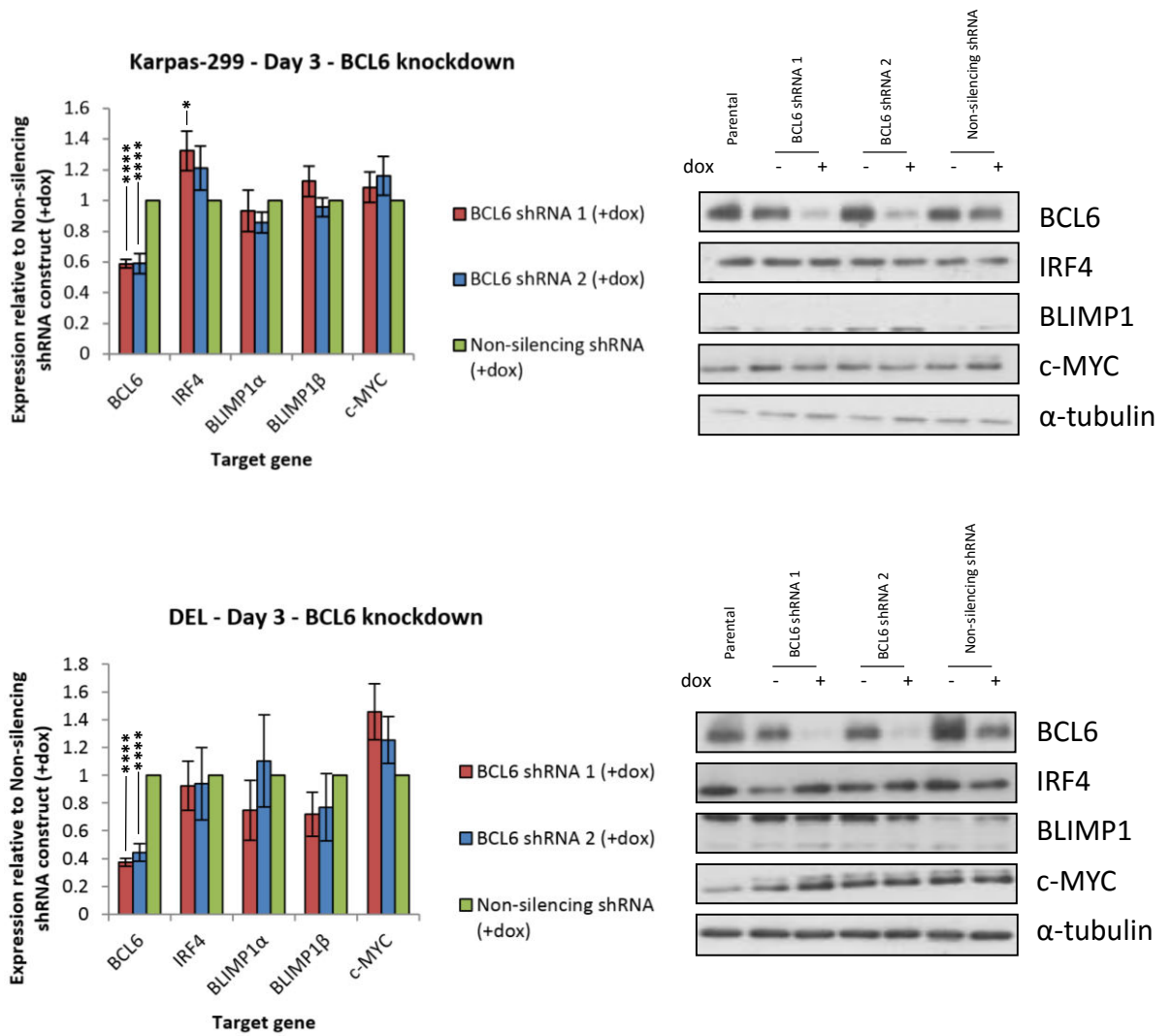


**Figure 3.13: The effect of BCL6 shRNA knockdown on the expression of BCL6, IRF4, and BLIMP1 in Karpas-299 and DEL**

Transcript and protein levels of transcription factors after induction of shRNA and maintenance of culture with 2 $\mu$ g/ml doxycycline-containing medium at Day 0 in A) Karpas-299 and B) DEL. Data is derived from 4 independent replicates; error bars indicate standard error of the mean. Significance calculated using a paired students t-test, \* p<0.05, \*\* p<0.01, \*\*\* p<0.001, \*\*\*\* p<0.0001.

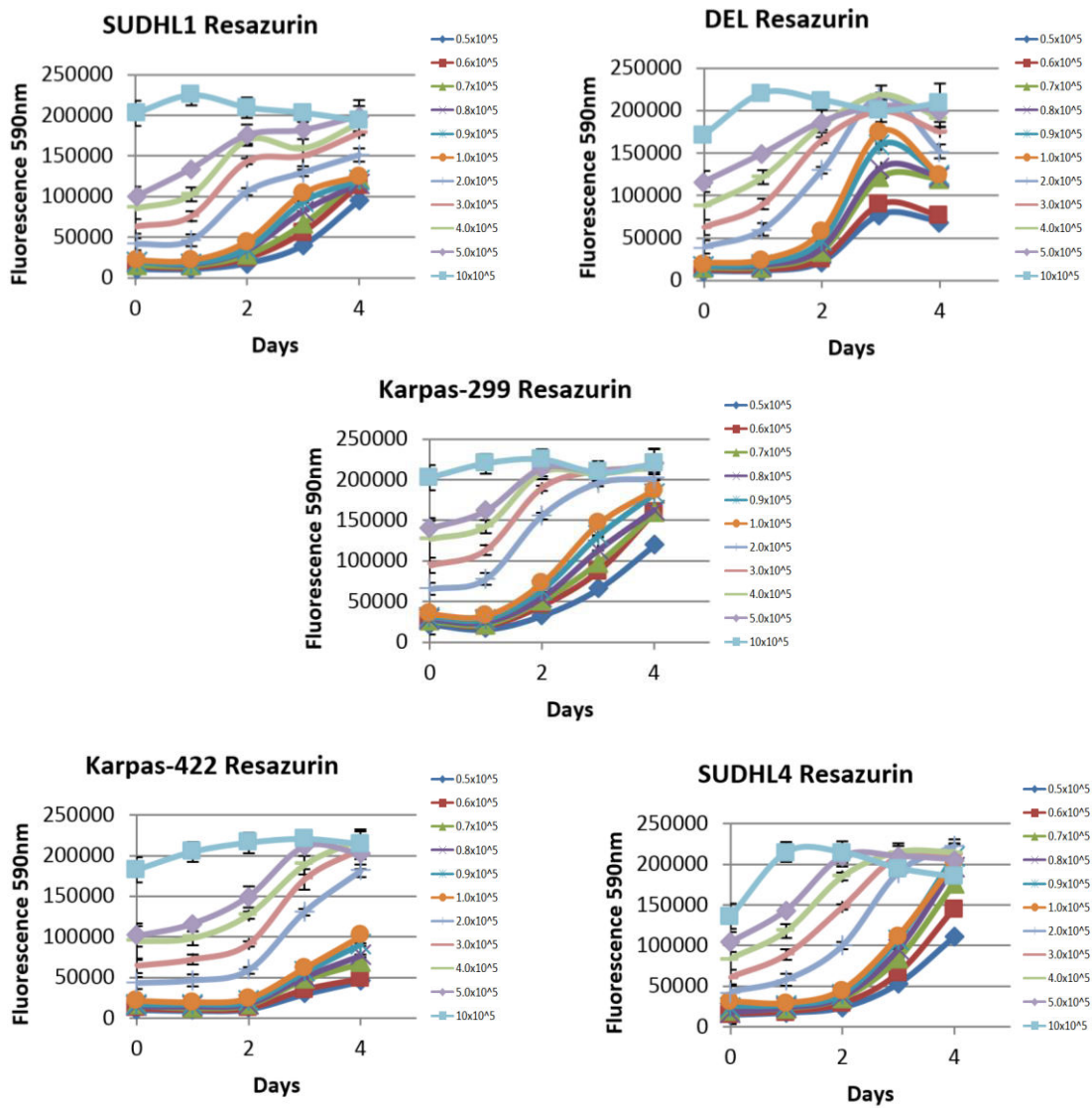


**Figure 3.13: Growth curve of lymphoma cell lines with Resazurin**

Raw fluorescent values of cells treated with Resazurin for 2 hours at each day. Results are derived from 3 independent replicates; error bars indicate standard error of the mean.

### **3.2.10 ALCL cell lines are sensitive to 79-6 inhibitor**

To further investigate the role of BCL6 in ALCL and to assess the possibility of pharmacological inhibition of BCL6 in these cells, cells were treated with increasing concentrations of 79-6 and assessed for proliferation/survival by a Resazurin assay. All cell lines, except from Karpas-422, were found to be sensitive to 79-6 treatment (figure 3.14). Based upon previously published data, a cell line which exhibits an IC<sub>50</sub> of below 936 $\mu$ M is deemed “BCL6-dependent” whilst an IC<sub>50</sub> above 15mM indicates a “BCL6-independent” cell line (Cerchietti et al., 2010a). In agreement with this study, the IC<sub>50</sub> value of the B-cell control line, SUDHL4, was 490.3 $\mu$ M indicating sensitivity to 79-6. In addition, all T-cell lines were found to be sensitive with a range of IC<sub>50</sub>s between 268.6 $\mu$ M and 583.0 $\mu$ M (figure 3.14A). However, the previously established “BCL6-independent” cell line, Toledo, demonstrated an IC<sub>50</sub> of 721.7 $\mu$ M. Furthermore, a cell line demonstrated to be insensitive to RI-BPI, Pfeiffer (Cerchietti et al., 2009), also exhibited an IC<sub>50</sub> of 375.2 $\mu$ M. As Karpas-422, another cell line insensitive to RI-BPI (Cerchietti et al., 2009), did not reach an IC<sub>50</sub> we sought to investigate this further. It was hypothesised that the apparent insensitivity may be caused by death occurring in the vehicle control due to the high concentration of DMSO required. Therefore cells were treated with increasing concentrations of DMSO for 72 hours and assessed by Resazurin analysis. It was revealed that Karpas-422 was sensitive to the vehicle DMSO concentration (1%) and exhibited 66% death after 72 hours (figure 3.14B) whilst other cell lines were not as sensitive. T-cell lymphoma cell lines were more resistant to DMSO than B-cell lymphoma cell lines (figure 3.14B).

### **3.2.11 79-6 induces apoptosis in all lymphoma cell lines**

To overcome the toxicity of cell lines to DMSO, cell lines were treated with either an IC<sub>50</sub> of 79-6, as determined by Resazurin analysis in figure 3.14A (an average of the IC<sub>50</sub> values of SUDHL4, SUDHL1, and Karpas-299 was used for Karpas-422) or the respective concentration of DMSO vehicle. Cells were treated for 24 hours and assessed for the presence of cleaved caspase-3 by flow cytometry. SUDHL1, Karpas-299, SUDHL4, and Karpas-422 showed significant increases in the level of apoptosis after 24 hours 79-6 treatment compared to vehicle controls (figure 3.15).

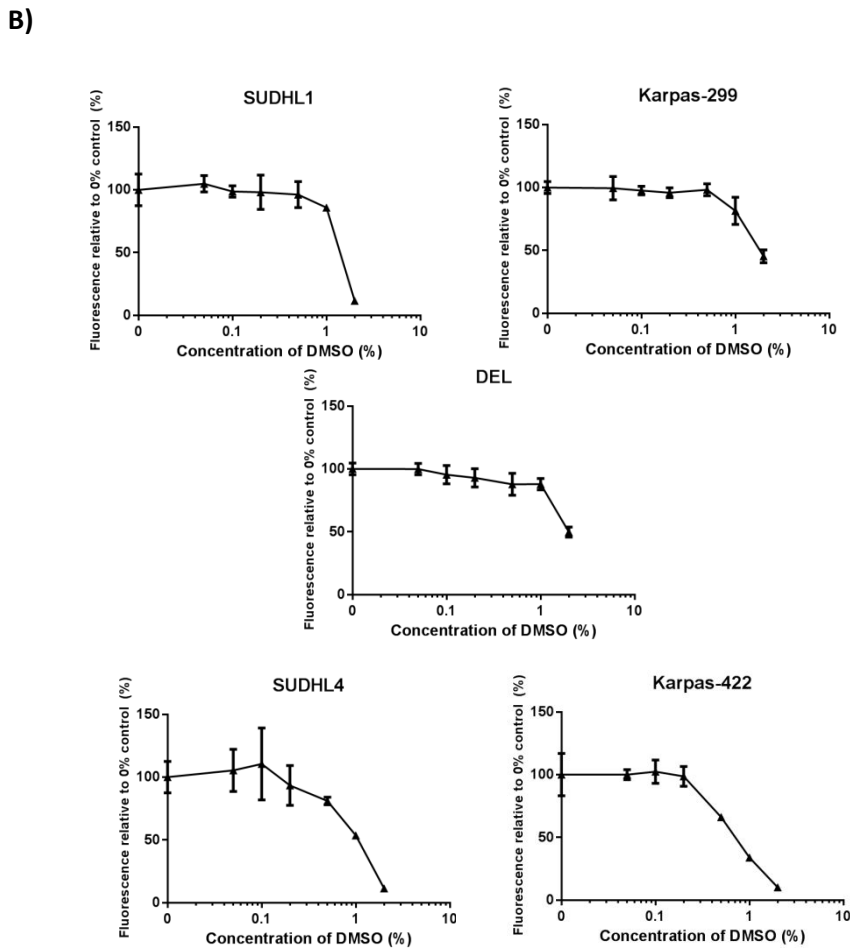
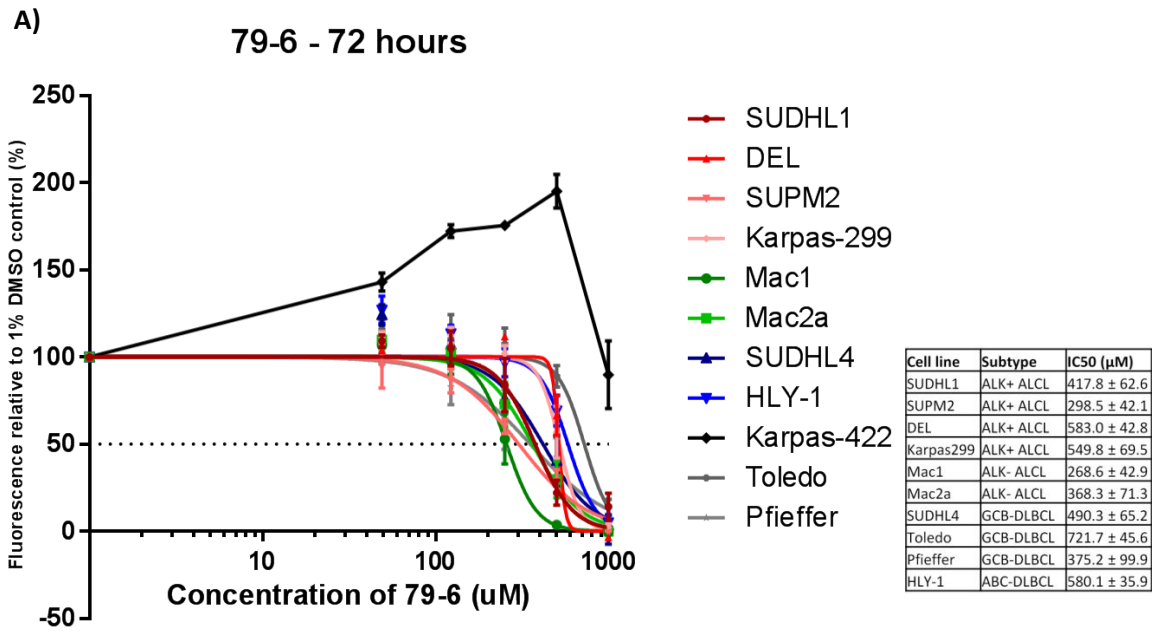


**Figure 3.14: Resazurin profiles of 79-6 and DMSO treated cell lines**

A) Growth inhibition curves of all lymphoma cell lines after 72 hours treatment with varying concentrations of 79-6. Cell lines previously reported to be insensitive to inhibition of BCL6 are: Toledo, Pfeiffer, and Karpas-422 B) Growth inhibition curves of lymphoma cell lines titrated with increasing concentrations of DMSO after 72 hours. All data is derived from 3 independent replicates, error bars indicate standard error of the mean.

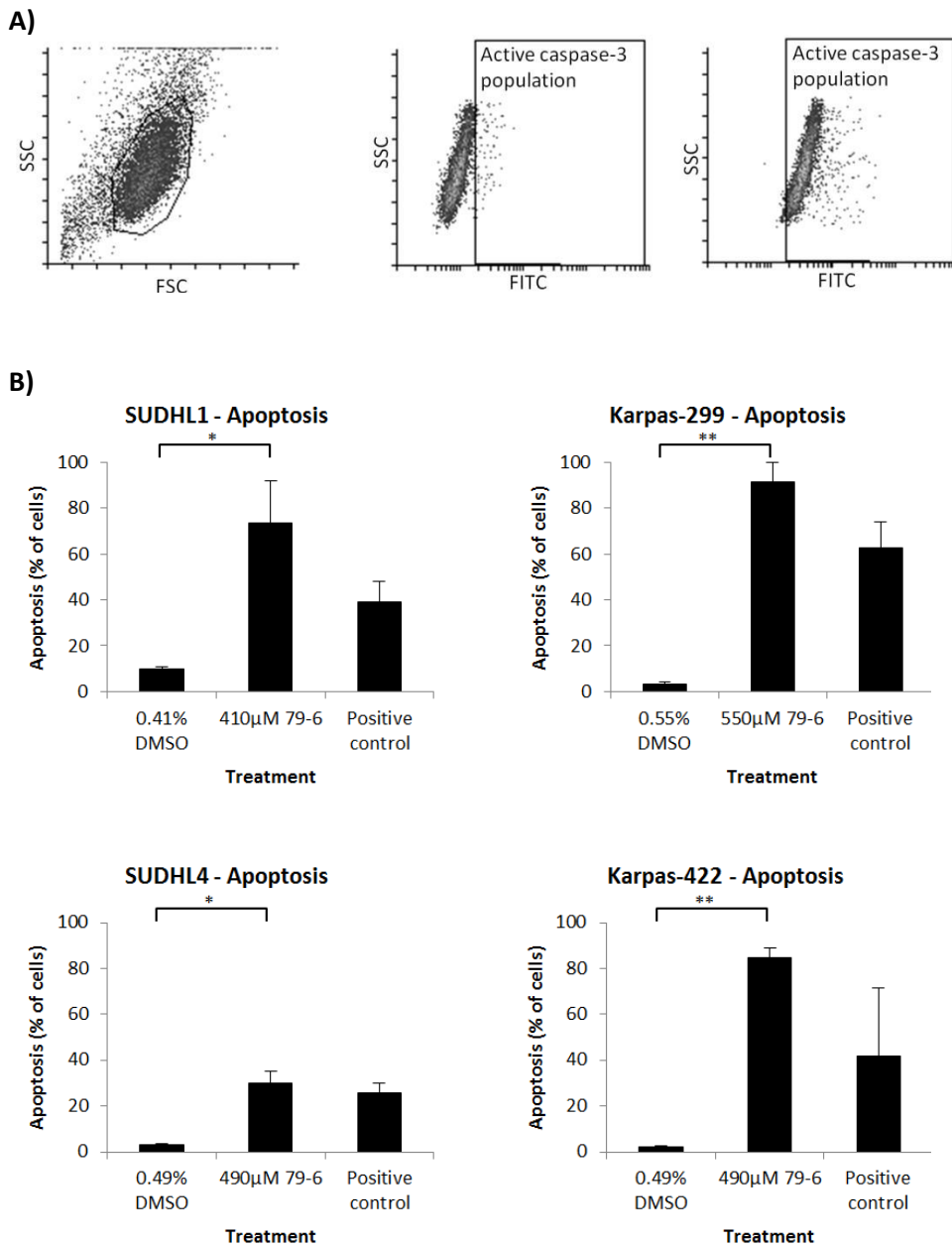


**Figure 3.15: Levels of apoptosis in lymphoma cell lines with 79-6 treatment**

A) Representative flow trace depicting gating method for defining apoptotic-populations, live cell population is gated as shown in the left panel, subsequent unstained cells are depicted in the middle pane, active caspase-3 stained cells are depicted in the right panel. B) Levels of apoptosis after 24 hours treatment with indicated drug concentration. Positive control for all samples is cells treated with 100μM staurosporine for 24 hours. Data is derived from 3 independent replicates, error bars indicate standard error of the mean. \* p<0.05, \*\* p<0.01.

Both T-cell lines exhibited high apoptosis whilst the B-cell control, SUDHL4, exhibited the lowest apoptotic induction (figure 3.15).

### **3.2.12 79-6 fails to induce changes in B-cell targets in T-cell lymphoma cell lines**

As no cell lines were found to be insensitive to 79-6 we hypothesised that the drug may not be working through BCL6. Therefore, mirroring a previously established experiment (Cerchiatti et al., 2010a), to elucidate if BCL6 is targeted by 79-6, cells were subjected to 50 $\mu$ M 79-6 or vehicle for 8 hours and assessed for changes in expression of a panel of B-cell BCL6 target genes. This panel was chosen as a T-cell panel of BCL6 targets was not yet established. 79-6 failed to produce significant changes in all BCL6 targets tested in the T-cell lines SUDHL1 and Karpas-299 (figure 3.16). 79-6 treatment resulted in a slight reduction of *BCL6* expression in SUDHL1 which was not reproducible in Karpas-299 (figure 3.16). As expected, SUDHL4 exhibited moderate increases in gene expression of *BCL6*, *IRF4*, *ATR*, *MYC*, *P21*, and *TP53* with 79-6 treatment, as BCL6 negatively regulates these genes, but unexpectedly 79-6 decreased *BLIMP1* expression. Changes exhibited in *IRF4*, *BLIMP1*, and *ATR* were the only genes significantly altered compared to vehicle control (*BCL6* p=0.2289, *IRF4* p=0.0301, *BLIMP1* p=0.037, *ATR* p=0.0156, c-MYC p=0.1057, p21 p=0.1376, TP53 p=0.23).

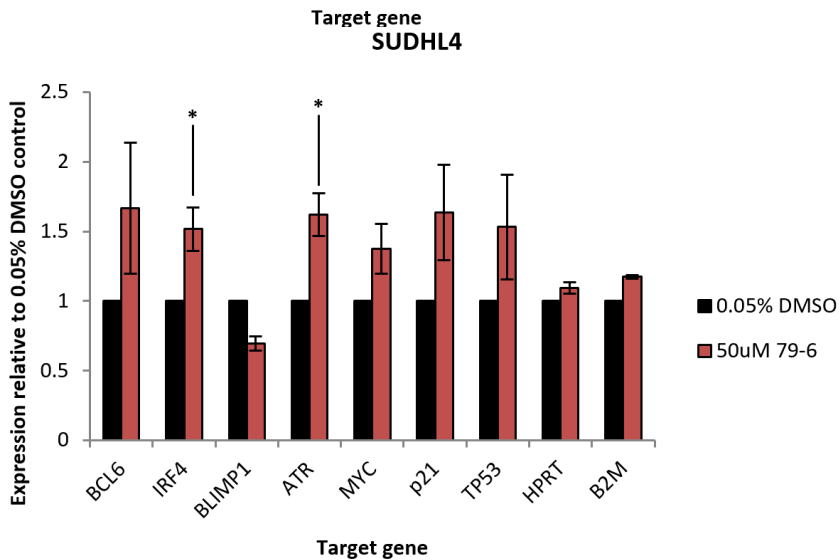
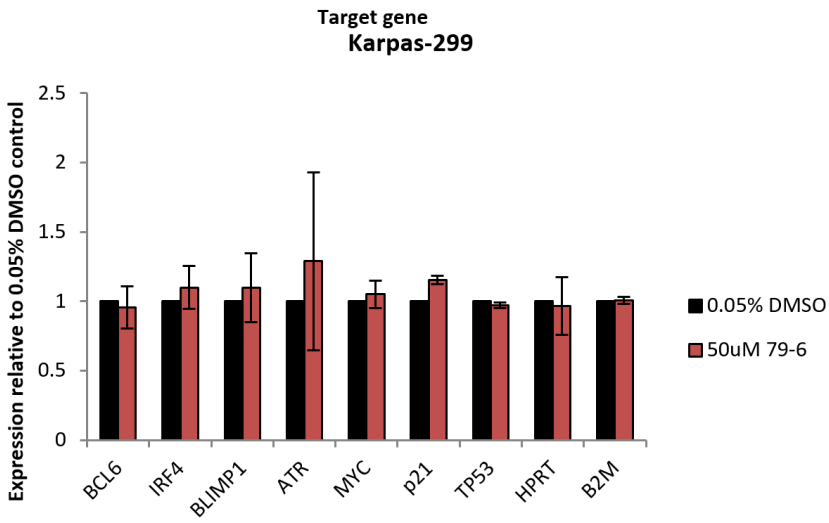
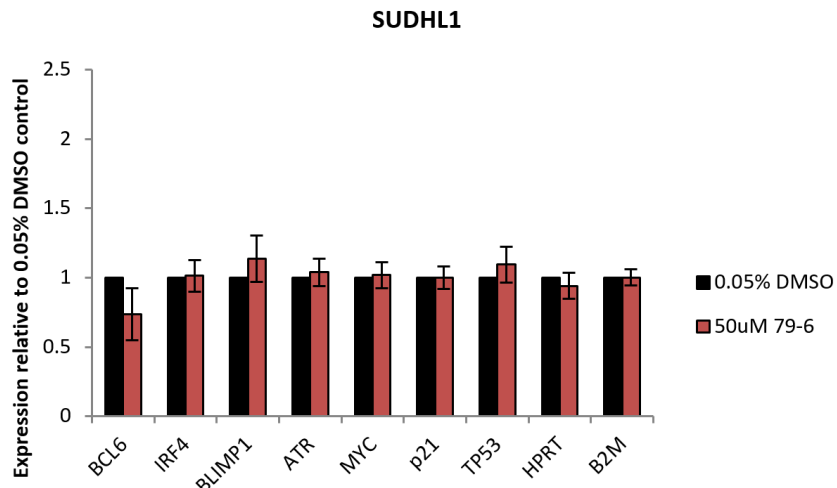


**Figure 3.16: Expression of BCL6 target genes after 8 hours with 79-6 treatment**

Relative mRNA abundance across lymphoma cell lines after treatment with 79-6 compared with 0.05% DMSO vehicle control. HPRT and B2M are included as control genes. Data is derived from 3 independent replicates; error bars indicate standard error of the mean.

### 3.3 Discussion

The data presented in this chapter shows that BCL6 may play a role in the proliferation and or survival of some ALCL cell lines. In addition, the data suggests a role of BCL6 for correct cell cycle progression and therefore is a potential therapeutic target for ALCL.

Whilst initially siRNA-mediated knockdown systems were employed for BCL6, this project moved to shRNA-mediated knockdown systems to overcome the drawbacks of siRNAs. Although siRNA provided a rapid BCL6 knockdown, the delivery of the siRNA induces cellular stress via electroporation. In addition, siRNA knockdown experiments suggested that loss of BCL6 did not cause a rapid deterioration of proliferation/survival (figure 3.5); therefore the shRNA knockdown system was employed to provide a stable knockdown. Knockdowns using shRNA are a useful tool as they allow persistent knockdown of a target in the presence of doxycycline allowing greater control over experimental parameters.

In agreement with published data (Ying et al., 2013), BCL6 knockdown reduced growth of lymphoma cell lines suggesting an important role for BCL6 in proliferation. Indeed, BCL6 knockdown resulted in a 50% decrease in shRNA-positive cells in the GCB-DLBCL cell line, SUDHL4 (figure 3.8A); a direct agreement with published data demonstrating a 30-70% reduction in shRNA-positive cells after two weeks (Ying et al., 2013). Whilst T-cell lymphoma cell lines exhibited a range of sensitivities to BCL6 knockdown, Karpas-299 reduced shRNA-positive populations at a similar rate to SUDHL4 indicating the importance of BCL6 in this cell line (figure 3.8A). However, SUDHL1 and DEL exhibited a delayed or less-marked response (figure 3.8A) despite marked BCL6 knockdown. Whilst DEL exhibited a small reduction in shRNA-positive populations in only 1 of 2 shRNAs, there was no evidence of apoptosis induction or changes in cell cycle (figures 3.9B and 3.10B); therefore it is plausible to conclude that DEL may be largely insensitive to BCL6 knockdown. The delayed response of RFP-reduction in SUDHL1 could be due to an important downstream BCL6 target, rather than the effect of BCL6 itself, that is important for proliferation. To evaluate this hypothesis, ChIP-Seq in combination with a Gene Expression Array would reveal any potentially important BCL6 targets. However, in SUDHL1 4 days post-combination, cells

harbouring BCL6 knockdown resulted in increased G2/M populations compared to RFP-negative cells suggesting an immediate effect of BCL6 knockdown also (figure 3.9B). BCL6 knockdown may therefore cause an effect on cellular growth initially but compensate this effect by upregulation of one or more pathways to promote survival. For example, SUDHL1 has been demonstrated to exhibit high expression of CDK6 and c-MYC (Nagel et al., 2008, Raetz et al., 2002), molecules demonstrated to be important in cell survival and cell cycle progression which may compensate for BCL6 inhibition (Scheicher et al., 2015, Weilemann et al., 2015). BCL6 has previously been demonstrated to be important in cell cycle progression in DLBCL cell lines, knockdown of BCL6 results in accumulation of cells in G1/G0 populations (Ying et al., 2013). In SUDHL1 cells, accumulation of cells in G2/M was observed with BCL6 knockdown (figure 3.9B) suggesting BCL6 may regulate the cell cycle in T-cells at a different stage to B-cells.

It has been reported that doxycycline can affect the metabolism and growth of a number of cell lines (Ahler et al., 2013, Pulvino et al., 2015). In one of these studies, exposure of cells to 1µg/ml doxycycline for 96 hours resulted in increased expression of metabolic pathway genes and increased production of lactate causing a reduction in the growth rate of cell lines (Ahler et al., 2013). Interestingly, in the work presented here a certain threshold of doxycycline was required to significantly down regulate IRF4 expression in SUDHL1 (figure 3.7A) suggesting doxycycline also affects pathways other than the metabolic pathway. Interestingly, knockdown of BCL6 at higher concentrations of doxycycline (2µg/ml) resulted in a greater effect on proliferation than at 0.5µg/ml in SUDHL1 suggesting BCL6 deficiency may synergise cells to stressful environments, such as the effects of doxycycline, however this data was not illustrated due to the confounding effect of reduction of IRF4 with doxycycline (figure 3.7A). In addition, BCL6 has been shown to repress the glycolytic pathway in CD8<sup>+</sup> mouse T-cells (Leavy, 2014, Man and Kallies, 2014, Oestreich et al., 2014) which could indicate a potential synergistic mechanism of action.

In order to address the issue of off-target doxycycline effects, a non-inducible knockdown system could be employed to eliminate the presence of doxycycline. The drawbacks of non-inducible systems include the inability to control unwanted effects from genomic integration as well as the inability to control induction of the shRNA.

Both inducible and non-inducible lentiviral knockdown systems rely on transducing different cells with a separate control virus which may give rise to specific growth bias if viral integrations differ between control and target shRNA cells. The benefit of the inducible system over the non-inducible system, however, is the ability to control for integration bias by comparing growth rates of transduced, non-induced cells against transduced, induced cells. In addition, inducible systems allow the evaluation of short-term knockdown effects, without adaptation of cells to knockdown, as well as allowing expansion of transduced cells harbouring shRNA which would be toxic if active. Therefore, a robust investigation of BCL6 knockdown would employ both inducible and non-inducible systems to alleviate the issues with both techniques. However, shRNA knockdown systems can induce immune responses giving rise to aberrant results. A technique has been recently developed which allows the deletion of genomic regions through exploitation of the CRISPR-Cas9 system employed by bacteria (Shalem et al., 2014). This technique would allow complete removal of *BCL6* DNA from the cell line genome eliminating any BCL6-mediated effects. This technique is only viable however, if BCL6 is not vital for cellular survival as knockout of *BCL6* may cause rapid death. This could be overcome by introducing a BCL6 coding sequence under the control of a tetracycline promoter, whereby presence of tetracycline switches off transcription of the expression cassette (Baron and Bujard, 2000).

All cell cycle profiles also exhibited increases in S-phase with induction of shRNA (figure 3.9A). This may indicate changes in transcriptional activity brought about by doxycycline by induction of the glycolytic pathway in these cells (Ahler et al., 2013). Alternatively, increased S-phase may be an artefact of inefficient flow cytometry compensation and be a result of detecting RFP expression in the FITC channel.

This work has demonstrated sensitivity to the BCL6 inhibitor, 79-6, across multiple lymphoma subtypes. All cell lines are sensitive to 79-6 treatment suggesting that, if 79-6 is targeting BCL6, BCL6 constitutes a putative therapeutic target. The sensitivity of cell lines to 79-6 does not appear to correlate with expression of BCL6. Out of the T-cell lines, Karpas-299 expresses the most BCL6 protein whilst DEL expresses the least (figure 3.2). However, despite this, the IC50s recorded for each are very similar. It is reasonable, therefore, to conclude that levels of BCL6 protein do not

determine sensitivity to this inhibitor. For example, SUDHL4 and Karpas-422 express the most BCL6 protein across the panel of cell lines (figure 3.2B). These cell lines are GCB-DLBCL which naturally express high quantities of BCL6 as their cell of origin is a GC B-cell (Basso and Dalla-Favera, 2010). However, despite this, SUDHL4 is considered BCL6 “dependent” whilst Karpas-422 is defined as a BCL6 “resistant” cell line when treated with RI-BPI (Cerchiatti et al., 2010a, Cerchiatti et al., 2009). Another problem arises with 79-6 however: those cell lines previously defined to be insensitive to RI-BPI, Karpas-422 and Pfeiffer, as well as Toledo, defined as requiring >15mM of 79-6 to achieve a 50% response (Cerchiatti et al., 2010a, Cerchiatti et al., 2009), were found to be sensitive in this study. Whilst Toledo exhibited the highest IC50 of all cells tested (721µM) which may be indicative of resistance, Pfeiffer exhibited a lower resistance (375µM) (figure 3.14A). Initially, Karpas-422 displayed pseudo-insensitivity by Resazurin analysis (figure 3.14A) however this was found to be caused by the high concentrations of DMSO required to solubilise a 1mM dose of 79-6 for cell lines (figure 3.13B). Further investigation revealing the sensitivity of Karpas-422 to 79-6 (figure 3.14) prompts the notion that 79-6 may not solely target BCL6. It is reasonable to believe that 79-6 works, at least in part, through BCL6 as B-cell targets of BCL6 were found to be upregulated by 79-6 treatment in SUDHL4 (figure 3.16). This is in agreement with previously published data which demonstrates that these targets were found to be greatly upregulated with 79-6 treatment (Cerchiatti et al., 2010a). In the T-cell lines however, it appears that 79-6 does not induce the expression of *P53*, *P21*, *c-MYC*, *IRF4*, or *BLIMP1* (figure 3.16).

The high concentration of 79-6 required to elicit a growth inhibition response discordance with published data cast doubts upon the specificity of the drug. It is generally accepted that anticancer drugs should be efficacious within the nanomolar region where possible as higher concentrations of drug lead to higher non-specific effects (Wong et al., 2012). The lack of 79-6 specificity for BCL6 may originate due to the design process utilised. Briefly, 79-6 was designed using computer aided drug design to screen for compounds which associated with the same residues of the lateral groove of BCL6 as SMRT. Next, compounds were selected based upon efficacy and binding conformation. Finally, selected compounds were further refined evaluating which compounds alleviated BCL6-mediated repression of a luciferase construct

through use of a GAL4 DNA binding domain-BCL6<sup>BTB</sup> construct with a GAL4 luciferase reporter construct (Cerchietti et al., 2010a). This assay yielded the compound 79-6 which was confirmed by X-ray crystallography to bind the lateral groove of BCL6. The authors test for the specificity of 79-6 by repeating the same luciferase reporter construct assay with GAL4 DNA binding domains fused to other BTB-containing proteins such as kaiso, hypermethylated in cancer 1, and promyelocytic zinc finger, demonstrating no discernible effect on luciferase levels. However, the authors do not test any other types of proteins for 79-6 binding. To fully elucidate if 79-6 targeted BCL6, the same luciferase reporter coupled assay could be utilised in this project to investigate if the BTB domains repressive activity on luciferase could be relieved with 79-6 treatment. Critically however, further biochemical investigations into the binding of 79-6 with a diverse range of proteins should be investigated to ascertain any potential non-specific binding.

In agreement with the 79-6 data, BCL6 shRNA knockdown could not significantly upregulate mRNA or protein expression of IRF4, BLIMP1, or c-MYC (figures 3.11A and figure 3.12A). This is in direct contrast to what is known about normal T-cell physiology, BCL6 and BLIMP1 antagonise one another's function and, in addition, directly bind and repress each other in T-cells (Cimmino et al., 2008, Johnston et al., 2009). It is possible that BCL6 has a mutated promoter site in ALCL cells that prevents the binding of BLIMP1 as well as BCL6 itself, as seen in DLBCL (Pasqualucci et al., 2003). This could, potentially, result in constitutive BCL6 expression which could overcome inhibitor efficiency through overexpression of the protein. Alternatively, as BLIMP1 is commonly mutated in ALCL it may be mutated or deleted to prevent the repressive effects of BCL6 on *PRDM1* transcriptional activity (Boi et al., 2013). In contrast to shRNA knockdown data, siRNA-mediated knockdown of BCL6 caused a modest increase in the RNA levels of IRF4 and BLIMP1 in SUDHL1, but not in Karpas-299 (figure 3.6B), which was lost after 72 hours. Therefore, it is possible that BCL6 exerts repressive activity on IRF4 and BLIMP1 initially but is then lost, as the earliest time point assessed for shRNA-mediated knockdown is 72 hours post-induction (figure 3.11 and figure 3.12) and therefore the cells may have compensated for BCL6 knockdown by this point. However, it should be noted that BCL6 targets are not the same between cells. A recent study showed that only 50% of BCL6 target genes are common between

breast cancer and B-cell lymphoma cancers (Walker et al., 2014). Interestingly, BCL6 is still required for the survival of these cell lines; however, BCL6 did not affect BLIMP1 transcription activity (Walker et al., 2014). A recent study into targets of BCL6 in T<sub>FH</sub> cells has also demonstrated that BCL6 represses a number of targets involved in T-cell differentiation, signalling, and migration, including: *STAT4*, *IFNGR1*, *GIMAP1*, *RORA* and *GATA3* (Hatzi et al., 2015). As well, BCL6 activity varies between B and T-cell lineages suggesting BCL6 will have vastly different targets. For example, an inactivating mutation introduced into *Bcl6* into early B-cells in *Bcl6*<sup>-/-</sup> mice results in complete abrogation of GC and reduced T<sub>FH</sub> cell formation (Huang et al., 2013b). Conversely, introduction of the mutated *Bcl6* into early T-cells results in normal T<sub>FH</sub> cell production suggesting a different transcriptional programme between cell lineages (Huang et al., 2013b). Future work should therefore focus on investigation of the transcriptional control of known BCL6 T-cell target genes within T-cell lymphoma.

Further work could focus on investigating BCL6 as a therapeutic target in T-cell lymphoma. 79-6 is a weak and non-specific inhibitor of BCL6 as, in this project, all cells were killed by the drug irrespective of reported dependency on BCL6 (figures 3.14 and 3.15). RI-BPI however is a well-established BCL6 inhibitor proven to be very specific to BCL6 targeting (Cerchietti et al., 2010a, Cerchietti et al., 2010b, Walker et al., 2014). The primary drawbacks of RI-BPI as a therapeutic intervention are the inability for oral delivery, as well as the complexity and expense of synthesis of the peptide.

The data presented suggests, that BCL6 is required for effective growth of at least some T-cell lymphoma cell lines. Indeed loss of BCL6 in normal murine CD8<sup>+</sup> T-cells is detrimental to the growth of these cells (Ichii et al., 2002). One possible mechanism of action which has been highlighted by this data is the repression of the glycolytic pathway. The anaerobic metabolism pathway is less efficient than aerobic respiration but it allows the production of Adenine-Triphosphate (ATP) without oxygen which may be beneficial for solid tumour cells in a hypoxic microenvironment. This could result in a rapid proliferation rate of tumour cells in harsher environments aiding metastasis (Hanahan and Weinberg, 2000). Indeed, it has been demonstrated across multiple malignancies that upregulation of PI3K can result in loss of glycolysis-dependence, and more aggressive tumours (Kalaany and Sabatini, 2009). BCL6 may act in this way and inhibition may not produce a rapid response on its own; however if

BCL6 promotes anaerobic respiration it has the potential to synergise cells to treatments which may exploit anaerobic respiration.

Future work may focus on expanding the panel of cell lines, or development of murine xenograft models, to incorporate types of PTCL other than ALCL to assess the role of BCL6 in these lymphomas. In particular, AITL characteristically has high BCL6 expression and may be BCL6 dependent (Yuan et al., 2005). Of most importance, PTCL cell lines should be treated with RI-BPI to ascertain if cells are reliant upon BCL6 through comparison with established BCL6-dependent cell lines. In addition, work should focus on combination therapy of BCL6 inhibition with current CHOP drugs and c-MYC inhibitors to investigate if BCL6 inhibition synergises cells to these treatments. Furthermore, exploiting the RD2 domain of BCL6 could prove important. This domain has recently been demonstrated to be required for HDAC recruitment and transcriptional inhibition of some genes and its actions may represent a means by which cells might resist the effects of BTB domain inhibition (Bereshchenko et al., 2002, Fujita et al., 2004, Huang et al., 2014). A method of overcoming may be to rely on the RD2 domain to exert inhibitory actions on target genes. To improve BCL6 knockdown experiments, utilisation of CRISPR-mediated knockout could be undertaken to evaluate if complete removal of BCL6 is fatal to cellular proliferation/survival. Finally, ChIP-Seq and Gene Expression Arrays of PTCL cell lines could be utilised to find novel T-cell targets of BCL6 to determine if any are important for PTCL survival.

## **Chapter 4: IRF4 in the maintenance of T-cell lymphoma**



## 4. IRF4 in the maintenance of T-cell lymphoma

### 4.1 Introduction

IRF4 is a transcription factor required for the differentiation, metabolism, and survival of B- and T-cells through transcriptional regulation of *BCL6* and *BLIMP1*, amongst other targets (Yao et al., 2013, Bruhn et al., 2012, Mobini et al., 2009, Kwon et al., 2009). Whilst it is known that IRF4 promotes the activity of both BCL6 and BLIMP1 in T-cells, the reciprocal interactions are not as well established in T-cells as in B-cells (figure 4.1). Several pieces of evidence indicate that IRF4 may play a role in driving T-cell malignancies, including the identified role of IRF4 in HTLV-I transformed ATL (Wang et al., 2011a), the occurrence of IRF4 translocations in T-cell lymphoma, and the high expression of IRF4 exhibited across certain T-cell lymphomas subsets (Feldman et al., 2011, Feldman et al., 2009, Kwon et al., 2009).

Therapeutic targeting of IRF4 is potentially difficult and no direct inhibitors exist. However a link between the immunomodulatory drug, Lenalidomide, and IRF4 expression has been elucidated. Specifically, IRF4 expression correlates with Lenalidomide sensitivity in ABC-DLBCL and treatment with the drug leads to downregulation of IRF4 (Zhang et al., 2013). The drug has been used successfully for

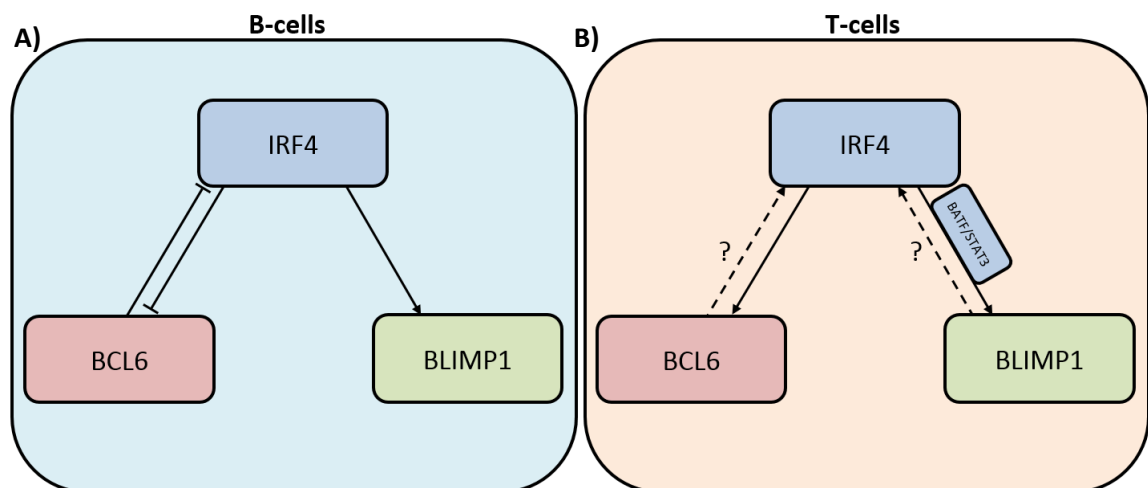


**Figure 4.1: Interaction of IRF4 with BCL6 and BLIMP1 in B-cells vs. T-cells**

A) In B-cells, IRF4 has a mutual inhibition of BCL6 whilst promoting BLIMP1 expression B) In T-cell differentiation, IRF4 interactions are less well characterised. IRF4 facilitates both BCL6 and BLIMP1 activities during T-cell development (Bollig et al., 2012, Honma et al., 2008). BCL6 expression, and subsequent  $T_{FH}$  cell differentiation is abrogated in  $Irf4^{-/-}$  mice demonstrating a positive interaction of IRF4 on BCL6 (Lohoff et al., 2002). IRF4 also forms complexes with BATF to facilitate chromatin remodelling, this complex can then associate with STAT3 to promoter expression of BLIMP1 (Li et al., 2012). The effect of BCL6 and BLIMP1 upon IRF4 expression is not known to date.

IRF4-driven malignancies such as CLL and MM (Herman et al., 2011, Li et al., 2011) and thus may be useful for T-cell lymphomas.

The aim of this chapter is therefore to investigate IRF4 as a potential oncoprotein in T-cell lymphoma. The chapter investigates the effect of IRF4 deficiency on proliferation, cell cycle, and induction of apoptosis of T-cell lymphoma cell lines. The chapter then examines the effect of targeting IRF4 therapeutically using Lenalidomide, as well as the determining the effect of IRF4 on expression of downstream targets BCL6, BLIMP1, and c-MYC.

## 4.2 Results

### 4.2.1 IRF4 siRNA knockdown results in a slight reduction in proliferation/survival of SUDHL1

In order to investigate the effect IRF4 siRNA knockdown had upon the proliferation/survival of ALK+ ALCL cell lines, SUDHL1 and Karpas-299 were electroporated with 500nM IRF4 siRNA or non-silencing siRNA and counted by Trypan Blue exclusion every 24 hours for 3 days. SUDHL1 exhibited a slight decrease in the total number of cells at every time point (figure 4.2). Despite the trend observed in this cell line, no result was found to be significant (24 hours  $p=0.055$ , 48 hours  $p=0.061$ , 72 hours  $p=0.137$ ). Karpas-299 was unaffected by siRNA knockdown at all timepoints (24 hours  $p=0.964$ , 48 hours  $p=0.564$ , 72 hours  $p=0.309$ ).

### 4.2.2 IRF4 siRNA knockdown has minimal, cell line-specific effects on BCL6 and BLIMP1 expression

RNA and protein was collected from SUDHL1 and Karpas-299 cells every 24 hours for 3 days post-electroporation and assessed by qPCR and western blot. Successful knockdown of RNA and protein was achieved in both cell lines (figure 4.3) with the greatest knockdown being recorded at 24 hours in both cell lines (SUDHL1: 24 hours  $p=0.0236$ , 48 hours  $p=0.0238$ , 72 hours  $p=0.041$ , Karpas-299: 24 hours  $p<0.0001$ , 48 hours  $p=0.0385$ , 72 hours  $p=0.175$ ). Knockdown of IRF4 in SUDHL1 resulted in increased expression of BCL6 protein at 24 hours which was not observed at 48 and 72 hours (figure 4.3A). No effect on BLIMP1 protein expression was observed in SUDHL1. In contrast, Karpas-299 exhibited a reduction in BCL6 protein expression with IRF4 knockdown (figure 4.3A), whilst no detectable effect was observed on BLIMP1 protein

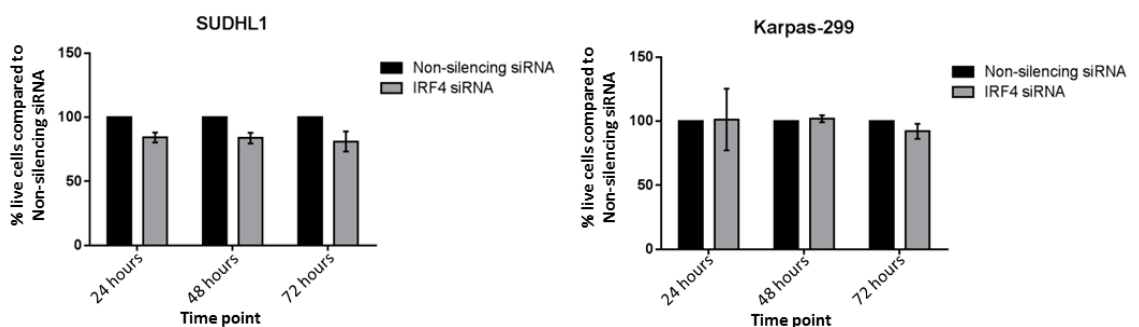


**Figure 4.2: Counts of IRF4 knockdown lymphoma cells**

Counts show total live cells treated with 500nM IRF4 siRNA normalised to non-silencing siRNA counts. Error bars indicate standard error of the mean, data is representative of three independent replicates. No counts were found to be significantly altered by a paired t-test.

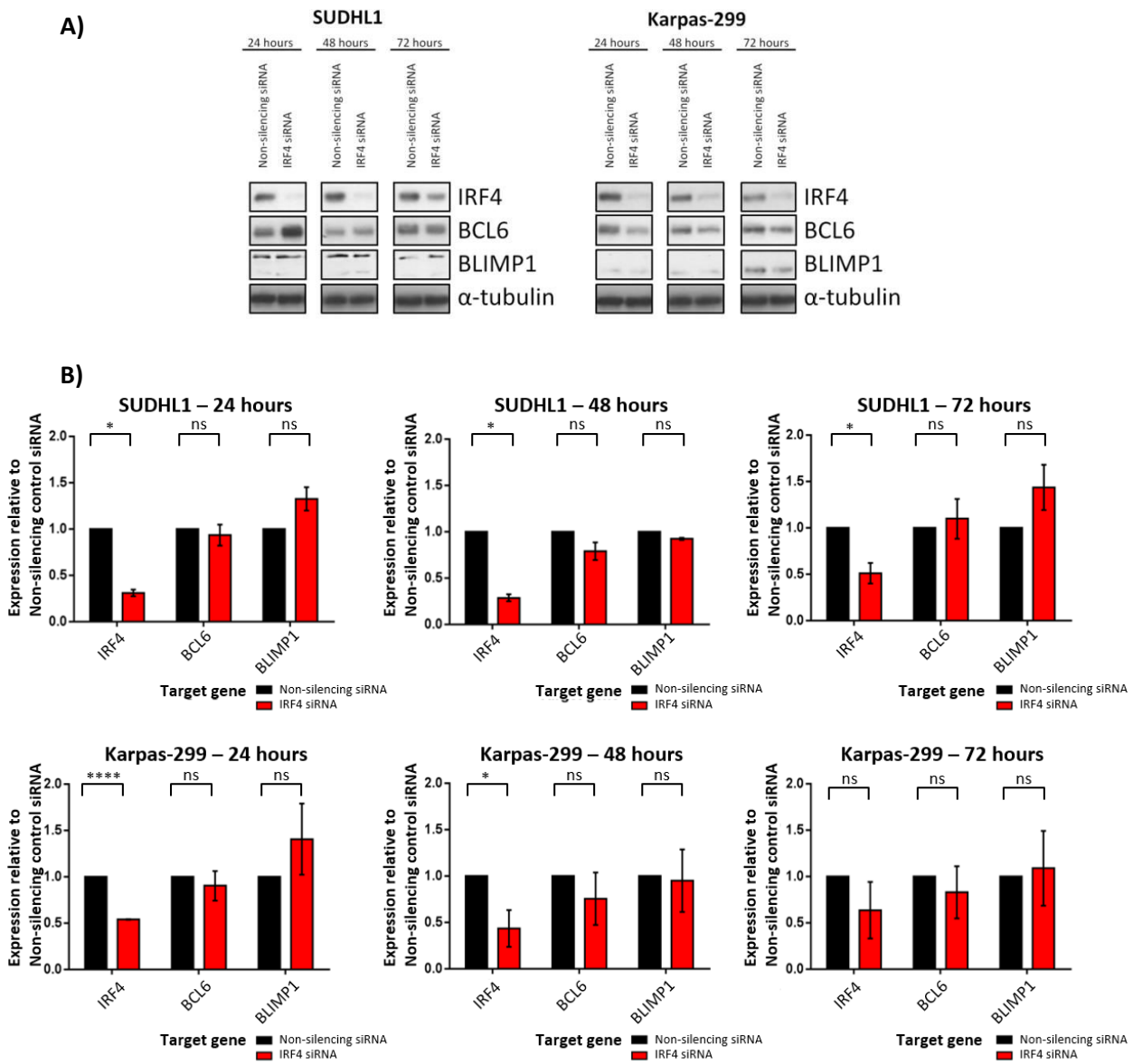


**Figure 4.3: Effect of IRF4 knockdown on the BCL6-IRF4-BLIMP1 transcription factor axis**

A) Timecourse western blot of SUDHL1 and Karpas-299 treated with non-silencing or IRF4 siRNA and assessed after the indicated time points. Results are representative of 3 independent experiments. Protein bands depicted for BLIMP1 in Karpas-299 are believed to be due to non-specific binding of the antibody. B) Relative mRNA levels in ALCL cell lines SUDHL1 and Karpas-299, n=3 error bars indicate standard error of the mean. Significance calculated using a paired students t-test, \* p<0.05, \*\* p<0.01, \*\*\* p<0.001, \*\*\*\* p<0.0001, ns = not significant.

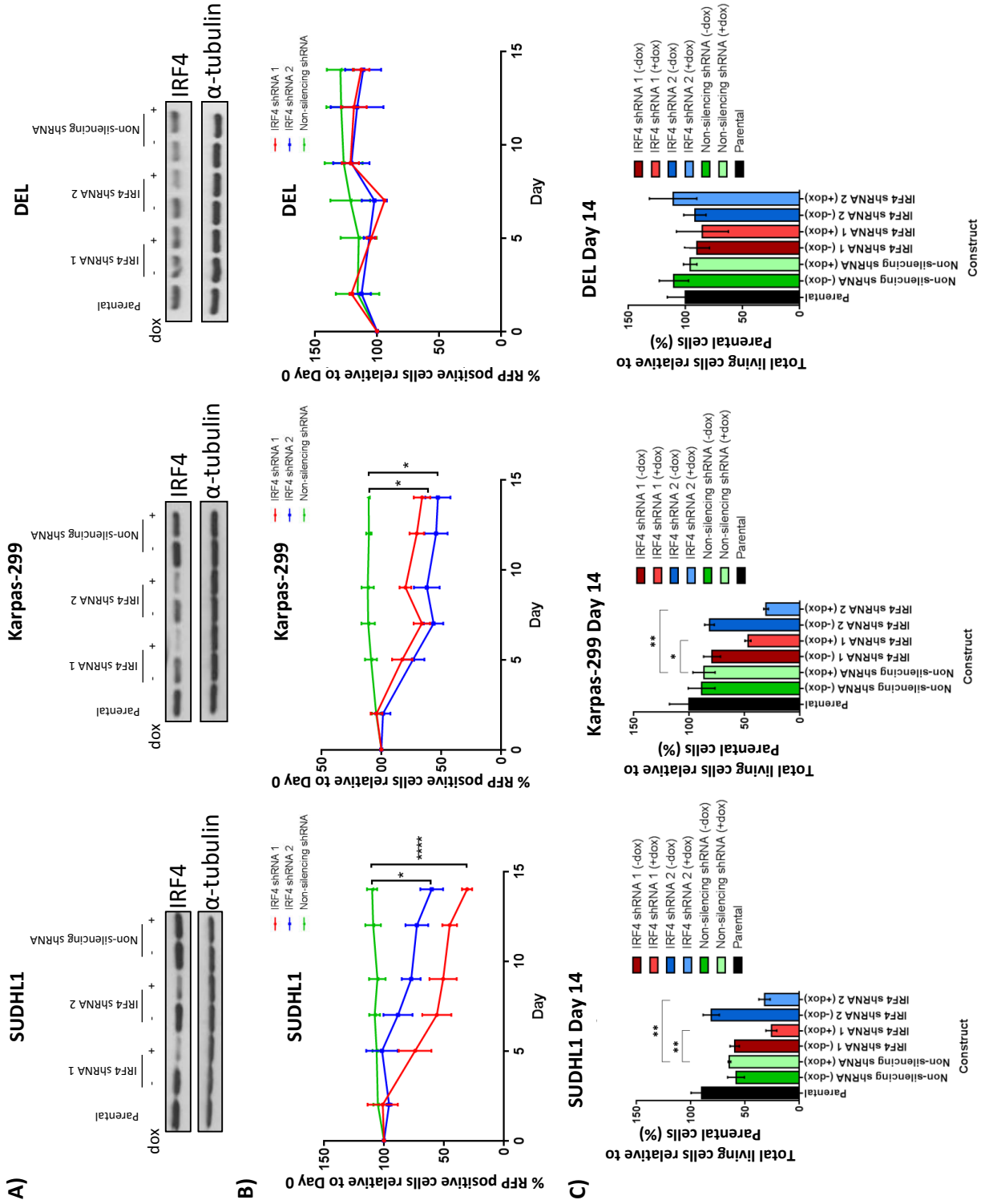
levels. Despite the effect IRF4 knockdown had upon BCL6 protein levels, at the mRNA level, IRF4 knockdown in SUDHL1 resulted in slightly decreased *BCL6* levels at 48 hours only which were not found to be significant (figure 4.3B) (24 hours  $p=0.5621$ , 48 hours  $p=0.1958$ , 72 hours  $p=0.637$ ). *BLIMP1* mRNA levels were increased by IRF4 knockdown at 24 and 72 hours in SUDHL1 but were not found to be significant (24 hours  $p=0.01701$ , 48 hours  $p=0.0675$ , 72 hours  $p=0.2391$ ) (figure 4.3B). Karpas-299 showed no significant effect on mRNA expression of BCL6 or BLIMP1 at any time point (figure 4.3B). However, there is a general trend of decreased BCL6 expression (24 hours  $p=0.3974$ , 48 hours  $p=0.2713$ , 72 hours  $p=0.3994$ ), consistent with protein expression data, and a modest increase in BLIMP1 mRNA levels with IRF4 knockdown (24 hours  $p=0.2075$ , 48 hours  $p=0.8181$ , 72 hours  $p=0.7441$ ) in these cells (figure 4.3B). Overall, there are small and inconsistent changes in *BCL6* and *BLIMP1* mRNA across both cell lines as well as between mRNA and protein levels.

#### **4.2.3 IRF4 shRNA knockdown results in reduced proliferation/survival of ALK+ ALCL cell lines**

Considering the subtle proliferation/survival phenotype and inconsistent changes in mRNA/protein levels caused by the siRNA knockdown of IRF4, shRNA knockdown was pursued to investigate if stable, prolonged, knockdown of IRF4 would produce a more marked effect. To ensure the IRF4 shRNAs could knockdown IRF4, SUDHL1, Karpas-299, and DEL cells were transduced with IRF4 shRNA or non-silencing shRNA constructs, selected with puromycin for 1 week, and induced with concentrations of doxycycline defined previously (see chapter 3, section 3.2.5). After 72 hours, protein levels showed a marked decrease in IRF4 levels with induction of IRF4 shRNAs in SUDHL1 and Karpas-299 but not in DEL (figure 4.4A). Due to the poor knockdown exhibited by DEL in shRNA 1 (figure 4.4A) and the inability to maintain knockdown levels using shRNA 2 (figure 4.9), the cell line was defined as a negative control for all experiments.

**Figure 4.4: IRF4 knockdown results in reduced growth rates of ALK+ ALCCL cell lines**

A) IRF4 shRNA knockdown achieved in SUDHL1 and Karpas-299 but not DEL. Transduced cell lines were incubated with and without doxycycline for 72 hours and lysed for protein analysis. B) RFP-tracking experiments in lymphoma cell lines. Transduced cells were induced with doxycycline for 72 hours, induced cells were then mixed in a 50:50 ratio transduced to non-transduced cells and maintained in doxycycline-containing medium. Samples for flow cytometric analysis were taken every 2-3 days for 2 weeks. Results are derived from 3 independent replicates, error bars indicate standard error of the mean. C) Total cell numbers in SUDHL1, Karpas-299, and DEL relative to parental cells after 14 days in culture, data is derived from 4 independent replicates, error bars indicate standard error of the mean. Significance calculated using a paired students t-test, \* p<0.05, \*\* p<0.01.



To evaluate the role of IRF4 on proliferation/survival of cell lines, transduced cell lines were combined in a 50:50 ratio with non-transduced cells and treated with doxycycline to induce shRNA knockdown and RFP expression. RFP levels were tracked by flow cytometry for 2 weeks post-mixing. IRF4 shRNA expression induced a reduction in RFP levels after 14 days in two out of three cell lines (figure 4.4B). At day 14, RFP-positive cells, indicative of IRF4 knockdown cells, were significantly reduced in SUDHL1 and Karpas-299 in proportion to non-silencing shRNA control (SUDHL1: shRNA 1  $p=0.001$ , shRNA 2  $p=0.045$ , Karpas-299: shRNA 1  $p=0.01$ , shRNA 2  $p=0.012$ ). Conversely, RFP-positive cells in DEL did not significantly alter in proportion to non-silencing counterparts (shRNA 1  $p=0.21$ , shRNA 2  $p=0.759$ ).

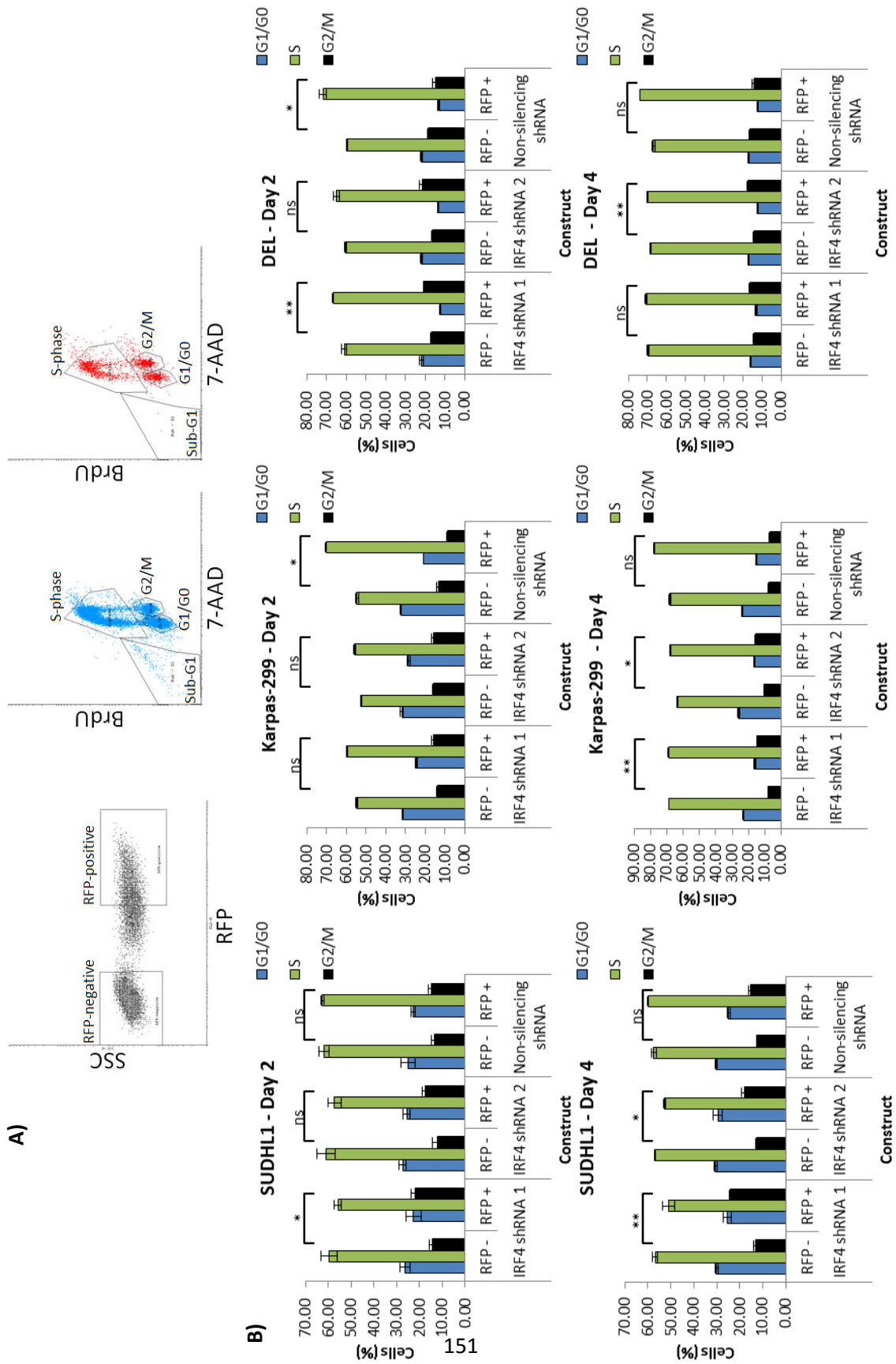
Consistent with these data, IRF4 knockdown in both SUDHL1 and Karpas-299 showed a significant reduction in the number of living cells by Trypan Blue exclusion with both shRNAs compared to non-silencing shRNA control (SUDHL1: shRNA 1  $p=0.009$ , shRNA 2  $p=0.005$ , Karpas-299: shRNA 1  $p=0.034$ , shRNA 2  $p=0.006$ ). Conversely, both IRF4 shRNAs expressed in DEL had no effect on live cell count compared to non-silencing shRNA control (shRNA 1  $p=0.675$ , shRNA 2  $p=0.104$ ) (figure 4.4C).

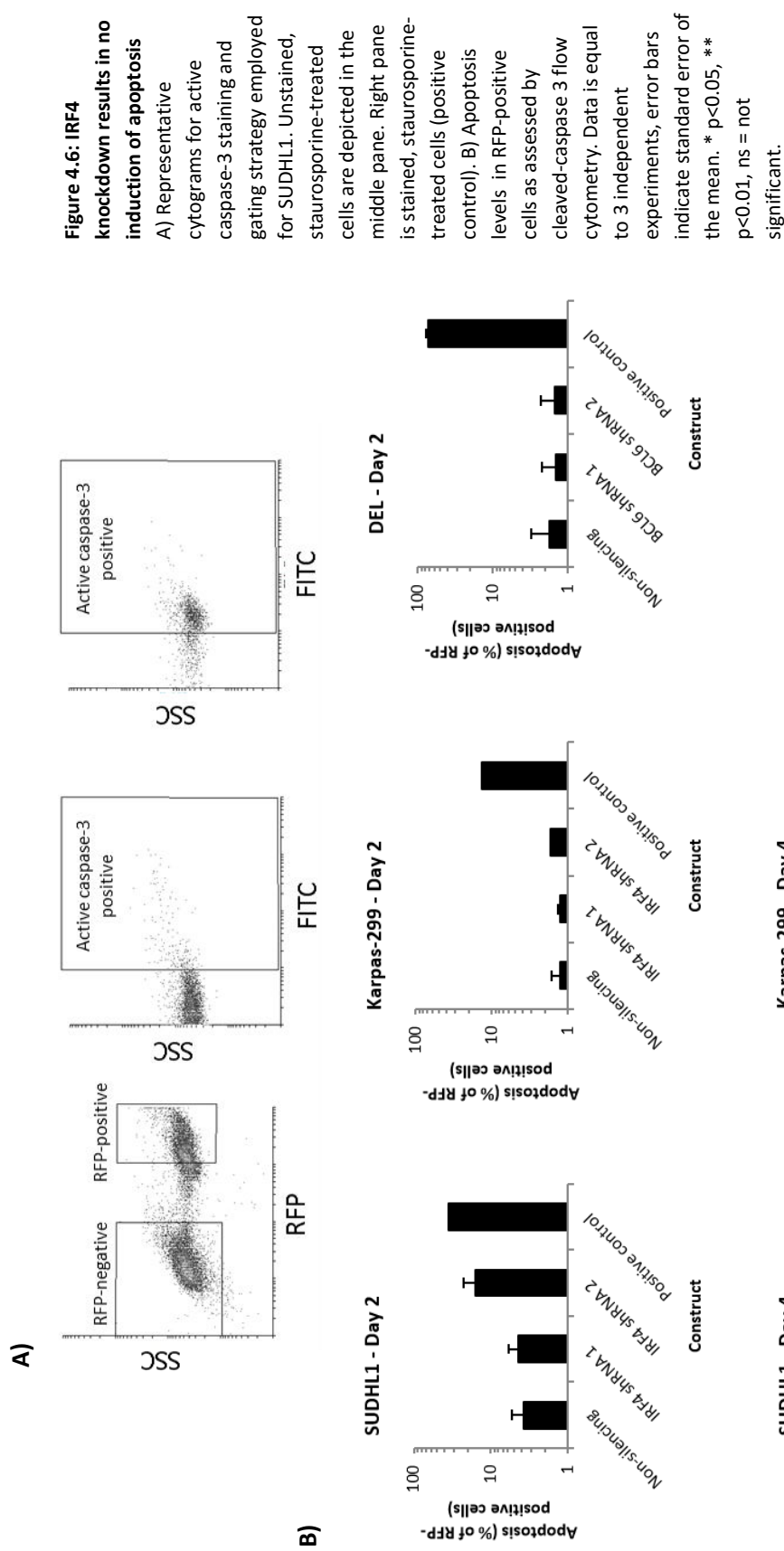
#### ***4.2.4 IRF4 shRNA knockdown results in a minor increase in G2/M populations***

To evaluate if IRF4 knockdown resulted in decreased proliferative activity by altering cell cycle kinetics, flow cytometric cell cycle analysis was undertaken (figure 4.5A). Samples were collected at days 2 and 4 of the RFP-tracking experiment shown in figure 4.5A. At day 2, RFP-positive populations of SUDHL1 showed a small increase in G2/M populations in only the IRF4 shRNA 1 culture ( $p=0.043$ ) whilst no significant effect was observed on the G2/M population fraction across the remaining shRNAs (figure 4.5B) (shRNA 2  $p=0.133$ , non-silencing shRNA  $p=0.455$ ). However, after 4 days in culture, both IRF4 shRNAs significantly increased G2/M populations in SUDHL1 which was not found in non-silencing shRNA cells (figure 4.5B) (shRNA 1  $p=0.001$ , shRNA 2  $p=0.017$ , non-silencing shRNA  $p=0.069$ ). Karpas-299 showed no significant effect on G2/M populations with IRF4 knockdown after 2 days in culture, although non-silencing shRNA treated cells did exhibit a significant small reduction in G2/M populations which was not found in IRF4 knockdown cells (figure 4.5B) (shRNA 1

**Figure 4.5: IRF4 knockdown results in accumulation of G2/M populations in ALK+ ALCL cell lines**

A) Representative cytograms for BrdU/7-AAD staining and gating strategy employed for SUDHL1 cells. RFP-negative cell cycle trace is depicted in blue (middle pane) whilst RFP-positive cell cycle trace is depicted in red (right pane). B) Respective cell cycle profiles of RFP-negative and RFP-positive cells within a culture as assessed by BrdU/7-AAD staining at 2 and 4 days post mixing. Data is derived from 3 independent experiments, error bars indicate standard error of the mean. \* p<0.05, \*\* p<0.01, ns = not significant.





$p=0.248$ , shRNA 2  $p=0.903$ , non-silencing shRNA  $p=0.026$ ). After 4 days in culture, Karpas-299 exhibited very slight (albeit significant) increases in G2/M populations with IRF4 shRNA compared to non-silencing shRNA (figure 4.5B) (shRNA 1  $p=0.003$ , shRNA 2  $p=0.014$ , non-silencing shRNA  $p=0.488$ ). By day 2, IRF4 knockdown in DEL resulted in a minor (but significant) increase in G2/M populations using IRF4 shRNA 1 ( $p=0.009$ ) but not IRF4 shRNA 2 ( $p=0.064$ ) or non-silencing shRNA ( $p=0.086$ ) (figure 4.5B).

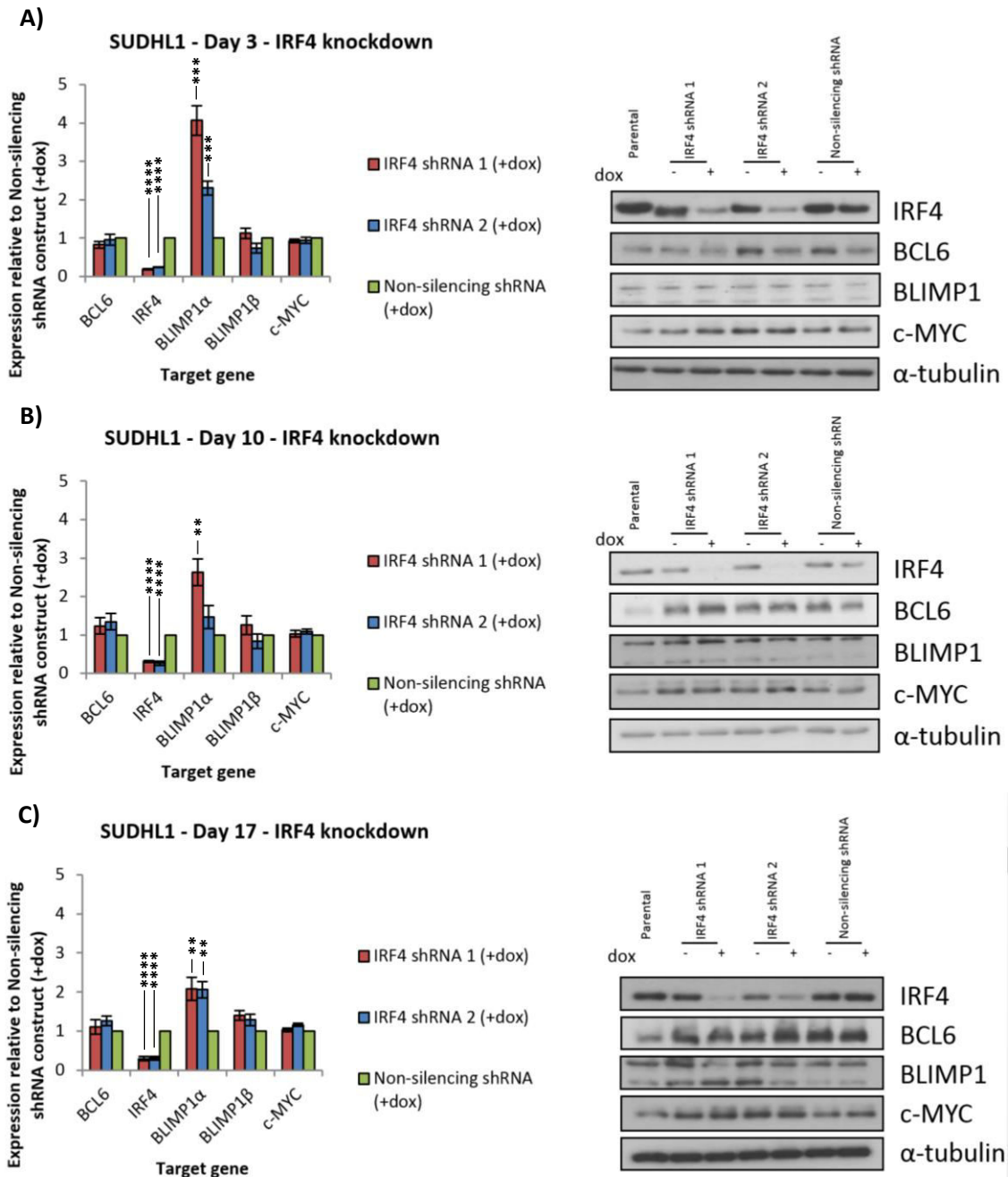
However, as seen with Karpas-299, non-silencing shRNA slightly decreased the G2/M population fraction which was not observed in IRF4 shRNA-treated counterparts. At day 4, IRF4 shRNA 1 treatment failed to increase G2/M populations ( $p=0.071$ ) whilst IRF4 shRNA 2 increased a miniscule but significant increase in G2/M populations, ( $p=0.006$ ) (figure 4.5B). These data demonstrate that cell lines sensitive to IRF4 knockdown, particularly SUDHL1, exhibit small increases in G2/M populations after 4 days culture in a competitive tracking experiment. Karpas-299 demonstrates a similar effect on cell cycle but to a much lower magnitude.

To assess apoptosis, samples were also taken at days 2 and 4 in culture, stained with active caspase-3 antibody, and assessed by flow cytometry (figure 4.6A). All cell lines harbouring IRF4 knockdown, apart from SUDHL1 IRF4 shRNA 1 and 2 at day 4 (shRNA 1  $p=0.0185$ , shRNA 2  $p=0.0039$ ), failed to reproducibly increase levels of apoptosis compared to non-silencing shRNA control (SUDHL1: day 2 shRNA 1  $p=0.8204$ , shRNA 2  $p=0.2939$ , Karpas-299: day 2 shRNA 1  $p=0.5227$ , shRNA 2  $p=0.9109$ , day 4 shRNA 1  $p=0.9277$ , shRNA 2  $p=0.21335$ , DEL: day 2 shRNA 1  $p=0.5992$ , shRNA 2  $p=0.247$ , day 4 shRNA 1  $p=0.5415$ , shRNA 2  $p=0.076$ ) (figure 4.6B). Whilst induction of apoptosis was not significant at day 2 with SUDHL1 IRF4 shRNA 2 there is a consistent induction of apoptosis with this IRF4 shRNA.

#### ***4.2.5 IRF4 promotes the expression of c-MYC with variable effects on BLIMP1 expression in Karpas-299***

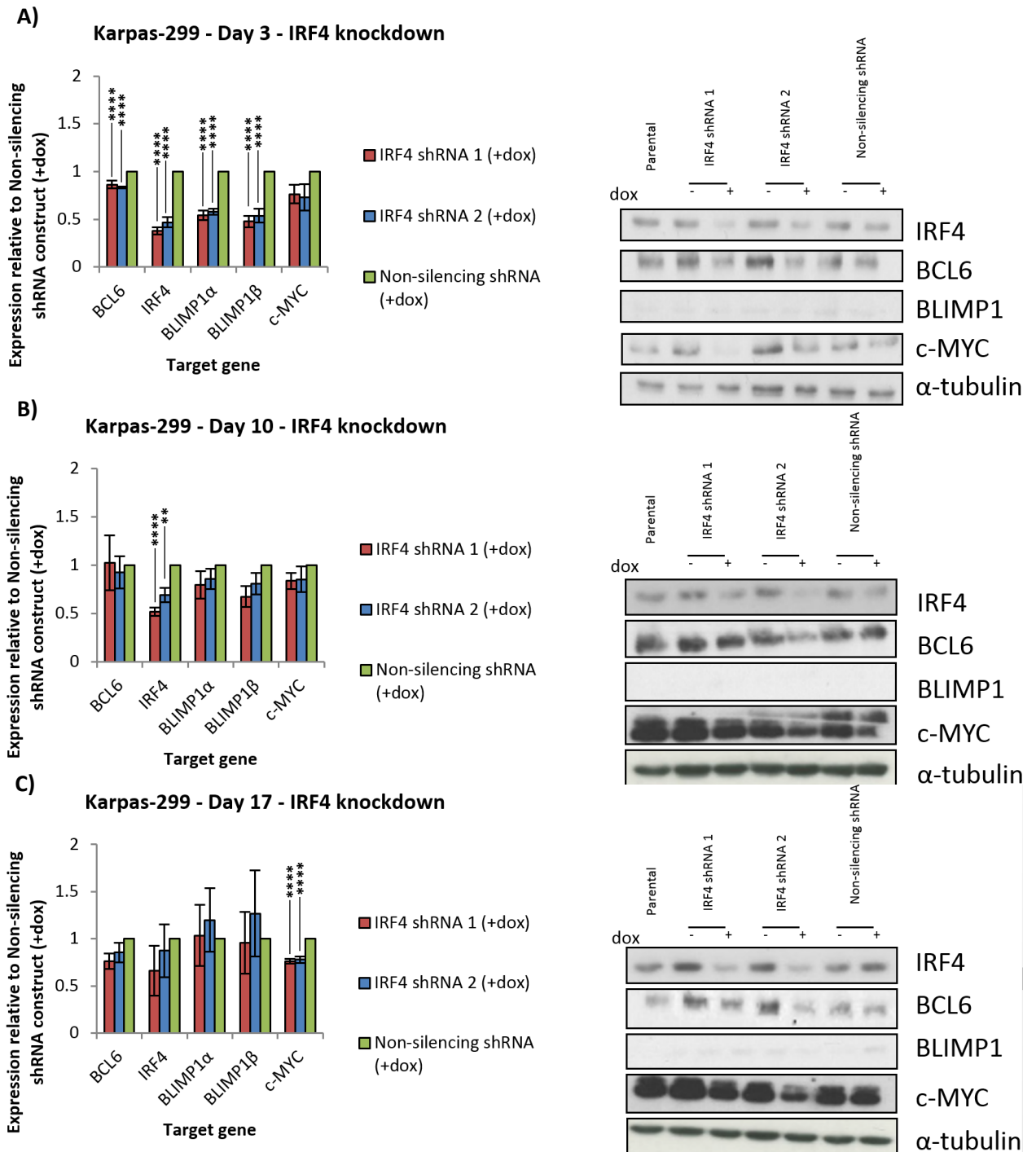
To assess the effect of IRF4 knockdown on expression of BCL6, IRF4, BLIMP1, and c-MYC, shRNA-transduced cells were cultured with doxycycline-containing medium for two weeks and lysed for RNA and protein analysis after 3, 10, and 17 days. SUDHL1 demonstrated significant IRF4 knockdown at both the RNA and protein level

across all days (both shRNAs and all days  $p < 0.0001$ ) whilst Karpas-299 demonstrated significant knockdown on days 3 and 10 at the RNA level (day 3: shRNA 1  $p < 0.0001$ , shRNA 2  $p < 0.001$ , day 10: shRNA 1  $p < 0.0001$ , shRNA 2  $p = 0.0067$ , day 17: shRNA 1  $p = 0.2472$ , shRNA 2  $p = 0.6676$ ) and across all days at the protein level (figures 4.7 and 4.8) whilst DEL only achieved significant knockdown at the RNA level on days 3 and 10 (day 3: shRNA 1  $p < 0.0001$ , shRNA 2  $p < 0.0001$ , day 10: shRNA 1  $p = 0.0238$ , shRNA 2  $p = 0.001$ , day 17: shRNA 1  $p = 0.33$ , shRNA 2  $p = 0.1679$ ) (figure 4.9).



**Figure 4.7: The effect of IRF4 shRNA knockdown on the expression of BCL6, IRF4, and BLIMP1 in SUDHL1**

Transcript and protein levels of transcription factors after induction of shRNA and maintenance of culture with 0.5µg/ml doxycycline-containing medium at A) Day 3, B) Day 10, C) Day 17. Data is derived from 4 independent replicates, error bars indicate standard error of the mean. Significance calculated using a paired students t-test, \* p<0.05, \*\* p<0.01, \*\*\* p<0.001, \*\*\*\* p<0.0001.



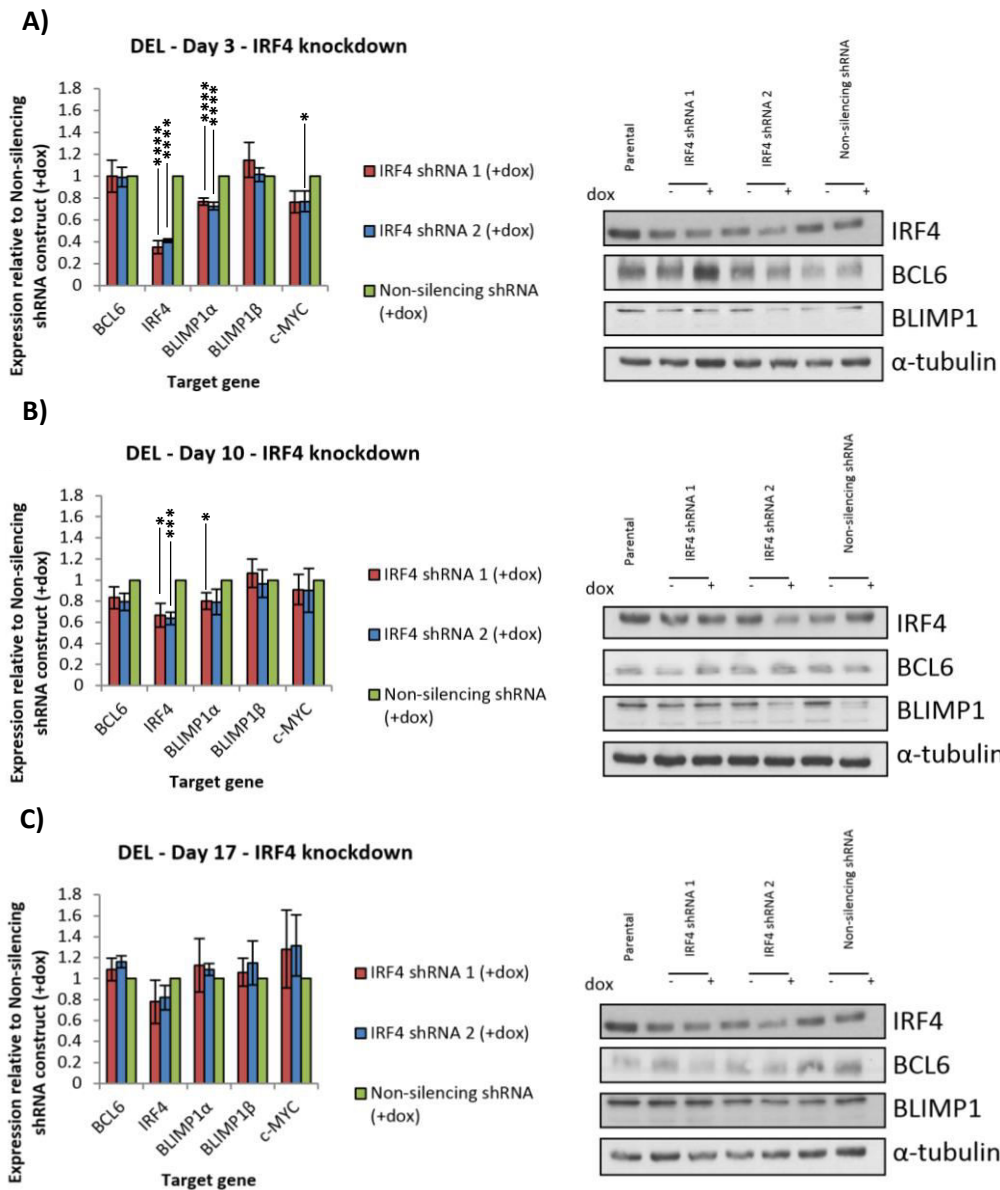


**Figure 4.10: The effect of IRF4 shRNA knockdown on the expression of BCL6, IRF4, and BLIMP1 in DEL**  
 Transcript and protein levels of transcription factors after induction of shRNA at A) Day 0, B) Day 7, C) Day 14. Day 0 is indicative of 72 hours treatment with 2 $\mu$ g/ml doxycycline. Data is equal to 4 independent replicates, error bars indicate standard error of the mean. Significance calculated using a paired students t-test, \*  $p < 0.05$ , \*\*  $p < 0.01$ , \*\*\*  $p < 0.001$ , \*\*\*\*  $p < 0.0001$ .

IRF4 knockdown resulted in a significant increase in *BLIMP1α* transcript levels at all timepoints in SUDHL1 (day 3: shRNA 1 p=0.0002, shRNA 2 p=0.0003, day 10: shRNA 1 p=0.0034, shRNA 2 p=0.0465, day 17: shRNA 1 p=0.0091, shRNA 2 p=0.0022) with no effect on *BCL6* (day 3: shRNA 1 p=0.0836, shRNA 2 p=0.779, day 10: shRNA 1 p=0.3036, shRNA 2 p=0.1495, day 17: shRNA 1 p=0.5943, shRNA 2 p=0.0724), *BLIMP1β* (day 3: shRNA 1 p=0.3811, shRNA 2 p=0.0746, day 10: shRNA 1 p=0.3317, shRNA 2 p=0.409, day 17: shRNA 1 p=0.9187, shRNA 2 p=0.5769), or *c-MYC* (day 3: shRNA 1 p=0.1824, shRNA 2 p=0.438, day 10: shRNA 1 p=0.3317, shRNA 2 p=0.409, day 17: shRNA 1 p=0.5282, shRNA 2 p=0.052) transcripts across all timepoints in SUDHL1 (figure 4.7). Despite having no effect on *BCL6* transcript levels, BCL6 protein levels were decreased with both IRF4 shRNAs as well as non-silencing shRNA-positive cells at day 3 only. No other transcription factors were affected (figure 4.7A). Parental cells showed a reduction in BCL6 protein levels compared to shRNA-positive cells, in SUDHL1, at days 10 and 17 (figure 4.7B and 4.7C).

Contrary to SUDHL1, IRF4 knockdown in Karpas-299 at day 3 resulted in significantly decreased *BLIMP1α* (day 3: shRNA 1 p=0.0001, shRNA 2 p<0.0001, day 10: shRNA 1 p=0.2721, shRNA 2 p=0.2305, day 17: shRNA 1 p=0.9187, shRNA 2 p=0.5769), and *BLIMP1β* (day 3: shRNA 1 p=0.0001, shRNA 2 p=0.0001, day 10: shRNA 1 p=0.0654, shRNA 2 p=0.1446, day 17: shRNA 1 p=0.9055, shRNA 2 p=0.5809) as well as *c-MYC* mRNA at day 17 (day 3: shRNA 1 p=0.0539, shRNA 2 p=0.0945, day 10: shRNA 1 p=0.1009, shRNA 2 p=0.3114, day 17: shRNA 1 p<0.0001, shRNA 2 p=0.0005), and a small, but significant decrease in *BCL6* mRNA at day 3 with both shRNAs and day 17 with shRNA 1 (day 3: shRNA 1 p<0.0001, shRNA 2 p<0.0001, day 10: shRNA 1: p=0.9298, shRNA 2: p=0.6796, day 17: shRNA 1 p=0.0284, shRNA 2 p=0.2157) (figure 4.8A and 4.8B). BCL6 and *c-MYC* reduction was also observed at the protein level at these timepoints. At day 17, *IRF4* mRNA levels were returning to basal levels whilst *BLIMP1α* and *BLIMP1β* were now unaffected by IRF4 knockdown (figure 4.8C). Reduction of *BCL6* and *c-MYC* mRNA was still evident at the RNA and protein level after 17 days (figure 4.8C).

DEL exhibited knockdown of IRF4 at the RNA level across days 3 and 10 (figure 4.9). However, protein knockdown was consistently unachievable at days 3 and 10 and was minimal by day 17 (figure 4.9C). Despite poor protein knockdown, loss of IRF4

resulted in decreased BCL6 protein levels at day 17 (figure 4.9C). In agreement with Karpas-299, IRF4 knockdown resulted in slightly decreased *BLIMP1α* (day 3: shRNA 1 p=0.0003, shRNA 2 p=0.0002, day 10: shRNA 1 p=0.0475, shRNA 2 p=0.1357, day 17: shRNA 1 p=0.635, shRNA 2 p=0.1753), but not *BLIMP1β* (day 3: shRNA 1 p=0.3987, shRNA 2 p=0.841, day 10: shRNA 1 p=0.643, shRNA 2 p=0.7936, day 17: shRNA 1 p=0.6636, shRNA 2 p=0.4968) RNA levels at days 3 and 10 (figure 4.9A and 4.9B). In addition, IRF4 knockdown caused a slight reduction in *c-MYC* transcript at day 3 (figure 4.9A) which recovered by day 17 (figure 4.9C) (day 3: shRNA 1 p=0.0579, shRNA 2 p=0.0471, day 10: shRNA 1 p=0.5556, shRNA 2 p=0.6534, day 17: shRNA 1 p=0.4778, shRNA 2 p=0.3224). Non-silencing shRNA cells treated with doxycycline decreased BCL6 protein levels at days 10 and 17 and BLIMP1 protein levels at day 10.

In summary, IRF4 knockdown was achieved in SUDHL1 and Karpas-299 but not DEL. All cell lines exhibited small variable effects on the expression of *BCL6*, *IRF4*, *BLIMP1*, and *c-MYC* with IRF4 knockdown. Of note, IRF4 knockdown in SUDHL1 resulted in an increase in only *BLIMP1α* mRNA but no effect on mRNA or protein of any other targets. Conversely, IRF4 knockdown in Karpas-299 resulted in a reduction of *BLIMP1α* mRNA and *c-MYC* mRNA and protein.

#### **4.2.6 PTCL cell lines are insensitive to Lenalidomide treatment**

To evaluate if Lenalidomide, a Cereblon inhibitor previously determined to downregulate expression of IRF4 in MM cell lines, would be a viable therapeutic intervention to target IRF4-sensitive cell lines, cells were incubated with the drug for 72 and 120 hours (figure 4.10). Myeloma cell lines and primary patient material have been previously demonstrated to be sensitive to Lenalidomide treatment below 10μM (Kronke et al., 2014, Rajkumar et al., 2005). Therefore, MM cell lines H929 and LP1 were used as positive controls.

Initial experiments focused on treatment of cells for 72 hours. However, most cells failed to achieve an IC50 at this timepoint (figure 4.10A). Therefore, cells were incubated for a longer timecourse (120 hours) and assessed for growth inhibition. Positive control cell lines were both partially sensitive to Lenalidomide treatment

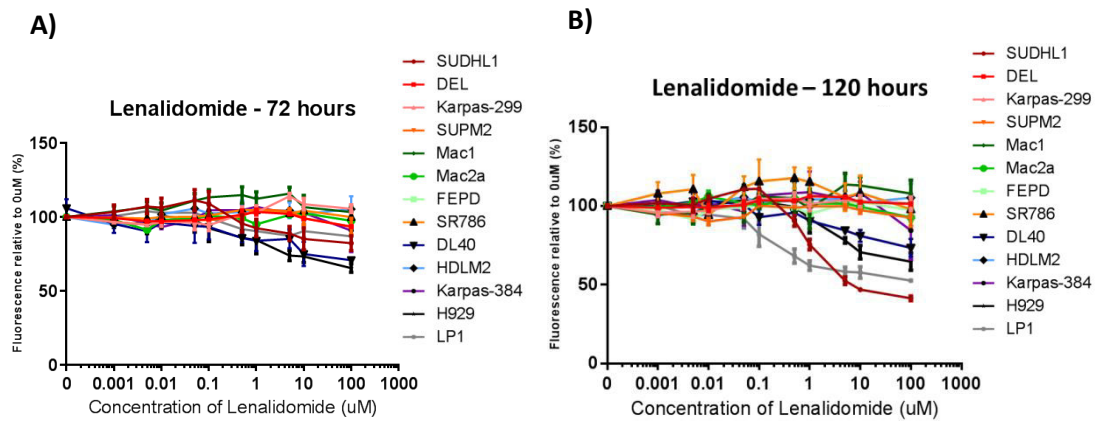


**Figure 4.10: Resazurin profiles of Lenalidomide treated cells**

Growth inhibition curves of all cell lines treated with increasing concentrations of Lenalidomide for A) 72 hours or B) 120 hours and assessed by Resazurin relative to 0.05% DMSO vehicle. Reported sensitive cells lines are: H929 and LP1. All data are derived from 3 independent replicates, error bars indicate standard error of the mean.

following 120 hours treatment but neither reached an IC<sub>50</sub> (figure 4.10B). The lymphoma cell line panel was insensitive to Lenalidomide after 120 hours apart from SUDHL1 and DL40 which showed a degree of sensitivity (figure 4.9B). SUDHL1 was the only cell line to achieve an IC<sub>50</sub>, at 5 $\mu$ M (figure 4.10B).

#### **4.2.7 ALK+ ALCL cell lines demonstrate increased sensitivity to JQ-1 with Lenalidomide treatment**

To investigate if the putative IRF4-MYC interaction demonstrated by IRF4 shRNA knockdown in Karpas-299 could be exploited therapeutically, cells were treated with a combination of a BRD4 inhibitor (c-MYC is a downstream target of BRD4), JQ-1, and Lenalidomide for 72 hours (figure 4.11). SUDHL1 and Karpas-299 did not reach an IC<sub>50</sub> value with JQ-1 treatment alone, however, with the addition of Lenalidomide, SUDHL1 achieved an IC<sub>50</sub> of 800nM and Karpas-299 achieved an IC<sub>50</sub> of 3 $\mu$ M (figure 4.11). FEPD and LP1 were found to be more sensitive to JQ-1 treatment than SUDHL1 or Karpas-299 and demonstrated minor additive effects of the drug combination, differences between curves at the highest concentration of JQ-1 were found to be significant in SUDHL1 and LP1 (SUDHL1  $p < 0.0001$ , Karpas-299  $p = 0.0891$ , FEPD  $p = 0.0591$ , LP1  $p = 0.0002$ ) (figure 4.11).

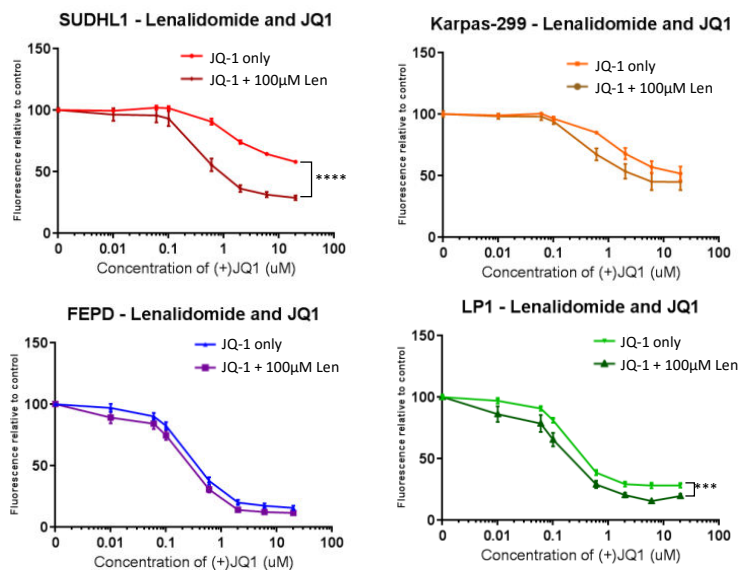


**Figure 4.11: Resazurin profiles of Lenalidomide and JQ-1 in combination**

Growth inhibition curves of all cell lines treated with increasing concentrations of JQ-1 only or JQ-1+100uM Lenalidomide (Len) relative to vehicle after 72 hours. Vehicle for JQ1 only treatment was 0.05% DMSO, vehicle for JQ-1+100uM Len was 100uM Lenalidomide in 0.05% DMSO. All data are derived from to 3 independent replicates, error bars indicate standard error of the mean. Significance calculated using a paired students t-test, \* p<0.05, \*\* p<0.01, \*\*\* p<0.001, \*\*\*\* p<0.0001.

### 4.3 Discussion

In this chapter, IRF4 has been established as important for the proliferation of ALK+ ALCL cell lines with one potential mechanism in some cell lines being a positive interaction between IRF4 and c-MYC. Furthermore, IRF4 has been demonstrated to promote G2/M progression, at least in SUDHL1 cells. In agreement with the data presented in this project, multiple groups have recently published data showing that IRF4 is required for ALK+ ALCL proliferation/survival (Weilemann et al., 2015, Boddicker et al., 2015).

IRF4 has been demonstrated to be important for the proliferation/survival of ALK+ ALCL cell lines. SUDHL1 and Karpas-299 displayed significant reductions in cell numbers with IRF4 shRNA knockdown as well as reduction in RFP-positive populations in competitive assays (figure 4.4B and 4.4C). However, siRNA knockdown of IRF4 in Karpas-299 in this project demonstrated no effect on proliferation/survival by Trypan Blue exclusion (figure 4.4B). This is in contrast to published data which demonstrates a reduction in cellular proliferation of Karpas-299 with IRF4 knockdown using a Thymidine Incorporation assay (Boddicker *et al.*, 2015). Whilst the exact nature of this discrepancy is not known, it could be due to the insufficient potency of knockdown achieved using siRNA in this project compared to Boddicker *et al.*, or due to the differences in sensitivity of the assays.

DEL did not display an effect on proliferation/survival upon IRF4 knockdown (figure 4.4), possible due to the poor levels of protein knockdown observed with IRF4 shRNAs (figures 4.4A and 4.9). Indeed, IRF4 shRNA knockdown has been demonstrated to reduce the proliferation/survival of DEL *in vitro* (Weilemann et al., 2015), suggesting knockdown in this project was not sufficient to induce a phenotype. To counteract this, transduced DEL cells could be seeded out in a colony forming assay in semi-solid agar to produce shRNA clones with increased IRF4 knockdown. Multiple clones would be required to ensure that any phenotypes observed are not a result of the clone-specific shRNA integration sites.

IRF4 knockdown caused increased G2/M populations compared to non-silencing counterparts in SUDHL1 and, to a lesser extent, in Karpas-299 (figure 4.5B) suggesting that IRF4 may exert its activity through promotion of cell cycle progression.

In agreement with this hypothesis, it has been previously reported that IRF4 is important for cell cycle progression in normal T-cell development and pre-B cells (Ma et al., 2008, Yao et al., 2013). Despite the effect IRF4 knockdown had upon cell cycle, knockdown of IRF4 did not consistently induce apoptosis between both IRF4 shRNAs (figure 4.6B). The induction of apoptosis caused by IRF4 shRNA 2 could be a true phenotype and additional to stalling of the cell cycle in G2/M. However, as there is no indication of any apoptosis induction in shRNA 1, a more plausible explanation could be that the phenotype is due to off-target effects of shRNA 2. To test this hypothesis, further IRF4 shRNA constructs should be employed in similar assays to assess if induction of apoptosis is true. Furthermore, a different method of detecting apoptosis could be undertaken using the current shRNAs, such as western blotting for cleaved PARP or caspase-3. This is because inefficient compensation can lead to a false-positive indication of apoptosis.

Thus these data currently suggest that IRF4 may play a more permissive role in the survival of ALCL cell lines, focusing primarily on rapid growth rate. In agreement with this, studies using *Irf4*-deficient murine CD8<sup>+</sup> T-cells demonstrate these cells proliferate slower than wild-type counterparts *in vitro* but did not induce apoptosis (Rackowski et al., 2013, Yao et al., 2013). However, a second independent study investigating deficiency of IRF4 in CD8<sup>+</sup> T-cells, provided evidence to suggest that loss of IRF4 does not affect the proliferation of these cells (Man et al., 2013). IRF4 has previously been demonstrated to promote the expression of metabolism genes, *FOXO1* and *HIF1A* and loss of IRF4 resulted in reduced oxygen consumption rate, decreased ATP production, and reduced glycolytic activity (Man et al., 2013). Thus, in ALK<sup>+</sup> ALCL, IRF4 may promote metabolic pathways to facilitate faster proliferation. In agreement with this, an independent study has revealed that knockdown of IRF4 in ALK<sup>+</sup> ALCL cell lines results in downregulation of a HIF1A gene signature (Weilemann et al., 2015). To investigate this effect, future work may focus on utilising gene expression arrays on IRF4 knockdown cells to identify putative IRF4 targets. Pathway analysis of these targets would elucidate if IRF4 is involved in the regulation of genes required for metabolic activity.

During this project, it was revealed that IRF4 promotes the expression of *c-MYC* mRNA in Karpas-299 and possibly DEL but not SUDHL1 cells (figures 4.7, 4.8, and 4.9)

and also promoted the expression of c-MYC protein in Karpas-299 (figure 4.8). A positive feedback loop between IRF4 and c-MYC resulting in overexpression of both transcription factors has been identified as a mechanism underlying the proliferation/survival of MM (Dib et al., 2008). c-MYC is a well characterised oncoprotein which, amongst other roles, can drive rapid proliferation in part by regulating important cell cycle regulators such as cyclins and CDKs (Dang et al., 2006, Eilers and Eisenman, 2008). A possible explanation for accumulation of G2/M populations in IRF4 knockdown cells could be reduced expression of these cell cycle regulators via downregulation of c-MYC in Karpas-299. In agreement with these data, others have recently demonstrated that knockdown of IRF4 in some ALK+ ALCL cell lines results in downregulation of c-MYC (Weilemann et al., 2015, Boddicker et al., 2015). Furthermore, one study has revealed that IRF4 knockdown in some ALCL cell lines can be rescued with overexpression of c-MYC (Weilemann et al., 2015). However, SUDHL1 does not exhibit this interaction between IRF4 and c-MYC (figure 4.7) suggesting other mechanisms of IRF4 dependency may exist in this cell line.

Whilst SUDHL1 expressed the lowest levels of IRF4 protein of all PTCL cell lines (see chapter 3, figure 3.2), it appears to rely on this expression for proliferation. SUDHL1 was sensitive to IRF4 knockdown and Lenalidomide treatment (figures 4.7 and 4.10), a drug known to downregulate IRF4 expression (Zhang et al., 2013). However, all remaining ALCL cell lines were insensitive to Lenalidomide treatment (figure 4.10). There are several possible explanations for the disagreement between IRF4 knockdown sensitivity and Lenalidomide treatment sensitivity in Karpas-299. For example, Lenalidomide downregulates multiple targets such as Ikaros, Aiolos, and phosphorylation of extracellular signal-regulated kinase (ERK), (Breitkreutz et al., 2008, Gandhi et al., 2014). Therefore, differences in expression or activity of these in ALCL may alter the sensitivity to Lenalidomide. In addition, Lenalidomide may require a longer incubation to induce an effect in a cell line dependent manner. Sensitivity to Lenalidomide may not be truly observed with the Resazurin assay however. The Resazurin assay is believed to exploit the chemical transfer of electrons from NADPH, FADH, and NADH during mitochondrial enzyme oxidation of these molecules (de Fries and Mitsuhashi, 1995). Therefore, the technique is not a direct measure of cellular survival but rather a measure of the metabolic activity of the cell culture as a whole.

Therefore, cells which arrest, but metabolise rapidly can be misconstrued as healthy dividing cells. A more robust method of assessing survival of these cells with Lenalidomide treatment would be to count cells directly by Trypan Blue exclusion or treat cells with Lenalidomide and assess survival via a clonogenic assay.

To investigate if IRF4 and c-MYC could be simultaneously targeted in ALCL as a therapeutic avenue, cell lines were treated with JQ-1, a BRD4 inhibitor demonstrated to potently repress c-MYC protein expression (Delmore et al., 2011). Combination of c-MYC inhibition and IRF4 inhibition has recently been suggested as a potential therapeutic approach for PTCL (Weilemann et al., 2015, Boddicker et al., 2015). Treatment with both drugs demonstrated that, albeit to a minor extent, SUDHL1, MM cell lines, and Karpas-299, survived less than either treatment alone (figure 4.10 and 4.11). These data suggest that dual targeting of the IRF4-BRD4 axis could be beneficial for some ALCL patients. To further investigate this avenue, direct c-MYC inhibitors should be employed in combination with Lenalidomide to elucidate if the effect of JQ-1 and Lenalidomide treatment is c-MYC-dependent or due to another target of BRD4. In addition, analysis of IRF4 levels in ALK+ ALCL cell lines after JQ-1 treatment should be undertaken to elucidate whether inhibition of BRD4 directly impacts IRF4 expression.

IRF4 shRNA knockdown resulted in an increase in *BLIMP1 $\alpha$* , but not *BLIMP1 $\beta$* , transcripts in SUDHL1 (figure 4.7) and, in addition, siRNA knockdown of IRF4 resulted in increased expression of *BLIMP1* (figure 4.3B). This is in direct contrast to Karpas-299 and DEL which demonstrated a reduction of *BLIMP1 $\alpha$*  and *BLIMP1 $\beta$*  with IRF4 shRNA knockdown (figure 4.8). These results may be indicative of different roles of IRF4 across the cell lines. In agreement with Karpas-299 and DEL, in normal T-cell and B-cell physiology, IRF4 promotes the expression of BLIMP1 (Kwon et al., 2009, Li et al., 2012, Yao et al., 2013). However, in SUDHL1, IRF4 appears to directly repress *BLIMP1 $\alpha$*  expression which could be a mechanism of downregulating the potential tumour suppressor gene expression. Karpas-299 and DEL displayed a minor reduction in the expression of *BCL6* mRNA with IRF4 knockdown (figures 4.3B, 4.7-4.9) suggesting IRF4 promoted the expression of *BCL6* in these lines, consistent with normal T-cell physiology (Kwon et al., 2009, Lohoff et al., 2002). Therefore, IRF4 may promote the expression of *BCL6* to maintain expression of a potential tumour promoter.

Future work for this study would utilise gene expression arrays in combination with CHIP-Seq analysis of PTCL cell lines to find novel IRF4 targets. Our results and those of Weilemann et al. suggest that while some ALCLs are addicted to IRF4 through interaction with c-MYC, others depend upon c-MYC-independent effects of IRF4. In this study IRF4 did not affect c-MYC expression in SUDHL1 cells (figure 4.7) and Weilemann et al. observed that c-MYC expression could only rescue IRF4 knockdown in 1 of 3 of their cell lines (Weilemann et al., 2015). Therefore, it would be beneficial to discover IRF4 targets other than c-MYC which contribute to ALCL survival as these may themselves present therapeutic targets.

Further investigation into the binding partners of IRF4 should be conducted. In B-cells IRF4 binds PU.1 to effect its activity, but PU.1 is not expressed in T-cells (Brass et al., 1996, Escalante et al., 2002). As a result, IRF4 must bind with other targets to affect transcription. Immunoprecipitation assays would reveal if IRF4 bound to some known T-cell transcriptional partners, such as BATF (Li et al., 2012), FOXO1 or HIF1A (Man et al., 2013). CHIP-Seq would allow investigation into whether IRF4 shared binding sites with other novel partners in T-cell lymphoma. Of particular interest would be to investigate the role of BATF3 in IRF4-dependent ALK+ ALCL. BATF3 is a transcriptional repressor which can heterodimerise with JUN and is required for the correction differentiation of CD8<sup>+</sup>α dendritic cells (Peng et al., 2014). Recently, *BATF3* has been implicated as one of the key genes specifically expressed by ALK+ ALCL (Iqbal et al., 2014). Whilst direct interaction of IRF4 and BATF3 has not been demonstrated, it is known that IRF8 (a close relation of IRF4) can interact with BATF3 (Hildner et al., 2008, Ise et al., 2011). Furthermore, IRF4 has demonstrated binding to BATF-JUN complexes during T-cell differentiation (Li et al., 2012). Therefore, it is plausible that a potential pro-tumour mechanism of action for IRF4 could be mediated through BATF3 interaction.

As IRF4 inhibitors are not currently available, it would be beneficial to explore downstream targets of IRF4 as a potential therapeutic avenue. Another aspect would be to investigate the use of c-MYC inhibitors on IRF4-dependent cell lines to exploit the c-MYC/IRF4 interaction observed in some ALCL cell lines. Further IRF4 knockdown experiments should be undertaken across different PTCL cell lines as well as primary patient cultures to investigate if IRF4 is required across PTCL cell lines as a whole and

whether IRF4 translates as a viable therapeutic target in patient samples. There is good rationale for IRF4 being a viable target as 91% of ALCL patient tumours have been previously demonstrated to be IRF4-positive by immunohistochemistry (Weilemann et al., 2015). Whilst gene expression arrays have already been utilised with IRF4 knockdown in ALCL cell lines: Karpas-299, DEL, and FEPD (Weilemann et al., 2015), it may be of interest to investigate how IRF4 works in our cell lines. For example, published data indicates that IRF4 knockdown does not affect the growth of SUDHL1 (Weilemann et al., 2015, Boddicker et al., 2015) which is a direct contrast to data presented in this report (figure 4.4A).

Although shRNA-mediated knockdown was useful in this project for overcoming the rapid recovery of IRF4 levels in SUDHL1 with siRNA knockdown (figure 4.3), the technique has some drawbacks. The lentiviral delivery system can be problematic as lentiviruses can typically integrate into preferential sites around the genome (Biffi et al., 2011). This is particularly problematic if the virus inserts a sequence into a specific locus causing deregulation of genes important for proliferation and survival and thus can produce spurious results. For example, *BACH2* contains a preferential integration site for EBV in BL (Takakuwa et al., 2004). However, this problem was overcome in this project through use of a bulk-transduced population, instead of individual clones, which will harbour intercellular variances in integrations. Furthermore, shRNA-mediated knockdown relies upon the micro-RNA processing pathway to be functional in these cells. Dysregulation of micro-RNA pathways is well established in cancers, therefore, the processing of shRNA may be hindered (Melo and Esteller, 2011). Additionally, a drawback of both siRNA and shRNA is the induction of interferon responses in cells leading to activation of immune responses (Bridge et al., 2003). A recent advancement has demonstrated the ability to knockout genes in human genomes via a CRISPR-mediated technique (Shalem et al., 2014). This may be a viable means of assessing the effect of complete loss of IRF4 on PTCL cell lines although a potential drawback in the technique is that if IRF4 is vital for these cell lines, then all cells will die rapidly. This issue can be overcome by combining knockout with an inducible expression vector containing IRF4 coding sequence to allow more control over experimental procedures.

## **Chapter 5: The transcriptional repressor, BLIMP1, as a tumour suppressor in ALCL**



## 5. The transcriptional repressor, BLIMP1, as a tumour suppressor in ALCL

### 5.1 Introduction

BLIMP1 is a transcriptional repressor encoded by the *PRDM1* gene which is required for B- and T-cell differentiation through interaction with many targets, including BCL6 and IRF4 (Shapiro-Shelef and Calame, 2005). The relationship between BLIMP1 and BCL6/IRF4 remain conserved between B- and T-cells (figure 5.1). There are two main isoforms of BLIMP1, designated BLIMP1 $\alpha$  and BLIMP1 $\beta$ , although others have been reported. BLIMP1 $\alpha$  has been demonstrated to exhibit greater repressive activity than BLIMP1 $\beta$  (Gyory et al., 2003). BLIMP1 is well established as a tumour suppressor in B-cell malignancies and is commonly inactivated or deleted in ABC-DLBCL (Pasqualucci et al., 2006, Tam et al., 2006, Mandelbaum et al., 2010). In addition, deletions of *PRDM1* were frequently found in NK-cell lymphomas and re-introduction of BLIMP1 into these neoplasms resulted in reduced cellular proliferation (Karube et al., 2011).

The aim of this chapter is therefore to investigate the role of BLIMP1 as a tumour suppressor in T-cell lymphoma and to establish its interactions with BCL6 and IRF4. The chapter will investigate the effect overexpression of BLIMP1 $\alpha$  or BLIMP1 $\beta$

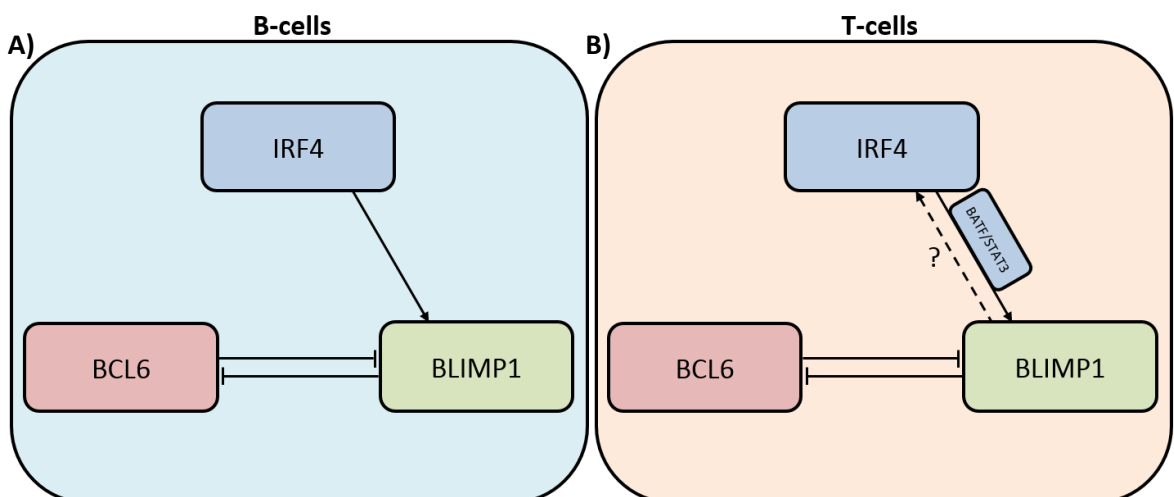


**Figure 5.1: Interaction of BLIMP1 with IRF4 and BCL6 in B-cells vs. T-cells**

A) In B-cells, BLIMP1 exhibits mutual inhibition with BCL6 to allow formation of slow-proliferation plasma cells (Shapiro-Shelef et al., 2003). B) In T-cell differentiation, BLIMP1 and BCL6 repress one another to achieve differentiation of T<sub>H</sub> cells. The effect of BLIMP1 on IRF4 expression is not known to date, however IRF4 can positively regulate expression of BLIMP1 via interaction with BATF and STAT3 (Li et al., 2012).

has upon the proliferation and survival of T-cell lines as well as the effect on expression of BCL6 and IRF4 mRNA and protein.

## 5.2 Results

### 5.2.1 *BLIMP1 overexpression is achievable in ALK+ ALCL cell lines*

To investigate the role of BLIMP1 in ALCL, we first needed a vector that could express both BLIMP1 isoforms to a detectable level. Endogenous BLIMP1 protein is difficult to detect due to the low levels of expression exhibited by PTCL cell lines. However, upon transduction of cells with pSIEW-BLIMP1 $\alpha$  and pSIEW-BLIMP1 $\beta$  vectors, protein was detectable after four days (figure 5.2A and B). SUDHL1 treated with 25 $\mu$ l of pSIEW-BLIMP1 $\alpha$  exhibited low viability whilst those treated with 25 $\mu$ l of pSIEW-BLIMP1 $\beta$ , or 15 $\mu$ l or 25 $\mu$ l of pSIEW virus, had completely died by 4 days. This was believed to be due to the multiple integrations of the viral vector into the host genome as all the populations were 100% GFP-positive. Karpas-299 was able to tolerate virus up to 25 $\mu$ l, however at 50 $\mu$ l of virus the cells spontaneously died (data not shown). There was not sufficient volume of surviving cells to assess protein levels in SUPM2 treated with pSIEW-BLIMP1 $\alpha$  and pSIEW-BLIMP1 $\beta$  at any virus concentration; however protein could be extracted from cells treated with 5 $\mu$ l pSIEW virus. The cell death exhibited by SUPM2 was believed to be a spurious effect caused by poor culturing. Therefore, to determine the ideal viral titre, GFP traces were analysed to determine which virus volumes produced similar transduction efficiencies to those found in SUDHL1 for SUPM2 (figure 5.2C). 15 $\mu$ l of pSIEW-BLIMP1 $\alpha$  and pSIEW-BLIMP1 $\beta$  viruses and 5 $\mu$ l of pSIN-SIEW virus for SUDHL1 and SUPM2 were selected based upon the transduction efficiency and non-specific cell death exhibited at these volumes. For Karpas-299, 25 $\mu$ l of all viruses was chosen for future transductions.

### 5.2.2 *BLIMP1 overexpression represses IRF4 and endogenous BLIMP1 in ALK+ ALCL*

BLIMP1 $\alpha$  overexpression resulted in significant increases in BLIMP1 $\alpha$  mRNA in all cell lines (SUDHL1 p=0.0257, Karpas-299 p=0.0139, SUPM2 p=0.0002). Overexpression of both BLIMP1 $\alpha$  and BLIMP1 $\beta$  proteins resulted in a marked decrease in IRF4 transcript levels in SUDHL1 (BLIMP1 $\alpha$  p<0.0001, BLIMP1 $\beta$  p<0.0001) (figure 5.3A). In addition, both constructs resulted in a depletion of detectable IRF4 protein

(figure 5.3D and F) in SUDHL1 and perhaps also in SUPM2. However, BCL6 expression was unaffected by either BLIMP1 isoform (BLIMP1 $\alpha$  p=0.1241, BLIMP1 $\beta$  p=0.1999).

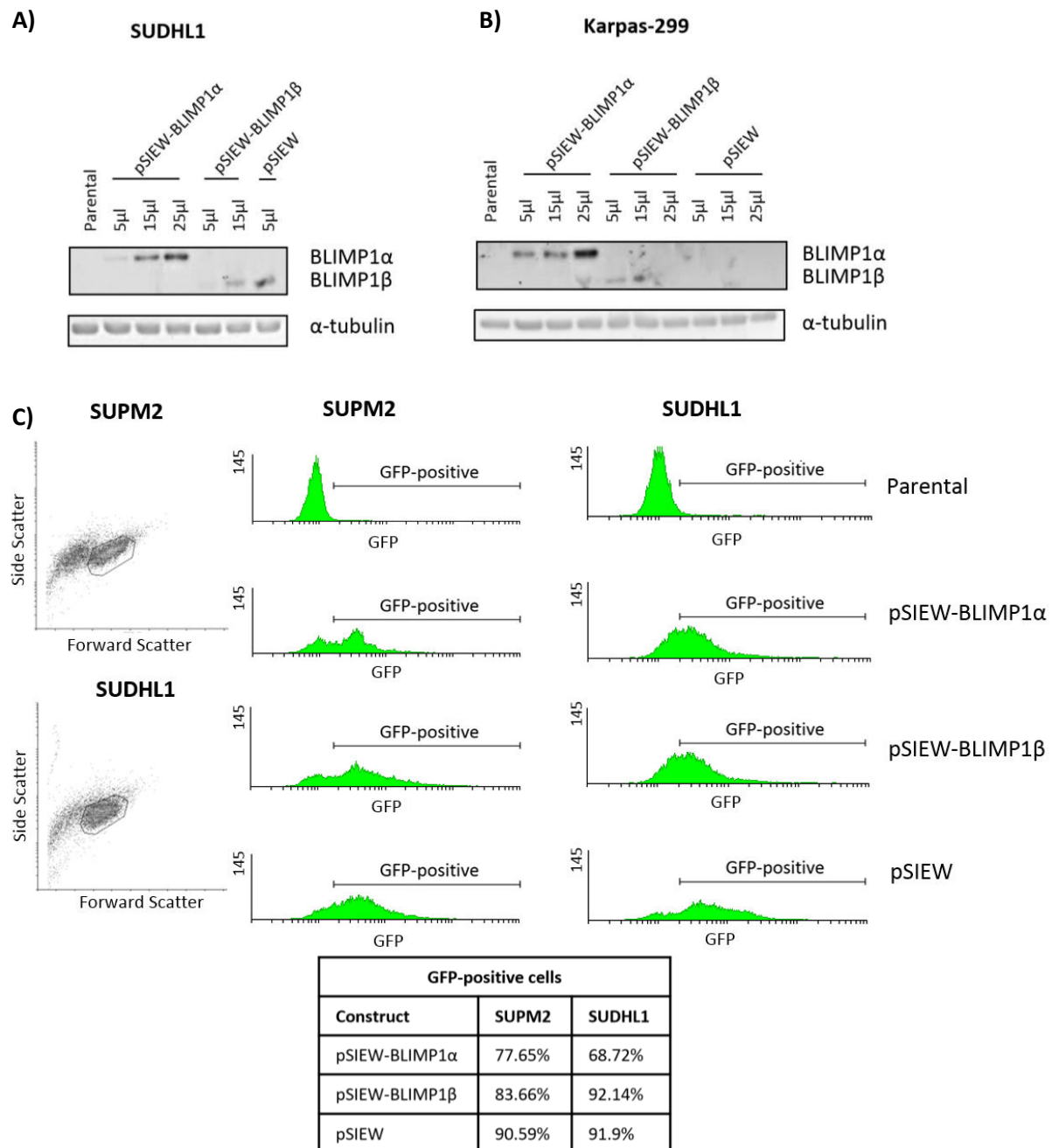


**Figure 5.2: Optimisation of pSIEW vector transduction in SUDHL1, SUPM2, and Karpas-299**

Cells were spininfected at 900g for 50 minutes with either 0 $\mu$ l, 5 $\mu$ l, 15 $\mu$ l, 25 $\mu$ l, or 50 $\mu$ l of virus and cultured as normal for 4 days. All samples containing 50 $\mu$ l of pSIEW-BLIMP1 $\alpha$ , pSIEW-BLIMP1 $\beta$ , or pSIEW died due to multiple integrations. A) Western blot after 4 days transduction in SUDHL1. There were no living cells in those treated with 25 $\mu$ l of SIEW-BLIMP1 $\beta$ , or 15 $\mu$ l and 25 $\mu$ l of SIN-SIEW virus. B) Western blot after 4 days transduction in Karpas-299. C) Live cells were gated according to the gate applied on forward scatter/side scatter plots. Subsequent GFP-traces for SUPM2 and SUDHL1 are depicted by histograms after 4 days with % GFP-positivity table.

Contrary to SUDHL1, SUPM2 and, to a lesser extent, Karpas-299 displayed a reduction in *c-MYC* mRNA levels with expression of BLIMP1 $\alpha$  (SUPM2 p=0.0197, Karpas-299 p=0.011), but not BLIMP1 $\beta$  (SUPM2 p=0.3645, Karpas-299 p=0.7801)

(figure 5.3B and 5.3C). However, in Karpas-299, expression of BLIMP1 $\alpha$  or BLIMP1 $\beta$  resulted in no change of *BCL6* or *IRF4* mRNA or protein levels (*BCL6* p=0.1473, *IRF4* p=0.3702) (figure 5.3B and 5.3E).

Whilst endogenous BLIMP1 $\alpha$  could not be detected whilst expressing SIEW-BLIMP1 $\alpha$ , using the primers in this study, endogenous *BLIMP1 $\beta$*  could be analysed. Interestingly, in all cell lines, expression of BLIMP1 $\alpha$  (and BLIMP1 $\beta$  in SUDHL1) caused reductions in *BLIMP1 $\beta$*  mRNA expression, significantly in SUDHL1 and SUPM2 (SUDHL1 p=0.0003, Karpas-299 p=0.2342, SUPM2 p=0.0004) (figure 5.3A-C). In addition, the expression of BLIMP1 $\beta$  had a small negative effect on the expression of *BLIMP1 $\alpha$*  in 2/3 cell lines (SUDHL1 p=0.0003, Karpas-299 p=0.8823, SUPM2 p=0.0483).

### **5.2.3 BLIMP1 overexpression reduces the proliferation/survival of ALK+ ALCL cell lines**

To investigate the role of BLIMP1 as a tumour suppressor, cells were transduced with virus according to the volumes defined in section 5.2.1. Flow cytometric samples were then collected every 2-3 days over a 2 week period and GFP-expression was assessed. GFP-expression was plotted against day 0 expression (48 hours after transduction) (figure 5.4). Both SUDHL1 and SUPM2 showed significant reduction of GFP-positive cells over time following BLIMP1 $\alpha$  or BLIMP1 $\beta$  expression compared to the pSIEW vector control (SUDHL1: BLIMP1 $\alpha$  p=0.001, BLIMP1 $\beta$  p=0.003, SUPM2: BLIMP1 $\alpha$  p=0.001, BLIMP1 $\beta$  p=0.001) (figure 5.4B and 5.4D). BLIMP1 $\alpha$ -expressing cells lost GFP expression faster than BLIMP1 $\beta$ -expressing counterparts. In Karpas-299 cells GFP-expression, however, remained stable throughout the experiment with both BLIMP1 constructs (figure 5.4C). In all cell lines, GFP expression tended to increase over time with the control vector.

### **5.2.4 BLIMP1 overexpression induces cell death in ALK+ ALCL cell lines**

To further evaluate the impact of BLIMP1 overexpression on sensitive cell lines, cells were stained with propidium iodide to assess cell cycle populations at days 0 and 2 of GFP-tracking (48 and 96 hours after transduction, respectively) (figure 5.5A). Both sensitive cell lines, SUDHL1 and SUPM2, showed significant increases in sub-G1 populations by day 2 compared to control vector with both pSIEW-BLIMP1 $\alpha$  (SUDHL1 p=0.002, SUPM2 p=0.011) and pSIEW-BLIMP1 $\beta$  (SUDHL1 p=0.049, SUPM2 p=0.006)

(figure 5.5B and D). Karpas-299 cell cycle profiles remained unchanged by pSIEW-BLIMP1 $\alpha$  and pSIEW-BLIMP1 $\beta$  compared to pSIEW control (figure 5.5C). A significant increase in sub-G1 populations was observed in SUDHL1 at day 0 with BLIMP1 $\beta$  expression but not BLIMP1 $\alpha$  (figure 5.5B). SUPM2 and Karpas-299 cell cycle profiles were not significantly altered at day 0 (figure 5.5C and D).

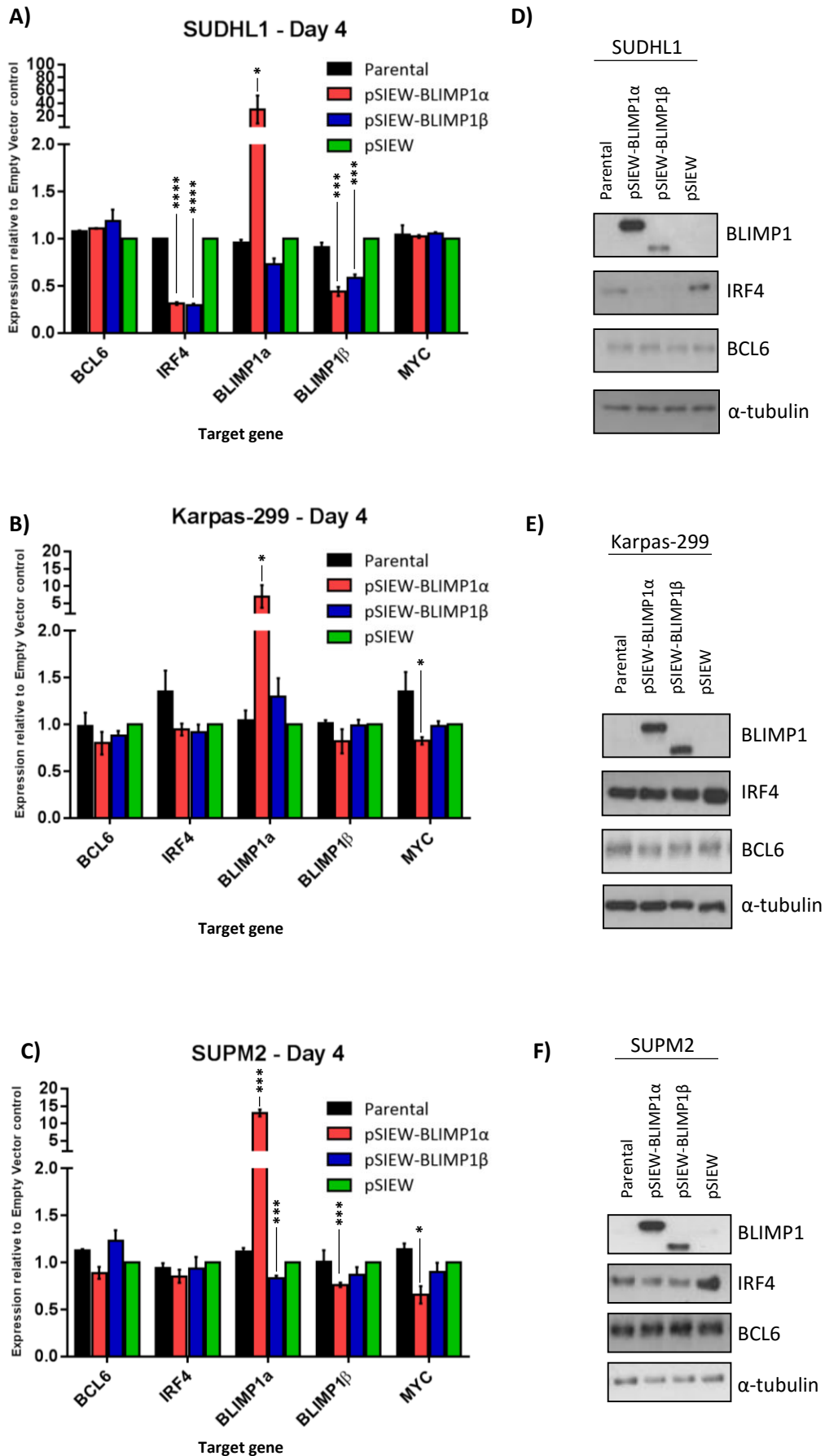


**Figure 5.3: Overexpression of BLIMP1α and BLIMP1β in ALK+ ALCL cell lines**

Quantitative PCR graphs for A) SUDHL1, B) Karpas-299, and C) SUPM2. Overexpression of BLIMP1β cannot be detected by qPCR as the primers target the only unique region of BLIMP1β, the 5'UTR, which is not present in the SIEW-BLIMP1β construct. Error bars are derived from 175 independent experiments and represent standard error of the mean. Respective western blots for D) SUDHL1, E) Karpas-299, and F) SUPM2. Significance calculated using a paired students t-test, \*  $p < 0.05$ , \*\*  $p < 0.01$ , \*\*\*  $p < 0.001$ , \*\*\*\*  $p < 0.0001$ .

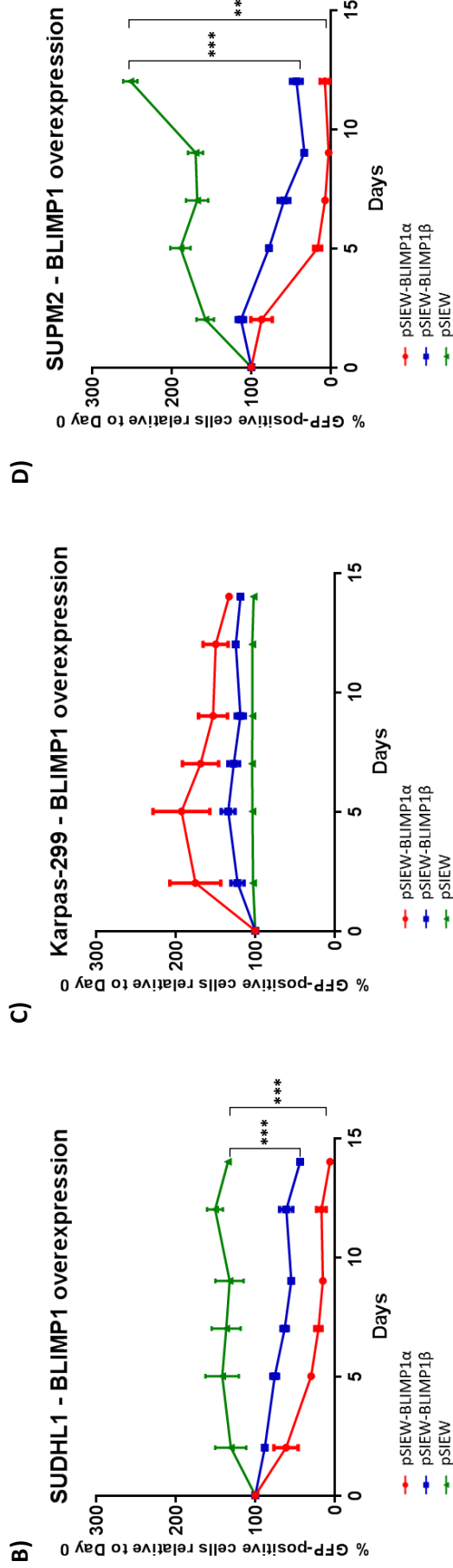
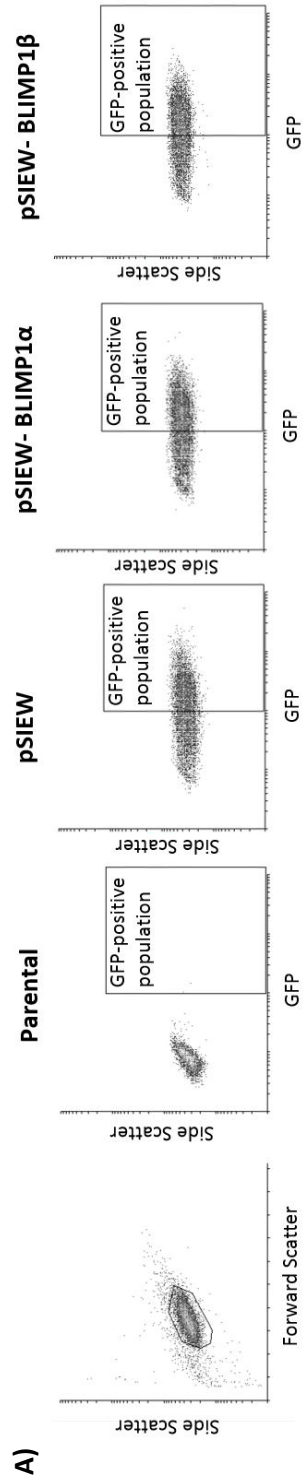


**Figure 5.4: Overexpression of BLIMP1 affects cell proliferation/survival**

A) Representative gating strategy for GFP-tracking experiment. Live cells analysed using gating strategy depicted in the left panel with subsequent GFP traces for each vector. GFP-tracking from 48 hours post-transduction in B) SUDHL1, C) Karpas-299, and D) SUPM2. Respective cell cycle distributions analysed using propidium iodide staining during tracking experiment on days 0 and 2 in D) SUDHL1, E) Karpas-299, and F) SUPM2. Error bars indicate standard error of the mean of 3 independent experiments. \* $\leq p < 0.05$ , \*\* $\leq p < 0.01$ , \*\*\* $\leq p < 0.001$ , statistical significance assessed using a paired students t-test.

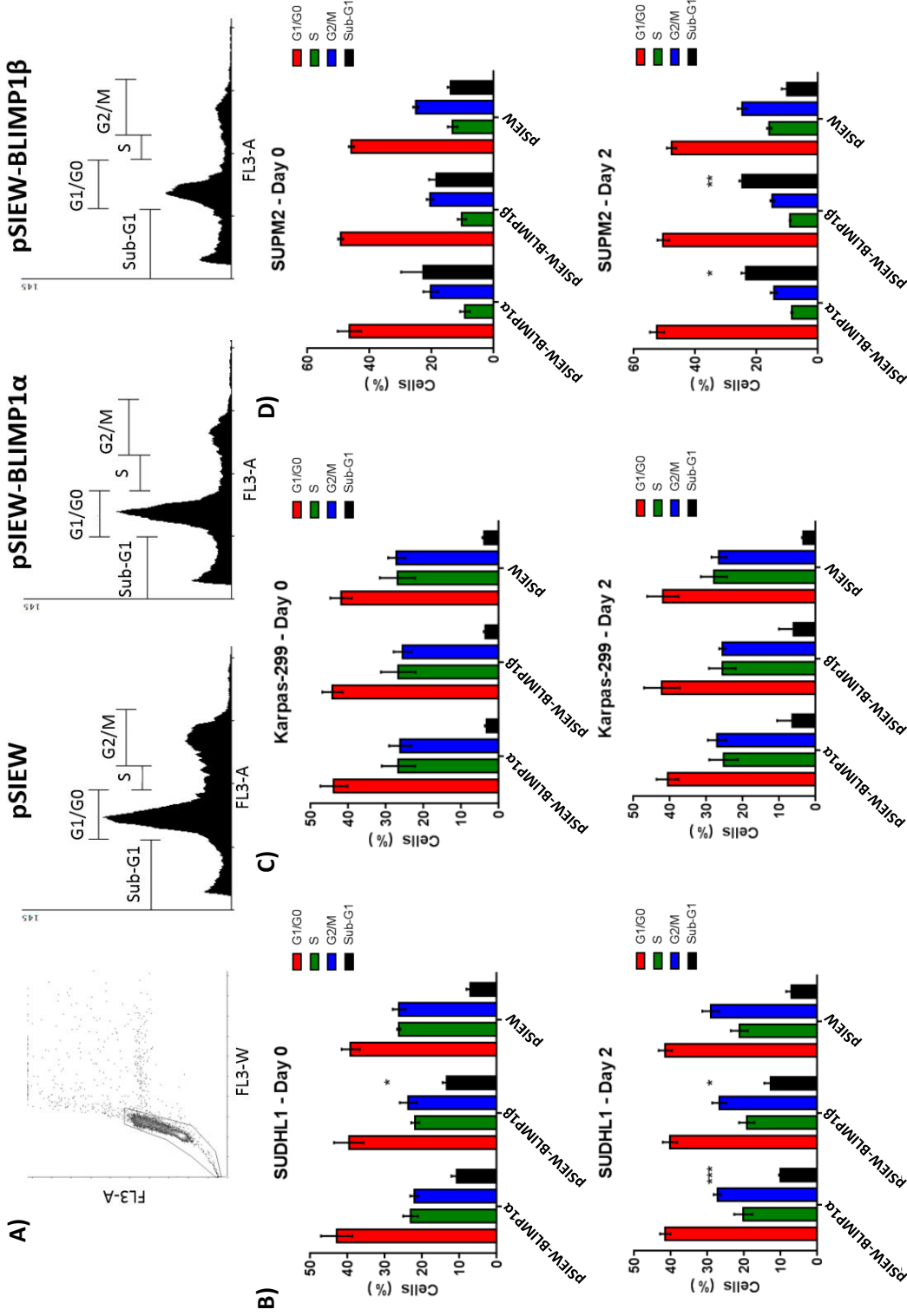


**Figure 5.5: Overexpression of BLIMP1 induces cellular death**

A) Representative cell cycle distribution staining by propidium iodide traces, single cells were analysed according to the left panel, gated population allows eradication of doublets from analysis, subsequent PI traces for each construct follow. Respective cell cycle distributions analysed using propidium iodide staining during tracking experiment on days 0 and 2 in B) SUDHL1, C) Karpas-299, and D) SUPM2. Data is derived from 3 independent replicates, error bars indicate standard error of the mean. \* $p < 0.05$ , \*\* $p < 0.01$ , \*\*\* $p < 0.001$ , statistical significance assessed using a paired students t-test.

### 5.3 Discussion

BLIMP1 is well established as a tumour suppressor in NK T-cell malignancies (Iqbal et al., 2009, Karube et al., 2011) and, during the course of this project, was discovered to be a tumour suppressor in ALK+ ALCL by another independent group (Boi et al., 2013). In agreement with this published data, overexpression of BLIMP1 $\alpha$  resulted in reduced proliferation/survival of SUDHL1 and SUPM2 cells in culture (figures 5.4B and 5.4D), accompanied by induction of apoptosis as reflected by an increase in sub-G1 population by flow cytometry (figures 5.5B and 5.5D). Therefore, this data as a whole suggests that BLIMP1 $\alpha$  and BLIMP1 $\beta$  may constrain the proliferation and survival of ALCL cells and that their transcriptional targets might be molecules which could be exploited for the treatment of ALK+ ALCL.

Overexpression experiments have revealed that BLIMP1 does not affect BCL6 mRNA or protein expression across all three ALK+ ALCL cell lines (figure 5.3), suggesting that BLIMP1 has lost the ability to repress BCL6 in ALCL cells. BLIMP1 has previously been shown to directly inhibit BCL6 expression in normal CD4<sup>+</sup> and CD8<sup>+</sup> T-cells (Cimmino et al., 2008). Loss of repressive activity of BLIMP1 on BCL6 could be indicative of a mutation/alteration in *BCL6* that could alleviate repression. Indeed BCL6 has been demonstrated to harbour mutations in its promoter region, in DLBCL, to prevent its own autoregulation or regulation by IRF4 (Pasqualucci et al., 2003, Saito et al., 2007).

However, overexpression of BLIMP1 $\alpha$  and BLIMP1 $\beta$  did result in repression of IRF4 mRNA and protein in SUDHL1 and SUPM2 (figure 5.3A and 5.3C). Little is known about the effect of BLIMP1 upon IRF4 in normal T-cells, however, this data agrees with published data showing that BLIMP1 represses IRF4 expression in ALK+ ALCL (Boi et al., 2013). In addition, overexpression of BLIMP1 $\alpha$  resulted in suppression of *c-MYC* mRNA levels in SUPM2 and, to a lesser extent, in Karpas-299 (figure 5.3B and 5.3C). Whilst BLIMP1 has been demonstrated to directly repress *c-MYC* in plasma cells (Lin et al., 1997), it is unknown whether the work presented in this report demonstrates a direct repressive effect of BLIMP1 or a secondary repressive effect via loss of IRF4 expression resulting in reduction of *c-MYC* (Weilemann et al., 2015). BLIMP1 ChIP could be used to determine if BLIMP1 binds *c-MYC* directly.

Both BLIMP1 $\alpha$  and BLIMP1 $\beta$  exhibit the same level of repression of *IRF4* mRNA (figure 5.3A and 5.3C). Therefore, contrary to one hypothesis suggesting that BLIMP1 $\beta$  may act as a competitive inhibitor of BLIMP1 $\alpha$  by binding BLIMP1 $\alpha$  sites and exerting lesser repressive activity to targets (Zhao et al., 2008), this data suggests both isoforms are able to repress expression equally. However, BLIMP1 $\alpha$  reproducibly resulted in a more rapid loss of GFP-positive cells compared to BLIMP1 $\beta$  in both SUDHL1 and SUPM2 (figure 5.4B and 5.4D) suggesting that BLIMP1 $\alpha$  can exert greater tumour suppressor activity than BLIMP1 $\beta$ . This effect, however, may be due to the fact that BLIMP1 $\alpha$  appears to be expressed to a higher level than BLIMP1 $\beta$  in both of these cell lines (figures 5.3D and 5.3F). Repression of *IRF4* by BLIMP1 may also reinforce the notion of *IRF4* as a tumour promoting protein in ALCL. Contrary to SUDHL1 and SUPM2, overexpression of BLIMP1 did not affect expression of *BCL6* or *IRF4* in Karpas-299 (figure 5.3B) which may be indicative of different transforming mechanisms between the cell lines. In addition to *IRF4*, BLIMP1 $\alpha$  has been demonstrated to suppress *miR155* in published data however this has not been demonstrated with BLIMP1 $\beta$  (Boi et al., 2013). *miR155* is a known oncogene that, amongst other roles, upregulates p-STAT3 levels (Merkel et al., 2015). The oncogenic role of *miR155* has been demonstrated in breast cancer (Czyzyk-Krzeska and Zhang, 2014) and more recently in ALK- ALCL (Merkel et al., 2015). The authors of the most recent paper conclude that *miR155* is not required for ALK+ ALCL due to the low intrinsic levels of expression (Merkel et al., 2015). In addition, treatment of ALK+ ALCL cell lines with Crizotinib resulted in no changes in *miR155* levels suggesting it was not regulated by ALK. These data as a whole, however, suggest that upregulation of *miR155* may occur, at least in part, through repression of BLIMP1 $\alpha$  in ALK+ ALCL and may constitute an oncogenic target in ALK+ ALCL.

Whilst all three ALK+ ALCL cell lines used in this chapter have been shown to exhibit BLIMP1 deletions by FISH (Boi et al., 2013), Karpas-299 is the only cell line to completely lack BLIMP1 $\alpha$  protein expression (see chapter 3, figure 3.2). Despite this, overexpression of BLIMP1 $\alpha$  did not slow the growth of these cells (figure 5.4C), nor significantly induce apoptosis (figure 5.5C). The exact reason for this is unknown; however it is possible to speculate a combination of factors resulting in BLIMP1 overexpression insensitivity. According to published data (Boi et al., 2013) and SNP 6.0

array data collected in our lab (data not shown), the BLIMP1 locus is deleted in Karpas-299. However, the deletion does not appear to be the reason for loss of protein expression as mRNA levels of *BLIMP1α* observed in Karpas-299 are similar to those observed in SUDHL1 and SUPM2, both of which contain detectable BLIMP1 protein (see chapter 3, figure 3.2A). Therefore, BLIMP1 may be mutated to give rise to aberrant transcripts. This type of activity has been observed in DLBCL whereby BLIMP1 has been demonstrated to harbour a wide spectra of mutations leading to truncated proteins, frameshift deletions, or nonsense mutations causing inactivation of one or more alleles of BLIMP1 (Pasqualucci et al., 2006). Furthermore, these cells lack BLIMP1 protein expression whilst retaining *BLIMP1* mRNA expression.

Alternatively, upregulation of proteasomal degradation pathways may be the cause of BLIMP1α protein loss in Karpas-299. One publication demonstrates that BLIMP1 is degraded by Small Ubiquitin-like Molecule 1 (SUMO-1) *in vitro* by a process known as SUMOylation (Shimshon et al., 2011). Therefore, a mechanism of overcoming BLIMP1 overexpression could be to upregulate proteasomal degradation pathways; whilst this could explain lack of endogenous BLIMP1α, it seems unlikely to be the cause of BLIMP1 overexpression insensitivity as BLIMP1 protein is detectable with overexpression vectors suggesting proteasomal degradation pathways have not targeted this protein (figure 5.3E). In addition, it could be hypothesised that mutations may be present in the BLIMP1 binding sites of critical BLIMP1 targets preventing the binding of BLIMP1α or BLIMP1β. Whilst this has not been demonstrated naturally in malignancies, mutations introduced to BLIMP1 target gene promoters in BL abrogated BLIMP1 repression (Cubedo et al., 2011). In agreement with this hypothesis, loss of BCL6 inhibition by BLIMP1 is evident across all cell lines tested (figure 5.3), though the exact mechanism of this is unknown. It could be speculated that BLIMP1-mediated repression of BCL6 is overridden by constitutive STAT3 signalling driven by the NPM-ALK translocation (Chiarle et al., 2008). Sequencing of the BCL6 locus in these cell lines could elucidate whether mutations of BLIMP1 binding sites are present, alternatively ChIP-Seq of BLIMP1 could also reveal if BLIMP1α or BLIMP1β still possess the ability to bind the *BCL6* locus.

Interestingly, overexpression of either BLIMP1α or BLIMP1β resulted in repression of endogenous *BLIMP1β* mRNA, whilst overexpression of BLIMP1β also

resulted in repression of endogenous *BLIMP1α* mRNA in SUDHL1 and SUPM2 cell lines (figure 5.3A and C). This repression may be an intrinsic method of compensating overexpression of BLIMP1. One mechanism may be through upregulation of B-cell lineage-specific activator protein (BSAC). BSAC has been demonstrated by CHIP to directly bind BLIMP1 and, when ectopically expressed, result in the repression of BLIMP1 expression (Mora-Lopez et al., 2007). Another important molecule may be BACH2 which has also been shown to bind and repress BLIMP1 expression in B-cells (Ochiai et al., 2006). Therefore, investigation into the levels of either BSAC or BACH2 with BLIMP1 overexpression may validate a role for these proteins in these cell lines.

These data have demonstrated that BLIMP1 is a bona fide tumour suppressor in ALK+ ALCL and may exert its activity via down regulation of multiple targets, such as IRF4 and c-MYC. Repeat experiments could focus on improving the control vector to contain a mutated, inactive version of BLIMP1  $\alpha$  or BLIMP1 $\beta$  to ensure the effect observed is specifically due to active BLIMP1. In addition, as propidium iodide staining does not distinguish between necrosis and apoptosis it may be necessary to prove that BLIMP1 induces apoptosis via an apoptosis assay. GFP expression is detected in the same fluorescent channel as the FITC caspase-3 flow cytometry assay employed during this project, which therefore would not be suitable in our experiments. However, collecting whole cell extracts of BLIMP1 overexpressing cells and probing for apoptotic proteins such as PARP, and caspase-3, would allow assessment of apoptosis induction. Future work would focus on expression arrays for BLIMP1 $\alpha$  and BLIMP1 $\beta$  overexpression to identify genes regulated by BLIMP1 in these cell lines. Of particular interest would be to utilise an array for the insensitive Karpas-299 and the sensitive SUDHL1 and SUPM2 to assess which genes are differentially regulated which could explain the different BLIMP1 sensitivities.

This would allow further investigation into the pathways that are specifically important to survival of SUDHL1 and SUPM2. Work investigating BLIMP1 overexpression in other subtypes of PTCL would be of use, particularly in AITL, characteristic for containing high BCL6 expression (Nurieva et al., 2009). It would also be of benefit to investigate if there are differences in gene expression targets between BLIMP1 $\alpha$  and BLIMP1 $\beta$  arrays to further elucidate the individual role of each. These experiments would demonstrate if BLIMP1 is important for the survival of all PTCLs, or

just ALCL, as well as clarify whether loss of BCL6 antagonism is specific to ALCL subtypes or is common across all PTCL.



## **Chapter 6: NPM-ALK in the regulation of the BCL6-IRF4-BLIMP1 Transcription Factor Axis**



## 6. NPM-ALK in the regulation of the BCL6-IRF4-BLIMP1 Transcription Factor Axis

### 6.1 Introduction

ALK is a tyrosine kinase which is believed to be required for the development of the nervous system in embryos (Iwahara et al., 1997, Morris et al., 1994). ALK is the target of chromosomal translocation or mutations in several types of tumour. Whilst many translocation partners exist for ALK, the most common in ALCL is the t(2;5)(p23;q35) creating the *NPM-ALK* fusion tyrosine kinase. In ALK+ ALCL, ALK is therefore constitutively active resulting in constitutive activation of STAT3 which directs cell survival and proliferation (Khoury et al., 2003, Zamo et al., 2002, Amin et al., 2004). Importantly, STAT3 can induce expression of BCL6 and IRF4 demonstrating putative therapeutic targets (Walker et al., 2013, Kwon et al., 2009).

ALK inhibitors have recently found utility for the treatment of ALK-rearranged non-small cell lung cancer and myofibroblastic tumours, and are in trials for ALCL (Butrynski et al., 2010, Gambacorti-Passerini et al., 2011, Kwak et al., 2010). Crizotinib is a dual ALK and c-Met inhibitor utilised in the treatment of these malignancies (Sahu et al., 2013). Crizotinib inhibits the phosphorylation, and subsequent activation, of ALK (Cui et al., 2011, Sahu et al., 2013).

The aim of this chapter is therefore to evaluate the role of ALK in regulating the BCL6-IRF4-BLIMP1 transcription factor axis in ALK+ ALCL by examining the effect of ALK inhibition, using Crizotinib, on cell proliferation/survival and the effect this has upon the mRNA and protein levels of BCL6, IRF4, and BLIMP1 in ALK+ vs. ALK- ALCL cell lines.

## 6.2 Results

### 6.2.1 ALK+ ALCL cell lines are selectively sensitive to Crizotinib

To assess the cell lines' sensitivity to ALK inhibition, ALCL cell lines were treated with Crizotinib for 72 hours and assessed by Resazurin assay. The ALK+ ALCL cell lines: SUDHL1, Karpas-299, and DEL were all sensitive to Crizotinib, reaching IC50s below 1µM, whilst the ALK- ALCL cell line Mac1 was resistant and failed to reach an IC50 (figure 6.1).

### 6.2.2 Inhibition of ALK reveals two distinct effects on RNA levels of BCL6, IRF4, BLIMP1, and c-MYC

To evaluate how ALK affected the BCL6-IRF4-BLIMP1 transcription factor axis, cells were treated with a low concentration of Crizotinib (50nM and 100nM) over a 24 hour period and lysed for RNA and protein analysis. All cell lines exhibited a reduction in *BCL6* mRNA and protein in a dose-dependent manner (SUDHL1: 50nM 4 hours  $p=0.001$ , 50nM 8 hours  $p=0.0022$ , 50nM 24 hours  $p<0.0001$ , 100nM 4 hours  $p=0.0005$ , 100nM 8 hours  $p<0.0001$ , 100nM 24 hours  $p<0.0001$ , Karpas-299: 50nM 4 hours  $p=0.0071$ , 50nM 8 hours  $p=0.0073$ , 50nM 24 hours  $p=0.0017$ , 100nM 4 hours  $p<0.0001$ , 100nM 8 hours  $p=0.0007$ , 100nM 24 hours  $p<0.0001$ , DEL: 50nM 4 hours  $p=0.0027$ , 50nM 8 hours  $p=0.0015$ , 50nM 24 hours  $p<0.0001$ , 100nM 4 hours  $p=0.0014$ , 100nM 8 hours  $p=<0.0001$ , 100nM 24 hours  $p<0.0001$ ) (figure 6.2).

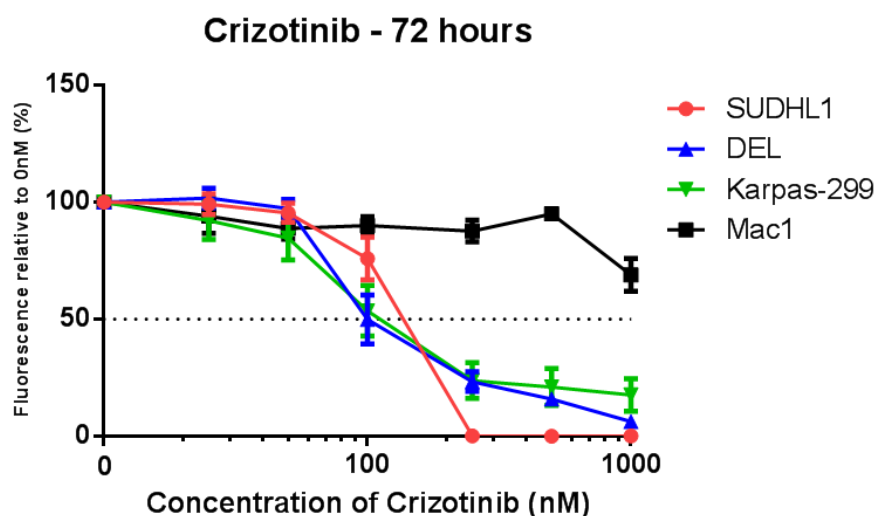
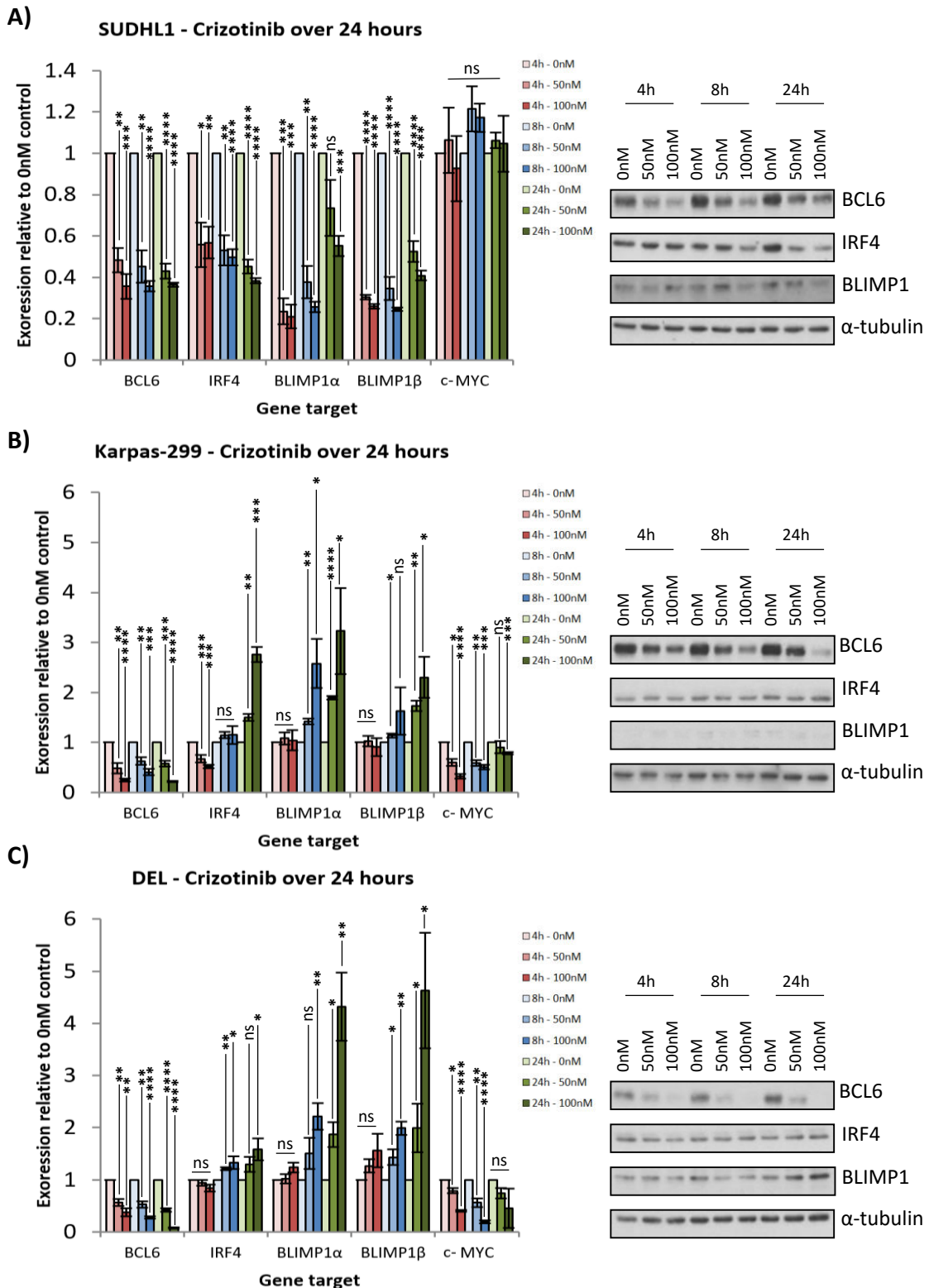


Figure 6.1: Survival curve of ALCL cell lines treated with Crizotinib

Growth inhibition curve as assessed by Resazurin fluorescence. Data is derived from 3 independent replicates, error bars indicate standard error of the mean.

There were two distinct patterns observed across the cell lines with respect to *IRF4*, *BLIMP1* and, *c-MYC* expression. SUDHL1 exhibited a reduction in *IRF4* (50nM 4 hours p=0.0148, 50nM 8 hours p=0.029, 50nM 24 hours p<0.0001, 100nM 4 hours p=0.005, 100nM 8 hours p<0.0001, 100nM 24 hours p<0.0001), *BLIMP1 $\alpha$*  (50nM 4 hours p=0.0002, 50nM 8 hours p=0.0013, 50nM 24 hours p=0.123, 100nM 4 hours p=0.0002, 100nM 8 hours p<0.0001, 100nM 24 hours p=0.0007), and *BLIMP1 $\beta$*  (50nM 4 hours p<0.0001, 50nM 8 hours p<0.0001, 50nM 24 hours p<0.001, 100nM 4 hours p<0.0001, 100nM 8 hours p<0.0001, 100nM 24 hours p<0.0001) mRNA levels with ALK inhibition whilst expression of *c-MYC* was unaltered *BLIMP1 $\beta$*  (50nM 4 hours p=0.7069, 50nM 8 hours p=0.1212, 50nM 24 hours p=0.1756, 100nM 4 hours p=0.6648, 100nM 8 hours p=0.066, 100nM 24 hours p=0.7485) (figure 6.2A). In agreement with this, *IRF4* and *BLIMP1* protein was reduced after 24 hours with Crizotinib treatment (figure 6.2A).

Karpas-299, and DEL to a minor degree, demonstrated initial reductions in *IRF4* mRNA levels at 4 hours with Crizotinib treatment (Karpas-299: 50nM p=0.0002, 100nM p=0.0002, DEL: 50nM p=0.3251, 100nM p=0.0837), however by 8 hours mRNA levels had returned to basal levels and at 24 hours mRNA was increased with Crizotinib treatment (Karpas-299: 50nM p=0.0015, 100nM p=0.003, DEL: 50nM p=0.1148, 100nM p=0.0476) (figure 6.2B and 6.2C). In addition, *BLIMP1 $\alpha$*  and *BLIMP1 $\beta$*  levels were unaffected at 4 hours (Karpas-299: *BLIMP1 $\alpha$*  50nM p=0.8489, *BLIMP1 $\alpha$*  100nM p=0.172, *BLIMP1 $\beta$*  50nM p=0.1055, *BLIMP1 $\beta$*  100nM p=0.6330, DEL: *BLIMP1 $\alpha$*  50nM p=0.8198, *BLIMP1 $\alpha$*  100nM p=0.072, *BLIMP1 $\beta$*  50nM p=0.1155, *BLIMP1 $\beta$*  100nM p=0.1572) but increased in a dose-dependent manner from 8 hours (Karpas-299: 8 hours: *BLIMP1 $\alpha$*  50nM p=0.0022, *BLIMP1 $\alpha$*  100nM p=0.0331, *BLIMP1 $\beta$*  50nM p=0.0280, *BLIMP1 $\beta$*  100nM p=0.2595, 24 hours: *BLIMP1 $\alpha$*  50nM p=0.0024, *BLIMP1 $\alpha$*  100nM p=0.0605, *BLIMP1 $\beta$*  50nM p=0.0024, *BLIMP1 $\beta$*  100nM p=0.0346, DEL: 8 hours: *BLIMP1 $\alpha$*  50nM p=0.172, *BLIMP1 $\alpha$*  100nM p=0.0083, *BLIMP1 $\beta$*  50nM p=0.0456, *BLIMP1 $\beta$*  100nM p=0.0015, 24 hours: *BLIMP1 $\alpha$*  50nM p=0.022, *BLIMP1 $\alpha$*  100nM p=0.0071, *BLIMP1 $\beta$*  50nM p=0.010, *BLIMP1 $\beta$*  100nM p=0.0306) across both cell lines (figure 6.2B and 6.2C).



**Figure 6.2: The effect of Crizotinib treatment on the expression of BCL6, IRF4, and BLIMP1 in ALK+ ALCL** Transcript and protein levels of transcription factors after 4, 8, and 24 hours treatment with Crizotinib in A) SUDHL1, B) Karpas-299, and C) DEL. Data is derived from 3 independent replicates, error bars indicate standard error of the mean.

Expression of *c-MYC* was reduced in a dose-dependent manner across both cell lines (Karpas-299: 8 hours: 50nM  $p=0.0026$ , 100nM  $p=0.0004$ , 24 hours: 50nM  $p=0.4835$ , 100nM  $p=0.0007$ , DEL: 8 hours: 50nM  $p=0.0062$ , 100nM  $p<0.0001$ , 24 hours: 50nM  $p=0.0654$ , BLIMP1 $\beta$  100nM  $p=0.2241$ ) (figure 6.2B and 6.2C). Despite the effect at the RNA level, the protein levels of IRF4 and BLIMP1 were largely unaffected in either cell line (figure 6.2B and 6.2C).

### 6.3 Discussion

In this chapter, all ALK+ ALCL cell lines were found to be selectively sensitive to the ALK inhibitor, Crizotinib, in agreement with published data and in keeping with development of Crizotinib as a clinical agent in ALK+ ALCL (Gambacorti-Passerini et al., 2011, Redaelli et al., 2013). In addition, inhibition of ALK lead to changes in the transcription of *BCL6*, *IRF4*, *BLIMP1*, and *c-MYC* indicating that ALK regulates this axis in ALK+ ALCL.

Crizotinib is a dual c-Met and ALK inhibitor (Sahu et al., 2013) and both c-Met and its ligand Hepatocyte Growth Factor have been detected by RT-PCR in ALCL cell lines. (Pons et al., 1998). It is therefore conceivable that the effects of Crizotinib on transcription factor expression in these experiments occurred through inhibition of c-Met-dependent as well as ALK-dependent events. However, as the survival of ALK+ ALCLs was sensitive to Crizotinib but that of the ALK- ALCL cell line, Mac1, was not (figure 6.1), it is likely that the Crizotinib-sensitive pathway of interest in these cell lines was downstream of ALK rather than c-Met.

Analysis of transcription factor levels after Crizotinib treatment yielded two patterns in the regulation of expression, summarised in figure 6.3. All cell lines treated with Crizotinib resulted in a downregulation of *BCL6* mRNA and protein (figure 6.2) indicating that *BCL6* expression is driven by NPM-ALK in ALK+ ALCLs. This is in agreement with previously published data which suggested that *BCL6* expression is driven by STAT3, a direct target of ALK (Walker et al., 2013).

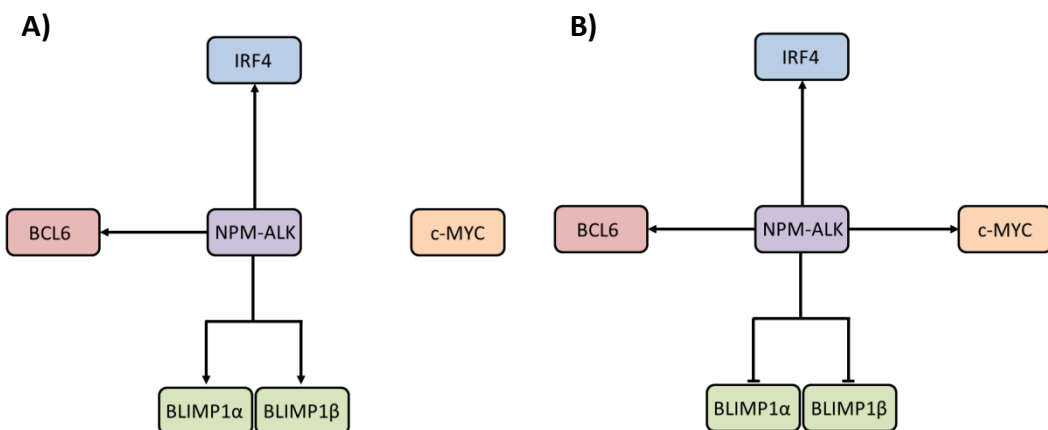


**Figure 6.3: Summary of the interactions of ALK across ALK+ ALCL cell lines**  
Interaction network of ALK based upon data in this chapter in A) SUDHL1 B) Karpas-299 and DEL.

In contrast the effect on *IRF4* mRNA expression was variable. *IRF4* was downregulated at all timepoints in SUDHL1 but upregulated in Karpas-299 and DEL (figure 6.2), albeit after an initial downregulation in Karpas-299 and perhaps also DEL. NPM-ALK may thus drive expression of IRF4 but in some cell lines ALK inhibition could result in upregulation of IRF4 as either a result of secondary regulatory effects downstream from ALK signalling or as a reflex upregulation of IRF4 as a pro-survival mechanism against Crizotinib treatment. This type of mechanism has been observed in other systems whereby treatment of ALL or CML cells with the BCR-ABL kinase inhibitor, Imatinib, results in upregulation of BCL6 for survival (Duy et al., 2011). Importantly however, the changes in *IRF4* mRNA levels seen were not recapitulated at the protein level (figure 6.2). Data published during the course of this project demonstrated that treatment of Karpas-299 cells with 150nM Crizotinib for 24 hours was sufficient to downregulate IRF4 protein expression (Weilemann et al., 2015). These contradictory data could be due to the use of different concentrations of Crizotinib, to differences in cell cultures conditions, or to differences between the cell lines used.

Crizotinib regulation of expression of BLIMP1 $\alpha$  and BLIMP1 $\beta$  also differs between cell lines. Whilst ALK inhibition appears to reduce the expression of both BLIMP1 isoforms in SUDHL1 (figure 6.2A), it promotes the expression of both isoforms in Karpas-299 and DEL (figure 6.2B and 6.2C). This discrepancy in regulation could be indicative of different fundamental interactions between the axis and BLIMP1. The expression of *BLIMP1 $\alpha$*  and *BLIMP1 $\beta$*  mRNA is only increased after 8 hours treatment in Karpas-299 and DEL (figure 6.2B and 6.2C) suggesting that the *BLIMP1* mRNA increase may be an indirect effect of ALK inhibition. Consistent with differences between cell lines, expression of *c-MYC* mRNA is reduced by ALK inhibition in Karpas-299 and DEL but not in SUDHL1 (figure 6.2). This suggests that ALK directly drives the expression of *c-MYC* in Karpas-299 and DEL whilst *c-MYC* may be driven by a different effector in SUDHL1.

The data presented in this chapter confirms that Crizotinib is a viable treatment for ALK+ ALCL. Furthermore, this data agrees with published data promoting the potential of utilising Crizotinib in a clinical setting.

It cannot be ruled out that c-Met may contribute to the effects seen and therefore future work could focus on using a different ALK inhibitor to assess if these results can be reproduced. In addition, STAT3 is a direct target of ALK (Zamo et al., 2002), and therefore cells could be treated with a STAT3 inhibitor to evaluate if the effects observed with Crizotinib are repeated with STAT3 inhibition. Alternatively, knockdown of ALK and STAT3 could be utilised to assess if similar effects are observed. Further analysis of other ALK+ ALCL cell lines should be undertaken to assess if there is a common effect on the axis expression with ALK inhibition.

## **Chapter 7: Conclusion and Discussion**



## 7. Conclusion and Discussion

The biology of PTCLs is poorly understood and as a result, they are difficult to classify and treat effectively. There is no standard, effective treatment for PTCLs; generally patients are treated with non-targeted multi-agent chemotherapy regimens such as CHOP (Vose et al., 2008). Consequently, long-term survival for patients is poor and novel therapies targeting critical biological dependencies are required. The BCL6-IRF4-BLIMP1 transcription factor axis plays a key role in the regulation of B-cell maturation and differentiation as well as that of CD4<sup>+</sup> and CD8<sup>+</sup> T-cells (Crotty et al., 2010, Johnston et al., 2009, Rutishauser et al., 2009). Recently, the axis has been implicated in a number of lymphoid malignancies including DLBCL and some types of NK/T-cell lymphoma (Boi et al., 2013, Pasqualucci et al., 2006, Pasqualucci et al., 2003, Shaffer et al., 2009, Weilemann et al., 2015). This project has examined and identified the importance of BCL6 and IRF4 expression and BLIMP1 suppression to the maintenance of proliferation and survival in ALCL.

Initial analysis of the expression of the transcription factor axis across PTCL cell lines revealed that ALK<sup>+</sup> ALCL cell lines express more BCL6 than other PTCLs. A possible explanation for this is that BCL6 expression is driven by the NPM-ALK fusion tyrosine kinase present in ALK<sup>+</sup> ALCLs. NPM-ALK is constitutively catalytically active ALK (Chiarle et al., 2005, Zamo et al., 2002) and has many targets, including STAT3, which it phosphorylates resulting in its activation (Chiarle et al., 2005, Zamo et al., 2002). Activated STAT3 has been demonstrated to drive the expression of many targets, including BCL6 and IRF4 (Walker et al., 2013, Zamo et al., 2002). In agreement with this, treatment of all ALK<sup>+</sup> ALCL cell lines tested with Crizotinib resulted in decreased mRNA and protein expression of BCL6 and, at early timepoints, IRF4. Therefore, BCL6, and to an extent IRF4, are driven by constitutively active ALK in ALK<sup>+</sup> ALCL. However, this does not explain the high expression of BCL6 protein exhibited in ALK<sup>-</sup> ALCL or  $\gamma\delta$  T-NHL cell lines. It could be speculated that BCL6 expression is a result of a STAT3 mutation resulting in constitutively active STAT3. Indeed, activating mutations of STAT3 have been reported in ALK<sup>-</sup> ALCLs as well as  $\gamma\delta$  T-NHL which have been implicated in the maintenance of cellular proliferation (Crescenzo et al., 2015, Kucuk et al., 2015).

Recently it was demonstrated that downregulation of *miR155* expression leads to reduction of p-STAT3 levels in ALK- ALCL (Merkel et al., 2015). This interaction is particularly important in the context of this study as p-STAT3 drives the expression of both BCL6 and IRF4 (Chiarle et al., 2008, Kwon et al., 2009, Walker et al., 2013, Zamo et al., 2002). However, Merkel et al. showed that the *miR155* gene is highly methylated in SUPM2 cells and thus expressed at low levels (Merkel et al., 2015). It is therefore difficult to ascertain the exact role of *miR155* in ALK+ ALCL currently but low level expression of *miR155* in ALK+ ALCL may nevertheless be sufficient for it to exert pro-tumour effects.

High BCL6 expression could be a result of downregulation of antagonistic transcription factors, for example BLIMP1. In normal T-cell physiology, BLIMP1 and BCL6 are mutually antagonistic and determine cell fate via this mechanism (Cimmino et al., 2008, Johnston et al., 2009). Of the PTCL cell lines presented in chapter 3, 50% exhibit low or no expression of at least one BLIMP1 isoform at the protein level. Despite this, some cell lines contain mutual expression of BLIMP1 and BCL6 protein suggesting mutual inhibition may be lost. In agreement with this, knockdown of BCL6 in this project did not cause any effect on the expression of BLIMP1 mRNA or protein in any of the cell lines tested whilst BLIMP1 overexpression failed to reduce the expression of *BCL6* mRNA or protein in this project and previously published data (Boi et al., 2013). As the cell of origin of ALCL is unknown, it is difficult to ascertain the interaction between BCL6 and BLIMP1 in these lymphomas. It is plausible that BCL6 and BLIMP1 targets differ between T-cell lymphoma and normal T-cell physiology. For example, BCL6 only shares 50% of its target genes between DLBCL and breast cancer (Walker et al., 2014), and, additionally in T<sub>FH</sub> cells, BCL6 targets effectors required for T-cell differentiation, migration, and signalling (Hatzi et al., 2015) suggesting that the BCL6 transcriptional programme varies according to cellular context.

To investigate if a direct BCL6-BLIMP1 interaction is present, there are multiple experiments which could be undertaken. ChIP-Seq would demonstrate if the transcription factors bound to the promoters of the antagonist, or a luciferase reporter construct coupled to a *BCL6/BLIMP1* promoter could be utilised to investigate if overexpression of BCL6/BLIMP1 caused repression of luciferase.

This project has demonstrated that BCL6 is required to sustain the proliferation of some ALK+ ALCL cell lines. Lentiviral-mediated knockdown of BCL6 caused reduced growth rates compared to controls but did not induce apoptosis. As knockdown of BCL6 caused increased G2/M population subsets in 2 of 3 cell lines, it is possible that BCL6 promotes cellular proliferation through the promotion of cell cycle progression. In agreement with this argument, previously published data demonstrates that knockdown of BCL6 in DLBCL causes G1 arrest and fails to induce apoptosis (Ying et al., 2013). The mechanism of this effect was not investigated but it seems not to involve suppression of p21 as *p21* expression was not altered by 79-6.

Recently, it has been identified that BCL6 is important for the control of metabolism in CD4<sup>+</sup> and CD8<sup>+</sup> T-cells through repression of glycolytic pathway genes (Oestreich et al., 2014). In addition, deficiency of Bcl6 in murine CD8<sup>+</sup> T-cells is detrimental to cellular growth (Ichii et al., 2002). Therefore, if ALCLs share traits with CD8<sup>+</sup> T-cells it is possible that BCL6 is working through the same mechanism. The glycolytic pathway is important for normal cellular production of ATP from glucose and oxygen; however repression of this pathway promotes the anaerobic respiration pathway. Whilst less efficient, the anaerobic pathway allows production of ATP in the absence of oxygen which would be beneficial for cells in oxygen-starved environments, such as those yet to undergo angiogenesis (Hanahan and Weinberg, 2000). Indeed, there are documented cases of the generation of more aggressive tumours via the removal of glycolysis-dependence (Kalaany and Sabatini, 2009).

The data in this project would suggest that loss of BCL6 activity does not induce apoptosis as BCL6 knockdown failed to induce apoptosis. However, treatment of all cell lines with 79-6 did induce apoptosis irrespective of their reported BCL6 dependency. As a result, it appears that 79-6 might exert off-target effects to induce apoptosis as published data on 79-6 demonstrates that the drug does not induce death in more than 40% of Toledo or OCI-Ly4 cells at 15mM (Cerchietti et al., 2010a). However, in this project, treatment of Toledo with 1mM of 79-6 was enough to kill all cells by Resazurin analysis.

The dependency of ALCL cell lines on BCL6 could be clarified by examining known BCL6 targets. Although not well documented in T-cells at the time of the

experiment, BCL6 targets were available for B-cells. BCL6 directly targets and represses the expression of genes involved in repressing apoptosis, namely *ATR* and *P53*, to allow DNA recombination for CSR and SHM as well as the cell cycle progression gene, *P21* to promote cell cycling (Cerchiatti et al., 2010a). However, treatment of ALCL cell lines with 79-6 failed to induce expression of these targets in the T-cell lines whilst expression was induced in DLBCL control suggesting that the BCL6 targets are not common between B-cells and T-cells or that 79-6 does not inhibit BCL6 in ALCL lines. It is possible that 79-6 is inhibiting BCL6, in part, based upon the induction of BCL6 target genes within SUDHL4. In light of this data, 79-6 does not constitute a viable therapeutic option for patients due to the poor specificity of the drug. More recently however, BCL6 targets for T<sub>FH</sub> cells have been published (Hatzi et al., 2015). Therefore, this experiment should be repeated using T-cell-specific BCL6 targets: *STAT4*, *IFNGR1*, *GIMAP1*, *RORA* and *GATA3*.

The transforming mechanism of *IRF4* is still unknown in PTCL; whilst translocations of the gene exist in a small percentage of PTCLs (Feldman et al., 2009), the oncogenic role of the translocation has never been proven. However, a number of activating *IRF4* mutations have been identified in ATL, MM, and CLL (Havelange et al., 2011, Kataoka, 2014, Melchor et al., 2014). These mutations all cluster in the DNA-binding domain of *IRF4* suggesting altered function of this domain is important for transformation of malignant cells. It is possible that *IRF4* mutations may exist across PTCLs and it is important to sequence *IRF4* in these tumours to identify any potential activating mutations. As well as coding mutations, SNPs present in *IRF4* intronic regions have also been demonstrated to contribute to constitutive IRF4 expression (Boddicker et al., 2015). To further investigate these mutations, knockdown of IRF4 in these cell lines could be performed in conjunction with rescue experiments with mutated sequences. Indeed, a more robust experiment would be to knockout IRF4, if the cells are viable, and introduce the mutated IRF4 and assess the effect on proliferation of these cells.

IRF4 has been demonstrated to be vital for the proliferation/survival of some ALCL cell lines in this project and, during the course of this work, similar findings have been published by two other groups (Boddicker et al., 2015, Weilemann et al., 2015). These data suggest that IRF4 plays a role in ALCL similar to that of MM, and HTLV- and

EBV-transformed cells (Dib et al., 2008, Wang et al., 2011a, Xu et al., 2008, Shaffer et al., 2008). In addition, 2 of the 3 cell lines examined in this project also demonstrated reduced *c-MYC* expression with IRF4 knockdown, suggesting a potential positive interaction between the transcription factors as observed in MM (Shaffer et al., 2008). Furthermore, recent work demonstrated that *c-MYC* inhibition resulted in IRF4 downregulation in ALCL, suggesting IRF4 is also driven by *c-MYC* in these cells (Boddicker et al., 2015). Regulation of *c-MYC* is critically important for any cancer. Translocations involving the gene are common across DLBCL and BL (Thieblemont and Briere, 2013) and are seen in rare cases of ALCL (Liang et al., 2013). In non-transformed cells, *c-MYC* is important for regulating both apoptosis and proliferation. However, overexpression of *c-MYC* can drive rapid proliferation and also cause deregulation of cell cycle regulators (Dang et al., 2006, Eilers and Eisenman, 2008). According to recently published data, treatment of ALK+ ALCL cell lines (Karpas-299, JB6) with 150nM Crizotinib for 24 hours results in downregulation of both IRF4 and *c-MYC* protein expression (Weilemann et al., 2015). The authors conclude that *c-MYC* downregulation is an effect of IRF4 downregulation. This is in agreement with data for the cell lines presented in the project, Karpas-299 and DEL, as knockdown of IRF4 in these cell lines causes downregulation of *c-MYC* in these cell lines and, additionally, *c-MYC* mRNA expression correlates with *IRF4* mRNA expression with Crizotinib treatment. In addition, it has been established that IRF4 also promotes CD30 and NF- $\kappa$ B expression in ALCL to drive its own expression (Boddicker et al., 2015). Therefore, collectively these data suggest that IRF4 is a putative tumour-promoting protein that drives its own expression through multiple pathways.

Interestingly, downregulation of IRF4 in this project lead to an increase in *BLIMP1 $\alpha$*  mRNA levels in SUDHL1 but not Karpas-299 or DEL. This interaction is contrary to normal T-cell function whereby IRF4 facilitates BLIMP1 activity (Li et al., 2012). However, this dysregulation may be expected in SUDHL1 as a mechanism of suppressing the tumour suppressor activity of BLIMP1 $\alpha$ . The data also demonstrates that Karpas-299 and DEL retain the positive effect of IRF4 expression upon BLIMP1 and thus suggest a different mechanism of overcoming BLIMP1 tumour suppressor activity.

Investigation into the inhibition of ALK lead to the observation that *IRF4* mRNA is initially downregulated in all ALK+ ALCL cell lines examined demonstrating that IRF4

is driven by ALK signalling. However, *IRF4* mRNA is then upregulated in 2 of the 3 cell lines which could be indicative of a potential compensatory mechanism for loss of ALK activity. This type of mechanism has been observed in BCR-ABL-positive ALL with Imatinib whereby treatment of cell lines with Imatinib lead to a sharp increase in the expression of BCL6. This effect was believed to be a compensatory mechanism for the loss of BCR-ABL to promote survival (Duy et al., 2011).

Interestingly, knockdown of IRF4 also induced stalling in the G2/M stage of the cell cycle and failed to induce apoptosis in most of the cell lines tested. However, in contrast to BCL6, IRF4 has been demonstrated to be important for the promotion of glycolysis, ATP production, and increased oxygen consumption (Man et al., 2013). In agreement with this, knockout of IRF4 in T-cells revealed IRF4 binds *HIF1A* which is required for cellular homeostasis (Man et al., 2013, Yao et al., 2013). Furthermore, gene expression profiling of ALK+ ALCL cells revealed an enrichment of the *HIF1A* gene signature suggesting this is a vital pathway in ALCL (Iqbal et al., 2014). Therefore, it is plausible that BCL6 and IRF4 promote proliferation of ALCL cells by promoting different metabolic pathways. Indeed, it is possible that both transcription factors are important for maintenance of proliferation and therefore dual-inhibition of both could be a useful therapeutic approach. To investigate this, knockdown of both BCL6 and IRF4 should be undertaken or, conversely, treatment of IRF4 knockdown cells with BCL6 inhibitor, to assess if a combinatory effect could be exploited. Alternatively, direct inhibition of the metabolic pathways would elucidate whether the pathway can be exploited in these malignancies. The overlapping functions suggest that ALCLs may also benefit from treatment with drugs exploiting metabolic pathways.

One unexplored aspect of the tumourigenic function of IRF4 in ALCLs is the identity of the transcription factors with which it cooperates. In B-cells, IRF4 typically binds PU.1 and SPIB to exert its activity (Basso and Dalla-Favera, 2012, Escalante et al., 2002), however due to the low quantities of these binding proteins in T-cells, IRF4 binds to other targets such as BATF and STAT3 to exert its effects (Kwon et al., 2009, Li et al., 2012, Murphy et al., 2013). It would be of interest to investigate the levels and functional dependencies of BATF, STAT3, PU.1, and SPIB in T-cell lymphomas to investigate whether these co-factors play any role in the survival of these cells in cooperation with IRF4. Indeed, published gene expression profiling of ALCLs

demonstrate a high BATF3 gene signature suggesting a potential role for BATF3 specifically in ALCL (Iqbal et al., 2014). This could also be reinforced with ChIP-Seq to demonstrate whether IRF4 shares the same binding sites as any of these co-factors. This work would be of benefit as it would offer another therapeutic alternative to targeting IRF4, as no inhibitors of the protein currently exist.

The data presented in chapter 5 demonstrated that overexpression of either BLIMP1 isoform is detrimental to the survival of 2 out of 3 of the ALCL cell lines. Therefore, it appears beneficial to cell line survival to reduce expression of BLIMP1 wherever possible. Whilst overexpression of either BLIMP1 $\alpha$  or BLIMP1 $\beta$  failed to induce changes in BCL6 expression, IRF4 expression was negatively regulated in 2 of the 3 cell lines by overexpression of either isoform. As BLIMP1 was defined as a tumour suppressor in these lymphomas, the data reinforces the concept of pro-tumorigenic IRF4 functions.

BLIMP1 may exert inhibitory effects on ALCL cells in several ways. For example, expression of BLIMP1 in the ALK+ ALCL cell line SUPM2 has been reported to result in downregulation of an oncogenic microRNA, *miR155* (Boi et al., 2013). Therefore, one possible mechanism by which BLIMP1 could suppress lymphoma development is through inhibition of *miR155* expression leading to downregulation of p-STAT3 and eventually BCL6 and IRF4, amongst other targets. However, BCL6 expression was not downregulated by BLIMP1 overexpression in any cell line in this study or in that of Boi et al. (Boi et al., 2013). Since BCL6 expression is mediated through NPM-ALK in all ALK+ ALCL cell lines tested, the repressive effect of BLIMP1 on BCL6 could be diminished by the constitutive expression of NPM-ALK. This effect may be confirmed in a previous study which demonstrates that overexpression of BLIMP1 $\alpha$  in ALK+ ALCL did not cause a detectable reduction in *BCL6* mRNA levels by gene expression array (Boi et al., 2013).

It is possible that critical BLIMP1 targets have been modified in some way within cell lines to prevent the binding of BLIMP1, or that BLIMP1 itself is mutated to render it dysfunctional. Whilst it has not been documented to date, mutations introduced into BLIMP1 targets in BL abrogate the binding of BLIMP1 to regulatory regions (Cubedo et al., 2011). It has previously been documented that *PRDM1* can harbour frameshift deletions, truncations, and point mutations in DLBCL leading to the

inactivation of the BLIMP1 protein (Pasqualucci et al., 2006). To this possibility in ALCL lines, the *PRDM1* gene of the cell lines would require sequencing. Sequencing of the *PRDM1* locus may be interesting in Karpas-299 in particular as this line harbours a deletion of 6q21 (Boi et al., 2013) and expresses no detectable levels of BLIMP1 $\alpha$  protein in this project but expresses large quantities of *BLIMP1* mRNA (data not shown). Therefore, the data suggests either a mutation resulting in protein instability or a deregulation of protein degradation. Interestingly, BLIMP1 $\alpha$  has been shown to be degraded following SUMOylation (Shimshon et al., 2011) so that hyperactivation of this pathway could result in increased degradation of BLIMP1 protein. Somewhat similarly, inactivation of the FBXO11 ubiquitin ligase protein in DLBCL leads to increased expression of BCL6 protein (Duan et al., 2012).

This project has highlighted a potential differing mechanism of transformation between certain ALK+ ALCL cell lines, namely between SUDHL1 and Karpas-299/DEL. Regarding the transcription factor axis, SUDHL1 responds differently to drug treatments compared to Karpas-299 and DEL. For example, treatment of SUDHL1 with Crizotinib results in reduction of *BCL6*, *IRF4*, and *BLIMP1* mRNA expression but not *c-MYC* expression. However, treatment of Karpas-299 and DEL with Crizotinib results in reduction of all targets initially, with *IRF4* and *BLIMP1* mRNA expression increasing after 24 hours suggesting that ALK may have differing interactions in these cell lines. SUDHL1 was also the only ALK+ ALCL cell line to show sensitivity to Lenalidomide treatment reinforcing the hypothesis of differing transforming mechanisms between SUDHL1 and other ALK+ ALCLs. In addition, loss of *IRF4* in SUDHL1 results in upregulation of *BLIMP1 $\alpha$* , but not *BLIMP1 $\beta$* , mRNA expression whilst Karpas-299 and DEL demonstrate reduction in both BLIMP1 isoforms. Taken together, these data suggest that a subset of ALK+ ALCLs may exist that would benefit from Lenalidomide treatment. This could be investigated further by conducting gene expression profiling of SUDHL1 vs. Karpas-299 and DEL and investigating any important differences between the cell lines. In addition, published data could be investigated for alterations between specific ALK+ ALCLs.

From this body of research, two key areas for future work are particularly evident. It is important to investigate if BCL6 and IRF4 promote proliferation across other PTCL subsets, particularly AITL whereby expression of BCL6 is high. Therefore

knockdown or CRISPR-mediated knockouts of BCL6 and/or IRF4 should be undertaken in other cell lines and proliferation/survival should be assessed. For AITL, due to the lack of cell line availability, either primary cell cultures or xenograft mouse models would be required to investigate this. It is also of interest to elucidate any BCL6 and IRF4 targets in T-cell lymphoma and assess how these contribute to proliferation. This would involve taking cell lines which are sensitive and insensitive to BCL6/IRF4 inhibition or knockdown and assessing the changes in gene expression. Targets important for proliferation could potentially be identified by analysing the gene expression differences between sensitive and insensitive lines. As cell lines appear to exhibit heterogeneity in the sensitivities of either BCL6/IRF4 knockdown or BLIMP1 overexpression it would be beneficial to understand the molecular events contributing to these sensitivities. Therefore further investigation into how the interactions of BCL6, IRF4, and BLIMP1 differ between both PTCL cell lines and normal T-cells, and the molecular mechanisms which perturb these interactions, should also be undertaken. This could be achieved through CRISPR-mediated knockout studies in conjunction with gene expression profiling.

The data presented in this project has demonstrated that the interactions between the BCL6-IRF4-BLIMP1 transcription factor axis varies between cell lines (figure 7.1). However, it is clear the axis plays a vital role in the survival of ALCL and highlights potential therapeutic avenues which could be exploited for the future treatment of these patients. Therapeutic options should focus on downregulating BCL6, IRF4, and NPM-ALK activity whilst promoting BLIMP1 activity. As direct targeting of IRF4 is not an option currently, indirect inhibition through targeting of BRD4, c-MYC, and NF- $\kappa$ B would exert anti-tumour effects on those malignancies sensitive to IRF4 knockdown. The use of metabolic inhibitors, STAT3 inhibitors, or ALK inhibitors (for ALK-driven malignancies) may yield a mechanism of targeting both BCL6 and IRF4 pathways simultaneously. The treatment of PTCL will improve only with greater understanding of the underlying mechanisms that drive it; this project provides the foundations for that work.

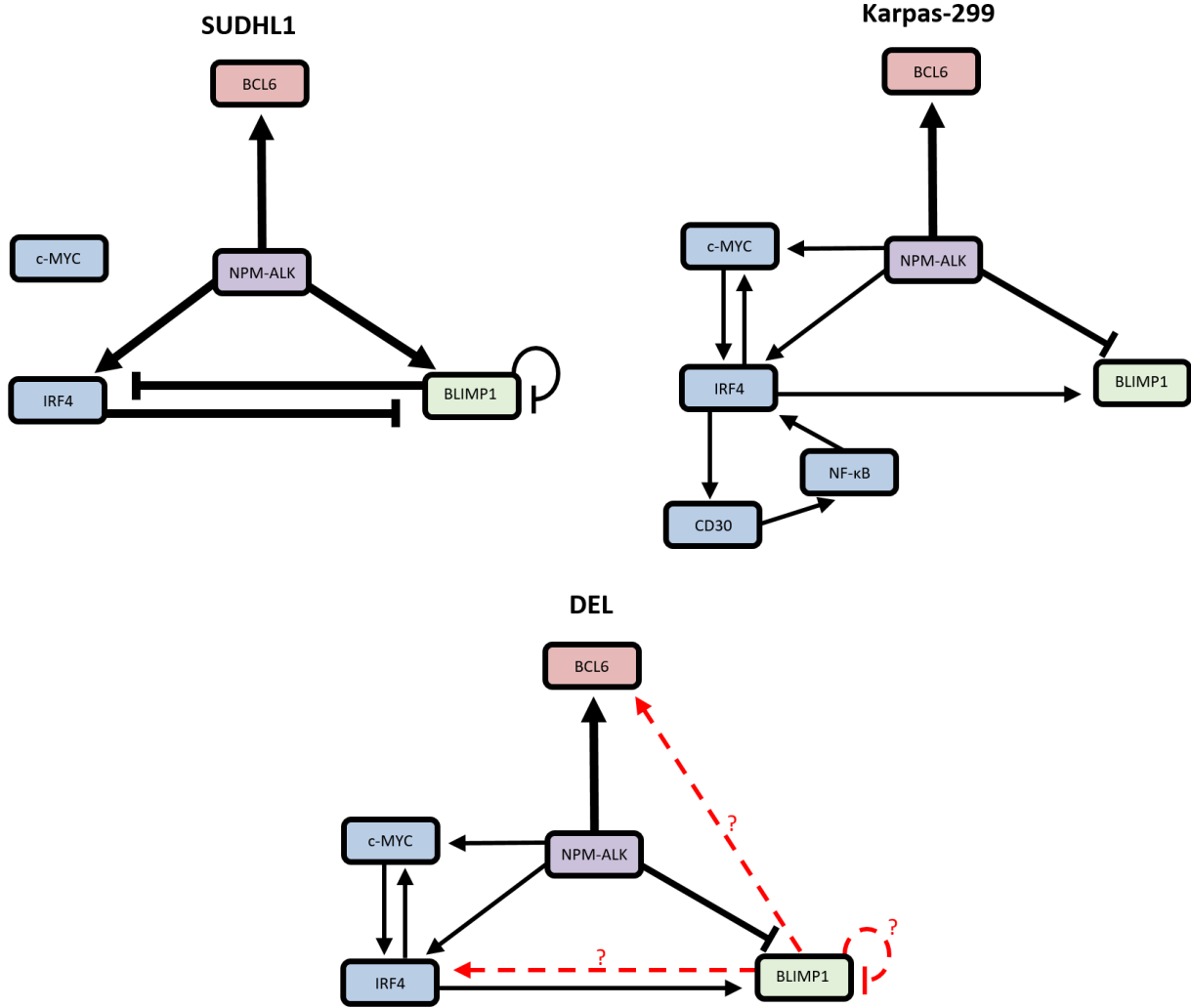


**Figure 7.1: Summary of the interactions between the BCL6-IRF4-BLIMP1 transcription factor axis in ALK+ ALCL cell lines**

Suggested interaction network of the BCL6-IRF4-BLIMP1 axis in the ALK+ ALCL based upon experiments conducted and published data. Arrow thickness indicates the magnitude of the interaction, dashed lines indicate the interaction has not been interrogated in this project.

## **Chapter 8: References**



## 8. References

- AFKARIAN, M., SEDY, J. R., YANG, J., JACOBSON, N. G., CEREB, N., YANG, S. Y., MURPHY, T. L. & MURPHY, K. M. 2002. T-bet is a STAT1-induced regulator of IL-12R expression in naive CD4+ T cells. *Nat Immunol*, 3, 549-57.
- AGNELLI, L., MEREU, E., PELLEGRINO, E., LIMONGI, T., KWEE, I., BERGAGGIO, E., PONZONI, M., ZAMO, A., IQBAL, J., PICCALUGA, P. P., NERI, A., CHAN, W. C., PILERI, S., BERTONI, F., INGHIRAMI, G. & PIVA, R. 2012. Identification of a 3-gene model as a powerful diagnostic tool for the recognition of ALK-negative anaplastic large-cell lymphoma. *Blood*, 120, 1274-81.
- AGRAWAL, N., DASARADHI, P. V., MOHMMED, A., MALHOTRA, P., BHATNAGAR, R. K. & MUKHERJEE, S. K. 2003. RNA interference: biology, mechanism, and applications. *Microbiol Mol Biol Rev*, 67, 657-85.
- AHEARNE, M. J., ALLCHIN, R. L., FOX, C. P. & WAGNER, S. D. 2014. Follicular helper T-cells: expanding roles in T-cell lymphoma and targets for treatment. *Br J Haematol*, 166, 326-35.
- AHLER, E., SULLIVAN, W. J., CASS, A., BRAAS, D., YORK, A. G., BENSINGER, S. J., GRAEBER, T. G. & CHRISTOFK, H. R. 2013. Doxycycline alters metabolism and proliferation of human cell lines. *PLoS One*, 8, e64561.
- AHMAD, K. F., MELNICK, A., LAX, S., BOUCHARD, D., LIU, J., KIANG, C. L., MAYER, S., TAKAHASHI, S., LICHT, J. D. & PRIVE, G. G. 2003. Mechanism of SMRT corepressor recruitment by the BCL6 BTB domain. *Mol Cell*, 12, 1551-64.
- AKASAKA, H., AKASAKA, T., KURATA, M., UEDA, C., SHIMIZU, A., UCHIYAMA, T. & OHNO, H. 2000. Molecular anatomy of BCL6 translocations revealed by long-distance polymerase chain reaction-based assays. *Cancer Res*, 60, 2335-41.
- ALINIKULA, J., NERA, K. P., JUNTTILA, S. & LASSILA, O. 2011. Alternate pathways for Bcl6-mediated regulation of B cell to plasma cell differentiation. *Eur J Immunol*, 41, 2404-13.
- AMIN, H. M. & LAI, R. 2007. Pathobiology of ALK+ anaplastic large-cell lymphoma. *Blood*, 110, 2259-67.
- AMIN, H. M., MCDONNELL, T. J., MA, Y., LIN, Q., FUJIO, Y., KUNISADA, K., LEVENTAKI, V., DAS, P., RASSIDAKIS, G. Z., CUTLER, C., MEDEIROS, L. J. & LAI, R. 2004. Selective inhibition of STAT3 induces apoptosis and G(1) cell cycle arrest in ALK-positive anaplastic large cell lymphoma. *Oncogene*, 23, 5426-34.
- ANDERSEN, C. L., ASMAR, F., KLAUSEN, T., HASSELBALCH, H. & GRONBAEK, K. 2012. Somatic mutations of the CREBBP and EP300 genes affect response to histone deacetylase inhibition in malignant DLBCL clones. *Leuk Res Rep*, 2, 1-3.
- ANNUNZIATO, F., COSMI, L., SANTARLASCIO, V., MAGGI, L., LIOTTA, F., MAZZINGHI, B., PARENTE, E., FILI, L., FERRI, S., FROSALI, F., GIUDICI, F., ROMAGNANI, P., PARRONCHI, P., TONELLI, F., MAGGI, E. & ROMAGNANI, S. 2007. Phenotypic and functional features of human Th17 cells. *J Exp Med*, 204, 1849-61.
- ARMITAGE, J. O. 2012. The aggressive peripheral T-cell lymphomas: 2012 update on diagnosis, risk stratification, and management. *Am J Hematol*, 87, 511-9.
- BACHEM, A., GUTTLER, S., HARTUNG, E., EBSTEIN, F., SCHAEFER, M., TANNERT, A., SALAMA, A., MOVASSAGHI, K., OPITZ, C., MAGES, H. W., HENN, V., KLOETZEL, P. M., GURKA, S. & KROCZEK, R. A. 2010. Superior antigen cross-presentation and XCR1 expression define human CD11c+CD141+ cells as homologues of mouse CD8+ dendritic cells. *J Exp Med*, 207, 1273-81.
- BARISH, G. D., YU, R. T., KARUNASIRI, M., OCAMPO, C. B., DIXON, J., BENNER, C., DENT, A. L., TANGIRALA, R. K. & EVANS, R. M. 2010. Bcl-6 and NF-kappaB cistromes mediate opposing regulation of the innate immune response. *Genes Dev*, 24, 2760-5.

- BARON, B. W., ANASTASI, J., MONTAG, A., HUO, D., BARON, R. M., KARRISON, T., THIRMAN, M. J., SUBUDHI, S. K., CHIN, R. K., FELSHER, D. W., FU, Y. X., MCKEITHAN, T. W. & BARON, J. M. 2004. The human BCL6 transgene promotes the development of lymphomas in the mouse. *Proc Natl Acad Sci U S A*, 101, 14198-203.
- BARON, U. & BUJARD, H. 2000. Tet repressor-based system for regulated gene expression in eukaryotic cells: principles and advances. *Methods Enzymol*, 327, 401-21.
- BARRANS, S., CROUCH, S., SMITH, A., TURNER, K., OWEN, R., PATMORE, R., ROMAN, E. & JACK, A. 2010. Rearrangement of MYC is associated with poor prognosis in patients with diffuse large B-cell lymphoma treated in the era of rituximab. *J Clin Oncol*, 28, 3360-5.
- BASSO, K. & DALLA-FAVERA, R. 2010. BCL6: master regulator of the germinal center reaction and key oncogene in B cell lymphomagenesis. *Adv Immunol*, 105, 193-210.
- BASSO, K. & DALLA-FAVERA, R. 2012. Roles of BCL6 in normal and transformed germinal center B cells. *Immunol Rev*, 247, 172-83.
- BASSO, K. & DALLA-FAVERA, R. 2015. Germinal centres and B cell lymphomagenesis. *Nat Rev Immunol*, 15, 172-84.
- BASSO, K., SAITO, M., SUMAZIN, P., MARGOLIN, A. A., WANG, K., LIM, W. K., KITAGAWA, Y., SCHNEIDER, C., ALVAREZ, M. J., CALIFANO, A. & DALLA-FAVERA, R. 2010. Integrated biochemical and computational approach identifies BCL6 direct target genes controlling multiple pathways in normal germinal center B cells. *Blood*, 115, 975-84.
- BATES, S. E., EISCH, R., LING, A., ROSING, D., TURNER, M., PITTALUGA, S., PRINCE, H. M., KIRSCHBAUM, M. H., ALLEN, S. L., ZAIN, J., GESKIN, L. J., JOSKE, D., POPPLEWELL, L., COWEN, E. W., JAFFE, E. S., NICHOLS, J., KENNEDY, S., STEINBERG, S. M., LIEWEHR, D. J., SHOWE, L. C., STEAKLEY, C., WRIGHT, J., FOJO, T., LITMAN, T. & PIEKARZ, R. L. 2015. Romidepsin in peripheral and cutaneous T-cell lymphoma: mechanistic implications from clinical and correlative data. *Br J Haematol*.
- BATLLE-LOPEZ, A., CORTIGUERA, M. G., ROSA-GARRIDO, M., BLANCO, R., DEL CERRO, E., TORRANO, V., WAGNER, S. D. & DELGADO, M. D. 2015. Novel CTCF binding at a site in exon1A of BCL6 is associated with active histone marks and a transcriptionally active locus. *Oncogene*, 34, 246-56.
- BEA, S., ZETTL, A., WRIGHT, G., SALAVERRIA, I., JEHN, P., MORENO, V., BUREK, C., OTT, G., PUIG, X., YANG, L., LOPEZ-GUILLERMO, A., CHAN, W. C., GREINER, T. C., WEISENBURGER, D. D., ARMITAGE, J. O., GASCOYNE, R. D., CONNORS, J. M., GROGAN, T. M., BRAZIEL, R., FISHER, R. I., SMELAND, E. B., KVALOY, S., HOLTE, H., DELABIE, J., SIMON, R., POWELL, J., WILSON, W. H., JAFFE, E. S., MONTSERRAT, E., MULLER-HERMELINK, H. K., STAUDT, L. M., CAMPO, E. & ROSENWALD, A. 2005. Diffuse large B-cell lymphoma subgroups have distinct genetic profiles that influence tumor biology and improve gene-expression-based survival prediction. *Blood*, 106, 3183-90.
- BELLEFROID, E. J., LECOCQ, P. J., BENHIDA, A., PONCELET, D. A., BELAYEW, A. & MARTIAL, J. A. 1989. The human genome contains hundreds of genes coding for finger proteins of the Kruppel type. *DNA*, 8, 377-87.
- BELZ, G. T. & KALLIES, A. 2010. Effector and memory CD8+ T cell differentiation: toward a molecular understanding of fate determination. *Curr Opin Immunol*, 22, 279-85.
- BENZ-LEMOINE, E., BRIZARD, A., HURET, J. L., BABIN, P., GUILHOT, F., COUET, D. & TANZER, J. 1988. Malignant histiocytosis: a specific t(2;5)(p23;q35) translocation? Review of the literature. *Blood*, 72, 1045-7.
- BERESHCHENKO, O. R., GU, W. & DALLA-FAVERA, R. 2002. Acetylation inactivates the transcriptional repressor BCL6. *Nat Genet*, 32, 606-13.
- BIFFI, A., BARTOLOMAE, C. C., CESANA, D., CARTIER, N., AUBOURG, P., RANZANI, M., CESANI, M., BENEDECENTI, F., PLATI, T., RUBAGOTTI, E., MERELLA, S., CAPOTONDO, A., SGUALDINO, J., ZANETTI, G., VON KALLE, C., SCHMIDT, M., NALDINI, L. & MONTINI, E. 2011. Lentiviral vector common integration sites in preclinical models and a clinical trial reflect a benign integration bias and not oncogenic selection. *Blood*, 117, 5332-9.

- BODDICKER, R. L., KIP, N. S., XING, X., ZENG, Y., YANG, Z. Z., LEE, J. H., ALMADA, L. L., ELSAWA, S. F., KNUDSON, R. A., LAW, M. E., KETTERLING, R. P., CUNNINGHAM, J. M., WU, Y., MAURER, M. J., O'BYRNE, M. M., CERHAN, J. R., SLAGER, S. L., LINK, B. K., PORCHER, J. C., GROTE, D. M., JELINEK, D. F., DOGAN, A., ANSELL, S. M., FERNANDEZ-ZAPICO, M. E. & FELDMAN, A. L. 2015. The oncogenic transcription factor IRF4 is regulated by a novel CD30/NF-kappaB positive feedback loop in peripheral T-cell lymphoma. *Blood*.
- BODEN, D., PUSCH, O., SILBERMANN, R., LEE, F., TUCKER, L. & RAMRATNAM, B. 2004. Enhanced gene silencing of HIV-1 specific siRNA using microRNA designed hairpins. *Nucleic Acids Res*, 32, 1154-8.
- BOI, M., RINALDI, A., KWEE, I., BONETTI, P., TODARO, M., TABBO, F., PIVA, R., RANCOITA, P. M., MATOLCSY, A., TIMAR, B., TOUSSEYN, T., RODRIGUEZ-PINILLA, S. M., PIRIS, M. A., BEA, S., CAMPO, E., BHAGAT, G., SWERDLOW, S. H., ROSENWALD, A., PONZONI, M., YOUNG, K. H., PICCALUGA, P. P., DUMMER, R., PILERI, S., ZUCCA, E., INGHIRAMI, G. & BERTONI, F. 2013. PRDM1/BLIMP1 is commonly inactivated in anaplastic large T-cell lymphoma. *Blood*.
- BOLLIG, N., BRUSTLE, A., KELLNER, K., ACKERMANN, W., ABASS, E., RAIFER, H., CAMARA, B., BRENDEL, C., GIEL, G., BOTHUR, E., HUBER, M., PAUL, C., ELLI, A., KROCZEK, R. A., NURIEVA, R., DONG, C., JACOB, R., MAK, T. W. & LOHOFF, M. 2012. Transcription factor IRF4 determines germinal center formation through follicular T-helper cell differentiation. *Proc Natl Acad Sci U S A*, 109, 8664-9.
- BRASS, A. L., KEHRLI, E., EISENBEIS, C. F., STORB, U. & SINGH, H. 1996. Pip, a lymphoid-restricted IRF, contains a regulatory domain that is important for autoinhibition and ternary complex formation with the Ets factor PU.1. *Genes Dev*, 10, 2335-47.
- BREITFELD, D., OHL, L., KREMMER, E., ELLWART, J., SALLUSTO, F., LIPP, M. & FORSTER, R. 2000. Follicular B helper T cells express CXC chemokine receptor 5, localize to B cell follicles, and support immunoglobulin production. *J Exp Med*, 192, 1545-52.
- BREITKREUTZ, I., RAAB, M. S., VALLET, S., HIDESHIMA, T., RAJE, N., MITSIADES, C., CHAUHAN, D., OKAWA, Y., MUNSHI, N. C., RICHARDSON, P. G. & ANDERSON, K. C. 2008. Lenalidomide inhibits osteoclastogenesis, survival factors and bone-remodeling markers in multiple myeloma. *Leukemia*, 22, 1925-32.
- BRESLER, S. C., WOOD, A. C., HAGLUND, E. A., COURTRIGHT, J., BELCASTRO, L. T., PLEGARIA, J. S., COLE, K., TOPOROVSKAYA, Y., ZHAO, H., CARPENTER, E. L., CHRISTENSEN, J. G., MARIS, J. M., LEMMON, M. A. & MOSSE, Y. P. 2011. Differential inhibitor sensitivity of anaplastic lymphoma kinase variants found in neuroblastoma. *Sci Transl Med*, 3, 108ra114.
- BRIDGE, A. J., PEBERNARD, S., DUCRAUX, A., NICOULAZ, A. L. & IGGO, R. 2003. Induction of an interferon response by RNAi vectors in mammalian cells. *Nat Genet*, 34, 263-4.
- BRUHN, S., BARRENAS, F., MOBINI, R., ANDERSSON, B. A., CHAVALI, S., EGAN, B. S., HOVIG, E., SANDVE, G. K., LANGSTON, M. A., ROGERS, G., WANG, H. & BENSON, M. 2012. Increased expression of IRF4 and ETS1 in CD4+ cells from patients with intermittent allergic rhinitis. *Allergy*, 67, 33-40.
- BRUSTLE, A., HEINK, S., HUBER, M., ROSENPLANTER, C., STADELMANN, C., YU, P., ARPAIA, E., MAK, T. W., KAMRADT, T. & LOHOFF, M. 2007. The development of inflammatory T(H)-17 cells requires interferon-regulatory factor 4. *Nat Immunol*, 8, 958-66.
- BUMCROT, D., MANOHARAN, M., KOTELIANSKY, V. & SAH, D. W. 2006. RNAi therapeutics: a potential new class of pharmaceutical drugs. *Nat Chem Biol*, 2, 711-9.
- BUTLER, M. P., IIDA, S., CAPELLO, D., ROSSI, D., RAO, P. H., NALLASIVAM, P., LOUIE, D. C., CHAGANTI, S., AU, T., GASCOYNE, R. D., GAIDANO, G., CHAGANTI, R. S. & DALLA-FAVERA, R. 2002. Alternative translocation breakpoint cluster region 5' to BCL-6 in B-cell non-Hodgkin's lymphoma. *Cancer Res*, 62, 4089-94.
- BUTRYNSKI, J. E., D'ADAMO, D. R., HORNICK, J. L., DAL CIN, P., ANTONESCU, C. R., JHANWAR, S. C., LADANYI, M., CAPELLETTI, M., RODIG, S. J., RAMAIYA, N., KWAK, E. L., CLARK, J. W., WILNER, K. D., CHRISTENSEN, J. G., JANNE, P. A., MAKI, R. G., DEMETRI, G. D. &

- SHAPIRO, G. I. 2010. Crizotinib in ALK-rearranged inflammatory myofibroblastic tumor. *N Engl J Med*, 363, 1727-33.
- CATTORETTI, G., CHANG, C. C., CECHOVA, K., ZHANG, J., YE, B. H., FALINI, B., LOUIE, D. C., OFFIT, K., CHAGANTI, R. S. & DALLA-FAVERA, R. 1995. BCL-6 protein is expressed in germinal-center B cells. *Blood*, 86, 45-53.
- CERCHIETTI, L. C., GHETU, A. F., ZHU, X., DA SILVA, G. F., ZHONG, S., MATTHEWS, M., BUNTING, K. L., POLO, J. M., FARES, C., ARROWSMITH, C. H., YANG, S. N., GARCIA, M., COOP, A., MACKERELL, A. D., JR., PRIVE, G. G. & MELNICK, A. 2010a. A small-molecule inhibitor of BCL6 kills DLBCL cells in vitro and in vivo. *Cancer Cell*, 17, 400-11.
- CERCHIETTI, L. C., HATZI, K., CALDAS-LOPES, E., YANG, S. N., FIGUEROA, M. E., MORIN, R. D., HIRST, M., MENDEZ, L., SHAKNOVICH, R., COLE, P. A., BHALLA, K., GASCOYNE, R. D., MARRA, M., CHIOSIS, G. & MELNICK, A. 2010b. BCL6 repression of EP300 in human diffuse large B cell lymphoma cells provides a basis for rational combinatorial therapy. *J Clin Invest*.
- CERCHIETTI, L. C., YANG, S. N., SHAKNOVICH, R., HATZI, K., POLO, J. M., CHADBURN, A., DOWDY, S. F. & MELNICK, A. 2009. A peptomimetic inhibitor of BCL6 with potent antilymphoma effects in vitro and in vivo. *Blood*, 113, 3397-405.
- CHALLEN, G. A., SUN, D., JEONG, M., LUO, M., JELINEK, J., BERG, J. S., BOCK, C., VASANTHAKUMAR, A., GU, H., XI, Y., LIANG, S., LU, Y., DARLINGTON, G. J., MEISSNER, A., ISSA, J. P., GODLEY, L. A., LI, W. & GOODELL, M. A. 2012. Dnmt3a is essential for hematopoietic stem cell differentiation. *Nat Genet*, 44, 23-31.
- CHAPMAN, M. A., LAWRENCE, M. S., KEATS, J. J., CIBULSKIS, K., SOUGNEZ, C., SCHINZEL, A. C., HARVIEW, C. L., BRUNET, J. P., AHMANN, G. J., ADLI, M., ANDERSON, K. C., ARDLIE, K. G., AUCLAIR, D., BAKER, A., BERGSAGEL, P. L., BERNSTEIN, B. E., DRIER, Y., FONSECA, R., GABRIEL, S. B., HOFMEISTER, C. C., JAGANNATH, S., JAKUBOWIAK, A. J., KRISHNAN, A., LEVY, J., LIEFELD, T., LONIAL, S., MAHAN, S., MFUKO, B., MONTI, S., PERKINS, L. M., ONOFRIO, R., PUGH, T. J., RAJKUMAR, S. V., RAMOS, A. H., SIEGEL, D. S., SIVACHENKO, A., STEWART, A. K., TRUDEL, S., VIJ, R., VOET, D., WINCKLER, W., ZIMMERMAN, T., CARPTEN, J., TRENT, J., HAHN, W. C., GARRAWAY, L. A., MEYERSON, M., LANDER, E. S., GETZ, G. & GOLUB, T. R. 2011. Initial genome sequencing and analysis of multiple myeloma. *Nature*, 471, 467-72.
- CHATTOPADHYAY, A., TATE, S. A., BESWICK, R. W., WAGNER, S. D. & KO FERRIGNO, P. 2006. A peptide aptamer to antagonize BCL-6 function. *Oncogene*, 25, 2223-33.
- CHEN, Q., YANG, W., GUPTA, S., BISWAS, P., SMITH, P., BHAGAT, G. & PERNIS, A. B. 2008. IRF-4-binding protein inhibits interleukin-17 and interleukin-21 production by controlling the activity of IRF-4 transcription factor. *Immunity*, 29, 899-911.
- CHEN, W., IIDA, S., LOUIE, D. C., DALLA-FAVERA, R. & CHAGANTI, R. S. 1998. Heterologous promoters fused to BCL6 by chromosomal translocations affecting band 3q27 cause its deregulated expression during B-cell differentiation. *Blood*, 91, 603-7.
- CHIARLE, R., GONG, J. Z., GUASPARRI, I., PESCI, A., CAI, J., LIU, J., SIMMONS, W. J., DHALL, G., HOWES, J., PIVA, R. & INGHIRAMI, G. 2003. NPM-ALK transgenic mice spontaneously develop T-cell lymphomas and plasma cell tumors. *Blood*, 101, 1919-27.
- CHIARLE, R., SIMMONS, W. J., CAI, H., DHALL, G., ZAMO, A., RAZ, R., KARRAS, J. G., LEVY, D. E. & INGHIRAMI, G. 2005. Stat3 is required for ALK-mediated lymphomagenesis and provides a possible therapeutic target. *Nat Med*, 11, 623-9.
- CHIARLE, R., VOENA, C., AMBROGIO, C., PIVA, R. & INGHIRAMI, G. 2008. The anaplastic lymphoma kinase in the pathogenesis of cancer. *Nat Rev Cancer*, 8, 11-23.
- CHOI, Y. S., YANG, J. A., YUSUF, I., JOHNSTON, R. J., GREENBAUM, J., PETERS, B. & CROTTY, S. 2013. Bcl6 Expressing Follicular Helper CD4 T Cells Are Fate Committed Early and Have the Capacity To Form Memory. *J Immunol*.
- CIMMINO, L., MARTINS, G. A., LIAO, J., MAGNUSDOTTIR, E., GRUNIG, G., PEREZ, R. K. & CALAME, K. L. 2008. Blimp-1 attenuates Th1 differentiation by repression of ifng, tbx21, and bcl6 gene expression. *J Immunol*, 181, 2338-47.

- CIOFANI, M., MADAR, A., GALAN, C., SELLARS, M., MACE, K., PAULI, F., AGARWAL, A., HUANG, W., PARKURST, C. N., MURATET, M., NEWBERRY, K. M., MEADOWS, S., GREENFIELD, A., YANG, Y., JAIN, P., KIRIGIN, F. K., BIRCHMEIER, C., WAGNER, E. F., MURPHY, K. M., MYERS, R. M., BONNEAU, R. & LITTMAN, D. R. 2012. A Validated Regulatory Network for Th17 Cell Specification. *Cell*.
- COLLEONI, G. W., BRIDGE, J. A., GARICOCHEA, B., LIU, J., FILIPPA, D. A. & LADANYI, M. 2000. ATIC-ALK: A novel variant ALK gene fusion in anaplastic large cell lymphoma resulting from the recurrent cryptic chromosomal inversion, inv(2)(p23q35). *Am J Pathol*, 156, 781-9.
- COOLS, J., WLODARSKA, I., SOMERS, R., MENTENS, N., PEDEUTOUR, F., MAES, B., DE WOLF-PEETERS, C., PAUWELS, P., HAGEMEIJER, A. & MARYNEN, P. 2002. Identification of novel fusion partners of ALK, the anaplastic lymphoma kinase, in anaplastic large-cell lymphoma and inflammatory myofibroblastic tumor. *Genes Chromosomes Cancer*, 34, 354-62.
- COURONNE, L., BASTARD, C. & BERNARD, O. A. 2012. TET2 and DNMT3A mutations in human T-cell lymphoma. *N Engl J Med*, 366, 95-6.
- CRESCENZO, R., ABATE, F., LASORSA, E., TABBO, F., GAUDIANO, M., CHIESA, N., DI GIACOMO, F., SPACCAROTELLA, E., BARBAROSSA, L., ERCOLE, E., TODARO, M., BOI, M., ACQUAVIVA, A., FICARRA, E., NOVERO, D., RINALDI, A., TOUSSEYN, T., ROSENWALD, A., KENNER, L., CERRONI, L., TZANKOV, A., PONZONI, M., PAULLI, M., WEISENBURGER, D., CHAN, W. C., IQBAL, J., PIRIS, M. A., ZAMO, A., CIARDULLO, C., ROSSI, D., GAIDANO, G., PILERI, S., TIACCI, E., FALINI, B., SHULTZ, L. D., MEVELLEC, L., VIALARD, J. E., PIVA, R., BERTONI, F., RABADAN, R. & INGHIRAMI, G. 2015. Convergent mutations and kinase fusions lead to oncogenic STAT3 activation in anaplastic large cell lymphoma. *Cancer Cell*, 27, 516-32.
- CRETNEY, E., XIN, A., SHI, W., MINNICH, M., MASSON, F., MIASARI, M., BELZ, G. T., SMYTH, G. K., BUSSLINGER, M., NUTT, S. L. & KALLIES, A. 2011. The transcription factors Blimp-1 and IRF4 jointly control the differentiation and function of effector regulatory T cells. *Nat Immunol*, 12, 304-11.
- CROTTY, S., JOHNSTON, R. J. & SCHOENBERGER, S. P. 2010. Effectors and memories: Bcl-6 and Blimp-1 in T and B lymphocyte differentiation. *Nat Immunol*, 11, 114-20.
- CUBEDO, E., MAURIN, M., JIANG, X., LOSSOS, I. S. & WRIGHT, K. L. 2011. PRDM1/Blimp1 downregulates expression of germinal center genes LMO2 and HGAL. *FEBS J*, 278, 3065-75.
- CUENCO, G. M., NUCIFORA, G. & REN, R. 2000. Human AML1/MDS1/EVI1 fusion protein induces an acute myelogenous leukemia (AML) in mice: a model for human AML. *Proc Natl Acad Sci U S A*, 97, 1760-5.
- CUI, J. J., TRAN-DUBE, M., SHEN, H., NAMBU, M., KUNG, P. P., PAIRISH, M., JIA, L., MENG, J., FUNK, L., BOTROUS, I., MCTIGUE, M., GRODSKY, N., RYAN, K., PADRIQUE, E., ALTON, G., TIMOFEEVSKI, S., YAMAZAKI, S., LI, Q., ZOU, H., CHRISTENSEN, J., MROCZKOWSKI, B., BENDER, S., KANIA, R. S. & EDWARDS, M. P. 2011. Structure based drug design of crizotinib (PF-02341066), a potent and selective dual inhibitor of mesenchymal-epithelial transition factor (c-MET) kinase and anaplastic lymphoma kinase (ALK). *J Med Chem*, 54, 6342-63.
- CZYZYK-KRZESKA, M. F. & ZHANG, X. 2014. MiR-155 at the heart of oncogenic pathways. *Oncogene*, 33, 677-8.
- D'COSTA, K., EMSLIE, D., METCALF, D., SMYTH, G. K., KARNOWSKI, A., KALLIES, A., NUTT, S. L. & CORCORAN, L. M. 2009. Blimp1 is limiting for transformation in a mouse plasmacytoma model. *Blood*, 113, 5911-9.
- DANG, C. V., O'DONNELL, K. A., ZELLER, K. I., NGUYEN, T., OSTHUS, R. C. & LI, F. 2006. The c-Myc target gene network. *Semin Cancer Biol*, 16, 253-64.

- DE FRIES, R. & MITSUHASHI, M. 1995. Quantification of mitogen induced human lymphocyte proliferation: comparison of alamarBlue assay to 3H-thymidine incorporation assay. *J Clin Lab Anal*, 9, 89-95.
- DE LEVAL, L., RICKMAN, D. S., THIELEN, C., REYNIES, A., HUANG, Y. L., DELSOL, G., LAMANT, L., LEROY, K., BRIERE, J., MOLINA, T., BERGER, F., GISSELBRECHT, C., XERRI, L. & GAULARD, P. 2007. The gene expression profile of nodal peripheral T-cell lymphoma demonstrates a molecular link between angioimmunoblastic T-cell lymphoma (AITL) and follicular helper T (TFH) cells. *Blood*, 109, 4952-63.
- DE SILVA, N. S. & KLEIN, U. 2015. Dynamics of B cells in germinal centres. *Nat Rev Immunol*, 15, 137-48.
- DE SILVA, N. S., SIMONETTI, G., HEISE, N. & KLEIN, U. 2012. The diverse roles of IRF4 in late germinal center B-cell differentiation. *Immunol Rev*, 247, 73-92.
- DEJEAN, E., RENALIER, M. H., FOISSEAU, M., AGIRRE, X., JOSEPH, N., DE PAIVA, G. R., AL SAATI, T., SOULIER, J., DESJOBERT, C., LAMANT, L., PROSPER, F., FELSHER, D. W., CAVAILLE, J., PRATS, H., DELSOL, G., GIURIATO, S. & MEGGETTO, F. 2011. Hypoxia-microRNA-16 downregulation induces VEGF expression in anaplastic lymphoma kinase (ALK)-positive anaplastic large-cell lymphomas. *Leukemia*, 25, 1882-90.
- DEL PRETE, G. 1992. Human Th1 and Th2 lymphocytes: their role in the pathophysiology of atopy. *Allergy*, 47, 450-5.
- DELMORE, J. E., ISSA, G. C., LEMIEUX, M. E., RAHL, P. B., SHI, J., JACOBS, H. M., KASTRITIS, E., GILPATRICK, T., PARANAL, R. M., QI, J., CHESI, M., SCHINZEL, A. C., MCKEOWN, M. R., HEFFERNAN, T. P., VAKOC, C. R., BERGSAGEL, P. L., GHOBRIAL, I. M., RICHARDSON, P. G., YOUNG, R. A., HAHN, W. C., ANDERSON, K. C., KUNG, A. L., BRADNER, J. E. & MITSIADES, C. S. 2011. BET bromodomain inhibition as a therapeutic strategy to target c-Myc. *Cell*, 146, 904-17.
- DENT, A. L., SHAFFER, A. L., YU, X., ALLMAN, D. & STAUDT, L. M. 1997. Control of inflammation, cytokine expression, and germinal center formation by BCL-6. *Science*, 276, 589-92.
- DHORDAIN, P., ALBAGLI, O., HONORE, N., GUIDEZ, F., LANTOINE, D., SCHMID, M., THE, H. D., ZELENT, A. & KOKEN, M. H. 2000. Colocalization and heteromerization between the two human oncogene POZ/zinc finger proteins, LAZ3 (BCL6) and PLZF. *Oncogene*, 19, 6240-50.
- DHORDAIN, P., ALBAGLI, O., LIN, R. J., ANSIEAU, S., QUIEF, S., LEUTZ, A., KERCKAERT, J. P., EVANS, R. M. & LEPRINCE, D. 1997. Corepressor SMRT binds the BTB/POZ repressing domain of the LAZ3/BCL6 oncoprotein. *Proc Natl Acad Sci U S A*, 94, 10762-7.
- DHORDAIN, P., LIN, R. J., QUIEF, S., LANTOINE, D., KERCKAERT, J. P., EVANS, R. M. & ALBAGLI, O. 1998. The LAZ3(BCL-6) oncoprotein recruits a SMRT/mSIN3A/histone deacetylase containing complex to mediate transcriptional repression. *Nucleic Acids Res*, 26, 4645-51.
- DIB, A., GABREA, A., GLEBOV, O. K., BERGSAGEL, P. L. & KUEHL, W. M. 2008. Characterization of MYC translocations in multiple myeloma cell lines. *J Natl Cancer Inst Monogr*, 25-31.
- DUAN, S., CERMAK, L., PAGAN, J. K., ROSSI, M., MARTINENGO, C., DI CELLE, P. F., CHAPUY, B., SHIPP, M., CHIARLE, R. & PAGANO, M. 2012. FBXO11 targets BCL6 for degradation and is inactivated in diffuse large B-cell lymphomas. *Nature*, 481, 90-3.
- DUDLEY, D. D., CHAUDHURI, J., BASSING, C. H. & ALT, F. W. 2005. Mechanism and control of V(D)J recombination versus class switch recombination: similarities and differences. *Adv Immunol*, 86, 43-112.
- DUY, C., HURTZ, C., SHOJAEI, S., CERCHIETTI, L., GENG, H., SWAMINATHAN, S., KLEMM, L., KWEON, S. M., NAHAR, R., BRAIG, M., PARK, E., KIM, Y. M., HOFMANN, W. K., HERZOG, S., JUMAA, H., KOEFFLER, H. P., YU, J. J., HEISTERKAMP, N., GRAEBER, T. G., WU, H., YE, B. H., MELNICK, A. & MUSCHEN, M. 2011. BCL6 enables Ph+ acute lymphoblastic leukaemia cells to survive BCR-ABL1 kinase inhibition. *Nature*, 473, 384-8.
- EILERS, M. & EISENMAN, R. N. 2008. Myc's broad reach. *Genes Dev*, 22, 2755-66.
- EILERS, M., EISENMAN, R. N. 2008. Myc's broad reach. *Genes Dev*, 22, 2755-66.

- ESCALANTE, C. R., BRASS, A. L., PONGUBALA, J. M., SHATOVA, E., SHEN, L., SINGH, H. & AGGARWAL, A. K. 2002. Crystal structure of PU.1/IRF-4/DNA ternary complex. *Mol Cell*, 10, 1097-105.
- EVANS, S. E., GOULT, B. T., FAIRALL, L., JAMIESON, A. G., KO FERRIGNO, P., FORD, R., SCHWABE, J. W. & WAGNER, S. D. 2014. The ansamycin antibiotic, rifamycin SV, inhibits BCL6 transcriptional repression and forms a complex with the BCL6-BTB/POZ domain. *PLoS One*, 9, e90889.
- FALINI, B., FIZZOTTI, M., PUCCIARINI, A., BIGERNA, B., MARAFIOTI, T., GAMBACORTA, M., PACINI, R., ALUNNI, C., NATALI-TANCI, L., UGOLINI, B., SEBASTIANI, C., CATTORETTI, G., PILERI, S., DALLA-FAVERA, R. & STEIN, H. 2000. A monoclonal antibody (MUM1p) detects expression of the MUM1/IRF4 protein in a subset of germinal center B cells, plasma cells, and activated T cells. *Blood*, 95, 2084-92.
- FALINI, B., PILERI, S., PIZZOLO, G., DURKOP, H., FLENGHI, L., STIRPE, F., MARTELLI, M. F. & STEIN, H. 1995. CD30 (Ki-1) molecule: a new cytokine receptor of the tumor necrosis factor receptor superfamily as a tool for diagnosis and immunotherapy. *Blood*, 85, 1-14.
- FALINI, B., PILERI, S., ZINZANI, P. L., CARBONE, A., ZAGONEL, V., WOLF-PEETERS, C., VERHOEF, G., MENESTRINA, F., TODESCHINI, G., PAULLI, M., LAZZARINO, M., GIARDINI, R., AIELLO, A., FOSS, H. D., ARAUJO, I., FIZZOTTI, M., PELICCI, P. G., FLENGHI, L., MARTELLI, M. F. & SANTUCCI, A. 1999. ALK+ lymphoma: clinico-pathological findings and outcome. *Blood*, 93, 2697-706.
- FAZILLEAU, N., MCHEYZER-WILLIAMS, L. J., ROSEN, H. & MCHEYZER-WILLIAMS, M. G. 2009. The function of follicular helper T cells is regulated by the strength of T cell antigen receptor binding. *Nat Immunol*, 10, 375-84.
- FELDMAN, A. L., DOGAN, A., SMITH, D. I., LAW, M. E., ANSELL, S. M., JOHNSON, S. H., PORCHER, J. C., OZSAN, N., WIEBEN, E. D., ECKLOFF, B. W. & VASMATZIS, G. 2011. Discovery of recurrent t(6;7)(p25.3;q32.3) translocations in ALK-negative anaplastic large cell lymphomas by massively parallel genomic sequencing. *Blood*, 117, 915-9.
- FELDMAN, A. L., LAW, M., REMSTEIN, E. D., MACON, W. R., ERICKSON, L. A., GROGG, K. L., KURTIN, P. J. & DOGAN, A. 2009. Recurrent translocations involving the IRF4 oncogene locus in peripheral T-cell lymphomas. *Leukemia*, 23, 574-80.
- FINLAY, D. K., ROSENZWEIG, E., SINCLAIR, L. V., FEIJOO-CARNERO, C., HUKELMANN, J. L., ROLF, J., PANTELEYEV, A. A., OKKENHAUG, K. & CANTRELL, D. A. 2012. PDK1 regulation of mTOR and hypoxia-inducible factor 1 integrate metabolism and migration of CD8+ T cells. *J Exp Med*, 209, 2441-53.
- FISCHER, P., NACHEVA, E., MASON, D. Y., SHERRINGTON, P. D., HOYLE, C., HAYHOE, F. G. & KARPAS, A. 1988. A Ki-1 (CD30)-positive human cell line (Karpas 299) established from a high-grade non-Hodgkin's lymphoma, showing a 2;5 translocation and rearrangement of the T-cell receptor beta-chain gene. *Blood*, 72, 234-40.
- FOSS, F. M., ZINZANI, P. L., VOSE, J. M., GASCOYNE, R. D., ROSEN, S. T. & TOBINAI, K. 2011. Peripheral T-cell lymphoma. *Blood*, 117, 6756-67.
- FRIBOULET, L., LI, N., KATAYAMA, R., LEE, C. C., GAINOR, J. F., CRYSTAL, A. S., MICHELLYS, P. Y., AWAD, M. M., YANAGITANI, N., KIM, S., PFERDEKAMPER, A. C., LI, J., KASIBHATLA, S., SUN, F., SUN, X., HUA, S., MCNAMARA, P., MAHMOOD, S., LOCKERMAN, E. L., FUJITA, N., NISHIO, M., HARRIS, J. L., SHAW, A. T. & ENGELMAN, J. A. 2014. The ALK inhibitor ceritinib overcomes crizotinib resistance in non-small cell lung cancer. *Cancer Discov*, 4, 662-73.
- FUJITA, N., JAYE, D. L., GEIGERMAN, C., AKYILDIZ, A., MOONEY, M. R., BOSS, J. M. & WADE, P. A. 2004. MTA3 and the Mi-2/NuRD complex regulate cell fate during B lymphocyte differentiation. *Cell*, 119, 75-86.
- FUJIWARA, S. I., YAMASHITA, Y., NAKAMURA, N., CHOI, Y. L., UENO, T., WATANABE, H., KURASHINA, K., SODA, M., ENOMOTO, M., HATANAKA, H., TAKADA, S., ABE, M., OZAWA, K. & MANO, H. 2008. High-resolution analysis of chromosome copy number

- alterations in angioimmunoblastic T-cell lymphoma and peripheral T-cell lymphoma, unspecified, with single nucleotide polymorphism-typing microarrays. *Leukemia*, 22, 1891-8.
- GAMBACORTI-PASSERINI, C., MESSA, C. & POGLIANI, E. M. 2011. Crizotinib in anaplastic large-cell lymphoma. *N Engl J Med*, 364, 775-6.
- GANDHI, A. K., KANG, J., HAVENS, C. G., CONKLIN, T., NING, Y., WU, L., ITO, T., ANDO, H., WALDMAN, M. F., THAKURTA, A., KLIPPEL, A., HANDA, H., DANIEL, T. O., SCHAFER, P. H. & CHOPRA, R. 2014. Immunomodulatory agents lenalidomide and pomalidomide co-stimulate T cells by inducing degradation of T cell repressors Ikaros and Aiolos via modulation of the E3 ubiquitin ligase complex CRL4(CRBN.). *Br J Haematol*, 164, 811-21.
- GARCIA, J. F., RONCADOR, G., SANZ, A. I., MAESTRE, L., LUCAS, E., MONTES-MORENO, S., FERNANDEZ VICTORIA, R., MARTINEZ-TORRECUADRARA, J. L., MARAFIOTI, T., MASON, D. Y. & PIRIS, M. A. 2006. PRDM1/BLIMP-1 expression in multiple B and T-cell lymphoma. *Haematologica*, 91, 467-74.
- GASCOYNE, R. D., AOUN, P., WU, D., CHHANABHAI, M., SKINNIDER, B. F., GREINER, T. C., MORRIS, S. W., CONNORS, J. M., VOSE, J. M., VISWANATHA, D. S., COLDMAN, A. & WEISENBURGER, D. D. 1999. Prognostic significance of anaplastic lymphoma kinase (ALK) protein expression in adults with anaplastic large cell lymphoma. *Blood*, 93, 3913-21.
- GEARHART, M. D., CORCORAN, C. M., WAMSTAD, J. A. & BARDWELL, V. J. 2006. Polycomb group and SCF ubiquitin ligases are found in a novel BCOR complex that is recruited to BCL6 targets. *Mol Cell Biol*, 26, 6880-9.
- GEBHARDT, T., WAKIM, L. M., EIDSMO, L., READING, P. C., HEATH, W. R. & CARBONE, F. R. 2009. Memory T cells in nonlymphoid tissue that provide enhanced local immunity during infection with herpes simplex virus. *Nat Immunol*, 10, 524-30.
- GERBER, D. E. & MINNA, J. D. 2010. ALK inhibition for non-small cell lung cancer: from discovery to therapy in record time. *Cancer Cell*, 18, 548-51.
- GHETU, A. F., CORCORAN, C. M., CERCHIETTI, L., BARDWELL, V. J., MELNICK, A. & PRIVE, G. G. 2008. Structure of a BCOR corepressor peptide in complex with the BCL6 BTB domain dimer. *Mol Cell*, 29, 384-91.
- GODFREY, D. I. & ZLOTNIK, A. 1993. Control points in early T-cell development. *Immunol Today*, 14, 547-53.
- GONG, D. & MALEK, T. R. 2007. Cytokine-dependent Blimp-1 expression in activated T cells inhibits IL-2 production. *J Immunol*, 178, 242-52.
- GROGG, K. L., MORICE, W. G. & MACON, W. R. 2007. Spectrum of bone marrow findings in patients with angioimmunoblastic T-cell lymphoma. *Br J Haematol*, 137, 416-22.
- GRUMONT, R. J. & GERONDAKIS, S. 2000. Rel induces interferon regulatory factor 4 (IRF-4) expression in lymphocytes: modulation of interferon-regulated gene expression by rel/nuclear factor kappaB. *J Exp Med*, 191, 1281-92.
- GUPTA, S., JIANG, M., ANTHONY, A. & PERNIS, A. B. 1999. Lineage-specific modulation of interleukin 4 signaling by interferon regulatory factor 4. *J Exp Med*, 190, 1837-48.
- GYORY, I., FEJER, G., GHOSH, N., SETO, E. & WRIGHT, K. L. 2003. Identification of a functionally impaired positive regulatory domain I binding factor 1 transcription repressor in myeloma cell lines. *J Immunol*, 170, 3125-33.
- HALE, J. S. & AHMED, R. 2015. Memory T follicular helper CD4 T cells. *Front Immunol*, 6, 16.
- HALE, J. S., YOUNGBLOOD, B., LATNER, D. R., MOHAMMED, A. U., YE, L., AKONDY, R. S., WU, T., IYER, S. S. & AHMED, R. 2013. Distinct memory CD4+ T cells with commitment to T follicular helper- and T helper 1-cell lineages are generated after acute viral infection. *Immunity*, 38, 805-17.
- HALLBERG, B. & PALMER, R. H. 2013. Mechanistic insight into ALK receptor tyrosine kinase in human cancer biology. *Nat Rev Cancer*, 13, 685-700.
- HANAHAHAN, D. & WEINBERG, R. A. 2000. The hallmarks of cancer. *Cell*, 100, 57-70.

- HARLOW, E. & LANE, D. 2006. Lysing tissue-culture cells for immunoprecipitation. *CSH Protoc*, 2006.
- HARTMANN, E. M., OTT, G. & ROSENWALD, A. 2008. Molecular biology and genetics of lymphomas. *Hematol Oncol Clin North Am*, 22, 807-23, vii.
- HARTY, J. T. & BADOVINAC, V. P. 2008. Shaping and reshaping CD8+ T-cell memory. *Nat Rev Immunol*, 8, 107-19.
- HATZI, K., NANCE, J. P., KROENKE, M. A., BOTHWELL, M., HADDAD, E. K., MELNICK, A. & CROTTY, S. 2015. BCL6 orchestrates Tfh cell differentiation via multiple distinct mechanisms. *J Exp Med*, 212, 539-53.
- HAVELANGE, V., PEKARSKY, Y., NAKAMURA, T., PALAMARCHUK, A., ALDER, H., RASSENTI, L., KIPPS, T. & CROCE, C. M. 2011. IRF4 mutations in chronic lymphocytic leukemia. *Blood*, 118, 2827-9.
- HEASMAN, S. J., CARLIN, L. M., COX, S., NG, T. & RIDLEY, A. J. 2010. Coordinated RhoA signaling at the leading edge and uropod is required for T cell transendothelial migration. *J Cell Biol*, 190, 553-63.
- HERMAN, S. E., GORDON, A. L., HERTLEIN, E., RAMANUNNI, A., ZHANG, X., JAGLOWSKI, S., FLYNN, J., JONES, J., BLUM, K. A., BUGGY, J. J., HAMDY, A., JOHNSON, A. J. & BYRD, J. C. 2011. Bruton tyrosine kinase represents a promising therapeutic target for treatment of chronic lymphocytic leukemia and is effectively targeted by PCI-32765. *Blood*, 117, 6287-96.
- HERMANN-KLEITER, N. & BAIER, G. 2010. NFAT pulls the strings during CD4+ T helper cell effector functions. *Blood*, 115, 2989-97.
- HERNANDEZ, L., PINYOL, M., HERNANDEZ, S., BEA, S., PULFORD, K., ROSENWALD, A., LAMANT, L., FALINI, B., OTT, G., MASON, D. Y., DELSOL, G. & CAMPO, E. 1999. TRK-fused gene (TFG) is a new partner of ALK in anaplastic large cell lymphoma producing two structurally different TFG-ALK translocations. *Blood*, 94, 3265-8.
- HIKONO, H., KOHLMEIER, J. E., TAKAMURA, S., WITTMER, S. T., ROBERTS, A. D. & WOODLAND, D. L. 2007. Activation phenotype, rather than central- or effector-memory phenotype, predicts the recall efficacy of memory CD8+ T cells. *J Exp Med*, 204, 1625-36.
- HILDNER, K., EDELSON, B. T., PURTHA, W. E., DIAMOND, M., MATSUSHITA, H., KOHYAMA, M., CALDERON, B., SCHRAML, B. U., UNANUE, E. R., DIAMOND, M. S., SCHREIBER, R. D., MURPHY, T. L. & MURPHY, K. M. 2008. Batf3 deficiency reveals a critical role for CD8alpha+ dendritic cells in cytotoxic T cell immunity. *Science*, 322, 1097-100.
- HONMA, K., KIMURA, D., TOMINAGA, N., MIYAKODA, M., MATSUYAMA, T. & YUI, K. 2008. Interferon regulatory factor 4 differentially regulates the production of Th2 cytokines in naive vs. effector/memory CD4+ T cells. *Proc Natl Acad Sci U S A*, 105, 15890-5.
- HUANG, C., GENG, H., BOSS, I., WANG, L. & MELNICK, A. 2013a. Cooperative transcriptional repression by BCL6 and BACH2 in germinal center B-cell differentiation. *Blood*.
- HUANG, C., GONZALEZ, D. G., COTE, C. M., JIANG, Y., HATZI, K., TEATER, M., DAI, K., HLA, T., HABERMAN, A. M. & MELNICK, A. 2014. The BCL6 RD2 Domain Governs Commitment of Activated B Cells to Form Germinal Centers. *Cell Rep*.
- HUANG, C., HATZI, K. & MELNICK, A. 2013b. Lineage-specific functions of Bcl-6 in immunity and inflammation are mediated by distinct biochemical mechanisms. *Nat Immunol*, 14, 380-8.
- HUANG, S., SHAO, G. & LIU, L. 1998. The PR domain of the Rb-binding zinc finger protein RIZ1 is a protein binding interface and is related to the SET domain functioning in chromatin-mediated gene expression. *J Biol Chem*, 273, 15933-9.
- HUBER, M., BRUSTLE, A., REINHARD, K., GURALNIK, A., WALTER, G., MAHINY, A., VON LOW, E. & LOHOFF, M. 2008. IRF4 is essential for IL-21-mediated induction, amplification, and stabilization of the Th17 phenotype. *Proc Natl Acad Sci U S A*, 105, 20846-51.
- HUBER, M. & LOHOFF, M. 2014. IRF4 at the crossroads of effector T-cell fate decision. *Eur J Immunol*, 44, 1886-95.

- HURTZ, C., HATZI, K., CERCHIETTI, L., BRAIG, M., PARK, E., KIM, Y. M., HERZOG, S., RAMEZANI-RAD, P., JUMAA, H., MULLER, M. C., HOFMANN, W. K., HOCHHAUS, A., YE, B. H., AGARWAL, A., DRUKER, B. J., SHAH, N. P., MELNICK, A. M. & MUSCHEN, M. 2011. BCL6-mediated repression of p53 is critical for leukemia stem cell survival in chronic myeloid leukemia. *J Exp Med*, 208, 2163-74.
- HUYNH, K. D., FISCHLE, W., VERDIN, E. & BARDWELL, V. J. 2000. BCoR, a novel corepressor involved in BCL-6 repression. *Genes Dev*, 14, 1810-23.
- ICHII, H., SAKAMOTO, A., HATANO, M., OKADA, S., TOYAMA, H., TAKI, S., ARIMA, M., KURODA, Y. & TOKUHISA, T. 2002. Role for Bcl-6 in the generation and maintenance of memory CD8+ T cells. *Nat Immunol*, 3, 558-63.
- ICHII, H., SAKAMOTO, A., KURODA, Y. & TOKUHISA, T. 2004. Bcl6 acts as an amplifier for the generation and proliferative capacity of central memory CD8+ T cells. *J Immunol*, 173, 883-91.
- IIDA, S., RAO, P. H., BUTLER, M., CORRADINI, P., BOCCADORO, M., KLEIN, B., CHAGANTI, R. S. & DALLA-FAVERA, R. 1997. Deregulation of MUM1/IRF4 by chromosomal translocation in multiple myeloma. *Nat Genet*, 17, 226-30.
- INGHIRAMI, G., CHAN, W. C. & PILERI, S. 2015. Peripheral T-cell and NK cell lymphoproliferative disorders: cell of origin, clinical and pathological implications. *Immunol Rev*, 263, 124-59.
- INLAY, M., ALT, F. W., BALTIMORE, D. & XU, Y. 2002. Essential roles of the kappa light chain intronic enhancer and 3' enhancer in kappa rearrangement and demethylation. *Nat Immunol*, 3, 463-8.
- INTLEKOFER, A. M., TAKEMOTO, N., KAO, C., BANERJEE, A., SCHAMBACH, F., NORTHROP, J. K., SHEN, H., WHERRY, E. J. & REINER, S. L. 2007. Requirement for T-bet in the aberrant differentiation of unhelped memory CD8+ T cells. *J Exp Med*, 204, 2015-21.
- IQBAL, J., KUCUK, C., DELEEUW, R. J., SRIVASTAVA, G., TAM, W., GENG, H., KLINKEBIEL, D., CHRISTMAN, J. K., PATEL, K., CAO, K., SHEN, L., DYBKAER, K., TSUI, I. F., ALI, H., SHIMIZU, N., AU, W. Y., LAM, W. L. & CHAN, W. C. 2009. Genomic analyses reveal global functional alterations that promote tumor growth and novel tumor suppressor genes in natural killer-cell malignancies. *Leukemia*, 23, 1139-51.
- IQBAL, J., WEISENBURGER, D. D., GREINER, T. C., VOSE, J. M., MCKEITHAN, T., KUCUK, C., GENG, H., DEFFENBACHER, K., SMITH, L., DYBKAER, K., NAKAMURA, S., SETO, M., DELABIE, J., BERGER, F., LOONG, F., AU, W. Y., KO, Y. H., SNG, I., ARMITAGE, J. O. & CHAN, W. C. 2010. Molecular signatures to improve diagnosis in peripheral T-cell lymphoma and prognostication in angioimmunoblastic T-cell lymphoma. *Blood*, 115, 1026-36.
- IQBAL, J., WRIGHT, G., WANG, C., ROSENWALD, A., GASCOYNE, R. D., WEISENBURGER, D. D., GREINER, T. C., SMITH, L., GUO, S., WILCOX, R. A., TEH, B. T., LIM, S. T., TAN, S. Y., RIMSZA, L. M., JAFFE, E. S., CAMPO, E., MARTINEZ, A., DELABIE, J., BRAZIEL, R. M., COOK, J. R., TUBBS, R. R., OTT, G., GEISSINGER, E., GAULARD, P., PICCALUGA, P. P., PILERI, S. A., AU, W. Y., NAKAMURA, S., SETO, M., BERGER, F., DE LEVAL, L., CONNORS, J. M., ARMITAGE, J., VOSE, J., CHAN, W. C. & STAUDT, L. M. 2014. Gene expression signatures delineate biological and prognostic subgroups in peripheral T-cell lymphoma. *Blood*, 123, 2915-23.
- ISE, W., KOHYAMA, M., SCHRAML, B. U., ZHANG, T., SCHWER, B., BASU, U., ALT, F. W., TANG, J., OLTZ, E. M., MURPHY, T. L. & MURPHY, K. M. 2011. The transcription factor BATF controls the global regulators of class-switch recombination in both B cells and T cells. *Nat Immunol*, 12, 536-43.
- IVANOV, II, MCKENZIE, B. S., ZHOU, L., TADOKORO, C. E., LEPELLEY, A., LAFAILLE, J. J., CUA, D. J. & LITTMAN, D. R. 2006. The orphan nuclear receptor ROR $\gamma$  directs the differentiation program of proinflammatory IL-17+ T helper cells. *Cell*, 126, 1121-33.

- IWAHARA, T., FUJIMOTO, J., WEN, D., CUPPLES, R., BUCAY, N., ARAKAWA, T., MORI, S., RATZKIN, B. & YAMAMOTO, T. 1997. Molecular characterization of ALK, a receptor tyrosine kinase expressed specifically in the nervous system. *Oncogene*, 14, 439-49.
- JABEEN, R., GOSWAMI, R., AWE, O., KULKARNI, A., NGUYEN, E. T., ATTENASIO, A., WALSH, D., OLSON, M. R., KIM, M. H., TEPPER, R. S., SUN, J., KIM, C. H., TAPAROWSKY, E. J., ZHOU, B. & KAPLAN, M. H. 2013. Th9 cell development requires a BATF-regulated transcriptional network. *J Clin Invest*, 123, 4641-53.
- JO, S. H., SCHATZ, J. H., ACQUAVIVA, J., SINGH, H. & REN, R. 2010. Cooperation between deficiencies of IRF-4 and IRF-8 promotes both myeloid and lymphoid tumorigenesis. *Blood*, 116, 2759-67.
- JOHNSON, K., HASHIMSHONY, T., SAWAI, C. M., PONGUBALA, J. M., SKOK, J. A., AIFANTIS, I. & SINGH, H. 2008. Regulation of immunoglobulin light-chain recombination by the transcription factor IRF-4 and the attenuation of interleukin-7 signaling. *Immunity*, 28, 335-45.
- JOHNSTON, R. J., POHOLEK, A. C., DITORO, D., YUSUF, I., ETO, D., BARNETT, B., DENT, A. L., CRAFT, J. & CROTTY, S. 2009. Bcl6 and Blimp-1 are reciprocal and antagonistic regulators of T follicular helper cell differentiation. *Science*, 325, 1006-10.
- JUTEL, M. & AKDIS, C. A. 2008. T-cell regulatory mechanisms in specific immunotherapy. *Chem Immunol Allergy*, 94, 158-77.
- KAECH, S. M. & WHERRY, E. J. 2007. Heterogeneity and cell-fate decisions in effector and memory CD8+ T cell differentiation during viral infection. *Immunity*, 27, 393-405.
- KALAANY, N. Y. & SABATINI, D. M. 2009. Tumours with PI3K activation are resistant to dietary restriction. *Nature*, 458, 725-31.
- KALLIES, A., HASBOLD, J., TARLINTON, D. M., DIETRICH, W., CORCORAN, L. M., HODGKIN, P. D. & NUTT, S. L. 2004. Plasma cell ontogeny defined by quantitative changes in blimp-1 expression. *J Exp Med*, 200, 967-77.
- KALLIES, A., HAWKINS, E. D., BELZ, G. T., METCALF, D., HOMMEL, M., CORCORAN, L. M., HODGKIN, P. D. & NUTT, S. L. 2006. Transcriptional repressor Blimp-1 is essential for T cell homeostasis and self-tolerance. *Nat Immunol*, 7, 466-74.
- KALLIES, A., XIN, A., BELZ, G. T. & NUTT, S. L. 2009. Blimp-1 transcription factor is required for the differentiation of effector CD8(+) T cells and memory responses. *Immunity*, 31, 283-95.
- KARAI, L. J., KADIN, M. E., HSI, E. D., SLUZEVICH, J. C., KETTERLING, R. P., KNUDSON, R. A. & FELDMAN, A. L. 2013. Chromosomal rearrangements of 6p25.3 define a new subtype of lymphomatoid papulosis. *Am J Surg Pathol*, 37, 1173-81.
- KARUBE, K., NAKAGAWA, M., TSUZUKI, S., TAKEUCHI, I., HONMA, K., NAKASHIMA, Y., SHIMIZU, N., KO, Y. H., MORISHIMA, Y., OHSHIMA, K., NAKAMURA, S. & SETO, M. 2011. Identification of FOXO3 and PRDM1 as tumor-suppressor gene candidates in NK-cell neoplasms by genomic and functional analyses. *Blood*, 118, 3195-204.
- KATAOKA, K., NAGATA, Y., KITANAKA, A., TOTOKI, Y., JUN-ICHIROU, Y., KOTANI, S., SATO-OTSUBO, A., SANADA, M., SHIRAISHI, Y., SHIMAMURA, T., CHIBA, K., TANAKA, H., SUZUKI, H., SATO, Y., SHIOZAWA, Y., YOSHIZATO, T., KON, A., YOSHIDA, K., HISHIZAWA, M., MUNAKATA, W., NAKAMURA, H., HAMA, N., SHIDE, K., KUBUKI, Y., HIDAKA, T., KAMEDA, T., ISHIYAMA, K., MIYAWAKE, S., ISHII, R., NUREKI, O., NAGAE, G., ABURATANI, H., MIYANO, S., TAKAORI-KONDO, A., WATANABE, T., MATSUOKA, M., SHIBATA, T., SHIMODA, K. 2014. Landscape of Genetic Alterations in Adult T-cell Leukemia/Lymphoma. *ASH 2014*.
- KELLER, A. D. & MANIATIS, T. 1992. Only two of the five zinc fingers of the eukaryotic transcriptional repressor PRDI-BF1 are required for sequence-specific DNA binding. *Mol Cell Biol*, 12, 1940-9.
- KERL, K., VONLANTHEN, R., NAGY, M., BOLZONELLO, N. J., GINDRE, P., HURWITZ, N., GUDAT, F., NADOR, R. G. & BORISCH, B. 2001. Alterations on the 5' noncoding region of the

- BCL-6 gene are not correlated with BCL-6 protein expression in T cell non-Hodgkin lymphomas. *Lab Invest*, 81, 1693-702.
- KHOORY, J. D., MEDEIROS, L. J., RASSIDAKIS, G. Z., YARED, M. A., TSIOLI, P., LEVENTAKI, V., SCHMITT-GRAEFF, A., HERLING, M., AMIN, H. M. & LAI, R. 2003. Differential expression and clinical significance of tyrosine-phosphorylated STAT3 in ALK+ and ALK- anaplastic large cell lymphoma. *Clin Cancer Res*, 9, 3692-9.
- KIKUCHI, M., MIKI, T., KUMAGAI, T., FUKUDA, T., KAMIYAMA, R., MIYASAKA, N. & HIROSAWA, S. 2000. Identification of negative regulatory regions within the first exon and intron of the BCL6 gene. *Oncogene*, 19, 4941-5.
- KINNEY, M. C., HIGGINS, R. A. & MEDINA, E. A. 2011. Anaplastic large cell lymphoma: twenty-five years of discovery. *Arch Pathol Lab Med*, 135, 19-43.
- KLEIN, U., CASOLA, S., CATTORETTI, G., SHEN, Q., LIA, M., MO, T., LUDWIG, T., RAJEWSKY, K. & DALLA-FAVERA, R. 2006. Transcription factor IRF4 controls plasma cell differentiation and class-switch recombination. *Nat Immunol*, 7, 773-82.
- KRONKE, J., UDESHI, N. D., NARLA, A., GRAUMAN, P., HURST, S. N., MCCONKEY, M., SVINKINA, T., HECKL, D., COMER, E., LI, X., CIARLO, C., HARTMAN, E., MUNSHI, N., SCHENONE, M., SCHREIBER, S. L., CARR, S. A. & EBERT, B. L. 2014. Lenalidomide causes selective degradation of IKZF1 and IKZF3 in multiple myeloma cells. *Science*, 343, 301-5.
- KUCUK, C., JIANG, B., HU, X., ZHANG, W., CHAN, J. K., XIAO, W., LACK, N., ALKAN, C., WILLIAMS, J. C., AVERY, K. N., KAVAK, P., SCUTO, A., SEN, E., GAULARD, P., STAUDT, L., IQBAL, J., ZHANG, W., CORNISH, A., GONG, Q., YANG, Q., SUN, H., D'AMORE, F., LEPPA, S., LIU, W., FU, K., DE LEVAL, L., MCKEITHAN, T. & CHAN, W. C. 2015. Activating mutations of STAT5B and STAT3 in lymphomas derived from gammadelta-T or NK cells. *Nat Commun*, 6, 6025.
- KUKITA, T., ARIMA, N., MATSUSHITA, K., ARIMURA, K., OHTSUBO, H., SAKAKI, Y., FUJIWARA, H., OZAKI, A., MATSUMOTO, T. & TEI, C. 2002. Autocrine and/or paracrine growth of adult T-cell leukaemia tumour cells by interleukin 15. *Br J Haematol*, 119, 467-74.
- KUPPERS, R., ENGERT, A. & HANSMANN, M. L. 2012. Hodgkin lymphoma. *J Clin Invest*, 122, 3439-47.
- KWAK, E. L., BANG, Y. J., CAMIDGE, D. R., SHAW, A. T., SOLOMON, B., MAKI, R. G., OU, S. H., DEZUBE, B. J., JANNE, P. A., COSTA, D. B., VARELLA-GARCIA, M., KIM, W. H., LYNCH, T. J., FIDIAS, P., STUBBS, H., ENGELMAN, J. A., SEQUIST, L. V., TAN, W., GANDHI, L., MINO-KENUDSON, M., WEI, G. C., SHREEVE, S. M., RATAIN, M. J., SETTLEMAN, J., CHRISTENSEN, J. G., HABER, D. A., WILNER, K., SALGIA, R., SHAPIRO, G. I., CLARK, J. W. & IAFRATE, A. J. 2010. Anaplastic lymphoma kinase inhibition in non-small-cell lung cancer. *N Engl J Med*, 363, 1693-703.
- KWON, H., THIERRY-MIEG, D., THIERRY-MIEG, J., KIM, H. P., OH, J., TUNYAPLIN, C., CAROTTA, S., DONOVAN, C. E., GOLDMAN, M. L., TAILOR, P., OZATO, K., LEVY, D. E., NUTT, S. L., CALAME, K. & LEONARD, W. J. 2009. Analysis of interleukin-21-induced Prdm1 gene regulation reveals functional cooperation of STAT3 and IRF4 transcription factors. *Immunity*, 31, 941-52.
- KWON, M. & FIRESTEIN, B. L. 2013. DNA transfection: calcium phosphate method. *Methods Mol Biol*, 1018, 107-10.
- LAMANT, L., DASTUGUE, N., PULFORD, K., DELSOL, G. & MARIAME, B. 1999. A new fusion gene TPM3-ALK in anaplastic large cell lymphoma created by a (1;2)(q25;p23) translocation. *Blood*, 93, 3088-95.
- LAMANT, L., DE REYNIES, A., DUPLANTIER, M. M., RICKMAN, D. S., SABOURDY, F., GIURIATO, S., BRUGIERES, L., GAULARD, P., ESPINOS, E. & DELSOL, G. 2007. Gene-expression profiling of systemic anaplastic large-cell lymphoma reveals differences based on ALK status and two distinct morphologic ALK+ subtypes. *Blood*, 109, 2156-64.
- LAMANT, L., GASCOYNE, R. D., DUPLANTIER, M. M., ARMSTRONG, F., RAGHAB, A., CHHANABHAI, M., RAJCAN-SEPAROVIC, E., RAGHAB, J., DELSOL, G. & ESPINOS, E. 2003.

- Non-muscle myosin heavy chain (MYH9): a new partner fused to ALK in anaplastic large cell lymphoma. *Genes Chromosomes Cancer*, 37, 427-32.
- LAWRIE, C. H. 2013. MicroRNAs and lymphomagenesis: a functional review. *Br J Haematol*, 160, 571-81.
- LEAVY, O. 2014. Signalling: BCL-6 curbs glycolysis. *Nat Rev Immunol*, 14, 650-1.
- LECHNER, M. G., MEGIEL, C., CHURCH, C. H., ANGELL, T. E., RUSSELL, S. M., SEVELL, R. B., JANG, J. K., BRODY, G. S. & EPSTEIN, A. L. 2012. Survival signals and targets for therapy in breast implant-associated ALK--anaplastic large cell lymphoma. *Clin Cancer Res*, 18, 4549-59.
- LEHNER, B., SANDNER, B., MARSCHALLINGER, J., LEHNER, C., FURTNER, T., COUILLARD-DESPRES, S., RIVERA, F. J., BROCKHOFF, G., BAUER, H. C., WEIDNER, N. & AIGNER, L. 2011. The dark side of BrdU in neural stem cell biology: detrimental effects on cell cycle, differentiation and survival. *Cell Tissue Res*, 345, 313-28.
- LENZ, G., DAVIS, R. E., NGO, V. N., LAM, L., GEORGE, T. C., WRIGHT, G. W., DAVE, S. S., ZHAO, H., XU, W., ROSENWALD, A., OTT, G., MULLER-HERMELINK, H. K., GASCOYNE, R. D., CONNORS, J. M., RIMSZA, L. M., CAMPO, E., JAFFE, E. S., DELABIE, J., SMELAND, E. B., FISHER, R. I., CHAN, W. C. & STAUDT, L. M. 2008a. Oncogenic CARD11 mutations in human diffuse large B cell lymphoma. *Science*, 319, 1676-9.
- LENZ, G., WRIGHT, G. W., EMRE, N. C., KOHLHAMMER, H., DAVE, S. S., DAVIS, R. E., CARTY, S., LAM, L. T., SHAFFER, A. L., XIAO, W., POWELL, J., ROSENWALD, A., OTT, G., MULLER-HERMELINK, H. K., GASCOYNE, R. D., CONNORS, J. M., CAMPO, E., JAFFE, E. S., DELABIE, J., SMELAND, E. B., RIMSZA, L. M., FISHER, R. I., WEISENBURGER, D. D., CHAN, W. C. & STAUDT, L. M. 2008b. Molecular subtypes of diffuse large B-cell lymphoma arise by distinct genetic pathways. *Proc Natl Acad Sci U S A*, 105, 13520-5.
- LEPRETRE, S., BUCHONNET, G., STAMATOULLAS, A., LENAIN, P., DUVAL, C., D'ANJOU, J., CALLAT, M. P., TILLY, H. & BASTARD, C. 2000. Chromosome abnormalities in peripheral T-cell lymphoma. *Cancer Genet Cytogenet*, 117, 71-9.
- LI, P., SPOLSKI, R., LIAO, W., WANG, L., MURPHY, T. L., MURPHY, K. M. & LEONARD, W. J. 2012. BATF-JUN is critical for IRF4-mediated transcription in T cells. *Nature*, 490, 543-6.
- LI, S., PAL, R., MONAGHAN, S. A., SCHAFFER, P., OUYANG, H., MAPARA, M., GALSON, D. L. & LENTZSCH, S. 2011. IMiD immunomodulatory compounds block C/EBP{beta} translation through eIF4E down-regulation resulting in inhibition of MM. *Blood*, 117, 5157-65.
- LIANG, X., BRANCHFORD, B., GREFFE, B., MCGAVRAN, L., CARSTENS, B., MELTESEN, L., ALBANO, E. A., QUINONES, R., COOK, B. & GRAHAM, D. K. 2013. Dual ALK and MYC rearrangements leading to an aggressive variant of anaplastic large cell lymphoma. *J Pediatr Hematol Oncol*, 35, e209-13.
- LIN, L., GERTH, A. J. & PENG, S. L. 2004. Active inhibition of plasma cell development in resting B cells by microphthalmia-associated transcription factor. *J Exp Med*, 200, 115-22.
- LIN, Y., WONG, K. & CALAME, K. 1997. Repression of c-myc transcription by Blimp-1, an inducer of terminal B cell differentiation. *Science*, 276, 596-9.
- LIU, C., IQBAL, J., TERUYA-FELDSTEIN, J., SHEN, Y., DABROWSKA, M. J., DYBKAER, K., LIM, M. S., PIVA, R., BARRECA, A., PELLEGRINO, E., SPACCAROTELLA, E., LACHEL, C. M., KUCUK, C., JIANG, C. S., HU, X., BHAGAVATHI, S., GREINER, T. C., WEISENBURGER, D. D., AOUN, P., PERKINS, S. L., MCKEITHAN, T. W., INGHIRAMI, G. & CHAN, W. C. 2013. MicroRNA expression profiling identifies molecular signatures associated with anaplastic large cell lymphoma. *Blood*, 122, 2083-92.
- LIU, Y., HERNANDEZ, A. M., SHIBATA, D. & CORTOPASSI, G. A. 1994. BCL2 translocation frequency rises with age in humans. *Proc Natl Acad Sci U S A*, 91, 8910-4.
- LIVAK, K. J. & SCHMITTGEN, T. D. 2001. Analysis of relative gene expression data using real-time quantitative PCR and the 2(-Delta Delta C(T)) Method. *Methods*, 25, 402-8.
- LOHOFF, M., MITTRUCKER, H. W., PRECHTL, S., BISCHOF, S., SOMMER, F., KOCK, S., FERRICK, D. A., DUNCAN, G. S., GESSNER, A. & MAK, T. W. 2002. Dysregulated T helper cell

- differentiation in the absence of interferon regulatory factor 4. *Proc Natl Acad Sci U S A*, 99, 11808-12.
- LOPEZ-GIRONA, A., HEINTEL, D., ZHANG, L. H., MENDY, D., GAIDAROVA, S., BRADY, H., BARTLETT, J. B., SCHAFER, P. H., SCHREDER, M., BOLOMSKY, A., HILGARTH, B., ZOJER, N., GISSLINGER, H., LUDWIG, H., DANIEL, T., JAGER, U. & CHOPRA, R. 2011. Lenalidomide downregulates the cell survival factor, interferon regulatory factor-4, providing a potential mechanistic link for predicting response. *Br J Haematol*, 154, 325-36.
- LOVISA, F., COZZA, G., CRISTIANI, A., CUZZOLIN, A., ALBIERO, A., MUSSOLIN, L., PILLON, M., MORO, S., BASSO, G., ROSOLEN, A. & BONVINI, P. 2015. ALK Kinase Domain Mutations in Primary Anaplastic Large Cell Lymphoma: Consequences on NPM-ALK Activity and Sensitivity to Tyrosine Kinase Inhibitors. *PLoS One*, 10, e0121378.
- LU, R., MEDINA, K. L., LANCKI, D. W. & SINGH, H. 2003. IRF-4,8 orchestrate the pre-B-to-B transition in lymphocyte development. *Genes Dev*, 17, 1703-8.
- LUCKHEERAM, R. V., ZHOU, R., VERMA, A.D., XIA, B. 2012. CD4<sup>+</sup> T Cells: Differentiation and Functions. *Clinical and Developmental Immunology*, 2012.
- LUGO-VILLARINO, G., MALDONADO-LOPEZ, R., POSSEMATO, R., PENARANDA, C. & GLIMCHER, L. H. 2003. T-bet is required for optimal production of IFN-gamma and antigen-specific T cell activation by dendritic cells. *Proc Natl Acad Sci U S A*, 100, 7749-54.
- LUTHJE, K., KALLIES, A., SHIMOHAKAMADA, Y., BELZ, G. T., LIGHT, A., TARLINTON, D. M. & NUTT, S. L. 2012. The development and fate of follicular helper T cells defined by an IL-21 reporter mouse. *Nat Immunol*, 13, 491-8.
- MA, S., PATHAK, S., TRINH, L. & LU, R. 2008. Interferon regulatory factors 4 and 8 induce the expression of Ikaros and Aiolos to down-regulate pre-B-cell receptor and promote cell-cycle withdrawal in pre-B-cell development. *Blood*, 111, 1396-403.
- MA, Z., COOLS, J., MARYNEN, P., CUI, X., SIEBERT, R., GESK, S., SCHLEGELBERGER, B., PEETERS, B., DE WOLF-PEETERS, C., WLODARSKA, I. & MORRIS, S. W. 2000. Inv(2)(p23q35) in anaplastic large-cell lymphoma induces constitutive anaplastic lymphoma kinase (ALK) tyrosine kinase activation by fusion to ATIC, an enzyme involved in purine nucleotide biosynthesis. *Blood*, 95, 2144-9.
- MAMANE, Y., GRANDVAUX, N., HERNANDEZ, E., SHARMA, S., INNOCENTE, S. A., LEE, J. M., AZIMI, N., LIN, R. & HISCOTT, J. 2002. Repression of IRF-4 target genes in human T cell leukemia virus-1 infection. *Oncogene*, 21, 6751-65.
- MAMANE, Y., LOIGNON, M., PALMER, J., HERNANDEZ, E., CESAIRE, R., ALAOUI-JAMALI, M. & HISCOTT, J. 2005. Repression of DNA repair mechanisms in IRF-4-expressing and HTLV-I-infected T lymphocytes. *J Interferon Cytokine Res*, 25, 43-51.
- MAN, K. & KALLIES, A. 2014. Bcl-6 gets T cells off the sugar. *Nat Immunol*, 15, 904-5.
- MAN, K., MIASARI, M., SHI, W., XIN, A., HENSTRIDGE, D. C., PRESTON, S., PELLEGRINI, M., BELZ, G. T., SMYTH, G. K., FEBBRAIO, M. A., NUTT, S. L. & KALLIES, A. 2013. The transcription factor IRF4 is essential for TCR affinity-mediated metabolic programming and clonal expansion of T cells. *Nat Immunol*, 14, 1155-65.
- MANDELBAUM, J., BHAGAT, G., TANG, H., MO, T., BRAHMACHARY, M., SHEN, Q., CHADBURN, A., RAJEWSKY, K., TARAKHOVSKY, A., PASQUALUCCI, L. & DALLA-FAVERA, R. 2010. BLIMP1 is a tumor suppressor gene frequently disrupted in activated B cell-like diffuse large B cell lymphoma. *Cancer Cell*, 18, 568-79.
- MANSO, R., RODRIGUEZ-PINILLA, S. M., GONZALEZ-RINCON, J., GOMEZ, S., MONSALVO, S., LLAMAS, P., ROJO, F., PEREZ-CALLEJO, D., CERECEDA, L., LIMERES, M. A., MAESO, C., FERRANDO, L., PEREZ-SEOANE, C., RODRIGUEZ, G., ARRINDA, J. M., GARCIA-BRAGADO, F., FRANCO, R., RODRIGUEZ-PERALTO, J. L., GONZALEZ-CARRERO, J., MARTIN-DAVILA, F., PIRIS, M. A. & SANCHEZ-BEATO, M. 2015. Recurrent presence of the PLCG1 S345F mutation in nodal peripheral T-cell lymphomas. *Haematologica*, 100, e25-7.
- MANSO, R., SANCHEZ-BEATO, M., MONSALVO, S., GOMEZ, S., CERECEDA, L., LLAMAS, P., ROJO, F., MOLLEJO, M., MENARGUEZ, J., ALVES, J., GARCIA-COSIO, M., PIRIS, M. A. &

- RODRIGUEZ-PINILLA, S. M. 2014. The RHOA G17V gene mutation occurs frequently in peripheral T-cell lymphoma and is associated with a characteristic molecular signature. *Blood*, 123, 2893-4.
- MARINER, J. M., MAMANE, Y., HISCOTT, J., WALDMANN, T. A. & AZIMI, N. 2002. IFN regulatory factor 4 participates in the human T cell lymphotropic virus type I-mediated activation of the IL-15 receptor alpha promoter. *J Immunol*, 168, 5667-74.
- MARTINS, G. & CALAME, K. 2008. Regulation and functions of Blimp-1 in T and B lymphocytes. *Annu Rev Immunol*, 26, 133-69.
- MARTINS, G. A., CIMMINO, L., LIAO, J., MAGNUSDOTTIR, E. & CALAME, K. 2008. Blimp-1 directly represses Il2 and the Il2 activator Fos, attenuating T cell proliferation and survival. *J Exp Med*, 205, 1959-65.
- MARTINS, G. A., CIMMINO, L., SHAPIRO-SHELEF, M., SZABOLCS, M., HERRON, A., MAGNUSDOTTIR, E. & CALAME, K. 2006. Transcriptional repressor Blimp-1 regulates T cell homeostasis and function. *Nat Immunol*, 7, 457-65.
- MATHIVET, T., MAZOT, P. & VIGNY, M. 2007. In contrast to agonist monoclonal antibodies, both C-terminal truncated form and full length form of Pleiotrophin failed to activate vertebrate ALK (anaplastic lymphoma kinase)? *Cell Signal*, 19, 2434-43.
- MCCARTHY, P. L., OWZAR, K., HOFMEISTER, C. C., HURD, D. D., HASSOUN, H., RICHARDSON, P. G., GIRALT, S., STADTMAUER, E. A., WEISDORF, D. J., VIJ, R., MOREB, J. S., CALLANDER, N. S., VAN BESIEEN, K., GENTILE, T., ISOLA, L., MAZIARZ, R. T., GABRIEL, D. A., BASHEY, A., LANDAU, H., MARTIN, T., QAZILBASH, M. H., LEVITAN, D., MCCLUNE, B., SCHLOSSMAN, R., HARS, V., POSTIGLIONE, J., JIANG, C., BENNETT, E., BARRY, S., BRESSLER, L., KELLY, M., SEILER, M., ROSENBAUM, C., HARI, P., PASQUINI, M. C., HOROWITZ, M. M., SHEA, T. C., DEVINE, S. M., ANDERSON, K. C. & LINKER, C. 2012. Lenalidomide after stem-cell transplantation for multiple myeloma. *N Engl J Med*, 366, 1770-81.
- MCCLELLAN, A. J., XIA, Y., DEUTSCHBAUER, A. M., DAVIS, R. W., GERSTEIN, M. & FRYDMAN, J. 2007. Diverse cellular functions of the Hsp90 molecular chaperone uncovered using systems approaches. *Cell*, 131, 121-35.
- MCDERMOTT, J. & JIMENO, A. 2014. Belinostat for the treatment of peripheral T-cell lymphomas. *Drugs Today (Barc)*, 50, 337-45.
- MCDONNELL, T. J., DEANE, N., PLATT, F. M., NUNEZ, G., JAEGER, U., MCKEARN, J. P. & KORSMEYER, S. J. 1989. bcl-2-immunoglobulin transgenic mice demonstrate extended B cell survival and follicular lymphoproliferation. *Cell*, 57, 79-88.
- MCILWAIN, D. R., BERGER, T. & MAK, T. W. 2013. Caspase functions in cell death and disease. *Cold Spring Harb Perspect Biol*, 5, a008656.
- MEECH, S. J., MCGAVRAN, L., ODOM, L. F., LIANG, X., MELTESEN, L., GUMP, J., WEI, Q., CARLSEN, S. & HUNGER, S. P. 2001. Unusual childhood extramedullary hematologic malignancy with natural killer cell properties that contains tropomyosin 4--anaplastic lymphoma kinase gene fusion. *Blood*, 98, 1209-16.
- MELCHOR, L., BRIOLI, A., WARDELL, C. P., MURISON, A., POTTER, N. E., KAISER, M. F., FRYER, R. A., JOHNSON, D. C., BEGUM, D. B., HULKKI WILSON, S., VIJAYARAGHAVAN, G., TITLEY, I., CAVO, M., DAVIES, F. E., WALKER, B. A. & MORGAN, G. J. 2014. Single-cell genetic analysis reveals the composition of initiating clones and phylogenetic patterns of branching and parallel evolution in myeloma. *Leukemia*, 28, 1705-15.
- MELO, S. A. & ESTELLER, M. 2011. Dysregulation of microRNAs in cancer: playing with fire. *FEBS Lett*, 585, 2087-99.
- MENDEZ, L. M., POLO, J. M., YU, J. J., KRUPSKI, M., DING, B. B., MELNICK, A. & YE, B. H. 2008. CtBP is an essential corepressor for BCL6 autoregulation. *Mol Cell Biol*, 28, 2175-86.
- MERKEL, O., HAMACHER, F., GRIESSL, R., GRABNER, L., SCHIEFER, A. I., PRUTSCH, N., BAER, C., EGGER, G., SCHLEDERER, M., KRENN, P. W., HARTMANN, T. N., SIMONITSCH-KLUPP, I., PLASS, C., STABER, P. B., MORIGGL, R., TURNER, S. D., GREIL, R. & KENNER, L. 2015.

- Oncogenic role of miR-155 in anaplastic large cell lymphoma lacking the t(2;5) translocation. *J Pathol*, 236, 445-56.
- MERKEL, O., HAMACHER, F., LAIMER, D., SIFFT, E., TRAJANOSKI, Z., SCHEIDELER, M., EGGER, G., HASSLER, M. R., THALLINGER, C., SCHMATZ, A., TURNER, S. D., GREIL, R. & KENNER, L. 2010. Identification of differential and functionally active miRNAs in both anaplastic lymphoma kinase (ALK)+ and ALK- anaplastic large-cell lymphoma. *Proc Natl Acad Sci U S A*, 107, 16228-33.
- MITTRUCKER, H. W., MATSUYAMA, T., GROSSMAN, A., KUNDIG, T. M., POTTER, J., SHAHINIAN, A., WAKEHAM, A., PATTERSON, B., OHASHI, P. S. & MAK, T. W. 1997. Requirement for the transcription factor LSIRF/IRF4 for mature B and T lymphocyte function. *Science*, 275, 540-3.
- MOBINI, R., ANDERSSON, B. A., ERJEFALT, J., HAHN-ZORIC, M., LANGSTON, M. A., PERKINS, A. D., CARDELL, L. O. & BENSON, M. 2009. A module-based analytical strategy to identify novel disease-associated genes shows an inhibitory role for interleukin 7 Receptor in allergic inflammation. *BMC Syst Biol*, 3, 19.
- MOMBAERTS, P., CLARKE, A. R., RUDNICKI, M. A., IACOMINI, J., ITOHARA, S., LAFAILLE, J. J., WANG, L., ICHIKAWA, Y., JAENISCH, R., HOOPER, M. L. & ET AL. 1992. Mutations in T-cell antigen receptor genes alpha and beta block thymocyte development at different stages. *Nature*, 360, 225-31.
- MOOG-LUTZ, C., DEGOUTIN, J., GOUZI, J. Y., FROBERT, Y., BRUNET-DE CARVALHO, N., BUREAU, J., CREMINON, C. & VIGNY, M. 2005. Activation and inhibition of anaplastic lymphoma kinase receptor tyrosine kinase by monoclonal antibodies and absence of agonist activity of pleiotrophin. *J Biol Chem*, 280, 26039-48.
- MORA-LOPEZ, F., REALES, E., BRIEVA, J. A. & CAMPOS-CARO, A. 2007. Human BSAP and BLIMP1 conform an autoregulatory feedback loop. *Blood*, 110, 3150-7.
- MORRIS, S. W., KIRSTEIN, M. N., VALENTINE, M. B., DITTMER, K. G., SHAPIRO, D. N., SALTMAN, D. L. & LOOK, A. T. 1994. Fusion of a kinase gene, ALK, to a nucleolar protein gene, NPM, in non-Hodgkin's lymphoma. *Science*, 263, 1281-4.
- MOSALPURIA, K., BOCIEK, R. G. & VOSE, J. M. 2014. Angioimmunoblastic T-cell lymphoma management. *Semin Hematol*, 51, 52-8.
- MOSSE, Y. P., LIM, M. S., VOSS, S. D., WILNER, K., RUFFNER, K., LALIBERTE, J., ROLLAND, D., BALIS, F. M., MARIS, J. M., WEIGEL, B. J., INGLE, A. M., AHERN, C., ADAMSON, P. C. & BLANEY, S. M. 2013. Safety and activity of crizotinib for paediatric patients with refractory solid tumours or anaplastic large-cell lymphoma: a Children's Oncology Group phase 1 consortium study. *Lancet Oncol*, 14, 472-80.
- MOTEGI, A., FUJIMOTO, J., KOTANI, M., SAKURABA, H. & YAMAMOTO, T. 2004. ALK receptor tyrosine kinase promotes cell growth and neurite outgrowth. *J Cell Sci*, 117, 3319-29.
- MOURALI, J., BENARD, A., LOURENCO, F. C., MONNET, C., GREENLAND, C., MOOG-LUTZ, C., RACAUD-SULTAN, C., GONZALEZ-DUNIA, D., VIGNY, M., MEHLEN, P., DELSOL, G. & ALLOUCHE, M. 2006. Anaplastic lymphoma kinase is a dependence receptor whose proapoptotic functions are activated by caspase cleavage. *Mol Cell Biol*, 26, 6209-22.
- MURPHY, T. L., TUSSIWAND, R. & MURPHY, K. M. 2013. Specificity through cooperation: BATF-IRF interactions control immune-regulatory networks. *Nat Rev Immunol*, 13, 499-509.
- MURRAY, H. W., RUBIN, B. Y., CARRIERO, S. M., HARRIS, A. M. & JAFFEE, E. A. 1985. Human mononuclear phagocyte antiprotozoal mechanisms: oxygen-dependent vs oxygen-independent activity against intracellular *Toxoplasma gondii*. *J Immunol*, 134, 1982-8.
- MUTO, A., OCHIAI, K., KIMURA, Y., ITOH-NAKADAI, A., CALAME, K. L., IKEBE, D., TASHIRO, S. & IGARASHI, K. 2010. Bach2 represses plasma cell gene regulatory network in B cells to promote antibody class switch. *EMBO J*, 29, 4048-61.
- MUTO, A., TASHIRO, S., NAKAJIMA, O., HOSHINO, H., TAKAHASHI, S., SAKODA, E., IKEBE, D., YAMAMOTO, M. & IGARASHI, K. 2004. The transcriptional programme of antibody class switching involves the repressor Bach2. *Nature*, 429, 566-71.

- NAGEL, S., LEICH, E., QUENTMEIER, H., MEYER, C., KAUFMANN, M., DREXLER, H. G., ZETTL, A., ROSENWALD, A. & MACLEOD, R. A. 2008. Amplification at 7q22 targets cyclin-dependent kinase 6 in T-cell lymphoma. *Leukemia*, 22, 387-92.
- NELSON, M., HORSMAN, D. E., WEISENBURGER, D. D., GASCOYNE, R. D., DAVE, B. J., LOBERIZA, F. R., LUDKOVSKI, O., SAVAGE, K. J., ARMITAGE, J. O. & SANGER, W. G. 2008. Cytogenetic abnormalities and clinical correlations in peripheral T-cell lymphoma. *Br J Haematol*, 141, 461-9.
- NIU, H., YE, B. H. & DALLA-FAVERA, R. 1998. Antigen receptor signaling induces MAP kinase-mediated phosphorylation and degradation of the BCL-6 transcription factor. *Genes Dev*, 12, 1953-61.
- NURIEVA, R. I., CHUNG, Y., MARTINEZ, G. J., YANG, X. O., TANAKA, S., MATSKEVITCH, T. D., WANG, Y. H. & DONG, C. 2009. Bcl6 mediates the development of T follicular helper cells. *Science*, 325, 1001-5.
- OCHIAI, K., KATO, Y., IKURA, T., HOSHIKAWA, Y., NODA, T., KARASUYAMA, H., TASHIRO, S., MUTO, A. & IGARASHI, K. 2006. Plasmacytic transcription factor Blimp-1 is repressed by Bach2 in B cells. *J Biol Chem*, 281, 38226-34.
- OCHIAI, K., MUTO, A., TANAKA, H., TAKAHASHI, S. & IGARASHI, K. 2008. Regulation of the plasma cell transcription factor Blimp-1 gene by Bach2 and Bcl6. *Int Immunol*, 20, 453-60.
- ODEJIDE, O., WEIGERT, O., LANE, A. A., TOSCANO, D., LUNNING, M. A., KOPP, N., KIM, S., VAN BODEGOM, D., BOLLA, S., SCHATZ, J. H., TERUYA-FELDSTEIN, J., HOCHBERG, E., LOUIS SAINT, A., DORFMAN, D., STEVENSON, K., RODIG, S. J., PICCALUGA, P. P., JACOBSEN, E., PILERI, S. A., HARRIS, N. L., FERRERO, S., INGHIRAMI, G., HORWITZ, S. M. & WEINSTOCK, D. M. 2014. A targeted mutational landscape of angioimmunoblastic T-cell lymphoma. *Blood*, 123, 1293-6.
- OESTREICH, K. J., READ, K. A., GILBERTSON, S. E., HOUGH, K. P., MCDONALD, P. W., KRISHNAMOORTHY, V. & WEINMANN, A. S. 2014. Bcl-6 directly represses the gene program of the glycolysis pathway. *Nat Immunol*, 15, 957-64.
- OTT, G. & ROSENWALD, A. 2008. Molecular pathogenesis of follicular lymphoma. *Haematologica*, 93, 1773-6.
- PALOMERO, T., COURONNE, L., KHIABANIAN, H., KIM, M. Y., AMBESI-IMPIOMBATO, A., PEREZ-GARCIA, A., CARPENTER, Z., ABATE, F., ALLEGRETTA, M., HAYDU, J. E., JIANG, X., LOSSOS, I. S., NICOLAS, C., BALBIN, M., BASTARD, C., BHAGAT, G., PIRIS, M. A., CAMPO, E., BERNARD, O. A., RABADAN, R. & FERRANDO, A. A. 2014. Recurrent mutations in epigenetic regulators, RHOA and FYN kinase in peripheral T cell lymphomas. *Nat Genet*, 46, 166-70.
- PAPADOPOULOU, V., POSTIGO, A., SANCHEZ-TILLO, E., PORTER, A. C. & WAGNER, S. D. 2010. ZEB1 and CtBP form a repressive complex at a distal promoter element of the BCL6 locus. *Biochem J*, 427, 541-50.
- PARRILLA CASTELLAR, E. R., JAFFE, E. S., SAID, J. W., SWERDLOW, S. H., KETTERLING, R. P., KNUDSON, R. A., SIDHU, J. S., HSI, E. D., KARIKEHALLI, S., JIANG, L., VASMATZIS, G., GIBSON, S. E., ONDREJKA, S., NICOLAE, A., GROGG, K. L., ALLMER, C., RISTOW, K. M., WILSON, W. H., MACON, W. R., LAW, M. E., CERHAN, J. R., HABERMANN, T. M., ANSELL, S. M., DOGAN, A., MAURER, M. J. & FELDMAN, A. L. 2014. ALK-negative anaplastic large cell lymphoma is a genetically heterogeneous disease with widely disparate clinical outcomes. *Blood*, 124, 1473-80.
- PASQUALUCCI, L., COMPAGNO, M., HOULDSWORTH, J., MONTI, S., GRUNN, A., NANDULA, S. V., ASTER, J. C., MURTY, V. V., SHIPP, M. A. & DALLA-FAVERA, R. 2006. Inactivation of the PRDM1/BLIMP1 gene in diffuse large B cell lymphoma. *J Exp Med*, 203, 311-7.
- PASQUALUCCI, L. & DALLA-FAVERA, R. 2014. SnapShot: diffuse large B cell lymphoma. *Cancer Cell*, 25, 132-132 e1.
- PASQUALUCCI, L., KHIABANIAN, H., FANGAZIO, M., VASISHTHA, M., MESSINA, M., HOLMES, A. B., OUILLETTE, P., TRIFONOV, V., ROSSI, D., TABBO, F., PONZONI, M., CHADBURN, A.,

- MURTY, V. V., BHAGAT, G., GAIDANO, G., INGHIRAMI, G., MALEK, S. N., RABADAN, R. & DALLA-FAVERA, R. 2014. Genetics of follicular lymphoma transformation. *Cell Rep*, 6, 130-40.
- PASQUALUCCI, L., MIGLIAZZA, A., BASSO, K., HOULDSWORTH, J., CHAGANTI, R. S. & DALLA-FAVERA, R. 2003. Mutations of the BCL6 proto-oncogene disrupt its negative autoregulation in diffuse large B-cell lymphoma. *Blood*, 101, 2914-23.
- PATHAK, S., MA, S., TRINH, L. & LU, R. 2008. A role for interferon regulatory factor 4 in receptor editing. *Mol Cell Biol*, 28, 2815-24.
- PENG, L., SPOLSKI, R., LIAO, W. & LEONARD, W. J. 2014. Complex interactions of transcription factors in mediated cytokine biology in T-cells. *Immunol Rev*, 261, 141-156.
- PEPPER, M., PAGAN, A. J., IGYARTO, B. Z., TAYLOR, J. J. & JENKINS, M. K. 2011. Opposing signals from the Bcl6 transcription factor and the interleukin-2 receptor generate T helper 1 central and effector memory cells. *Immunity*, 35, 583-95.
- PEREZ-GALAN, P., MORA-JENSEN, H., WENIGER, M. A., SHAFFER, A. L., 3RD, RIZZATTI, E. G., CHAPMAN, C. M., MO, C. C., STENNETT, L. S., RADER, C., LIU, P., RAGHAVACHARI, N., STETLER-STEVENSON, M., YUAN, C., PITTALUGA, S., MARIC, I., DUNLEAVY, K. M., WILSON, W. H., STAUDT, L. M. & WIESTNER, A. 2011. Bortezomib resistance in mantle cell lymphoma is associated with plasmacytic differentiation. *Blood*, 117, 542-52.
- PETRIE, H. T., LIVAK, F., BURTRUM, D. & MAZEL, S. 1995. T cell receptor gene recombination patterns and mechanisms: cell death, rescue, and T cell production. *J Exp Med*, 182, 121-7.
- PHAN, R. T. & DALLA-FAVERA, R. 2004. The BCL6 proto-oncogene suppresses p53 expression in germinal-centre B cells. *Nature*, 432, 635-9.
- PHAN, R. T., SAITO, M., BASSO, K., NIU, H. & DALLA-FAVERA, R. 2005. BCL6 interacts with the transcription factor Miz-1 to suppress the cyclin-dependent kinase inhibitor p21 and cell cycle arrest in germinal center B cells. *Nat Immunol*, 6, 1054-60.
- PHAN, R. T., SAITO, M., KITAGAWA, Y., MEANS, A. R. & DALLA-FAVERA, R. 2007. Genotoxic stress regulates expression of the proto-oncogene Bcl6 in germinal center B cells. *Nat Immunol*, 8, 1132-9.
- PHILPOTT, K. L., VINEY, J. L., KAY, G., RASTAN, S., GARDINER, E. M., CHAE, S., HAYDAY, A. C. & OWEN, M. J. 1992. Lymphoid development in mice congenitally lacking T cell receptor alpha beta-expressing cells. *Science*, 256, 1448-52.
- PICCALUGA, P. P., AGOSTINELLI, C., CALIFANO, A., CARBONE, A., FANTONI, L., FERRARI, S., GAZZOLA, A., GLOGHINI, A., RIGHI, S., ROSSI, M., TAGLIAFICO, E., ZINZANI, P. L., ZUPO, S., BACCARANI, M. & PILERI, S. A. 2007. Gene expression analysis of angioimmunoblastic lymphoma indicates derivation from T follicular helper cells and vascular endothelial growth factor deregulation. *Cancer Res*, 67, 10703-10.
- PICCALUGA, P. P., AGOSTINELLI, C., TRIPODO, C., GAZZOLA, A., BACCI, F., SABATTINI, E. & PILERI, S. A. 2011. Peripheral T-cell lymphoma classification: the matter of cellular derivation. *Expert Rev Hematol*, 4, 415-25.
- PICCALUGA, P. P., GAZZOLA, A., MANNU, C., AGOSTINELLI, C., BACCI, F., SABATTINI, E., SAGRAMOSO, C., PIVA, R., RONCOLATO, F., INGHIRAMI, G. & PILERI, S. A. 2010. Pathobiology of Anaplastic Large Cell Lymphoma. *Adv Hematol*, 2010.
- PILERI, S. A. & PICCALUGA, P. P. 2012. New molecular insights into peripheral T cell lymphomas. *J Clin Invest*, 122, 3448-55.
- PIVA, R., AGNELLI, L., PELLEGRINO, E., TODOERTI, K., GROSSO, V., TAMAGNO, I., FORNARI, A., MARTINOGLIO, B., MEDICO, E., ZAMO, A., FACCHETTI, F., PONZONI, M., GEISSINGER, E., ROSENWALD, A., MULLER-HERMELINK, H. K., DE WOLF-PEETERS, C., PICCALUGA, P. P., PILERI, S., NERI, A. & INGHIRAMI, G. 2010. Gene expression profiling uncovers molecular classifiers for the recognition of anaplastic large-cell lymphoma within peripheral T-cell neoplasms. *J Clin Oncol*, 28, 1583-90.
- POLO, J. M., DELL'OSO, T., RANUNCOLO, S. M., CERCHIETTI, L., BECK, D., DA SILVA, G. F., PRIVE, G. G., LICHT, J. D. & MELNICK, A. 2004. Specific peptide interference reveals BCL6

- transcriptional and oncogenic mechanisms in B-cell lymphoma cells. *Nat Med*, 10, 1329-35.
- PONS, E., UPHOFF, C. C. & DREXLER, H. G. 1998. Expression of hepatocyte growth factor and its receptor c-met in human leukemia-lymphoma cell lines. *Leuk Res*, 22, 797-804.
- PRATT, A. J. & MACRAE, I. J. 2009. The RNA-induced silencing complex: a versatile gene-silencing machine. *J Biol Chem*, 284, 17897-901.
- PULVINO, M., CHEN, L., OLEKSYN, D., LI, J., COMPITELLO, G., ROSSI, R., SPENCE, S., BALAKRISHNAN, V., JORDAN, C., POLIGONE, B., CASULO, C., BURACK, R., SHAPIRO, J. L., BERNSTEIN, S., FRIEDBERG, J. W., DESHAIES, R. J., LAND, H. & ZHAO, J. 2015. Inhibition of COP9-signalosome (CSN) deneddylating activity and tumor growth of diffuse large B-cell lymphomas by doxycycline. *Oncotarget*, 14796-14813.
- QUERFELD, C., KHAN, I., MAHON, B., NELSON, B. P., ROSEN, S. T. & EVENS, A. M. 2010. Primary cutaneous and systemic anaplastic large cell lymphoma: clinicopathologic aspects and therapeutic options. *Oncology (Williston Park)*, 24, 574-87.
- QUIVORON, C., COURONNE, L., DELLA VALLE, V., LOPEZ, C. K., PLO, I., WAGNER-BALLON, O., DO CRUZEIRO, M., DELHOMMEAU, F., ARNULF, B., STERN, M. H., GODLEY, L., OPOLON, P., TILLY, H., SOLARY, E., DUFFOURD, Y., DESSEN, P., MERLE-BERAL, H., NGUYEN-KHAC, F., FONTENAY, M., VAINCHENKER, W., BASTARD, C., MERCHER, T. & BERNARD, O. A. 2011. TET2 inactivation results in pleiotropic hematopoietic abnormalities in mouse and is a recurrent event during human lymphomagenesis. *Cancer Cell*, 20, 25-38.
- RACZKOWSKI, F., RITTER, J., HEESCH, K., SCHUMACHER, V., GURALNIK, A., HOCKER, L., RAIFER, H., KLEIN, M., BOPP, T., HARB, H., KESPER, D. A., PFEFFERLE, P. I., GRUSDAT, M., LANG, P. A., MITTRUCKER, H. W. & HUBER, M. 2013. The transcription factor Interferon Regulatory Factor 4 is required for the generation of protective effector CD8+ T cells. *Proc Natl Acad Sci U S A*, 110, 15019-24.
- RAETZ, E. A., PERKINS, S. L., CARLSON, M. A., SCHOOLER, K. P., CARROLL, W. L. & VIRSHUP, D. M. 2002. The nucleophosmin-anaplastic lymphoma kinase fusion protein induces c-Myc expression in pediatric anaplastic large cell lymphomas. *Am J Pathol*, 161, 875-83.
- RAJKUMAR, S. V., HAYMAN, S. R., LACY, M. Q., DISPENZIERI, A., GEYER, S. M., KABAT, B., ZELDENRUST, S. R., KUMAR, S., GREIPP, P. R., FONSECA, R., LUST, J. A., RUSSELL, S. J., KYLE, R. A., WITZIG, T. E. & GERTZ, M. A. 2005. Combination therapy with lenalidomide plus dexamethasone (Rev/Dex) for newly diagnosed myeloma. *Blood*, 106, 4050-3.
- RANUNCOLO, S. M., POLO, J. M. & MELNICK, A. 2008a. BCL6 represses CHEK1 and suppresses DNA damage pathways in normal and malignant B-cells. *Blood Cells Mol Dis*, 41, 95-9.
- RANUNCOLO, S. M., WANG, L., POLO, J. M., DELL'OSO, T., DIEROV, J., GAYMES, T. J., RASSOOL, F., CARROLL, M. & MELNICK, A. 2008b. BCL6-mediated attenuation of DNA damage sensing triggers growth arrest and senescence through a p53-dependent pathway in a cell context-dependent manner. *J Biol Chem*, 283, 22565-72.
- RAO, D. D., VORHIES, J. S., SENZER, N. & NEMUNAITIS, J. 2009. siRNA vs. shRNA: similarities and differences. *Adv Drug Deliv Rev*, 61, 746-59.
- REDAELLI, S., FARINA, F., STASIA, A., CECCON, M., MOLOGNI, L., MESSA, C., GUERRA, L., GIUDICI, G., SALA, E., MUSSOLIN, L., DEEREN, D., KING, M., STEURER, M., ORDEMANN, R., COHEN, A., GRUBE, M., BERNARD, L., CHIARIANO, G. & PIAZZA, R. 2013. High Response Rates To Crizotinib In Advanced, Chemoresistant ALK+ Lymphoma Patients. *ASH 2013*.
- REN, B., CHEE, K. J., KIM, T. H. & MANIATIS, T. 1999. PRDI-BF1/Blimp-1 repression is mediated by corepressors of the Groucho family of proteins. *Genes Dev*, 13, 125-37.
- RENGARAJAN, J., MOWEN, K. A., MCBRIDE, K. D., SMITH, E. D., SINGH, H. & GLIMCHER, L. H. 2002. Interferon regulatory factor 4 (IRF4) interacts with NFATc2 to modulate interleukin 4 gene expression. *J Exp Med*, 195, 1003-12.
- RUTISHAUSER, R. L., MARTINS, G. A., KALACHIKOV, S., CHANDELE, A., PARISH, I. A., MEFFRE, E., JACOB, J., CALAME, K. & KAECH, S. M. 2009. Transcriptional repressor Blimp-1

- promotes CD8(+) T cell terminal differentiation and represses the acquisition of central memory T cell properties. *Immunity*, 31, 296-308.
- SACKS, D. & NOBEN-TRAUTH, N. 2002. The immunology of susceptibility and resistance to *Leishmania major* in mice. *Nat Rev Immunol*, 2, 845-58.
- SAGLAM, A. & UNER, A. H. 2011. Immunohistochemical expression of Mum-1, Oct-2 and Bcl-6 in systemic anaplastic large cell lymphomas. *Tumori*, 97, 634-8.
- SAHU, A., PRABHASH, K., NORONHA, V., JOSHI, A. & DESAI, S. 2013. Crizotinib: A comprehensive review. *South Asian J Cancer*, 2, 91-7.
- SAITO, M., GAO, J., BASSO, K., KITAGAWA, Y., SMITH, P. M., BHAGAT, G., PERNIS, A., PASQUALUCCI, L. & DALLA-FAVERA, R. 2007. A signaling pathway mediating downregulation of BCL6 in germinal center B cells is blocked by BCL6 gene alterations in B cell lymphoma. *Cancer Cell*, 12, 280-92.
- SAKATA-YANAGIMOTO, M., ENAMI, T., YOSHIDA, K., SHIRAIISHI, Y., ISHII, R., MIYAKE, Y., MUTO, H., TSUYAMA, N., SATO-OTSUBO, A., OKUNO, Y., SAKATA, S., KAMADA, Y., NAKAMOTO-MATSUBARA, R., TRAN, N. B., IZUTSU, K., SATO, Y., OHTA, Y., FURUTA, J., SHIMIZU, S., KOMENO, T., SATO, Y., ITO, T., NOGUCHI, M., NOGUCHI, E., SANADA, M., CHIBA, K., TANAKA, H., SUZUKAWA, K., NANMOKU, T., HASEGAWA, Y., NUREKI, O., MIYANO, S., NAKAMURA, N., TAKEUCHI, K., OGAWA, S. & CHIBA, S. 2014. Somatic RHOA mutation in angioimmunoblastic T cell lymphoma. *Nat Genet*, 46, 171-5.
- SALAVERRIA, I., BEA, S., LOPEZ-GUILLERMO, A., LESPINET, V., PINYOL, M., BURKHARDT, B., LAMANT, L., ZETTL, A., HORSMAN, D., GASCOYNE, R., OTT, G., SIEBERT, R., DELSOL, G. & CAMPO, E. 2008. Genomic profiling reveals different genetic aberrations in systemic ALK-positive and ALK-negative anaplastic large cell lymphomas. *Br J Haematol*, 140, 516-26.
- SALLUSTO, F., LENIG, D., FORSTER, R., LIPP, M. & LANZAVECCHIA, A. 1999. Two subsets of memory T lymphocytes with distinct homing potentials and effector functions. *Nature*, 401, 708-12.
- SASAKI, O., MEGURO, K., TOHMIYA, Y., FUNATO, T., SHIBAHARA, S. & SASAKI, T. 2002. Altered expression of retinoblastoma protein-interacting zinc finger gene, RIZ, in human leukaemia. *Br J Haematol*, 119, 940-8.
- SCHATZ, J. H., HORWITZ, S. M., TERUYA-FELDSTEIN, J., LUNNING, M. A., VIALE, A., HUBERMAN, K., SOCCI, N. D., LAILLER, N., HEGUY, A., DOLGALEV, I., MIGLIACCI, J. C., PIRUN, M., PALOMBA, M. L., WEINSTOCK, D. M. & WENDEL, H. G. 2015. Targeted mutational profiling of peripheral T-cell lymphoma not otherwise specified highlights new mechanisms in a heterogeneous pathogenesis. *Leukemia*, 29, 237-41.
- SCHEICHER, R., HOELBL-KOVACIC, A., BELLUTTI, F., TIGAN, A. S., PRCHAL-MURPHY, M., HELLER, G., SCHNECKENLEITHNER, C., SALAZAR-ROA, M., ZOCHBAUER-MULLER, S., ZUBER, J., MALUMBRES, M., KOLLMANN, K. & SEXL, V. 2015. CDK6 as a key regulator of hematopoietic and leukemic stem cell activation. *Blood*, 125, 90-101.
- SCIAMMAS, R., SHAFFER, A. L., SCHATZ, J. H., ZHAO, H., STAUDT, L. M. & SINGH, H. 2006. Graded expression of interferon regulatory factor-4 coordinates isotype switching with plasma cell differentiation. *Immunity*, 25, 225-36.
- SHAFFER, A. L., 3RD, YOUNG, R. M. & STAUDT, L. M. 2012. Pathogenesis of human B cell lymphomas. *Annu Rev Immunol*, 30, 565-610.
- SHAFFER, A. L., EMRE, N. C., LAMY, L., NGO, V. N., WRIGHT, G., XIAO, W., POWELL, J., DAVE, S., YU, X., ZHAO, H., ZENG, Y., CHEN, B., EPSTEIN, J. & STAUDT, L. M. 2008. IRF4 addiction in multiple myeloma. *Nature*, 454, 226-31.
- SHAFFER, A. L., EMRE, N. C., ROMESSER, P. B. & STAUDT, L. M. 2009. IRF4: Immunity. Malignancy! Therapy? *Clin Cancer Res*, 15, 2954-61.
- SHAFFER, A. L., LIN, K. I., KUO, T. C., YU, X., HURT, E. M., ROSENWALD, A., GILTNAME, J. M., YANG, L., ZHAO, H., CALAME, K. & STAUDT, L. M. 2002. Blimp-1 orchestrates plasma cell differentiation by extinguishing the mature B cell gene expression program. *Immunity*, 17, 51-62.

- SHAFFER, A. L., ROSENWALD, A., HURT, E. M., GILTANNE, J. M., LAM, L. T., PICKERAL, O. K. & STAUDT, L. M. 2001. Signatures of the immune response. *Immunity*, 15, 375-85.
- SHAFFER, A. L., SHAPIRO-SHELEF, M., IWAKOSHI, N. N., LEE, A. H., QIAN, S. B., ZHAO, H., YU, X., YANG, L., TAN, B. K., ROSENWALD, A., HURT, E. M., PETROULAKIS, E., SONENBERG, N., YEWEDELL, J. W., CALAME, K., GLIMCHER, L. H. & STAUDT, L. M. 2004. XBP1, downstream of Blimp-1, expands the secretory apparatus and other organelles, and increases protein synthesis in plasma cell differentiation. *Immunity*, 21, 81-93.
- SHAFFER, A. L., WRIGHT, G., YANG, L., POWELL, J., NGO, V., LAMY, L., LAM, L. T., DAVIS, R. E. & STAUDT, L. M. 2006. A library of gene expression signatures to illuminate normal and pathological lymphoid biology. *Immunol Rev*, 210, 67-85.
- SHAFFER, A. L., YU, X., HE, Y., BOLDRICK, J., CHAN, E. P. & STAUDT, L. M. 2000. BCL-6 represses genes that function in lymphocyte differentiation, inflammation, and cell cycle control. *Immunity*, 13, 199-212.
- SHALEM, O., SANJANA, N. E., HARTENIAN, E., SHI, X., SCOTT, D. A., MIKKELSEN, T. S., HECKL, D., EBERT, B. L., ROOT, D. E., DOENCH, J. G. & ZHANG, F. 2014. Genome-scale CRISPR-Cas9 knockout screening in human cells. *Science*, 343, 84-7.
- SHAPIRO-SHELEF, M. & CALAME, K. 2005. Regulation of plasma-cell development. *Nat Rev Immunol*, 5, 230-42.
- SHAPIRO-SHELEF, M., LIN, K. I., MCHEYZER-WILLIAMS, L. J., LIAO, J., MCHEYZER-WILLIAMS, M. G. & CALAME, K. 2003. Blimp-1 is required for the formation of immunoglobulin secreting plasma cells and pre-plasma memory B cells. *Immunity*, 19, 607-20.
- SHARMA, S., MAMANE, Y., GRANDVAUX, N., BARTLETT, J., PETROPOULOS, L., LIN, R. & HISCOTT, J. 2000. Activation and regulation of interferon regulatory factor 4 in HTLV type 1-infected T lymphocytes. *AIDS Res Hum Retroviruses*, 16, 1613-22.
- SHEN, Y., GE, B., RAMACHANDRAREDDY, H., MCKEITHAN, T. & CHAN, W. C. 2008. Alternative splicing generates a short BCL6 (BCL6S) isoform encoding a compact repressor. *Biochem Biophys Res Commun*, 375, 190-3.
- SHIMSHON, L., MICHAELI, A., HADAR, R., NUTT, S. L., DAVID, Y., NAVON, A., WAISMAN, A. & TIROSH, B. 2011. SUMOylation of Blimp-1 promotes its proteasomal degradation. *FEBS Lett*, 585, 2405-9.
- SHIN, H., BLACKBURN, S. D., INTLEKOFER, A. M., KAO, C., ANGELOSANTO, J. M., REINER, S. L. & WHERRY, E. J. 2009. A role for the transcriptional repressor Blimp-1 in CD8(+) T cell exhaustion during chronic viral infection. *Immunity*, 31, 309-20.
- SHINKAI, Y., KOYASU, S., NAKAYAMA, K., MURPHY, K. M., LOH, D. Y., REINHERZ, E. L. & ALT, F. W. 1993. Restoration of T cell development in RAG-2-deficient mice by functional TCR transgenes. *Science*, 259, 822-5.
- SHIOTA, M., FUJIMOTO, J., SEMBA, T., SATOH, H., YAMAMOTO, T. & MORI, S. 1994. Hyperphosphorylation of a novel 80 kDa protein-tyrosine kinase similar to Ltk in a human Ki-1 lymphoma cell line, AMS3. *Oncogene*, 9, 1567-74.
- SHUSTIK, J., HAN, G., FARINHA, P., JOHNSON, N. A., BEN NERIAH, S., CONNORS, J. M., SEHN, L. H., HORSMAN, D. E., GASCOYNE, R. D. & STEIDL, C. 2010. Correlations between BCL6 rearrangement and outcome in patients with diffuse large B-cell lymphoma treated with CHOP or R-CHOP. *Haematologica*, 95, 96-101.
- SIEBERT, R., GESK, S., HARDER, L., STEINEMANN, D., GROTE, W., SCHLEGELBERGER, B., TIEMANN, M., WLODARSKA, I. & SCHEMMEL, V. 1999. Complex variant translocation t(1;2) with TPM3-ALK fusion due to cryptic ALK gene rearrangement in anaplastic large-cell lymphoma. *Blood*, 94, 3614-7.
- SMITH, A., CROUCH, S., LAX, S., LI, J., PAINTER, D., HOWELL, D., PATMORE, R., JACK, A. & ROMAN, E. 2015. Lymphoma incidence, survival and prevalence 2004-2014: sub-type analyses from the UK's Haematological Malignancy Research Network. *Br J Cancer*, 112, 1575-84.

- SMITH, M. A., MAURIN, M., CHO, H. I., BECKNELL, B., FREUD, A. G., YU, J., WEI, S., DJEU, J., CELIS, E., CALIGIURI, M. A. & WRIGHT, K. L. 2010. PRDM1/Blimp-1 controls effector cytokine production in human NK cells. *J Immunol*, 185, 6058-67.
- SNUDERL, M., KOLMAN, O. K., CHEN, Y. B., HSU, J. J., ACKERMAN, A. M., DAL CIN, P., FERRY, J. A., HARRIS, N. L., HASSERJIAN, R. P., ZUKERBERG, L. R., ABRAMSON, J. S., HOCHBERG, E. P., LEE, H., LEE, A. I., TOOMEY, C. E. & SOHANI, A. R. 2010. B-cell lymphomas with concurrent IGH-BCL2 and MYC rearrangements are aggressive neoplasms with clinical and pathologic features distinct from Burkitt lymphoma and diffuse large B-cell lymphoma. *Am J Surg Pathol*, 34, 327-40.
- SOKOL, C. L., CHU, N. Q., YU, S., NISH, S. A., LAUFER, T. M. & MEDZHITOV, R. 2009. Basophils function as antigen-presenting cells for an allergen-induced T helper type 2 response. *Nat Immunol*, 10, 713-20.
- SOMJA, J., BISIG, B., BONNET, C., HERENS, C., SIEBERT, R. & DE LEVAL, L. 2014. Peripheral T-cell lymphoma with t(6;14)(p25;q11.2) translocation presenting with massive splenomegaly. *Virchows Arch*, 464, 735-41.
- STAUDT, V., BOTHUR, E., KLEIN, M., LINGNAU, K., REUTER, S., GREBE, N., GERLITZKI, B., HOFFMANN, M., ULGES, A., TAUBE, C., DEHZAD, N., BECKER, M., STASSEN, M., STEINBORN, A., LOHOFF, M., SCHILD, H., SCHMITT, E. & BOPP, T. 2010. Interferon-regulatory factor 4 is essential for the developmental program of T helper 9 cells. *Immunity*, 33, 192-202.
- STEIN, H., FOSS, H. D., DURKOP, H., MARAFIOTI, T., DELSOL, G., PULFORD, K., PILERI, S. & FALINI, B. 2000. CD30(+) anaplastic large cell lymphoma: a review of its histopathologic, genetic, and clinical features. *Blood*, 96, 3681-95.
- STOICA, G. E., KUO, A., AIGNER, A., SUNITHA, I., SOUTTOU, B., MALERCZYK, C., CAUGHEY, D. J., WEN, D., KARAVANOV, A., RIEGEL, A. T. & WELLSTEIN, A. 2001. Identification of anaplastic lymphoma kinase as a receptor for the growth factor pleiotrophin. *J Biol Chem*, 276, 16772-9.
- STOICA, G. E., KUO, A., POWERS, C., BOWDEN, E. T., SALE, E. B., RIEGEL, A. T. & WELLSTEIN, A. 2002. Midkine binds to anaplastic lymphoma kinase (ALK) and acts as a growth factor for different cell types. *J Biol Chem*, 277, 35990-8.
- STREUBEL, B., VINATZER, U., WILLHEIM, M., RADERER, M. & CHOTT, A. 2006. Novel t(5;9)(q33;q22) fuses ITK to SYK in unspecified peripheral T-cell lymphoma. *Leukemia*, 20, 313-8.
- SU, L. D., SCHNITZER, B., ROSS, C. W., VASEF, M., MORI, S., SHIOTA, M., MASON, D. Y., PULFORD, K., HEADINGTON, J. T. & SINGLETON, T. P. 1997. The t(2;5)-associated p80 NPM/ALK fusion protein in nodal and cutaneous CD30+ lymphoproliferative disorders. *J Cutan Pathol*, 24, 597-603.
- SWERDLOW, S. H., CAMPO, E. & HARRIS, N. L. 2008. WHO Classification of Tumours of Haematopoietic and Lymphoid Tissues. Lyon, France: International Agency for Research On Cancer, 4th Edition.
- TAKAKUWA, T., LUO, W. J., HAM, M. F., SAKANE-ISHIKAWA, F., WADA, N. & AOZASA, K. 2004. Integration of Epstein-Barr virus into chromosome 6q15 of Burkitt lymphoma cell line (Raji) induces loss of BACH2 expression. *Am J Pathol*, 164, 967-74.
- TAM, W., GOMEZ, M., CHADBURN, A., LEE, J. W., CHAN, W. C. & KNOWLES, D. M. 2006. Mutational analysis of PRDM1 indicates a tumor-suppressor role in diffuse large B-cell lymphomas. *Blood*, 107, 4090-100.
- TANG, T. T., DOWBENKO, D., JACKSON, A., TONEY, L., LEWIN, D. A., DENT, A. L. & LASKY, L. A. 2002. The forkhead transcription factor AFX activates apoptosis by induction of the BCL-6 transcriptional repressor. *J Biol Chem*, 277, 14255-65.
- TANGYE, S. G. & TARLINTON, D. M. 2009. Memory B cells: effectors of long-lived immune responses. *Eur J Immunol*, 39, 2065-75.
- THIEBLEMONT, C. & BRIERE, J. 2013. MYC, BCL2, BCL6 in DLBCL: impact for clinics in the future? *Blood*, 121, 2165-6.

- THOMPSON, M. A., STUMPH, J., HENRICKSON, S. E., ROSENWALD, A., WANG, Q., OLSON, S., BRANDT, S. J., ROBERTS, J., ZHANG, X., SHYR, Y. & KINNEY, M. C. 2005. Differential gene expression in anaplastic lymphoma kinase-positive and anaplastic lymphoma kinase-negative anaplastic large cell lymphomas. *Hum Pathol*, 36, 494-504.
- TOKOYODA, K., EGAWA, T., SUGIYAMA, T., CHOI, B. I. & NAGASAWA, T. 2004. Cellular niches controlling B lymphocyte behavior within bone marrow during development. *Immunity*, 20, 707-18.
- TOMINAGA, N., OHKUSU-TSUKADA, K., UDONO, H., ABE, R., MATSUYAMA, T. & YUI, K. 2003. Development of Th1 and not Th2 immune responses in mice lacking IFN-regulatory factor-4. *Int Immunol*, 15, 1-10.
- TONEY, L. M., CATTORETTI, G., GRAF, J. A., MERGHOU, T., PANDOLFI, P. P., DALLA-FAVERA, R., YE, B. H. & DENT, A. L. 2000. BCL-6 regulates chemokine gene transcription in macrophages. *Nat Immunol*, 1, 214-20.
- TORT, F., PINYOL, M., PULFORD, K., RONCADOR, G., HERNANDEZ, L., NAYACH, I., KLUIN-NELEMANS, H. C., KLUIN, P., TOURIOL, C., DELSOL, G., MASON, D. & CAMPO, E. 2001. Molecular characterization of a new ALK translocation involving moesin (MSN-ALK) in anaplastic large cell lymphoma. *Lab Invest*, 81, 419-26.
- TOURIOL, C., GREENLAND, C., LAMANT, L., PULFORD, K., BERNARD, F., ROUSSET, T., MASON, D. Y. & DELSOL, G. 2000. Further demonstration of the diversity of chromosomal changes involving 2p23 in ALK-positive lymphoma: 2 cases expressing ALK kinase fused to CLTCL (clathrin chain polypeptide-like). *Blood*, 95, 3204-7.
- TSUBOI, K., IIDA, S., INAGAKI, H., KATO, M., HAYAMI, Y., HANAMURA, I., MIURA, K., HARADA, S., KIKUCHI, M., KOMATSU, H., BANNO, S., WAKITA, A., NAKAMURA, S., EIMOTO, T. & UEDA, R. 2000. MUM1/IRF4 expression as a frequent event in mature lymphoid malignancies. *Leukemia*, 14, 449-56.
- TSUJIMOTO, Y., COSSMAN, J., JAFFE, E. & CROCE, C. M. 1985. Involvement of the bcl-2 gene in human follicular lymphoma. *Science*, 228, 1440-3.
- TUNYAPLIN, C., SHAFFER, A. L., ANGELIN-DUCLOS, C. D., YU, X., STAUDT, L. M. & CALAME, K. L. 2004. Direct repression of prdm1 by Bcl-6 inhibits plasmacytic differentiation. *J Immunol*, 173, 1158-65.
- TUNYAPLIN, C., SHAPIRO, M. A. & CALAME, K. L. 2000. Characterization of the B lymphocyte-induced maturation protein-1 (Blimp-1) gene, mRNA isoforms and basal promoter. *Nucleic Acids Res*, 28, 4846-55.
- TURNER, C. A., JR., MACK, D. H. & DAVIS, M. M. 1994. Blimp-1, a novel zinc finger-containing protein that can drive the maturation of B lymphocytes into immunoglobulin-secreting cells. *Cell*, 77, 297-306.
- TUSZYNSKI, G. P. & MURPHY, A. 1990. Spectrophotometric quantitation of anchorage-dependent cell numbers using the bicinchoninic acid protein assay reagent. *Anal Biochem*, 184, 189-91.
- UEDA, C., AKASAKA, T., KURATA, M., MAESAKO, Y., NISHIKORI, M., ICHINOHASAMA, R., IMADA, K., UCHIYAMA, T. & OHNO, H. 2002. The gene for interleukin-21 receptor is the partner of BCL6 in t(3;16)(q27;p11), which is recurrently observed in diffuse large B-cell lymphoma. *Oncogene*, 21, 368-76.
- VAN DEN HAM, H. J., DE WAAL, L., ANDEWEG, A. C. & DE BOER, R. J. 2010. Identification of helper T cell master regulator candidates using the polar score method. *J Immunol Methods*, 361, 98-109.
- VASMATZIS, G., JOHNSON, S. H., KNUDSON, R. A., KETTERLING, R. P., BRAGGIO, E., FONSECA, R., VISWANATHA, D. S., LAW, M. E., KIP, N. S., OZSAN, N., GREBE, S. K., FREDERICK, L. A., ECKLOFF, B. W., THOMPSON, E. A., KADIN, M. E., MILOSEVIC, D., PORCHER, J. C., ASMANN, Y. W., SMITH, D. I., KOVTUN, I. V., ANSELL, S. M., DOGAN, A. & FELDMAN, A. L. 2012. Genome-wide analysis reveals recurrent structural abnormalities of TP63 and other p53-related genes in peripheral T-cell lymphomas. *Blood*, 120, 2280-9.

- VIEIRA, S. A., DEININGER, M. W., SOROUR, A., SINCLAIR, P., FORONI, L., GOLDMAN, J. M. & MELO, J. V. 2001. Transcription factor BACH2 is transcriptionally regulated by the BCR/ABL oncogene. *Genes Chromosomes Cancer*, 32, 353-63.
- VINUESA, C. G., TANGYE, S. G., MOSER, B. & MACKAY, C. R. 2005. Follicular B helper T cells in antibody responses and autoimmunity. *Nat Rev Immunol*, 5, 853-65.
- VOSE, J., ARMITAGE, J. & WEISENBURGER, D. 2008. International peripheral T-cell and natural killer/T-cell lymphoma study: pathology findings and clinical outcomes. *J Clin Oncol*, 26, 4124-30.
- VRZALIKOVA, K., LEONARD, S., FAN, Y., BELL, A., VOCKERODT, M., FLODR, P., WRIGHT, K. L., ROWE, M., TAO, Q. & MURRAY, P. G. 2012. Hypomethylation and Over-Expression of the Beta Isoform of BLIMP1 is Induced by Epstein-Barr Virus Infection of B Cells; Potential Implications for the Pathogenesis of EBV-Associated Lymphomas. *Pathogens*, 1, 83-101.
- WALKER, S. R., LIU, S., XIANG, M., NICOLAIS, M., HATZI, K., GIANNOPOULOU, E., ELEMENTO, O., CERCHIETTI, L., MELNICK, A. & FRANK, D. A. 2014. The transcriptional modulator BCL6 as a molecular target for breast cancer therapy. *Oncogene*.
- WALKER, S. R., NELSON, E. A., YEH, J. E., PINELLO, L., YUAN, G. C. & FRANK, D. A. 2013. STAT5 outcompetes STAT3 to regulate the expression of the oncogenic transcriptional modulator BCL6. *Mol Cell Biol*, 33, 2879-90.
- WANG, L., TOOMEY, N. L., DIAZ, L. A., WALKER, G., RAMOS, J. C., BARBER, G. N. & NING, S. 2011a. Oncogenic IRFs provide a survival advantage for Epstein-Barr virus- or human T-cell leukemia virus type 1-transformed cells through induction of BIC expression. *J Virol*, 85, 8328-37.
- WANG, R., DILLON, C. P., SHI, L. Z., MILASTA, S., CARTER, R., FINKELSTEIN, D., MCCORMICK, L. L., FITZGERALD, P., CHI, H., MUNGER, J. & GREEN, D. R. 2011b. The transcription factor Myc controls metabolic reprogramming upon T lymphocyte activation. *Immunity*, 35, 871-82.
- WANG, X., LI, Z., NAGANUMA, A. & YE, B. H. 2002. Negative autoregulation of BCL-6 is bypassed by genetic alterations in diffuse large B cell lymphomas. *Proc Natl Acad Sci U S A*, 99, 15018-23.
- WARNES, G. 2014. *Principles of Flow cytometry* [Online]. Institute of Cell and Molecular Science, Queen Mary, University of London. Available: <http://www.icms.qmul.ac.uk/flowcytometry/flowcytometry/principles/index.html> [Accessed 15 Aug 2014].
- WEAVER, C. T., HARRINGTON, L. E., MANGAN, P. R., GAVRIELI, M. & MURPHY, K. M. 2006. Th17: an effector CD4 T cell lineage with regulatory T cell ties. *Immunity*, 24, 677-88.
- WEILEMANN, A., GRAU, M., ERDMANN, T., MERKEL, O., SOBHIASHAR, U., ANAGNOSTOPOULOS, I., HUMMEL, M., SIEGERT, A., HAYFORD, C., MADLE, H., WOLLERT-WULF, B., FICHTNER, I., DORKEN, B., DIRNHOFER, S., MATHAS, S., JANZ, M., EMRE, N. C., ROSENWALD, A., OTT, G., LENZ, P., TZANKOV, A. & LENZ, G. 2015. Essential role of IRF4 and MYC signaling for survival of anaplastic large cell lymphoma. *Blood*, 125, 124-32.
- WEISENBURGER, D. D., SAVAGE, K. J., HARRIS, N. L., GASCOYNE, R. D., JAFFE, E. S., MACLENNAN, K. A., RUDIGER, T., PILERI, S., NAKAMURA, S., NATHWANI, B., CAMPO, E., BERGER, F., COIFFIER, B., KIM, W. S., HOLTE, H., FEDERICO, M., AU, W. Y., TOBINAI, K., ARMITAGE, J. O. & VOSE, J. M. 2011. Peripheral T-cell lymphoma, not otherwise specified: a report of 340 cases from the International Peripheral T-cell Lymphoma Project. *Blood*, 117, 3402-8.
- WILLIAMS, M. A. & BEVAN, M. J. 2007. Effector and memory CTL differentiation. *Annu Rev Immunol*, 25, 171-92.
- WONG, C. C., CHENG, K. W. & RIGAS, B. 2012. Preclinical predictors of anticancer drug efficacy: critical assessment with emphasis on whether nanomolar potency should be required of candidate agents. *J Pharmacol Exp Ther*, 341, 572-8.

- WOOD, G. S., HARDMAN, D. L., BONI, R., DUMMER, R., KIM, Y. H., SMOLLER, B. R., TAKESHITA, M., KIKUCHI, M. & BURG, G. 1996. Lack of the t(2;5) or other mutations resulting in expression of anaplastic lymphoma kinase catalytic domain in CD30+ primary cutaneous lymphoproliferative disorders and Hodgkin's disease. *Blood*, 88, 1765-70.
- WRIGHT, C. W., RUMBLE, J. M. & DUCKETT, C. S. 2007. CD30 activates both the canonical and alternative NF-kappaB pathways in anaplastic large cell lymphoma cells. *J Biol Chem*, 282, 10252-62.
- XU, B. & LIU, P. 2014. No survival improvement for patients with angioimmunoblastic T-cell lymphoma over the past two decades: a population-based study of 1207 cases. *PLoS One*, 9, e92585.
- XU, D., ZHAO, L., DEL VALLE, L., MIKLOSSY, J. & ZHANG, L. 2008. Interferon regulatory factor 4 is involved in Epstein-Barr virus-mediated transformation of human B lymphocytes. *J Virol*, 82, 6251-8.
- YAMAGATA, T., NISHIDA, J., TANAKA, S., SAKAI, R., MITANI, K., YOSHIDA, M., TANIGUCHI, T., YAZAKI, Y. & HIRAI, H. 1996. A novel interferon regulatory factor family transcription factor, ICSAT/Pip/LSIRF, that negatively regulates the activity of interferon-regulated genes. *Mol Cell Biol*, 16, 1283-94.
- YANG, Y., SHAFFER, A. L., 3RD, EMRE, N. C., CERIBELLI, M., ZHANG, M., WRIGHT, G., XIAO, W., POWELL, J., PLATIG, J., KOHLHAMMER, H., YOUNG, R. M., ZHAO, H., XU, W., BUGGY, J. J., BALASUBRAMANIAN, S., MATHEWS, L. A., SHINN, P., GUHA, R., FERRER, M., THOMAS, C., WALDMANN, T. A. & STAUDT, L. M. 2012. Exploiting Synthetic Lethality for the Therapy of ABC Diffuse Large B Cell Lymphoma. *Cancer Cell*, 21, 723-37.
- YAO, S., BUZO, B. F., PHAM, D., JIANG, L., TAPAROWSKY, E. J., KAPLAN, M. H. & SUN, J. 2013. Interferon regulatory factor 4 sustains CD8(+) T cell expansion and effector differentiation. *Immunity*, 39, 833-45.
- YE, B. H., CATTORETTI, G., SHEN, Q., ZHANG, J., HAWE, N., DE WAARD, R., LEUNG, C., NOURISHIRAZI, M., ORAZI, A., CHAGANTI, R. S., ROTHMAN, P., STALL, A. M., PANDOLFI, P. P. & DALLA-FAVERA, R. 1997. The BCL-6 proto-oncogene controls germinal-centre formation and Th2-type inflammation. *Nat Genet*, 16, 161-70.
- YE, B. H., RAO, P. H., CHAGANTI, R. S. & DALLA-FAVERA, R. 1993. Cloning of bcl-6, the locus involved in chromosome translocations affecting band 3q27 in B-cell lymphoma. *Cancer Res*, 53, 2732-5.
- YING, C. Y., DOMINGUEZ-SOLA, D., FABI, M., LORENZ, I. C., HUSSEIN, S., BANSAL, M., CALIFANO, A., PASQUALUCCI, L., BASSO, K. & DALLA-FAVERA, R. 2013. MEF2B mutations lead to deregulated expression of the oncogene BCL6 in diffuse large B cell lymphoma. *Nat Immunol*.
- YOO, H. Y., SUNG, M. K., LEE, S. H., KIM, S., LEE, H., PARK, S., KIM, S. C., LEE, B., RHO, K., LEE, J. E., CHO, K. H., KIM, W., JU, H., KIM, J., KIM, S. J., KIM, W. S., LEE, S. & KO, Y. H. 2014. A recurrent inactivating mutation in RHOA GTPase in angioimmunoblastic T cell lymphoma. *Nat Genet*, 46, 371-5.
- YOSHIDA, K., SAKAMOTO, A., YAMASHITA, K., ARGUNI, E., HORIGOME, S., ARIMA, M., HATANO, M., SEKI, N., ICHIKAWA, T. & TOKUHISA, T. 2006. Bcl6 controls granzyme B expression in effector CD8+ T cells. *Eur J Immunol*, 36, 3146-56.
- YU, D., RAO, S., TSAI, L. M., LEE, S. K., HE, Y., SUTCLIFFE, E. L., SRIVASTAVA, M., LINTERMAN, M., ZHENG, L., SIMPSON, N., ELLYARD, J. I., PARISH, I. A., MA, C. S., LI, Q. J., PARISH, C. R., MACKAY, C. R. & VINUESA, C. G. 2009. The transcriptional repressor Bcl-6 directs T follicular helper cell lineage commitment. *Immunity*, 31, 457-68.
- YU, J., ANGELIN-DUCLOS, C., GREENWOOD, J., LIAO, J. & CALAME, K. 2000. Transcriptional repression by blimp-1 (PRDI-BF1) involves recruitment of histone deacetylase. *Mol Cell Biol*, 20, 2592-603.
- YUAN, C. M., VERGILIO, J. A., ZHAO, X. F., SMITH, T. K., HARRIS, N. L. & BAGG, A. 2005. CD10 and BCL6 expression in the diagnosis of angioimmunoblastic T-cell lymphoma: utility of detecting CD10+ T cells by flow cytometry. *Hum Pathol*, 36, 784-91.

- ZACCHI, P., GOSTISSA, M., UCHIDA, T., SALVAGNO, C., AVOLIO, F., VOLINIA, S., RONAI, Z., BLANDINO, G., SCHNEIDER, C. & DEL SAL, G. 2002. The prolyl isomerase Pin1 reveals a mechanism to control p53 functions after genotoxic insults. *Nature*, 419, 853-7.
- ZAMO, A., CHIARLE, R., PIVA, R., HOWES, J., FAN, Y., CHILOSI, M., LEVY, D. E. & INGHIRAMI, G. 2002. Anaplastic lymphoma kinase (ALK) activates Stat3 and protects hematopoietic cells from cell death. *Oncogene*, 21, 1038-47.
- ZAN, H., LI, Z., YAMAJI, K., DRAMITINOS, P., CERUTTI, A. & CASALI, P. 2000. B cell receptor engagement and T cell contact induce Bcl-6 somatic hypermutation in human B cells: identity with Ig hypermutation. *J Immunol*, 165, 830-9.
- ZAPH, C., ROOK, K. A., GOLDSCHMIDT, M., MOHRS, M., SCOTT, P. & ARTIS, D. 2006. Persistence and function of central and effector memory CD4+ T cells following infection with a gastrointestinal helminth. *J Immunol*, 177, 511-8.
- ZDZALIK, D., DYMEK, B., GRYGIELEWICZ, P., GUNERKA, P., BUJAK, A., LAMPARSKA-PRZYBYSZ, M., WIECZOREK, M. & DZWONEK, K. 2014. Activating mutations in ALK kinase domain confer resistance to structurally unrelated ALK inhibitors in NPM-ALK-positive anaplastic large-cell lymphoma. *J Cancer Res Clin Oncol*, 140, 589-98.
- ZERRAHN, J., HELD, W. & RAULET, D. H. 1997. The MHC reactivity of the T cell repertoire prior to positive and negative selection. *Cell*, 88, 627-36.
- ZETTL, A., RUDIGER, T., KONRAD, M. A., CHOTT, A., SIMONITSCH-KLUPP, I., SONNEN, R., MULLER-HERMELINK, H. K. & OTT, G. 2004. Genomic profiling of peripheral T-cell lymphoma, unspecified, and anaplastic large T-cell lymphoma delineates novel recurrent chromosomal alterations. *Am J Pathol*, 164, 1837-48.
- ZHANG, L. H., KOSEK, J., WANG, M., HEISE, C., SCHAFER, P. H. & CHOPRA, R. 2013. Lenalidomide efficacy in activated B-cell-like subtype diffuse large B-cell lymphoma is dependent upon IRF4 and cereblon expression. *Br J Haematol*, 160, 487-502.
- ZHANG, S., WANG, F., KEATS, J., ZHU, X., NING, Y., WARDWELL, S. D., MORAN, L., MOHEMMAD, Q. K., ANJUM, R., WANG, Y., NARASIMHAN, N. I., DALGARNO, D., SHAKESPEARE, W. C., MIRET, J. J., CLACKSON, T. & RIVERA, V. M. 2011. Crizotinib-resistant mutants of EML4-ALK identified through an accelerated mutagenesis screen. *Chem Biol Drug Des*, 78, 999-1005.
- ZHAO, W. L., LIU, Y. Y., ZHANG, Q. L., WANG, L., LEBOEUF, C., ZHANG, Y. W., MA, J., GARCIA, J. F., SONG, Y. P., LI, J. M., SHEN, Z. X., CHEN, Z., JANIN, A. & CHEN, S. J. 2008. PRDM1 is involved in chemoresistance of T-cell lymphoma and down-regulated by the proteasome inhibitor. *Blood*, 111, 3867-71.
- ZHAO, W. L., MOURAH, S., MOUNIER, N., LEBOEUF, C., DANESHPOUY, M. E., LEGRES, L., MEIGNIN, V., OKSENHENDLER, E., MAIGNIN, C. L., CALVO, F., BRIERE, J., GISSELBRECHT, C. & JANIN, A. 2004. Vascular endothelial growth factor-A is expressed both on lymphoma cells and endothelial cells in angioimmunoblastic T-cell lymphoma and related to lymphoma progression. *Lab Invest*, 84, 1512-9.
- ZHENG, H., YOU, H., ZHOU, X. Z., MURRAY, S. A., UCHIDA, T., WULF, G., GU, L., TANG, X., LU, K. P. & XIAO, Z. X. 2002. The prolyl isomerase Pin1 is a regulator of p53 in genotoxic response. *Nature*, 419, 849-53.
- ZHENG, Y., CHAUDHRY, A., KAS, A., DEROOS, P., KIM, J. M., CHU, T. T., CORCORAN, L., TREUTING, P., KLEIN, U. & RUDENSKY, A. Y. 2009. Regulatory T-cell suppressor program co-opts transcription factor IRF4 to control T(H)2 responses. *Nature*, 458, 351-6.
- ZHU, Y. X., BRAGGIO, E., SHI, C. X., BRUINS, L. A., SCHMIDT, J. E., VAN WIER, S., CHANG, X. B., BJORKLUND, C. C., FONSECA, R., BERGSAGEL, P. L., ORLOWSKI, R. Z. & STEWART, A. K. 2011. Cereblon expression is required for the antimyeloma activity of lenalidomide and pomalidomide. *Blood*, 118, 4771-9.